Ceramic Regenerator Program

Contract NAS 3-25416

Final Report

NASA CR 189053

November 1991

Prepared For:

NASA/Lewis Research Center
21000 Brookpark Road
Cleveland, OH 44135

Aerojet Propulsion Division
P.O. Box 13222
Sacramento, CA 95813

TABLE OF CONTENTS

	Page
1.0 Introduction	1
2.0 Goals and Objectives	1
3.0 Summary of Accomplishments, Conclusions and Recommendations	1
4.0 ATR Specifications	3
5.0 Conceptual Design and Feasibility	6
5.1 Conceptual Design	6
5.2 Material Selection	14
5.3 Fabrication Processes.	21
5.3.1 Slip Casting	21
5.3.2 Ceramic Tape Cast Platelet Technology	21
6.0 Technical Discussion	25
6.1 Regenerator Design	25
6.1.1 Thermal Analysis	25
6.1.2 Structural Analysis and Vane Design	29
6.1.3 Manifold Design	33
6.1.4 Final Design	43
6.2 Regenerator Fabrication	57
6.2.1 Fabrication Experimentation	57
6.2.2 Final Regenerator Fabrication	64
6.3 Regenerator Testing	74
6.3.1 Objectives	74
6.3.2 Test Facility Description	81
6.3.3 Results	90
6.3.3.1 Leak, Proof and Burst Testing	90
6.3.3.2 Hot-Fire Testing	90
Appendices	
A Ceramic Regenerator Test Plan	A-1
B Detailed Design Drawings – Omitted From Draft	B-1

PRECEDING PAGE BLANK NOT FILMED

PAGE______INTENTIONALLY BLANK

LIST OF TABLES

Table No.		Page
1.0	Ceramic Regenerator Test Summary	3
4.1	Operating Parameters ATR Combustor Regenerator	5
5.2.1	Materials Data (Preliminary)	17
5.2.2	Comparison of Strength to Weight Ratios of Silicon Nitride With Other Engineering Materials	19
5.2.3	Typical Properties of PSG Silicon Nitride	19
6.1.1.1	Ceramic Heat Exchanger Gas Side Boundary Conditions	27
6.2.2.1	Dimension of Regenerator Vanes SN-1, SN-2, SN-3, and SN-4	80
6.3.3.1	Ceramic Regenerator Program Test Duration Summary. All Tests With GN_2 Coolant Except Where Noted With CH_4	91
6.3.3.2	ATR Ceramic Regenerator Program Summary of Program Accomplishments	92

PAGE____INTENTIONALLY BLANK

LIST OF FIGURES

Figure No.		Page
4.1	Advanced Materials Are Key to Lightweight Engines for High Speed Transport Aircraft	4
5.1.1	Layout of Vaned Regenerator Based on a 56-in. Diameter ATR Engine	7
5.1.2	Initial Regenerator Concepts	8
5.1.3	Prototype Ceramic Regenerator	9
5.1.4	Preliminary Design of 16 Channel, Silicon Nitride Regenerator	10
5.1.5	Preliminary Design of Manifolding for 16 Channel Ceramic Regenerator	11
5.1.6	Cross Flow ATR Ceramic Regenerator Concept	12
5.1.7	Multipass Ceramic Regenerator for ATR	13
5.1.8	Layered Ceramic Vane for Single Regenerator ATR	15
5.1.9	Ceramic Regenerator Vane, Current Design	16
5.2.1	Silicon Nitride Provides Lightweight, High Thermal Design Margin and is Not Ignitable in High Pressure O_2	18
5.2.2	Silicon Nitride Has a Higher Thermal Shock Capability Than Many Other Ceramics	20
5.3.1	Flow Sequence to Produce Integral Cast Regenerator Vane	22
5.3.2.1	Flow Diagram of Ceramic Platelet Fabrication Process	23
5.3.2.2	Tape Casting Process Uses a Doctor Bland and Continuous Reel of Mylar to Form the Green Ceramic Tape	23
6.1.1.1	Variation of Wall Temperature Gradient With Gas Side Heat Flux for Candidates Thickness of Silicon Carbide and Silicon Nitride	26
6.1.1.2	Coolant Velocity and Exit Temperature Calculated From Preliminary Thermal Hydraulic Analysis of Prototype Silicon Nitride Regenerator (16 Channels, 0.06 x 0.12 in.)	28
6.1.1.3	2-D ANSYS Finite Element Model of Cruise Condition (Worst Case)	30
6.1.1.4	Variation of Local Heat Transfer Coefficient Near Regenerator Vane Leading Edge for Sea Level Static (SLS), Cruise (Ma = 5), and Test Cell Conditions	31
6.1.2.1	Temperatures Input for 3D Thermal Model	32
6.1.2.2	Temperature Profile at Leading Edge	34
6.1.2.3	Temperature Profile at Trailing Edge	35
6.1.2.4	Temperature Profile Cross Section at Max Stress Location	36
6.1.2.5	Effective Stress Cross Section at Max Stress Location	37

LIST OF FIGURES (cont.)

Figure No.		Page
6.1.3.1	Assembly of Green Bond Regenerator Vane and Wax Cylinders. Top View is Exploded Section; Bottom View Shows Assembly Together	38
6.1.3.2a	Tape Wrapped Around Assembly From Figure 3	39
6.1.3.2b	Detail of Tape Wrap Manifold Approach	39
6.1.3.3	Top View Shows Overwrap Assembly After Green Machining to Trim Off Excess Material. Bottom View is Assembly After Sintering. A Metallic Tube is Shown Brazed Onto One Inlet. One Tube Was to be Brazed to Each Outlet for Controlling Methane Flow	40
6.1.3.4	Initial Unsuccessful Tubular Manifold Design	41
6.1.3.5a	Overall View of Ceramic Regenerator With Platelet Manifolds	42
6.1.3.5b	Cross Section of Platelet Manifolds for Ceramic Regenerator. Structure is Made Up From Multiple 0.016 in. Layers, Green Bonded, Machined and Fired	42
6.1.3.5c	Section B-B From Figure 6b. After Green Bonding of Manifold Stack, Manifold Tubes Are Machined Into Stack, the Ends Machined Round and Parts Fired	42
6.1.3.6a	Side Entry Ceramic Regenerator Concept. Manifolds Are Constructed From Layered Platelets	44
6.1.3.6b	Cross Section of Platelet Manifolds For Side Entry Manifold Concept. manifolds Are Green Machined Before Stacking and Green Bonding	44
6.1.3.6c	Manifold Design of Side Entry Ceramic Regenerator Corners and 0.5 in. Inlet Are Machined After Green Bonding	44
6.1.3.7a&b	Overall View of Improved Platelet Heat Exchanger Manifold Design	45&46
6.1.3.8a	Through View	47
6.1.3.8b	Flow Passage	47
6.1.3.9	Manifold Platelet Detail	48
6.1.3.10	Exploded View of Manifold Ends	49
6.1.4.1	Through View of Stacked Platelets For Ceramic Regenerator	50
6.1.4.2	Distribution Manifold Platelets For Ceramic Regenerator	51
6.1.4.3	Final Manifold and Channel Closeout Platelets	52
6.1.4.4	Regenerator Channel Platelet. Note the Wide Side Lands to be Trimmed After Being Bonded With P/N 1204477-2, Figure 3	53
6.1.4.5	Cross Section of Regenerator Vane Section	54
6.1.4.6	Regenerator Manifold Closeout Platelet	55

LIST OF FIGURES (cont.)

Figure No.		Page
6.1.4.7	Platelet Stacking Sequence for Ceramic Regenerator. Note the Thickness of the Vane Channels (P/N 1204477-3) Has Been Reduced to 2 Platelets	56
6.2.1	Prototype (Green Aluminum) Regenerator Platelets Showing Manifolds and Cooling Passages	58
6.2.2	Green Prototype (Alumina) Cooling Passage Platelet. Passages Are Optimized to Match Heat Input	59
6.2.3	Overall View of Prototype Alumina Regenerator Fabricated With an Earlier Design. This Part Was Sectioned For Evaluation	60
6.2.4	Edge View of Prototype Alumina Regenerator. The Warpage of the Vane Section is Due to Dragging of the Part on the Furnace Due to Shrinkage During Sintering	61
6.2.5	Edge View of Prototype Alumina Regenerator Manifold. The Delamination Is Due to Dragging of the Part On the Furnace Due to Shrinkage During Sintering	62
6.2.6	Cross Section of the Alumina Prototype Regenerator. Note the Misalignment of the Channels and Loads, the Droop in the Wide Channel and the Poor Alignment of the Edges of the Part. All of These Problems Have Been Addressed and Will be Eliminated in Future Parts	63
6.2.7	Large Scale "Green" Silicon Nitride Laminated Structure	65
6.2.2.1	Prototype Silicone Nitride Platelets	66
6.2.2.2	Alumina Prototype of the Final Regenerator Design	67
6.2.2.3	Location of Inspection Sections for Alumina Prototype Regenerator	68
6.2.2.4	Cross Section of the First Alumina Regenerator (Top) and Current Pre-Prototype Version (Bottom)	69
6.2.2.5	Detail of Sagging and Delamination of Wide Regenerator Channels	71
6.2.2.6	Prototype Alumina Regenerator. Deformation and Cracking is Due to Excessive Temperature and Pressure Used During Lamination	72
6.2.2.7	Cross Section of Manifold Region, Section C-C, Figure 2, Blistering and Delamination Due to Incomplete Burn-Out	73
6.2.2.8	Cross Section of the First Article Silicon Nitride Regenerator Vane – Design Cross Section of Vane Section	75
6.2.2.9	Section Through Manifold of Silicon Nitride Regenerator. Note the Laminations Are Free From Voids. The Rough Feature Edges Are Due to the Section Being a Small Cord Cut on Round Features	76
6.2.2.10	Section Through Manifold of Silicon Nitride Regenerator. Note the Straight Feature Edges. The Void is Due to the Lamination of an Unsupported Region	77

LIST OF FIGURES (cont.)

Figure No.		Page
6.2.2.11	Regenerators	78
6.2.2.12	Regenerators	79
6.3.2.1	Refractory Lined Combustion Chambers and Watercooled Test Section	82
6.3.2.2	Refractory Lined Combustion Chamber and Watercooled Test Section Setup in Test Area	83
6.3.2.3	Sketch of Water Cooled Test Section	84
6.3.2.4	Top View of Watercooled Test Section After Completion of Testing	85
6.3.2.5	Sketch of Test Section With Vane and Flanges Exploded in Place	86
6.3.2.6	Exploded View of Inlet and Exit Flanges for Ceramic Regenerator	87
6.3.2.7	Ceramic Regenerator Vane in Place in Test Section	88
6.3.2.8	Close-up View of Regenerator Vane in Test Section	89
6.3.3.1	Typical Heat Up and Cooling Transients During the Thermocycling Tests. Tests 32 and 33 on Part S-2	93
6.3.3.2	Heating and Cooling Rates of the Surface of the Silicon Nitride During Tests 32 and 33	94
6.3.3.3	Test Part SN-1, Fractured During Initial Heat-Up Cycle. Note the Crack in Center of Vane (Front)	96
6.3.3.4	Observe of Vane SN-1 (Rear)	97
6.3.3.5	SN-2 Thermocouple Tests #27 Through 40	98
6.3.3.6	Vane SN-2 After 40 Thermal Cycles and 09:40:11 (hr:min:sec) of Exposure (Front)	99
6.3.3.7	Observe of SN-2 After Testing (Rear)	100
6.3.3.8	Detail of Fracture of Vane SN-2 After Testing	101
6.3.3.9	Profile of Fracture of SN-2	102
6.3.3.10	Part No. SN-3 After 117:23:44 (hr:min:sec) of Exposure to Prepare Combustion Products (Front)	103
6.3.3.11	Observe of SN-3 After Long Duration Test (Rear)	104
6.3.3.12	Regenerator Vane No. SN-3 Test 9. Typical Thermal Cycle of Vane Surface Temperature During Methane Testing	105
6.3.3.13	Regenerator Vane No. SN-3, Methane Test No. 9 Coolant Outlet Temperature and Temperature Rise as the Coolant Passes Through the Heated Section	106
6.3.3.14	Vane SN-3 Coolant Flow Rate and Coolant Temperature Rise During Methane Test 9	107

LIST OF FIGURES (cont.)

Figure No.		Page
6.3.3.15	Long Duration Testing of SN-3 With GN_2, Combustion Gas Temperature, Vane Surface Temperature and Coolant Outlet Temperature	108
6.3.3.16	Long Duration Test of SN-3 Showing Coolant Flow Rate Inlet and Outlet Coolant Temperature	109
6.3.3.17	Heat Flux Variation During the Long Duration Test of SN-3	110
6.3.3.18	Leading Edge of SN-3 After Long Duration Test. Deposits from Tester	111
6.3.3.19	Trailing Edge of SN-3 After Long Duration Testing. Deposits Are From Tester	112
6.3.3.20	EDS Spectrum of Deposit Found on Leading Edge of SN-3. This Material is Believed to Originate in the Combustion Chamber and Water Cooled Section, and the Sulfur From the Propane Fuel	114
6.3.3.21	EDS Spectrum of Green Deposit on Trailing Edge of SN-3 After Testing	115
6.3.3.22	EDS Spectrum of Yellow Green Deposit Found on Trailing Edge of SN-3 After Testing	116
6.3.3.23	EDS Spectrum of Yellow/Brown Deposit Found on Inlet End of the Vane Face of SN-3 After Testing	117

PAGE INTENTIONALLY BLANK

1.0 INTRODUCTION

Advanced propulsion concepts such as the Air Turbo Ramjet (ATR) require light weight materials that are oxidation resistant and have good structural properties at high temperatures. Ceramic materials offer all of these advantages.

The ATR cycle Ref. 1 requires the delivery of 1800°R methane at 600 psi to drive the turbo pump. The liquid methane delivered from this pump is heated in a regenerator (heat exchanger) located in the ram air combustion chamber which operates at temperatures as high as 3749 R. This program addresses the materials and fabrication technologies required for a light weight heat exchanger.

The important design parameters in addition to weight, are durability and low pressure loss in both the fuel heating circuit and in the main hot gas flow stream. The heat exchanger must also be capable of operating over a wide range of flight conditions ranging from subsonic at take off and landing to supersonic cruise.

2.0 GOALS AND OBJECTIVES

The objectives of this feasibility demonstration program were to evaluate candidate ceramic material and fabrication concepts which have potential for an advanced lightweight regenerator which could meet the flight life and thermal requirements for the ATR. The specific goals of the program were to fabricate four test articles, using the selected design, material and fabrication concept and conduct proof pressure and leak tests and demonstrate 100 hours of operation and 36 thermal cycles in a simulated high temperature combustion gas environment.

3.0 SUMMARY OF ACCOMPLISHMENTS

Tape cast silicon nitride was selected as the preferred material to meet the thermal, structural and environmental requirements of the ATR. The fabrication processes required to formulate the powder blend, prepare the tape, punch the cooling passages and manifolding and laminate the assembly using Aerojet platelet technology developed for metals, was successfully accomplished.

Designs were prepared and six articles successfully fabricated from .016 in. thick, green silicon nitride tape, which was punched, laminated and thermally processed to a high density state.

Evaluation

The regenerators were visually and dimensionally analyzed as well as leak and proof tested. In addition, two of the regenerators were exposed to 500 fps, 3100°F propane combustion gases.

Two of the silicon nitride regenerators were sectioned to evaluate the internal features. A cross section of one of the sectioned regenerators is shown in Figure 1.0, along with the designed cross section. In the fully sintered state, there was no bond line visible between the individual platelets except in areas where there is clear non-contact.

Leak Testing

Four of the regenerators were subject to low pressure leak test by pressurizing the circuits with GN_2. One of the regenerators showed leakage through the face of the part as a result of being insufficiently sintered. This part was not subjected to further testing. Another showed a small leak at the edge of the manifold but this was not considered a deterrent to additional testing. The other two regenerators were leak free.

Proof Testing

Three remaining regenerators were subject to proof testing at 900 psi, 1.5 times their design operating pressure. No additional leaks were noted during this procedure and the leak noted during the low pressure GN_2 leak check did not manifest itself during the water testing. One of the regenerators was pressure tested to burst at 1575 psi, 2.6 times the operating pressure. The area of fracture was at one of the wider spans of the manifold which can easily be strengthened for higher pressure use.

Thermal Exposure

Three of the regenerators were subject to thermal cycling and exposure testing in a ATR simulator using 600 psi GN_2 and methane (CH_4) as coolants. The nominal operating environment for the exposure was propane combustion products at 500 fps and 3100°F. This environment produced regenerator surface temperatures as high as 2339°F and coolant exit temperatures of 1415°F with a ambient inlet temperature.

One of the test regenerators survived 40, 2000°F thermal cycles with GN_2 coolant for a total test exposure time of 09:40:11 (hr:min:sec) before fracturing during a rapid heating cycle. Another part underwent 10 methane thermal cycle tests and a single long duration test of

112:04:47 (hr:min:sec) with GN_2 as the coolant Table 1.0 gives a summary of the significant results of the regenerator evaluation and testing compared to goals.

TABLE 1.0. CERAMIC REGENERATOR TEST SUMMARY

	Goal	Attained
Proof Pressure	900 psi	900 psi
Leakage	None	None (2 parts)
Burst Pressure	900 psia	1575 psi (1 part)
Hot Testing	2 parts	2 Parts
Life	100 Hrs	117 Hrs
Max. Surface Temp.	2000 F	2339 F
Max Outlet Temp.	1250 F	1415 F
No. Thermal Cycles	36	40 (1 part)

Summary and Conclusions

The fabricability of silicon nitride regenerators with intricate internal passages using ceramic tape multilayer packaging techniques and Aerojet's platelet technology has been demonstrated. While the current example is fairly simple in design and execution, sufficient precedence has been established to proceed with larger and more complex and intricate ceramic components which will expand the application possibilities. Future efforts should also address the attachment of feedlines to the integral manifolds with emphasis on light weight and high reliability.

4.0 ATR SPECIFICATIONS AND DESIGN DRIVERS

The prototype regenerators built and tested on this program were designed to operate at the realistic service conditions anticipated of this component in the Air Turbo Ramjet (ATR) engine, Figure 4.1. The design operating conditions considered included propellant chemistry, flow rates, heat flux, gas-side and coolant temperatures and pressure differentials. Table 4.1 shows the operating parameters for the ATR baseline engine from the High Speed Civil Transport (HSCT) study contract AS-23468. These parameters were used as a portion of the design requirements for the ceramic heat exchanger test module. Two operating conditions are shown: (1) Sea-Level-Static (SLS) and (2) Cruise at Mach 5 and 83,000 ft altitude (M5/83K), at a minimum flow and thrust (17,700 lbf). There are wide ranges of thrust and altitude combinations at

PAGE____INTENTIONALLY BLANK

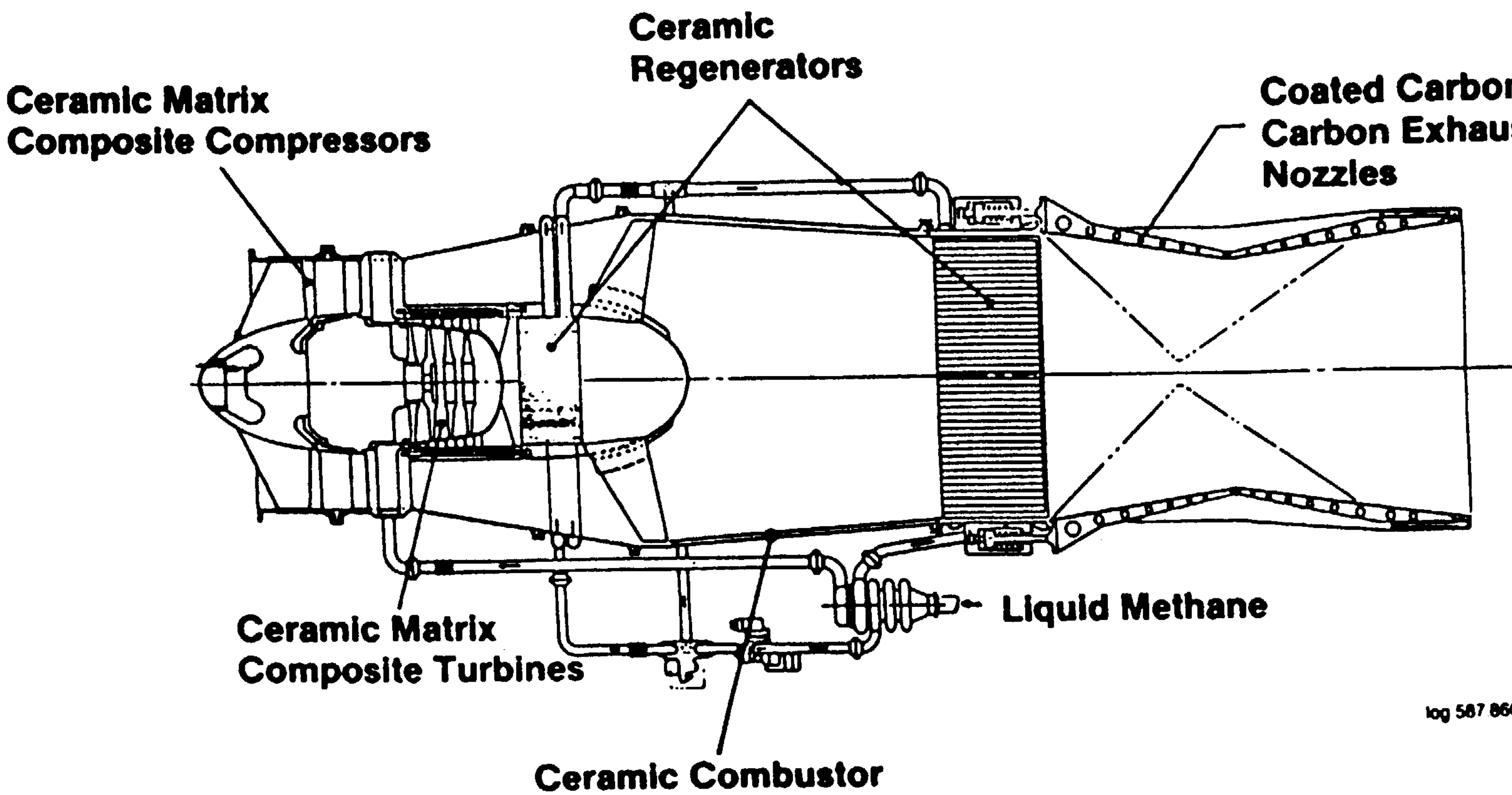

Figure 4.1 Advanced Materials Are Key to Lightweight Engines for High Speed Transport Aircraft

TABLE 4.1

OPERATING PARAMETERS
ATR COMBUSTOR REGENERATOR

Parameter	Units	S.L.S. (55K lbf)		M5/83K ft (17.7K lbf)	
		Cold Side	Hot Side	Cold Side	Hot Side
• Fluid	---	CH_4	Comb. Gas	CH_4	Comb. Gas
• Flow Rate	lb-sec	32.0	706.	7.73	277.
• Inlet Temp.	°R	200	3562	200	3844
• Outlet Temp.	°R	1860	3408	1860	3749
• Inlet Press.	psia	610	25	160	110
• Gas ΔP	psi	(1)	(2)	(1)	(2)
• Avg. Cp	Btu/lb-°R	0.75	0.366	0.75	0.366
• Mol. Wt	---	16	28.4	16	28.4
• Heat Trans.	Btu/sec	39840	39840	9624	9624
• Flow Area	in.^{2}	(3)	4610	(4)	4610(5)
• Length	in.	15	15	15	15

(1) As required; no significant effect on engine size, weight or performance. Suggest a maximum of 15% of inlet pressure.
(2) As low as possible; has a very pronounced effect on engine size, weight, and performance. Suggest a maximum of 5% of inlet pressure.
(3) As required but as low as possible; moderately affects the engine size and weight.
(4) As required to prevent over-heating of methane (1860°R limit for thermal decomposition). The regenerator system will shut off the methane flow to some of the platelets to give this required flow area.
(5) Combustion gas will flow around all platelets under all conditions even though some platelets will not always be cooled. Therefore, the uncooled platelet material must be capable of withstanding 3844°R.

which the engine must operate, but the two conditions shown are representative of the most important regimes of operation.

The assumed regenerator, which resulted in the parameters shown in Table 4.1, is one that contains a valve system which blocks the methane flow to a larger number of regenerator sections as the methane flow is reduced. As a result, the flow per active section is maintained high enough to prevent over-heating and thermally decomposing the methane when flow is less then the maximum value. The major impact on the regenerator design resulting from this regenerator system is that the ceramic material must be capable of withstanding the full combustion temperatures when the blocked platelets are not being actively cooled by the methane.

The two most important design parameters of the regenerator, as they effect vehicle performance, are the regenerator weight and the pressure drop in the combustion gas. It was recommended that the weight goal for the regenerator not exceed 1100 lbs. This weight represents 25% of the total engine weight. The engine without the regenerator is 3331 lbs. A preliminary heat transfer analysis indicated that this weight can be achieved if the ceramic wall is no more than 0.031 in thick.

Additionally, it was recommended that the hot gas pressure drop be no greater than 5% of the inlet pressure. Regenerator pressure drop has a very significant degrading effect on engine I_{sp}, which not only requires more fuel but also increases the engine size and weight. Based on a simplified mission analysis, i.e., Los Angeles to Tokyo, it was determined that the regenerator weight reduction required to compensate for an increase of 1% in the hot gas pressure drop is 488 lbs to maintain the same payload to initial weight fraction.

5.0 CONCEPTUAL DESIGN AND FEASIBILITY

5.1 CONCEPTUAL DESIGN

The initial regenerator concepts are show in Figures 5.1.1 and 5.1.2. In this concept, the regenerator is a group of pie sections which fit together in a 56 in. diameter ATR engine. An initial prototype concept is shown in Figure 5.1.3. This design simulated one vane of the pie section regenerator. This design utilized U-shaped channels of varying lengths and duel manifolds to allow the variation in flow for different operating conditions. Thermal analysis and potential fabrication difficulties resulted in a change in to a straight through flow design, Figure 5.1.4 and 5.1.5. This prototype was a result of a multi-pass, cross-flow ceramic regenerator concept which was defined for the program. This concept is shown in Figures 5.1.6 and 5.1.7. The multi-pass configuration was required to maintain the thermal stressed at an acceptable level.

Layout of Vaned Regenerator Based on a 56-in. Diameter ATR Engine.

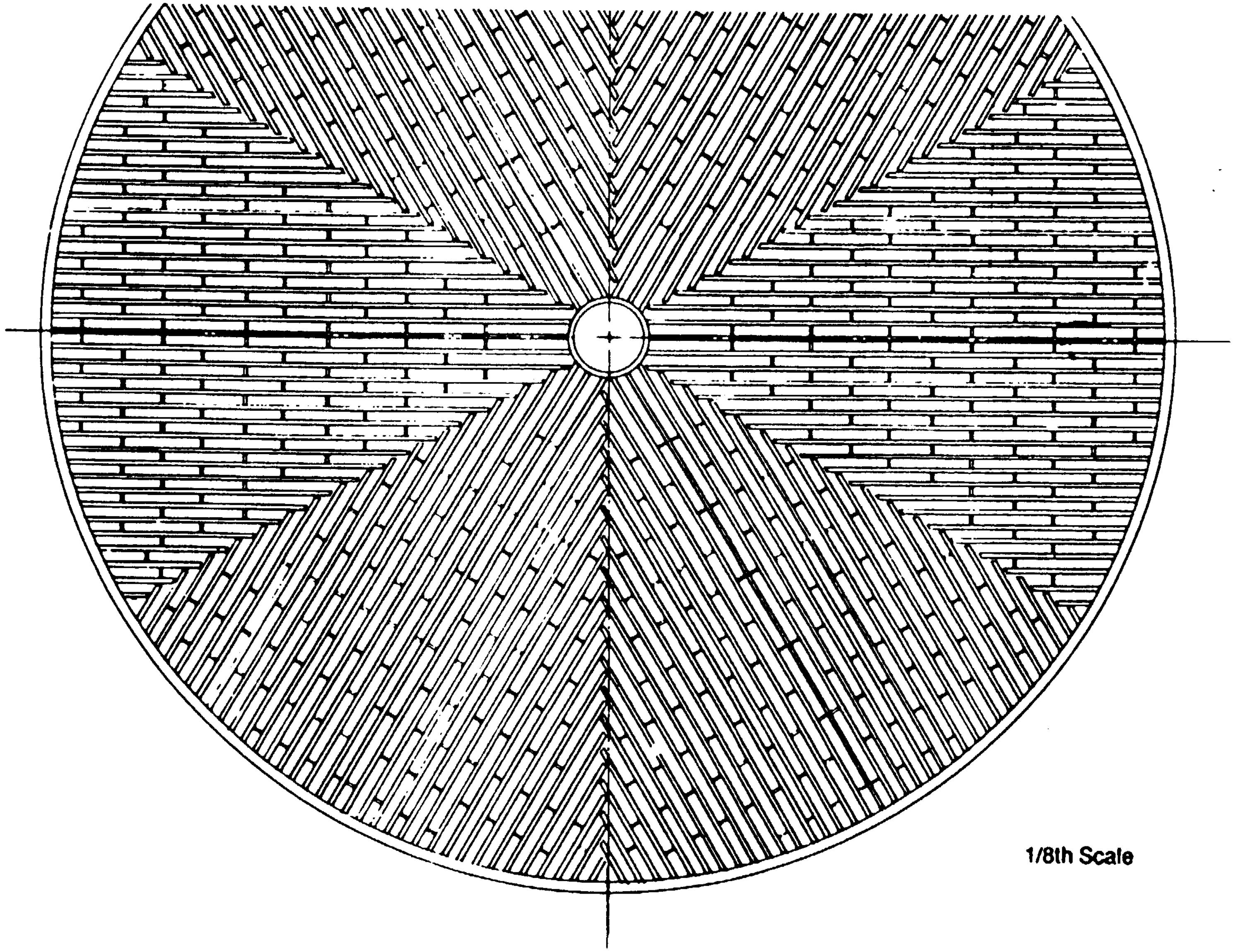

Figure 5.1.1 Layout of Vaned Regenerator Based on a 56-in. Diameter ATR Engine

Schematic of a Pie Section
of the Vaned Regenerator

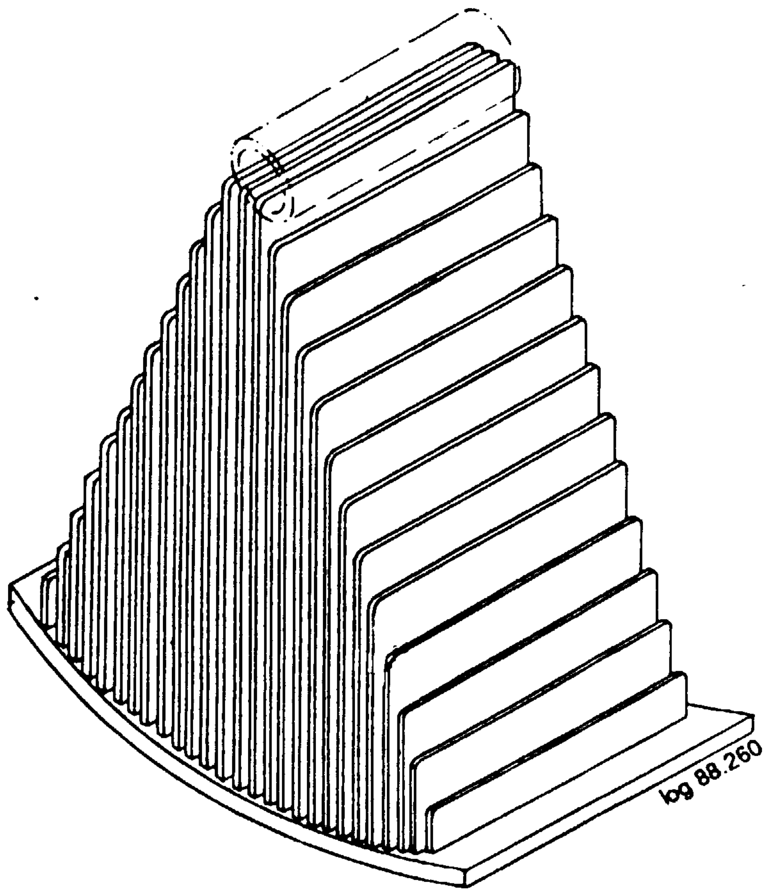

1/8th Scale

View through the Center of a
Vane in the Regenerator

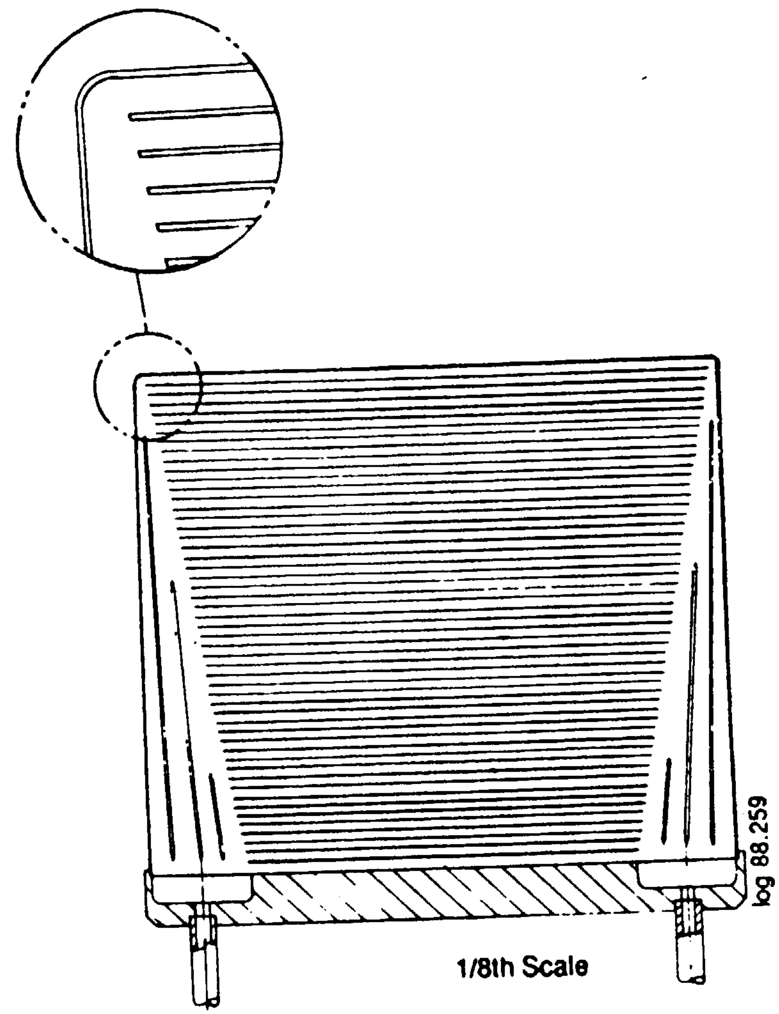

1/8th Scale

Figure 5.1.2 Initial Regeneration Concepts

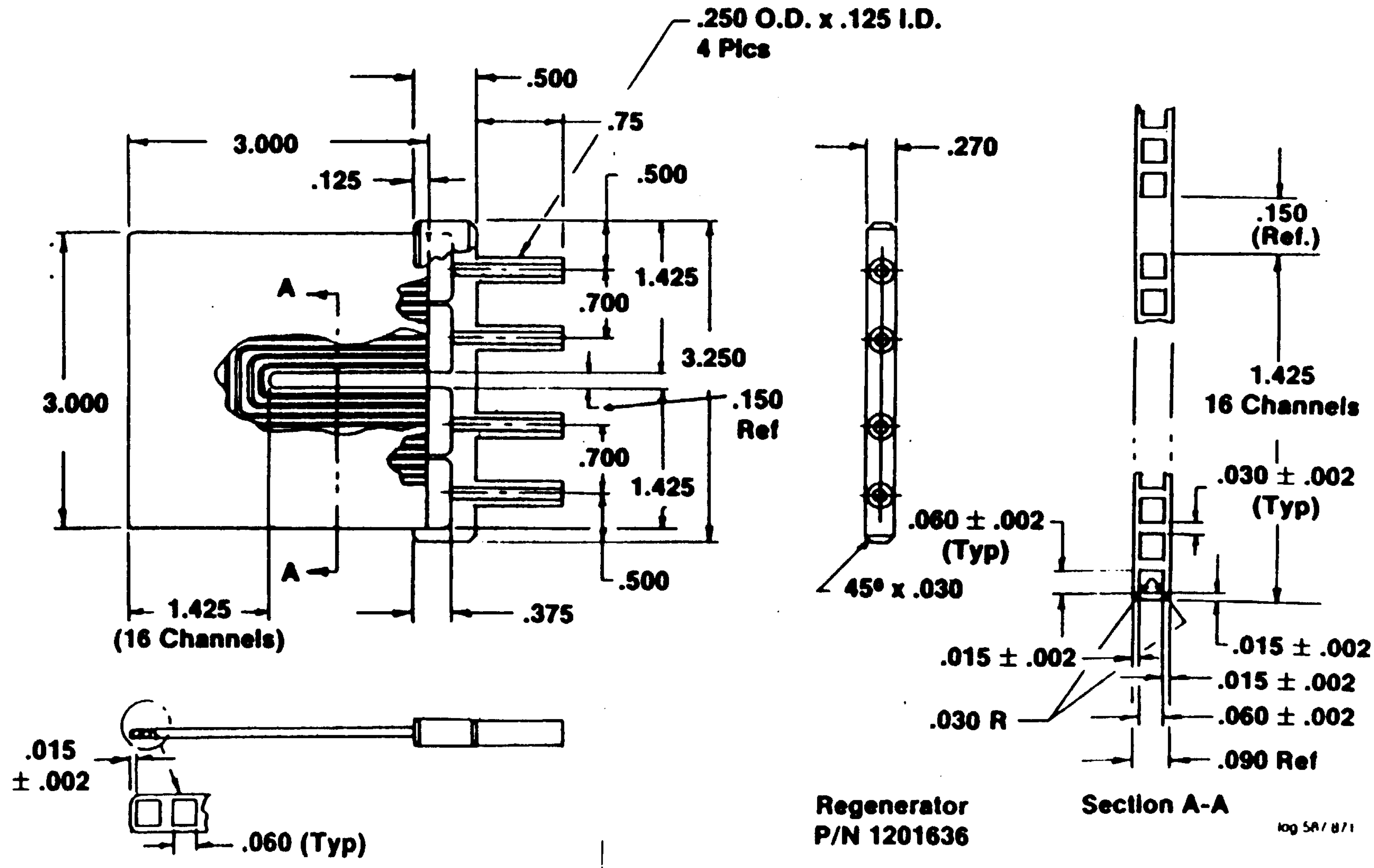

Figure 5.1.3 Prototype Ceramic Regenerator

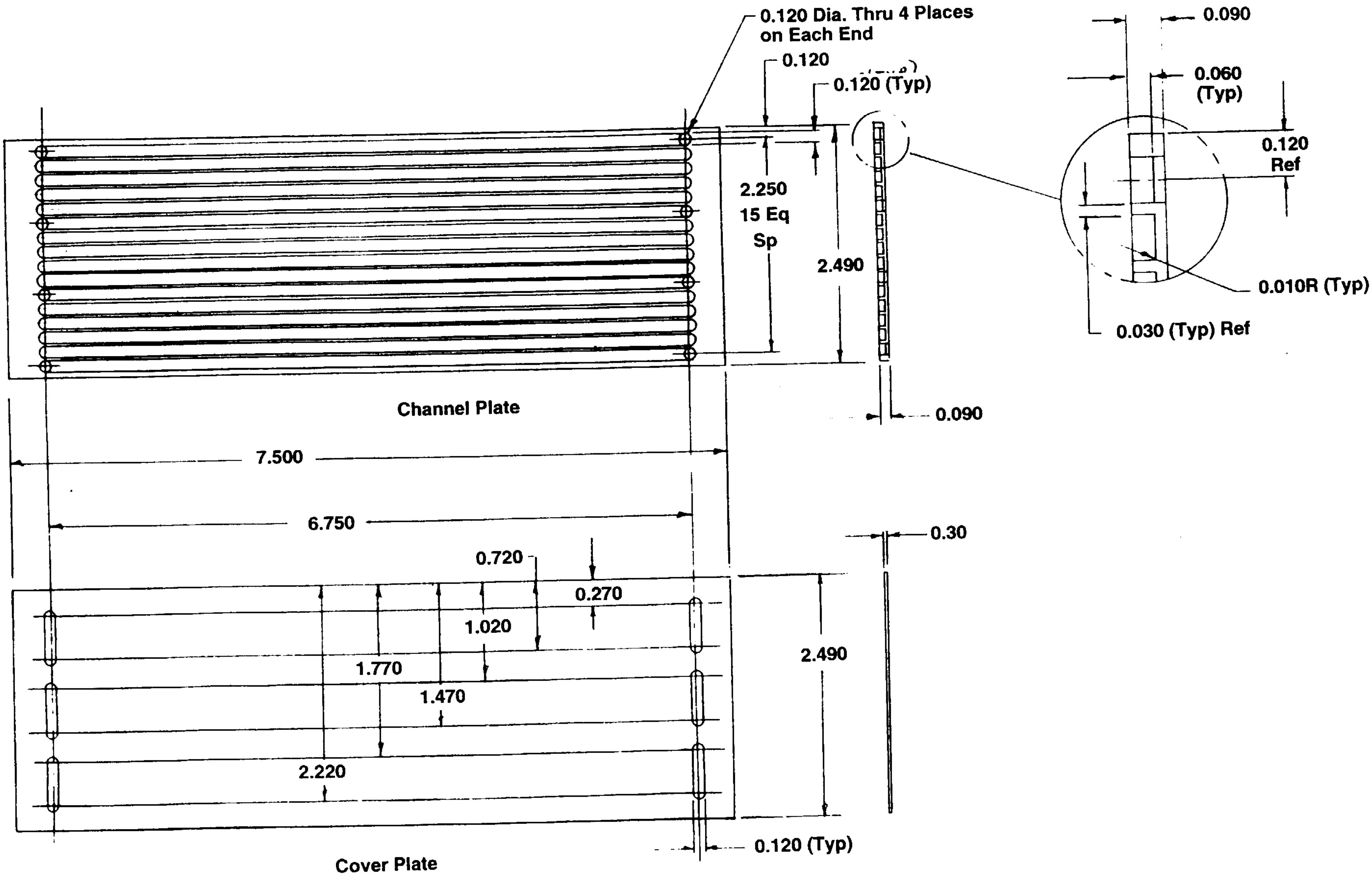

Figure 5.1.4 Preliminary Design of 16 Channel, Silicon Nitride Regenerator

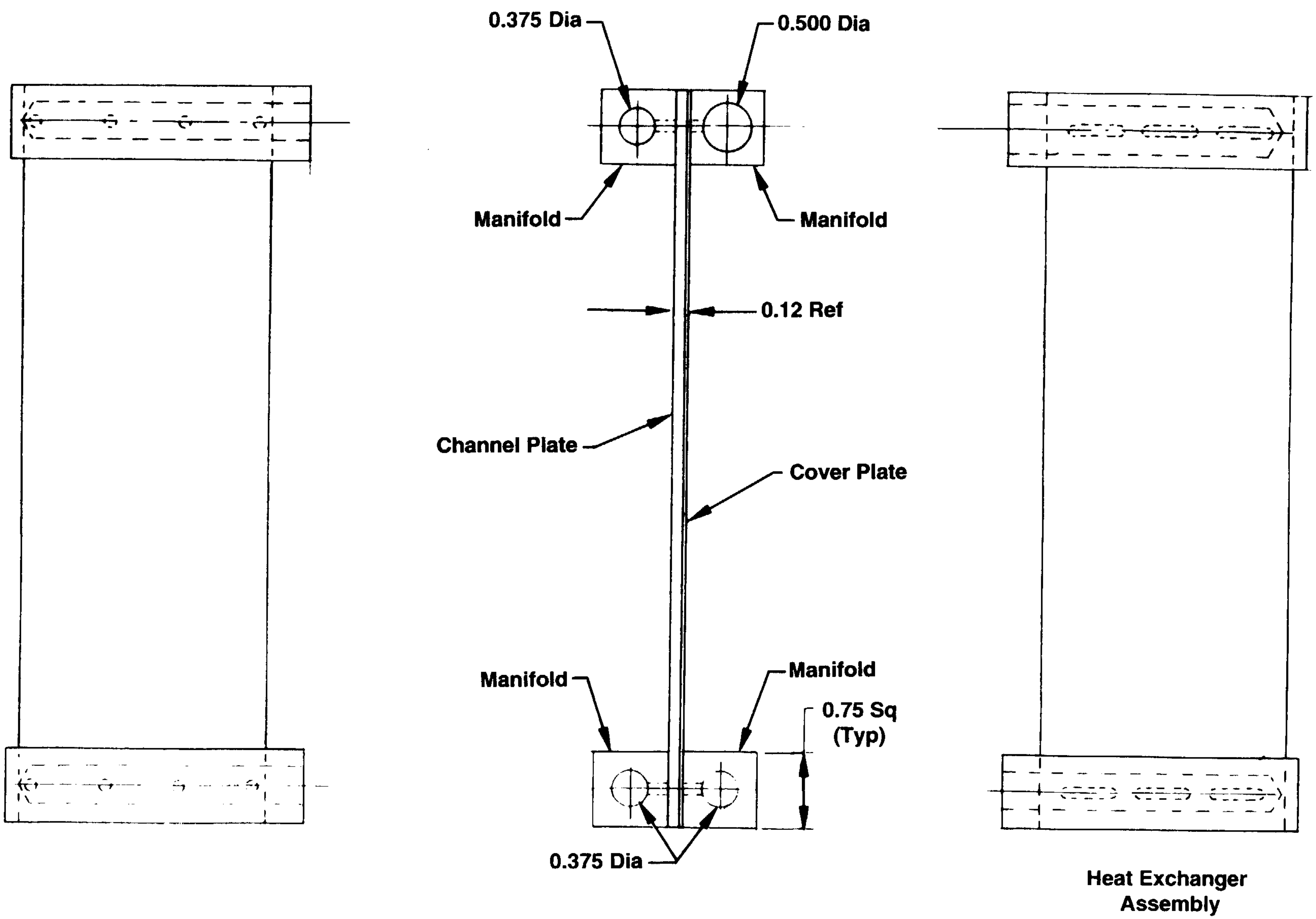

Figure 5.1.5 Preliminary Design of Manifolding for 16 Channel Ceramic Regenerator

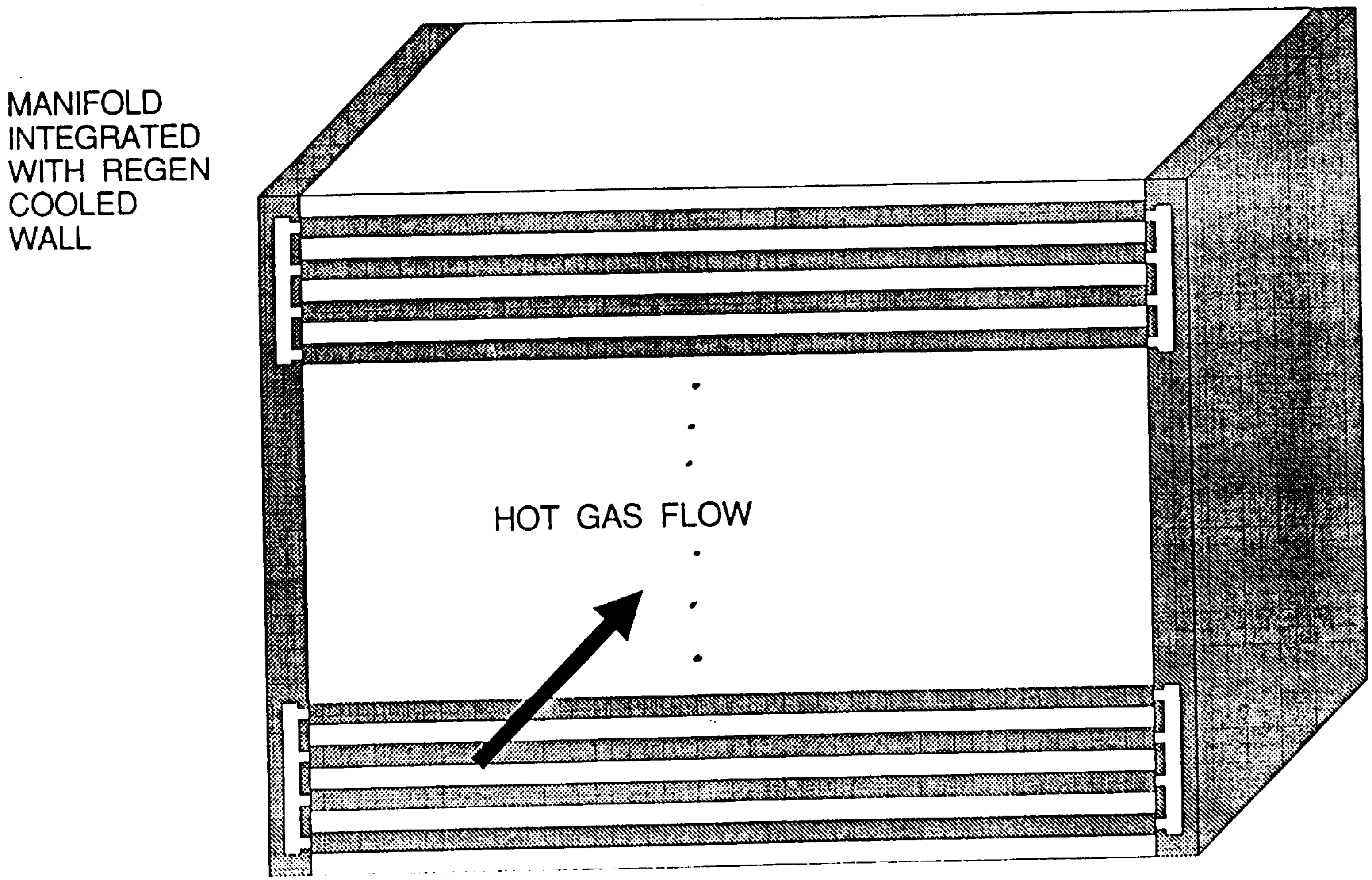

Figure 5.1.6 Cross Flow ATR Ceramic Regenerator Concept

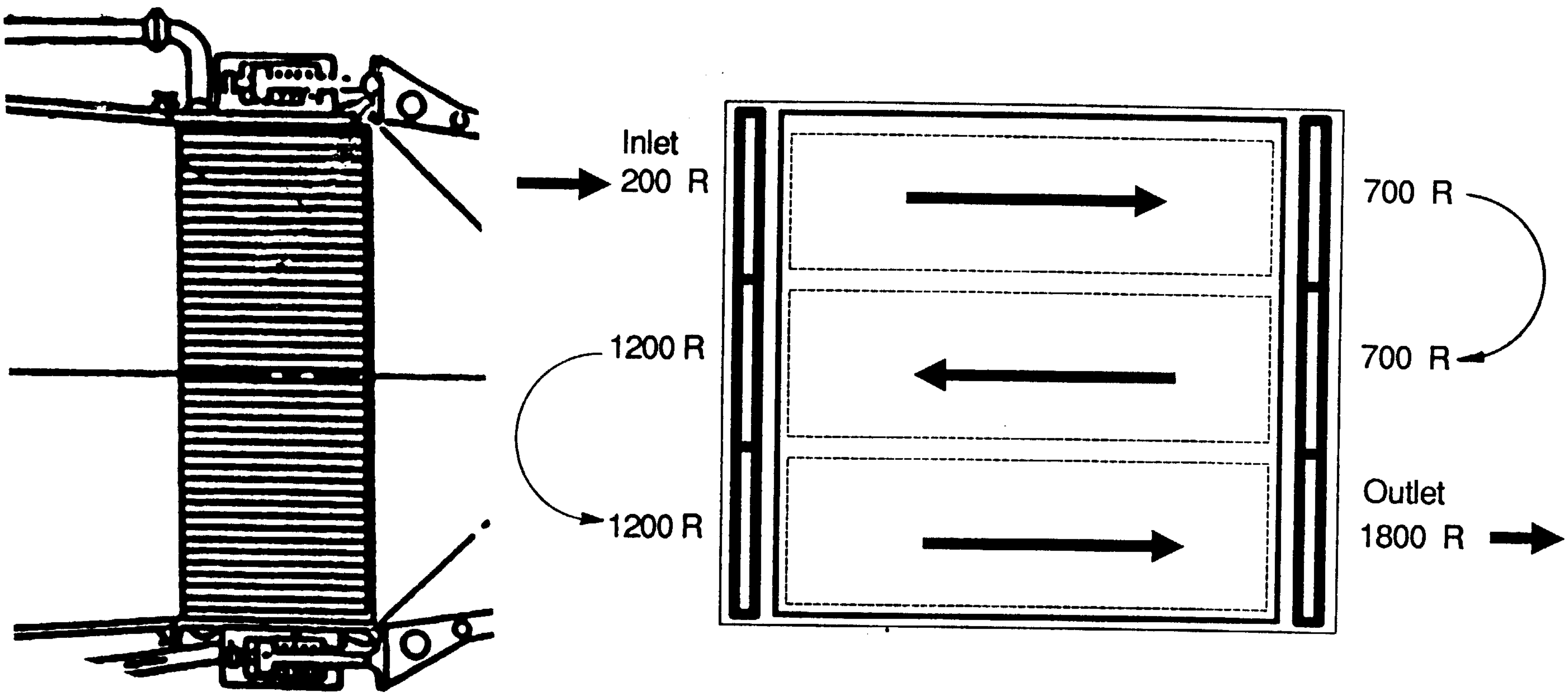

- Reduces Thermal Stresses

Figure 5.1.7 Multipass Ceramic Regenerator for ATR

Initially, this design incorporated two sets of manifolds. The lower manifolds had inlets and outlets for 1 out of 5 channels, while the upper manifolds had inlets and outlets for 4 out of 5 channels. During cruise operation, when the methane flow rate is 7.7 lb/sec, the coolant is directed to the lower manifold only. During SLS, both the upper and lower manifolds were to have flow. Single regenerator vane concepts for this type of ATR regenerator are seen in Figure 5.1.8. All of the channels would be flowing during take-off, but only those at the leading edge and in the center would be flowing during cruise. The final result of the conceptual analysis is the prototype cross flow ceramic regenerator vane shown in Figure 5.1.9. This vane was conceptually designed to permit evaluation of the temperatures, thermal gradients, and fuel compatibility. The variable channel sizes are required to obtain nearly equal methane exit bulk temperature from each of the channels. The straight through design simplified the channel design and analysis since all the coolant flow paths are the same length. A regenerator design model was used to determine the channel sizes by balancing the channel pressure drop, bulk temperature rise, and energy input to each channel.

This prototype ceramic regenerator vane design can be extended to actual ATR operation using a multi-pass design, i.e., increase methane temperature from 200 R to 1800 R in three passes through the combustion section as shown in Figure 5.1.7. The multi-pass arrangement is intended to reduce the thermal stresses due to thermal gradients within the vane.

5.2 MATERIAL SELECTION

A survey of ceramic material systems and vendors was conducted to determine the appropriate material and vendor for the fabrication of the regenerators. Initially, the material focus was on reaction bonded silicon nitride (RBSN) and reaction sintered silicon carbide (RSSC) for thermal shock reasons but was expanded to include other candidate materials. The survey list is shown in Table 5.2.1. Ultimately, two silicon nitride systems were chosen for further study, sintered silicon nitride (SSN) and RBSN.

A comparison of the thermal and engineering properties of silicon nitride with state-of-the-art metallic materials, such as titanium (6Al-4V), aluminum (6061), beryllium, and stainless steel (CRES 347), is shown in Figure 5.2.1. Silicon nitride has a density comparable to aluminum, a thermal conductivity twice that of stainless steel, and a melting temperature which exceeds stainless steel by nearly 850 F. The elevated temperature strength of silicon nitride is superior to all these metals when measured by the strength to weight ratio, Table 5.2.2.

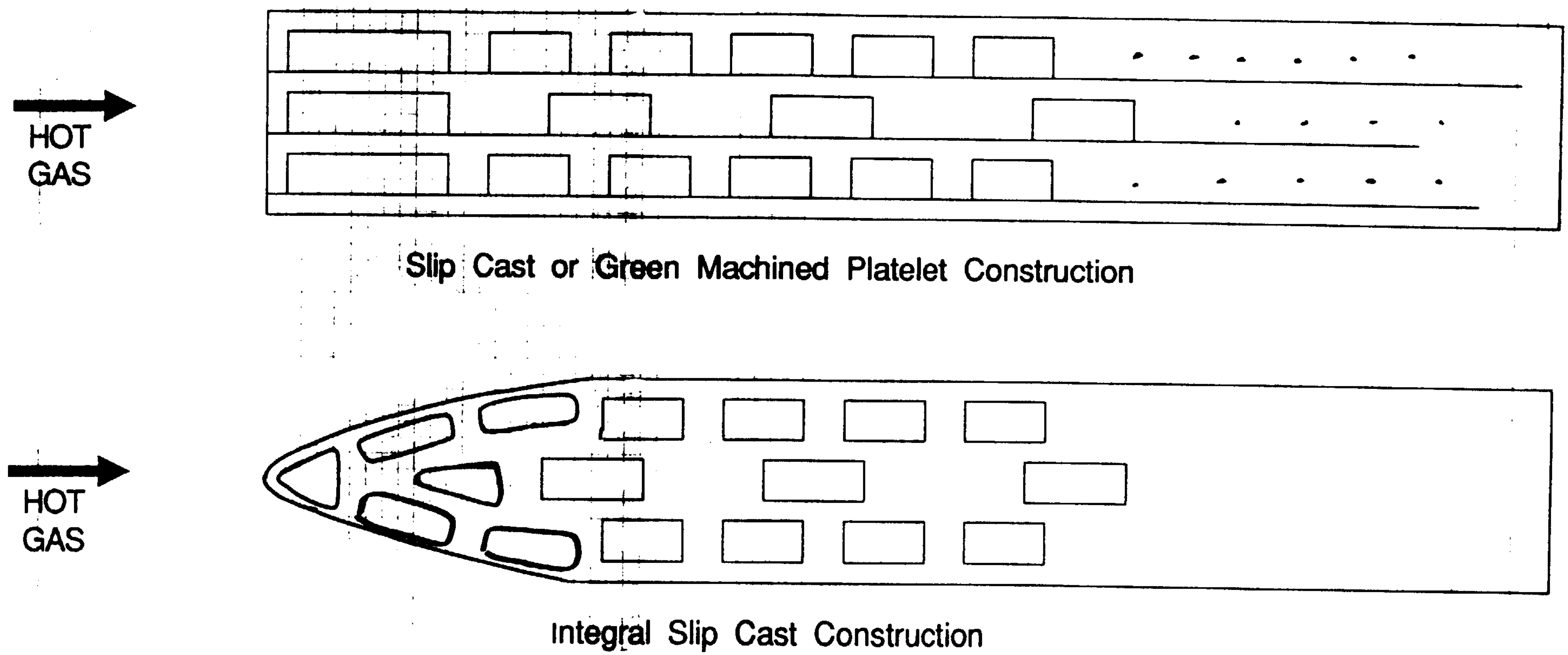

Figure 5.1.8 Layered Ceramic Vane for Single Regenerator ATR

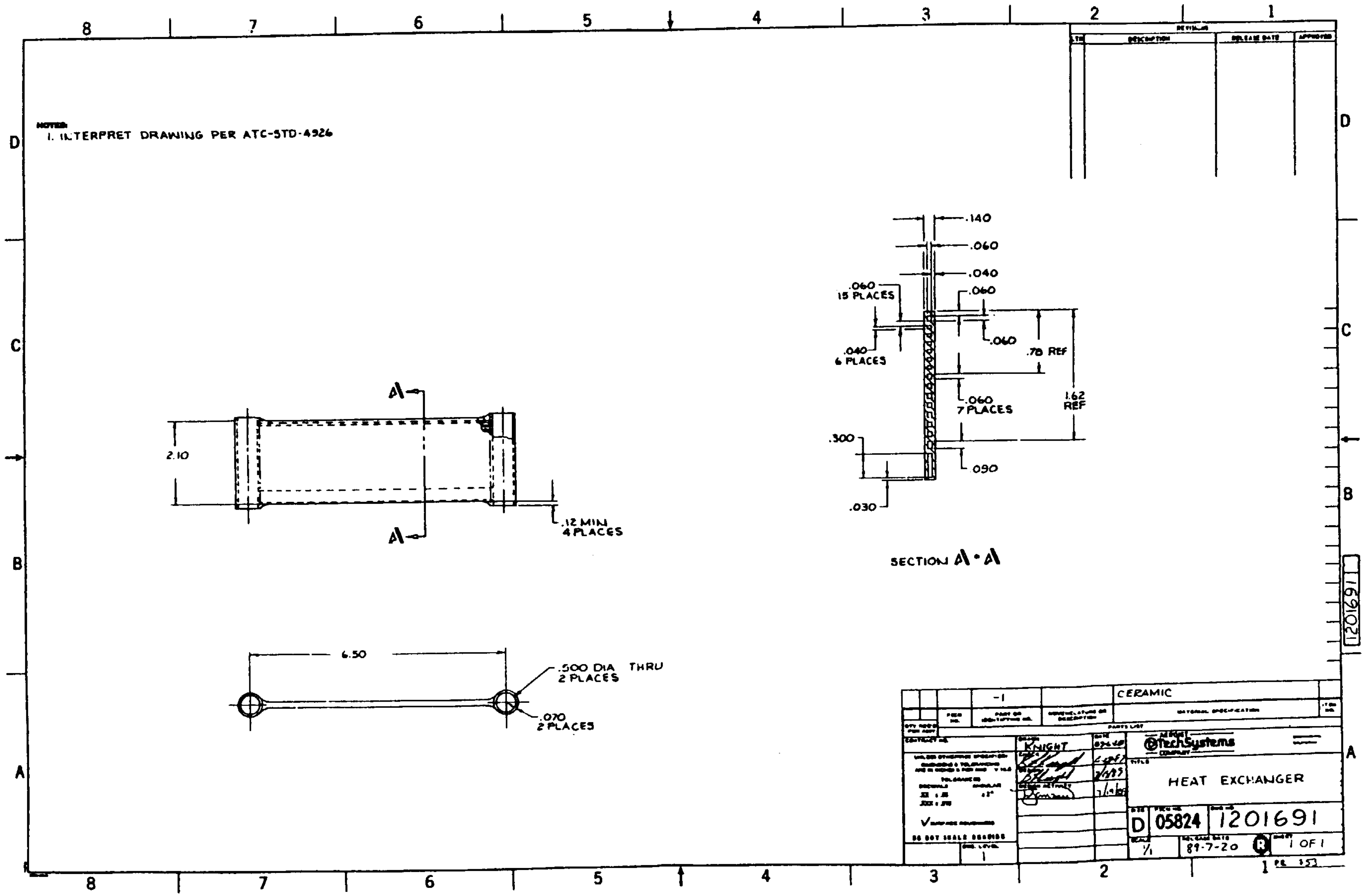

Figure 5.1.9 Ceramic Regenerator Vane, Current Design

TABLE 5.2.1

MATERIALS DATA (PRELIMINARY)

	Flex Strength, ksi	Thermal Expan., 10E-6/°C	Thermal Cond., W/m°K(RT)	Density, g/cc	Porosity %	Max. T (Air) °F
Reaction Sintered SiC						
Cercom ISD SiC-LG	35	4.5	---	3.05	0	---
Sohio KT (+Si)	40	5.04	129.7	3.09	---	2500
Sohio (KG (+Si+C))	7	4.50	112.4	2.70	---	1500
Sintered SiC						
Sohio SA	67	4.02	125.6	3.10	---	3000
Cercom "PAD"	78	4.5	108	3.14	---	---
Sintered Si3N4						
Cercom "PAD", CI	132	---	---	3.31	---	---
Kyocera, SN-220	86	3.2	16.7	3.2	<0.1	---
Reaction Bonded Si3N4						
Cercom	45	3.0	9-12	2.5	18-25	---
Reaction Bonded SiC						
Coors SCRB-2	75	3.0	124	3.10	---	2460
Nitride Bonded SiC						
Coors SCNB-19 (73SiC-24Si3N4-3 Oxides)	6.7	2.4	15.9 (1000 C)	2.65	---	2900
Oxides						
Zirconia, MgO P.S.						
Coors	60	2.7	---	5.4	---	---
Corning	65	3.9	2.0	5.5	---	---
Mullite (Coors)	27	3.7	4.1	2.82	---	3100
Alumina, Coors, AD-999	80	6.5	39.8	3.96	---	3450
Alumina, Ceramatec, CA-90	49	6.1	16.7	3.60	---	2730
Cordierite, Kyocera, C-600 (2MgO-2A12O3-5SiO2)	---	0.5	1.3	1.5	27	2190
Spinel, Kyocera, P-2101 (MgO.A12O3)	21	8.1	1.7	3.3	0	2012
Steatite, Kyocera, S-211	23	8.1	3.8	3.1	0	1832

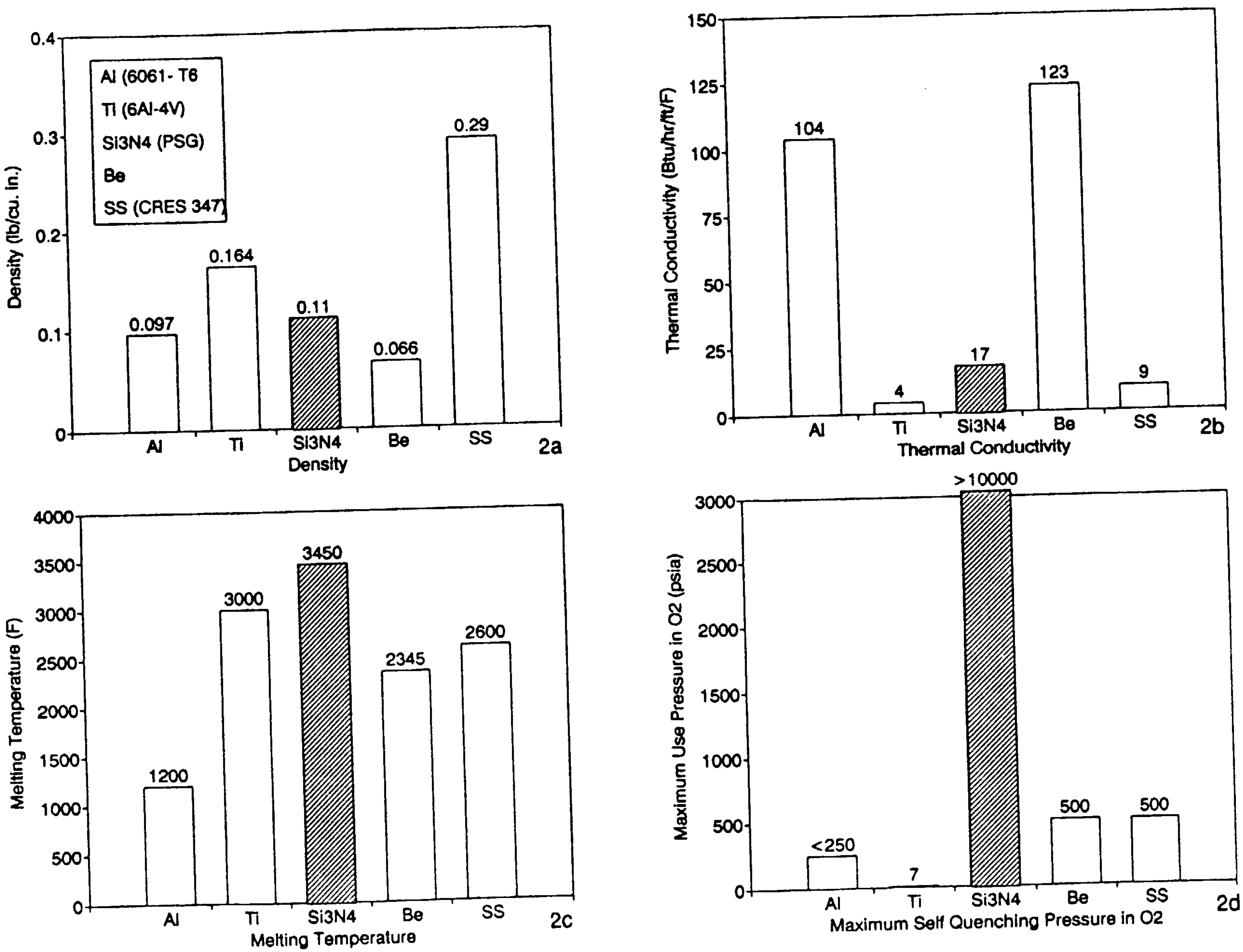

Figure 5.2.1 Silicon Nitride Provides Lightweight, High Thermal Design Margin and is Not Ignitable in High Pressure O_2

TABLE 5.2.2. COMPARISON OF STRENGTH TO WEIGHT RATIOS OF SILICON NITRIDE WITH OTHER ENGINEERING MATERIALS

Material	Si_3N_4	Al	Ti	Be	347 SS
	4 pt	6061	6Al-4V		
RT	840	459	812	552	260
1000°F	840	--	440	360	170
2000°F	830	--	--	--	20
2500°F	550	--	--	--	--

UTS/Density (ksi/lbm/in.^{3})

The silicon nitride material selected to be used in the fabrication of the regenerators was obtained from Cercom, Inc. of Vista, California. Their sintered material, PSG (Pressureless Sintered Glass) silicon nitride is a fully-dense, pressureless sintered ceramic specifically compounded to yield an amorphous intergranular phase. To produce the amorphous phase, 6% yttria (Y_2O_3) and 3% alumina (Al_2O_3) are added to the silicon nitride powder as a sintering aid. Pressureless sintering allows for net shape forming of complex components without the need for high pressure induced shear forces. Typical mechanical and physical properties are shown in Table 5.2.3. The material is isotropic as related to engineering properties and has been demonstrated to have excellent thermal shock resistance compared to many other ceramics, Figure 5.2.2.

TABLE 5.2.3. TYPICAL PROPERTIES OF PSG SILICON NITRIDE

Property	Value
Bulk Density (lb/in.^{3})	0.118
Hardness (45N)	88
Fracture Toughness (ksi in.$^{1/2}$) (ksi in.$^{1/2}$)	5.18
Characteristic Strength (RT, 4 pt, ksi)	109
Weibull Modulus	18
Elastic Modulus (MOE) (MPsi)	44
Poisson's Ratio	0.24
Thermal Expansion (10-6/F) (RT-1832 F)	1.9
Thermal Conductivity (Btu/hr/ft/F)	17.0
Thermal Shock Factor (Tc,F)	1215

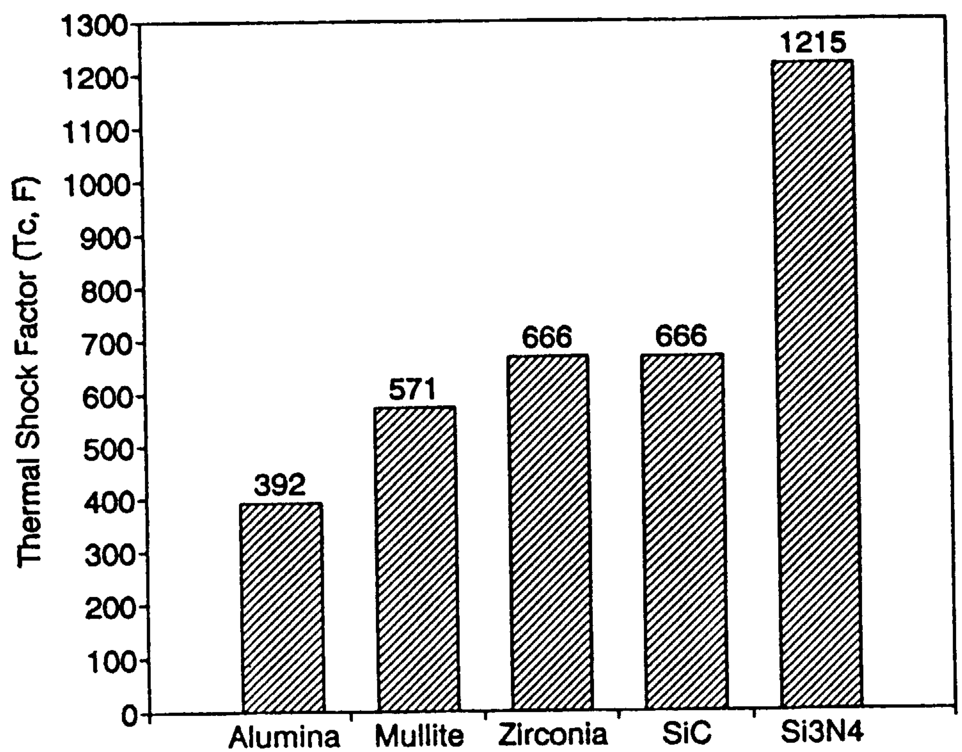

Figure 5.2.2 Silicon Nitride Has a Higher Thermal Shock Capability Than Many Other Ceramics

The reaction bonded silicon nitride has the same sintering aids (6% yttria and 3% alumina) added to silicon metal powder. This material does not produce the amorphous phase and therefore has a higher use temperature. This system was the preferred system due to less shrinkage and higher temperature capabilities.

5.3 FABRICATION PROCESSES.

5.3.1 Slip Casting

Initially slip casting was to be the primary process for the fabrication of the regenerator vanes and doctor blade/tape casting a secondary fabrication method. In the slip casting approach, leachable cores were to be bonded together and a slip cast around the integral unit within a plaster mold, Figure 5.3.1. Once the green slip has dried, the cores are leached away and the ceramic fired for densification. Initial experiments with the slip casting process were not successful. Slips were poured around 0.030 in diameter molybdenum wires to see if the wires could be removed after the slip had dried. All the slips cracked early in the drying process due to excessive green shrinkage. With these experiments and the success of the tape casting, the slip casting fabrication method was abandoned.

5.3.2 Ceramic Tape Cast Platelet Technology

The secondary fabrication method, which resulted in early success, was tape cast platelet construction. In this method of fabrication, the components consist of multiple laminated layers of ceramic material which contain intricate internal hydraulic passages. The process was developed jointly by Aerojet, Cercom Inc. of Vista, California and Coors Ceramics Co. of Golden Colorado. A flow chart illustrating the ceramic platelet fabrication process is shown in Figure 5.3.2.1. The technologies utilized in this process involve tape casting of the ceramic material, numerical controlled punching of the green tapes, green bonding or laminating and a burn-out cycle followed by a sintering operation.

The tape casting process begins with the formulation of the ceramic or silicon metal powders. In the PSG silicon nitride and the RBSN tape manufacturing process, yttria (Y_2O_3) and alumina (Al_2O_3) powders are added to the silicon nitride or silicon metal respectively. These oxides act as sintering aids and produce an amorphous (glassy) second phase in the PSG material but not in the RBSN. The mixture of powders is then wet ball milled. When the correct surface area of the powder is achieved the binder, plasticizer and deflocculant are added and the rheological properties of the slurry adjusted as needed. As a base line, polyvinylbuteral is added as a binder, K126 as a plasticizer and fishoil as a deflocculent for the

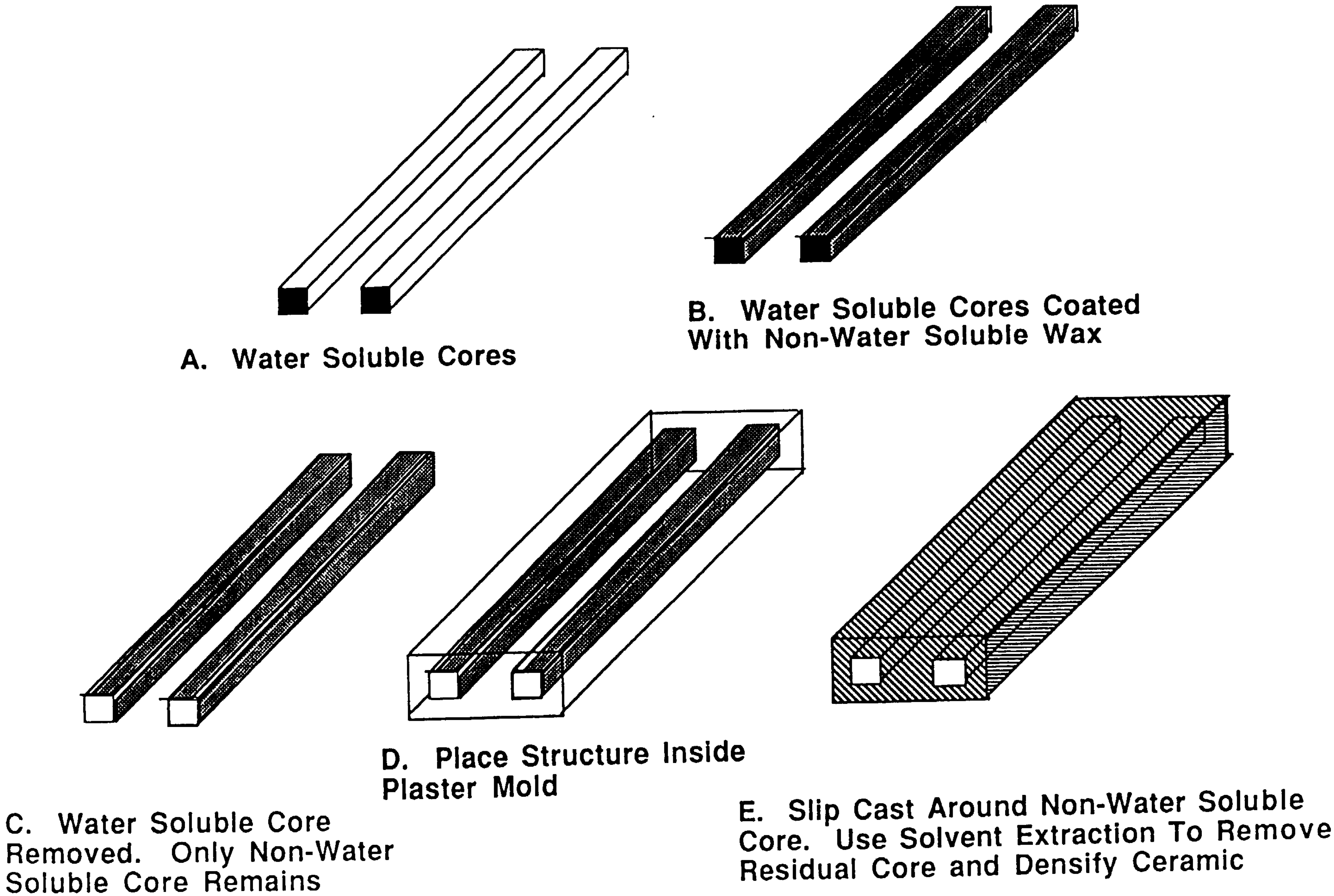

Figure 5.3.1 Flow Sequence to Produce Integral Cast Regenerator Vane

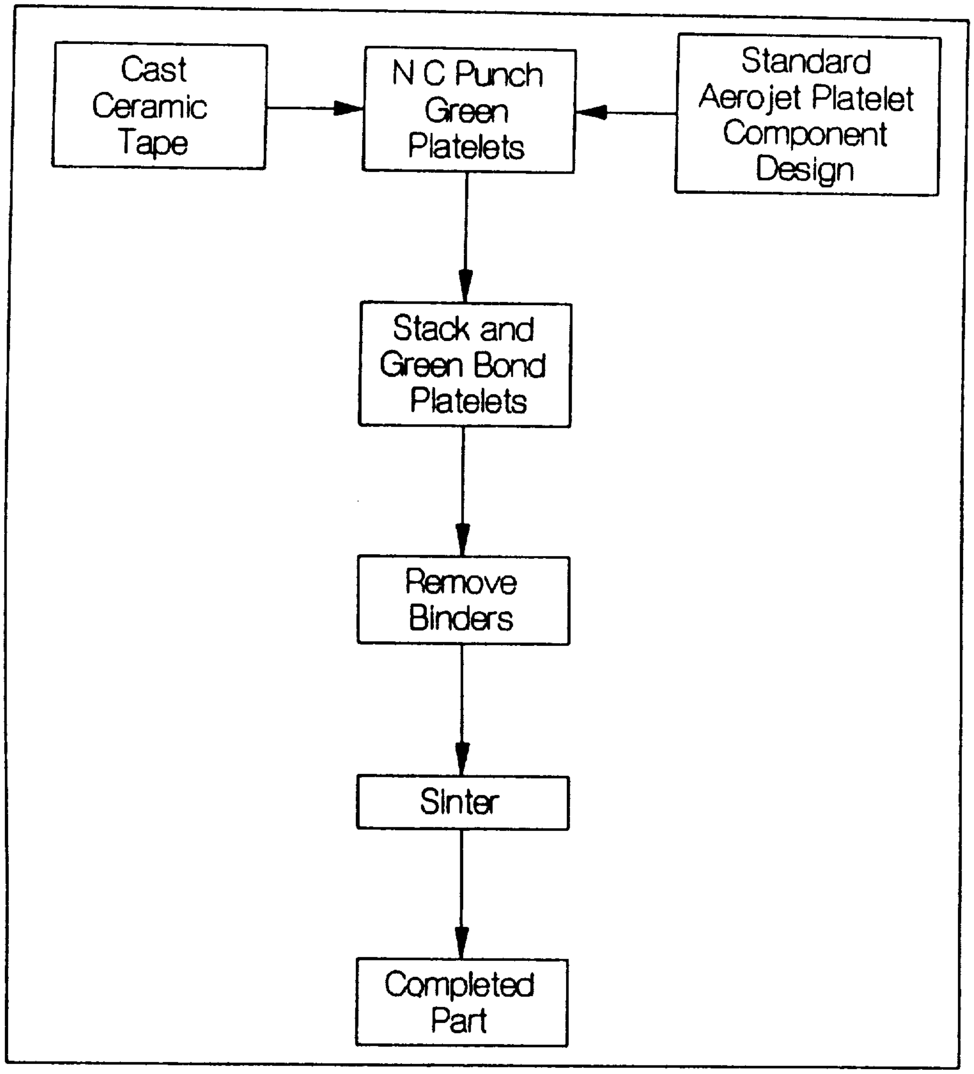

Figure 5.3.2.1 Flow Diagram of Ceramic Platelet Fabrication Process

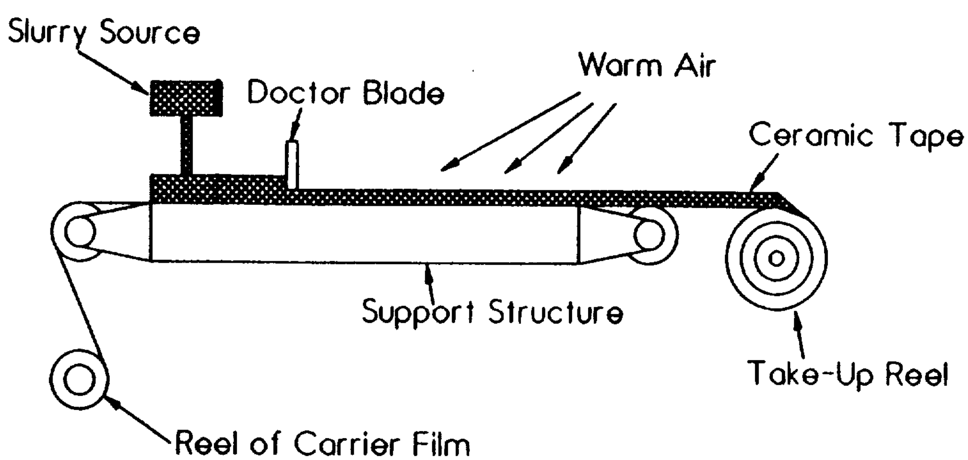

Figure 5.3.2.2 Tape Casting Process Uses a Doctor Blade and Continuous Reel of Mylar to Form the Green Ceramic Tape

PSG material. For the RBSN polyproylene carbonate binder and plasticizer are added. The binder contents are then adjusted to the powder size/surface area.

Once the slurry has been formulated the tape is cast using a doctor blade process. Figure 5.3.2.2 shows a schematic of the tape casting process. Mylar carrier film is laid over a support structure and attached to a take up reel. Above the mylar, the doctor blade is positioned to spread the slurry across the film. The height of the blade determines the thickness of the slurry which flows onto the mylar film. As the carrier film moves from the supply reel to the take-up reel over the support structure the ceramic slurry is spread over the film by the doctor blade. Moving away from the doctor blade the slurry is dried by warm air. The dried tape is then wound up on the take-up reel. Tape can be produced in 12 in. widths, 0.005 to 0.030 in. thick. The control of the thickness by the positioning of the doctor blade and the evaporation rate of the drying tape are the main process control parameters during tape fabrication. During tape casting development the PSG tape was the first material successfully cast. It was this material which was used for the remainder of the program.

Standard Aerojet metal platelet design techniques are used to engineer the individual platelets used in the design. When the design is finalized a numerically controlled punch is programmed and the green tape punched with the desired pattern.

Once the platelets are punched with the correct patterns a stacking and laminating schedule is developed and the components assembled for green bonding or lamination. The lamination is performed at about 5.5 MPa (800 psi) and 65 C (150 F).

After the platelets are green bonded the parts are burned-out at 650 C (1200 F) in a nitrogen atmosphere to remove the binders. The brown parts are then sintered at 1775 C (3200 F), to consolidate the parts to almost 100% dense.

This process lends itself to the fabrication of ceramic structures with intricate internal passages.

6.0 TECHNICAL DISCUSSION

6.1 REGENERATOR DESIGN

6.1.1 Thermal Analysis

A preliminary thermal analysis of the baseline regenerator shown in Figure 5.1.9 was preformed verify normal operating condition, i.e., gas side wall temperature (T_{wg}) and coolant velocity (v), for a maximum inside wall temperature of 1400 F. A temperature of 1400 F is specified as the limit to prevent thermal decomposition of the methane. A one dimensional, thermal-hydraulic model of the regenerator vane, including temperature dependent thermal conductivities, was used for the analysis.

Figure 6.1.1.1 shows the variation of wall temperature gradient as a function of heat flux for selected wall thickness of silicon carbide and silicon nitride for a fixed inside wall temperature of 1400 F. The predicted gradients indicate that the "normal" maximum vane surface temperature is 1450 F for silicon carbide and 1500 F for silicon nitride with a 0.015 in. thick wall. The temperatures at the corners of the leading edge of the vane are expected to exceed this value.

The gas side boundary condition for SLS, cruse and a test cell condition are summarized in Table 6.1.1.1, assuming a 5% blockage factor, i.e., regenerator frontal area divided by total flow area. At cruise conditions, the average gas side heat transfer coefficient is approximately 75% of that at SLS. In order for the single regenerator concept to work, i.e., maintain the coolant side wall temperature at or below 1400 F and achieve an exit temperature of at least 1340 F at both SLS and cruise condition, the total heat input to the regenerator must scale with the total coolant mass flow rate at SLS and cruise conditions. The mass flow rates vary by a factor of four, therefore, the total heat input must also vary by a factor of four. The decrease in heat input during cruise operation is achieved by two mechanisms. First, the lower heat transfer coefficient at the cruise condition accounts for approximately a 25% reduction in the heat input from SLS to cruise conditions. Second, the remaining heat input reduction is achieved through elevated regenerator mean surface temperature which reduces the surface heat flux during cruise operation.

A thermal hydraulic analysis was conducted to size the channels of the preliminary design. Figure 6.1.1.2 shows the methane exit temperature and average velocity for the prototype silicon nitride regenerator. The expected operating range for the 16 channel design,

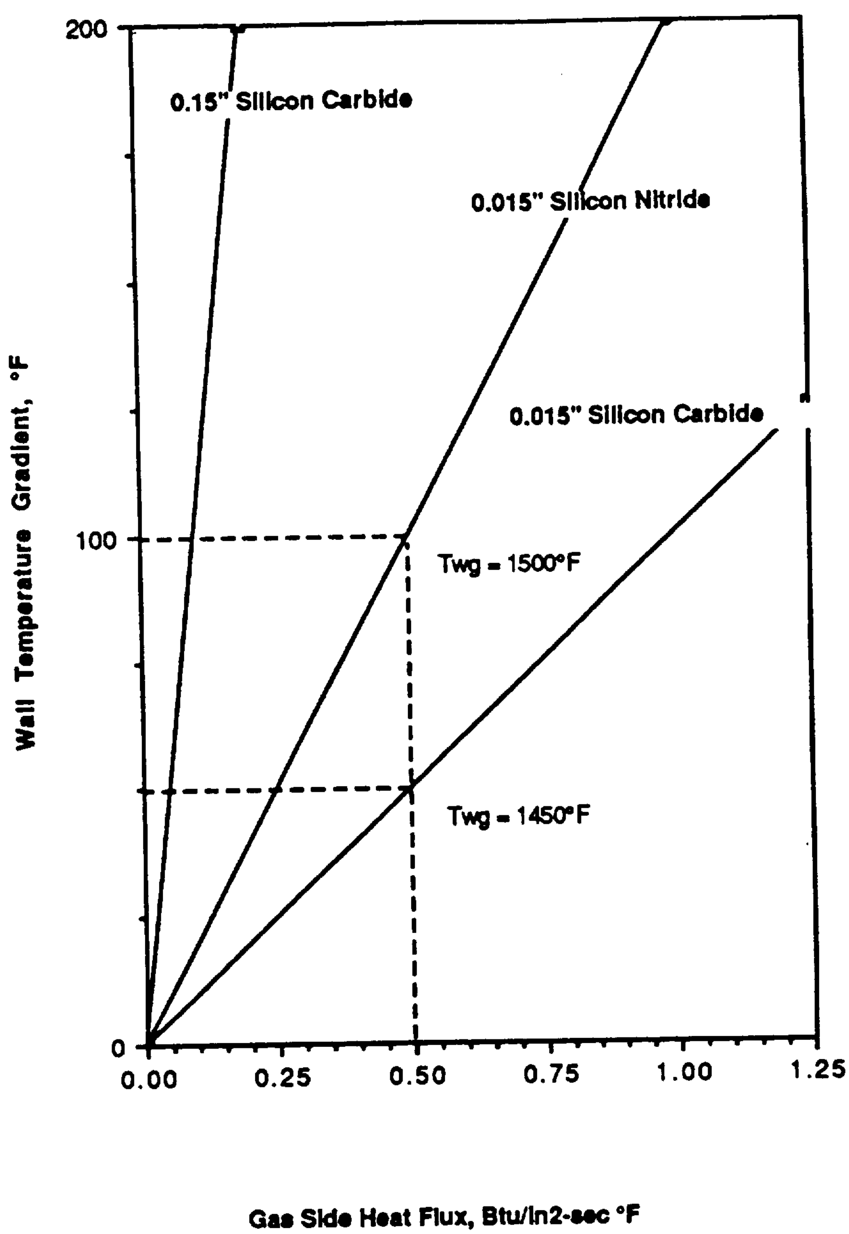

Figure 6.1.1.1 Variation of Wall Temperature Gradient With Gas Side Heat Flux for Candidates Thickness of Silicon Carbide and Silicon Nitride

TABLE 6.1.1.1

CERAMIC HEAT EXCHANGER GAS SIDE BOUNDARY CONDITIONS

Sea Level Static (SLS)		Mach 5/83 Kft (M5)		Test Cell	
Total Mass Flow	706 lbm/sec	Total Mass Flow	277 lbm/sec	Total Mass Flow	0.3 lbm/sec
T_c	3562 R	T_c	3844 R	T_c	3500 R
P_c	25 psia	P_c	110 psia	P_c	15.5 psia
Density	0.0185779 lbm/ft^3	Density	0.075746 lbm/ft^3	Density	0.011722 lbm/ft^3
Viscosity	0.000042 lbm/ft-sec	Viscosity	0.000045 lbm/ft-sec	Viscosity	0.000043 lbm/ft-sec
Conductivity, k	0.000002 Btu/in.-sec-R	Conductivity, k	0.000002 Btu/in.-sec-R	Conductivity	0.000002 Btu/in.-sec-R
Mole. Wt., MW	28.4 lbm/lbm-mole	Mole. Wt., MW	28.4 lbm/lbm-mole	Mole. Wt., MW	28.4 lbm/lbm-mole
Specific Heat, Cp	0.366 Btu/lbm	Specific Heat, Cp	0.366 Btu/lbm	Specific Heat, Cp	0.373 Btu/lbm
Prandl Number, Pr	0.64	Prandl Number, Pr	0.60	Prandl Number, Pr	0.67
Sonic Velocity, a	2793 ft/sec	Sonic Velocity, a	2901 ft/sec	Sonic Velocity, a	2768 ft/sec
Flow Area	4610 $in.^2$	Flow Area	4610 $in.^2$	Flow Area	8 $in.^2$
% Blockage	5	% Blockage	5	% Blockage	5
Velocity	1250 ft/sec	Velocity	120 ft/sec	Velocity	485 ft/sec
Mach Number, Ma	0.45	Mach Number, Ma	0.04	Mach Number, Ma	0.18
Vane Length	10 in.	Vane Length	10 in.	Vane Length	3 in.
Re_L	460587	Re_L	168665	Re_L	31946
Nu_L	389	Nu_L	230	Nu_L	104
Ave H.T. Coeff.	7.78‰-05 $Btu/in.^2$-sec-R	Ave H.T. Coeff.	5.29E-05 $Btu/in.^2$-sec-R	Ave H.T. Coeff.	7.17E-05 $Btu/in.^2$-sec-R

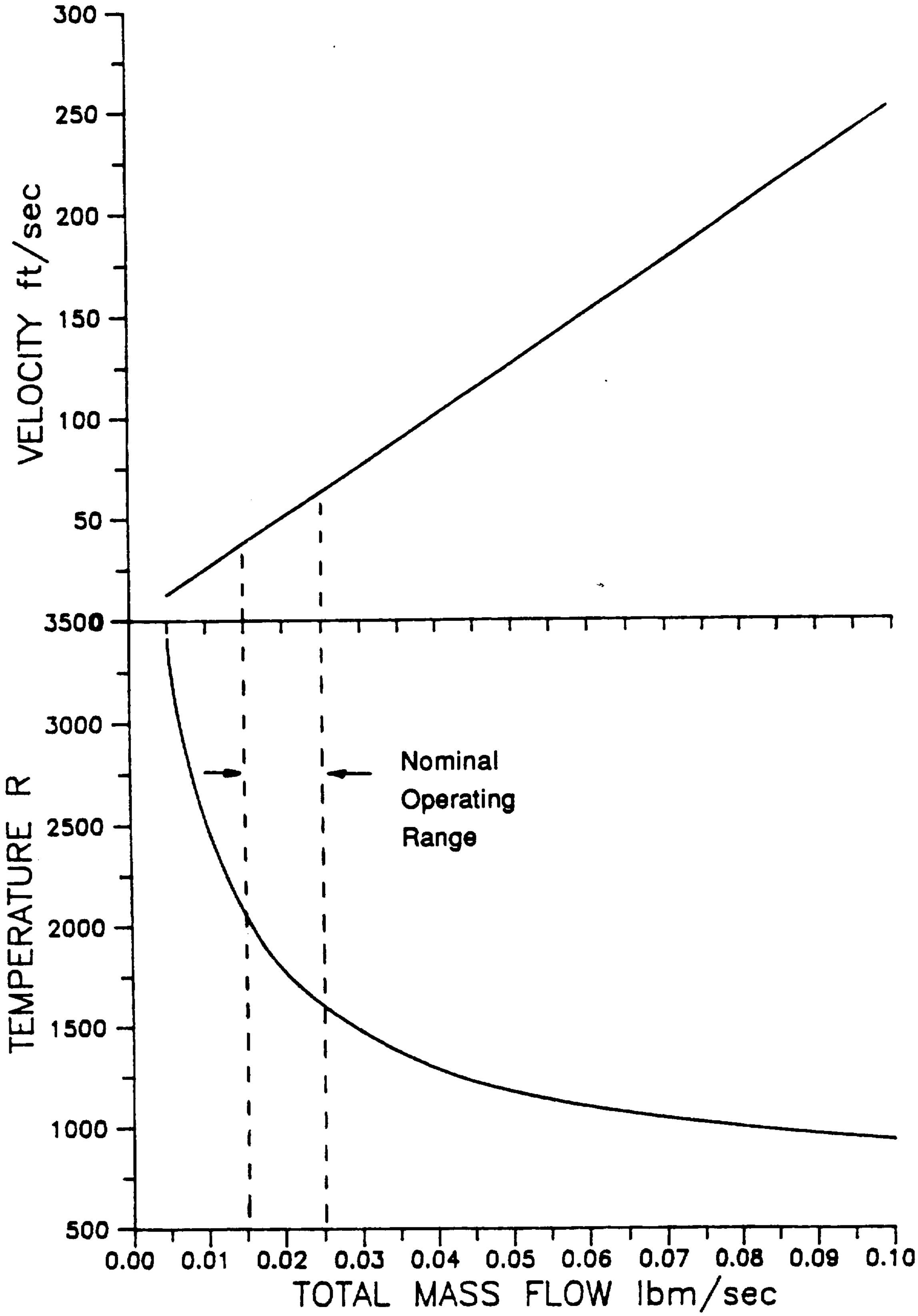

Figure 6.1.1.2 Coolant Velocity and Exit Temperature Calculated From Preliminary Thermal Hydraulic Analysis of Prototype Silicon Nitride Regenerator (16 Channels, 0.06 x 0.12")

shown in Figure 5.1.4, are temperatures between 1700 and 2050 F and coolant velocities between 30 and 65 ft/sec for a total mass flow of 0.015 to 0.025 lbm/sec. The test cell gas side boundary conditions in Table 6.1.1.1 were used and an inlet temperature of 660 F was assumed.

During SLS conditions with all channels flowing, a maximum temperature of less then 1540 F at the leading edge is expected. A finite element analysis using the ANSYS code was performed for cruise conditions with only one out of five channels flowing. A plot of the temperature distribution in the vane is shown in Figure 6.1.1.3. this shows the maximum temperature over the closed off channels to be 2550 F, within the temperature capability of the selected materials. This analysis assumed a constant average heat transfer coefficient typical of the leading edge region based on the flow rate, density, and velocity of the combustion gas a cruise conditions. Figure 6.1.1.4 shows the variation of the local heat transfer coefficient in the region of the leading edge for SLS and cruise conditions.

As can be seen from Figure 6.1.1.4, during cruise operation the coolant side wall temperature in channels not flowing will exceed 1400 F, the decomposition temperature of methane. An analysis of the effect of coking trapped methane in the channels assuming complete conversion of methane to soot, (CH_4 ----> $C_{(s)}$ + H_2) was conducted. At 30 psi (normal coolant pressure at cruise conditions) a 15% reduction of flow area occurs after approximately 100 cycles. If the cooled channels are vented to 5 psia, a 15% reduction occurs after 600 cycles. Assuming only one cycle per flight, the coking question would need to be addressed if the engine life is 5000 cycles. The regenerator could be changed out, assuming the weight savings of going from two to one regenerator is greater than the additional cost of 10 regenerators per engine. An alternative is to service the regenerator with warm hydrogen periodically to reverse the decomposition reaction and "clean" the regenerator channels. The estimate performed has assumed complete conversion, the actual conversion is rate dependent and, therefore, it is possible that coking may not limit the service life of the regenerator.

6.1.2 Structural Analysis and Vane Design

A 3D thermal and structural analysis was performed on the prototype regenerator vane assembly, Figure 5.1.9. Figure 6.1.2.1 shows the geometry of the model and temperatures assumed for the input into the PATRAN/PTHERMAL computer codes for thermal analysis. For these inputs a solid ceramic vane with tubular manifolds was assumed for simplicity. The temperatures assumed are consistent with the preliminary thermal analysis performed in 2D.

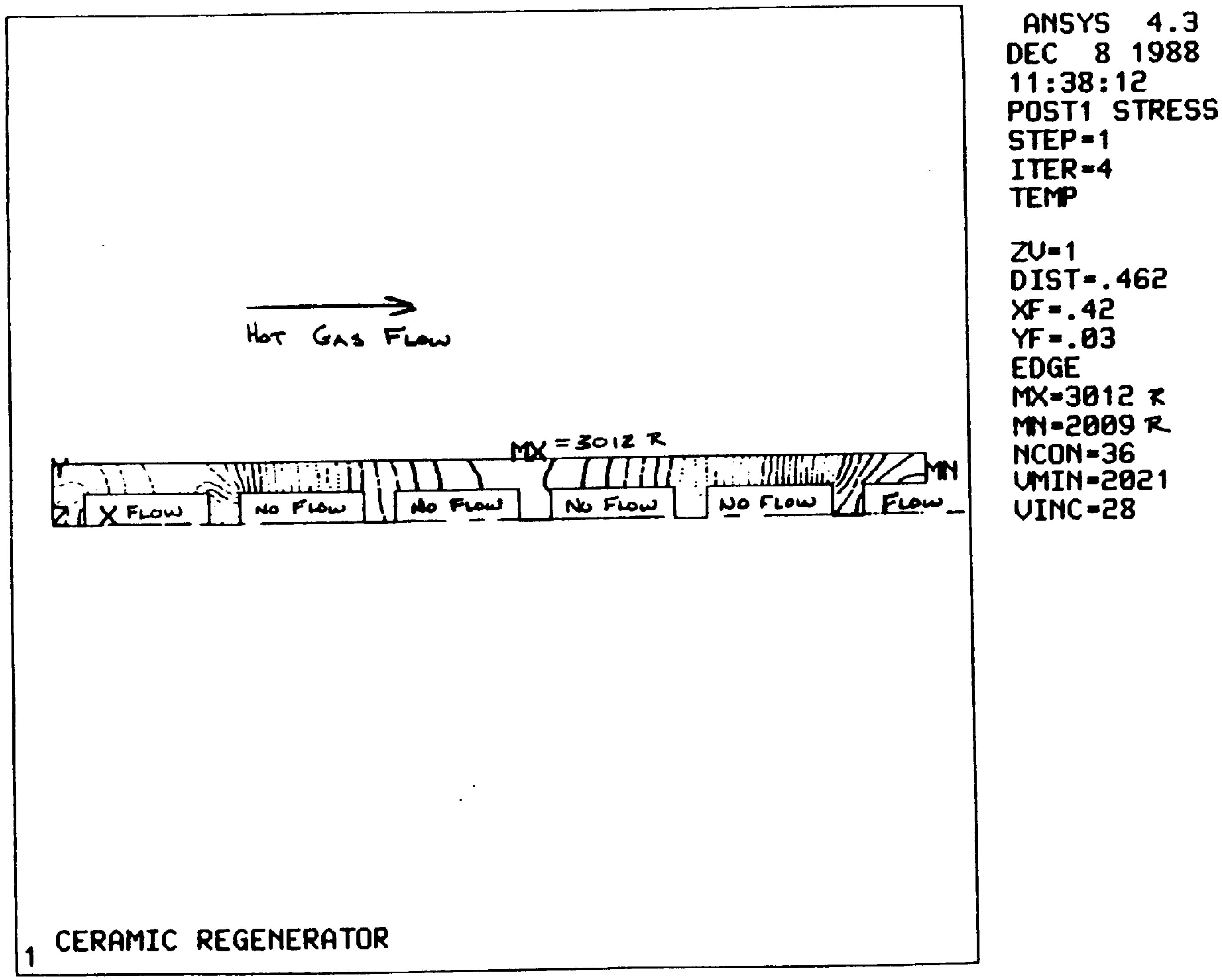

Figure 6.1.1.3 2-D ANSYS Finite Element Model of Cruise Condition (Worst Case)

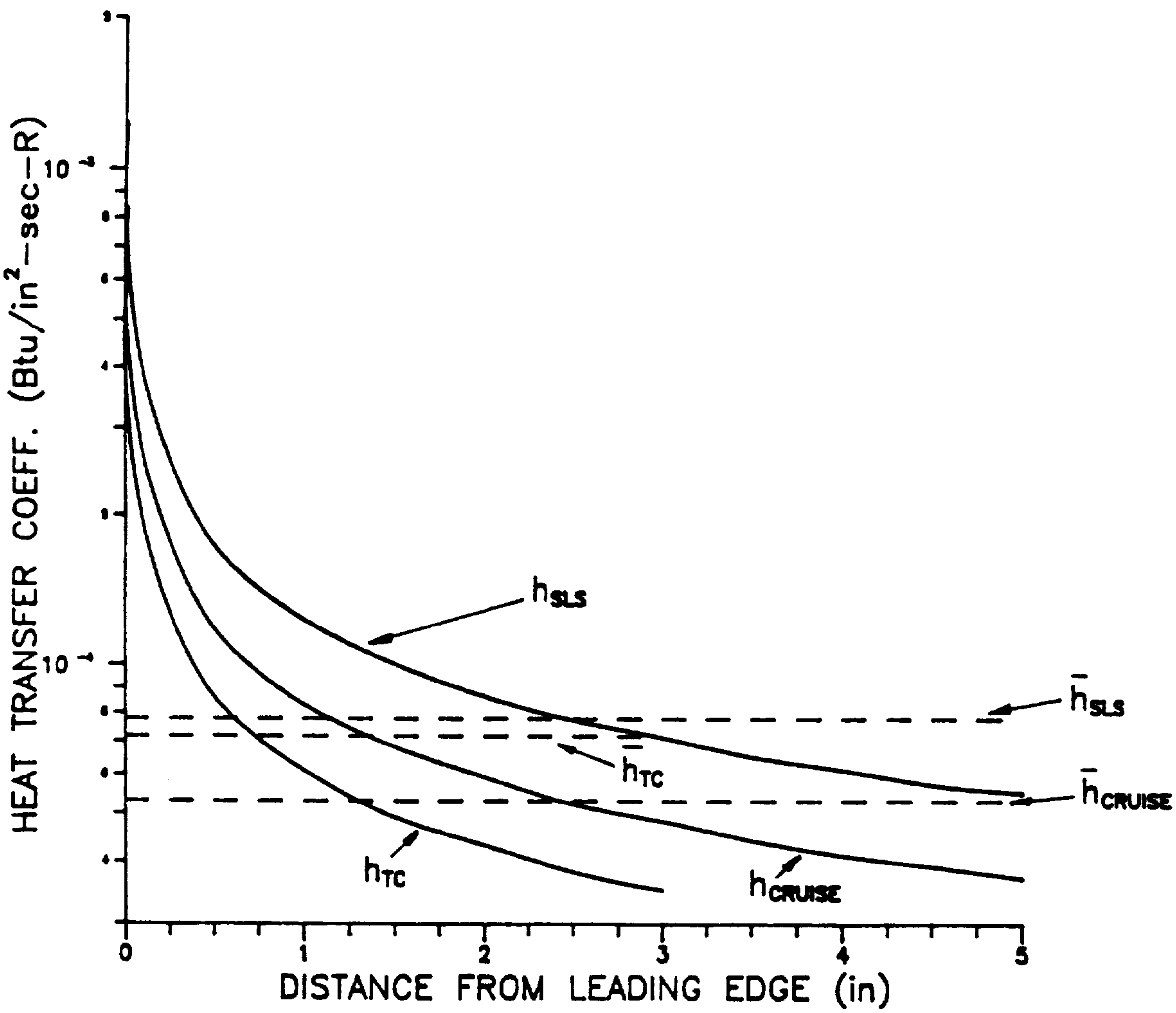

Figure 6.1.1.4 Variation of Local Heat Transfer Coefficient Near Regenerator Vane Leading Edge for Sea Level Static (SLS), Cruise (Ma=5), and Test Cell Conditions

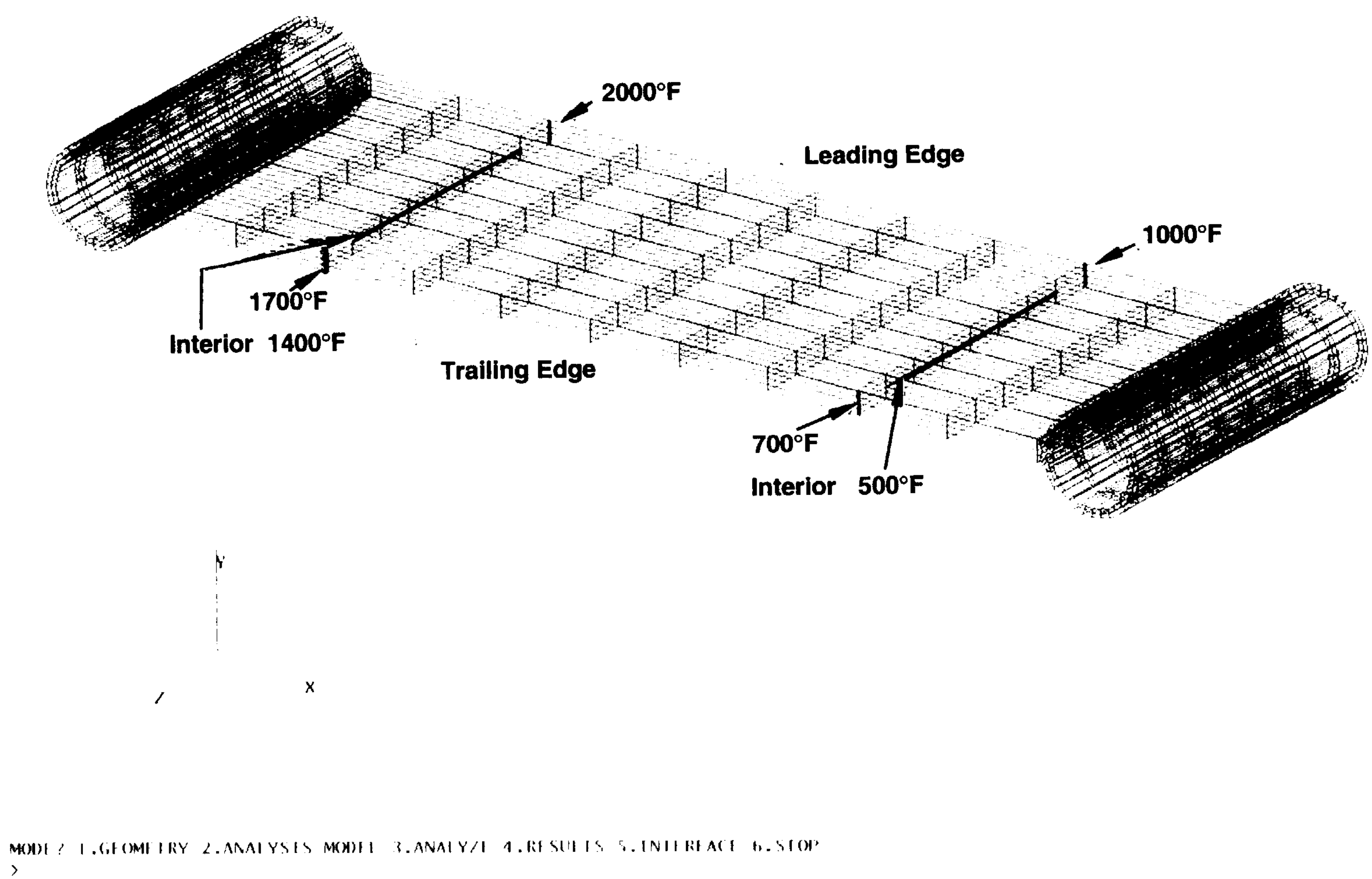

Figure 6.1.2.1 Temperatures Input for 3D Thermal Model

The results of the thermal analysis are shown in Figures 6.1.2.2 and 6.1.2.3 as input into ANSYS. These thermal profiles, together with the expected internal pressures of 640 psi in the manifolds, was input into the ANSYS computer code to determine the resultant thermal and pressure stresses. Figure 6.1.2.4 shows the thermal profile of a cross section at this location and Figure 6.1.2.5 show a profile of the effective stresses. The maximum computed effective stress was 14.6 ksi, located near the plane containing the maximum temperature. This is well below the estimated tensile stress of the PSG silicon nitride of 55 ksi (this is 1/2 of the reported value for 4 pt flexure strength for this material).

6.1.3 Manifold Design Concepts

The initial approach to fabricating the regenerator manifolds from tape was to wrap tape around cylindrical wax mandrels to make tubes and then green bond the tubes to the vane sections, Figure 6.1.3.1. The tubes would then be attached to the edges of the vane by an overwrap of additional tape, Figure 6.1.3.2. Several layers of tape would be required in order to build-up to the 0.070 inch thick manifolds. After overwrapping, the entire assembly is green bonded and then green machined in, order to trim off excess material, Figure 6.1.3.3. After burn out and sintering a metallic tube (Kovar) was to be brazed to each inlet and outlet for attachment to the methane source.

Unfortunately, fabrication of the tubular manifolds by this method proved to be unworkable. Experimental manifolds were constructed in the green state but upon sintering the outside edges of the manifolds cracked and the overwrapped layers delaminated, Figure 6.1.3.4. In addition, the manifolds did not remain round after sintering. Because of this problem, and the issues of sealing the ends of the manifold tubes and the sealing of the transition between the manifolds and the vane, it was decided to reassess the manifold fabrication.

An alternate concept to the manifold fabrication was to layer green tape at the ends of the vane section. The layers would be green bonded and then green machined to form tubular manifolds, Figure 6.1.3.5, similar to those shown in Figure 5.1.9. The layered platelet end structure is shown in cross section in Figure 6.1.3.5b. The base platelet material is 0.016 in. and many layers are needed to achieve a thickness needed for a 0.5 in. manifold. In this configuration 42 layers of material are needed. The vane section is precut and laminated prior to the manifold stack being bonded to it. The regenerator channels extend into the manifolds and when the 0.5 in. manifold is machined into the stack the passages are opened. Figure 6.1.3.5c shows section B-B of Figure 6.1.3.5b, the machined manifold. The ends of the two manifolds are machined round in order to accommodate the Kovar inlet and discharge tubes.

PAGE______INTENTIONALLY BLANK

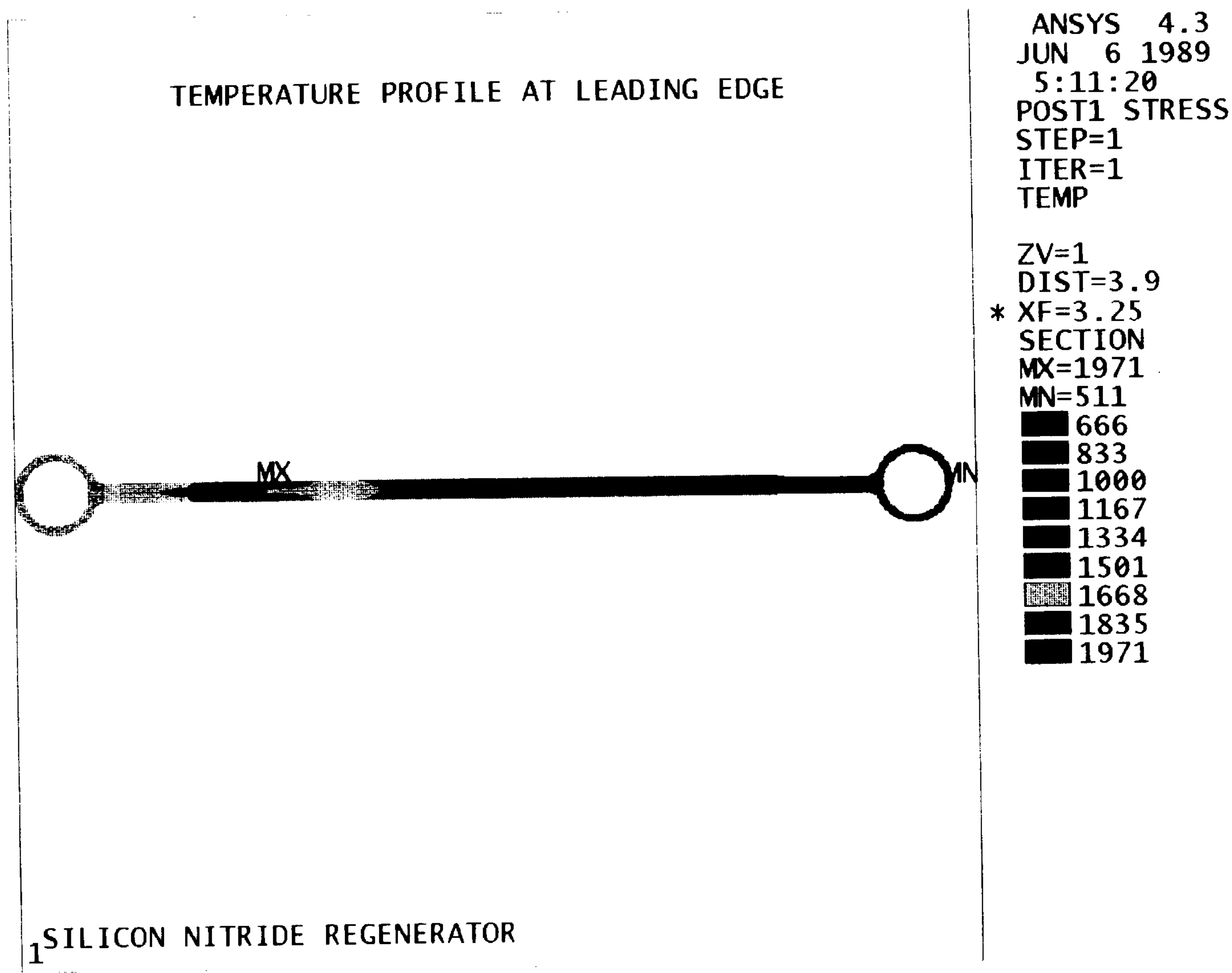

Figure 6.1.2.2 Temperature Profile at Leading Edge

ORIGINAL PAGE
COLOR PHOTOGRAPH

PAGE ____ INTENTIONALLY BLANK

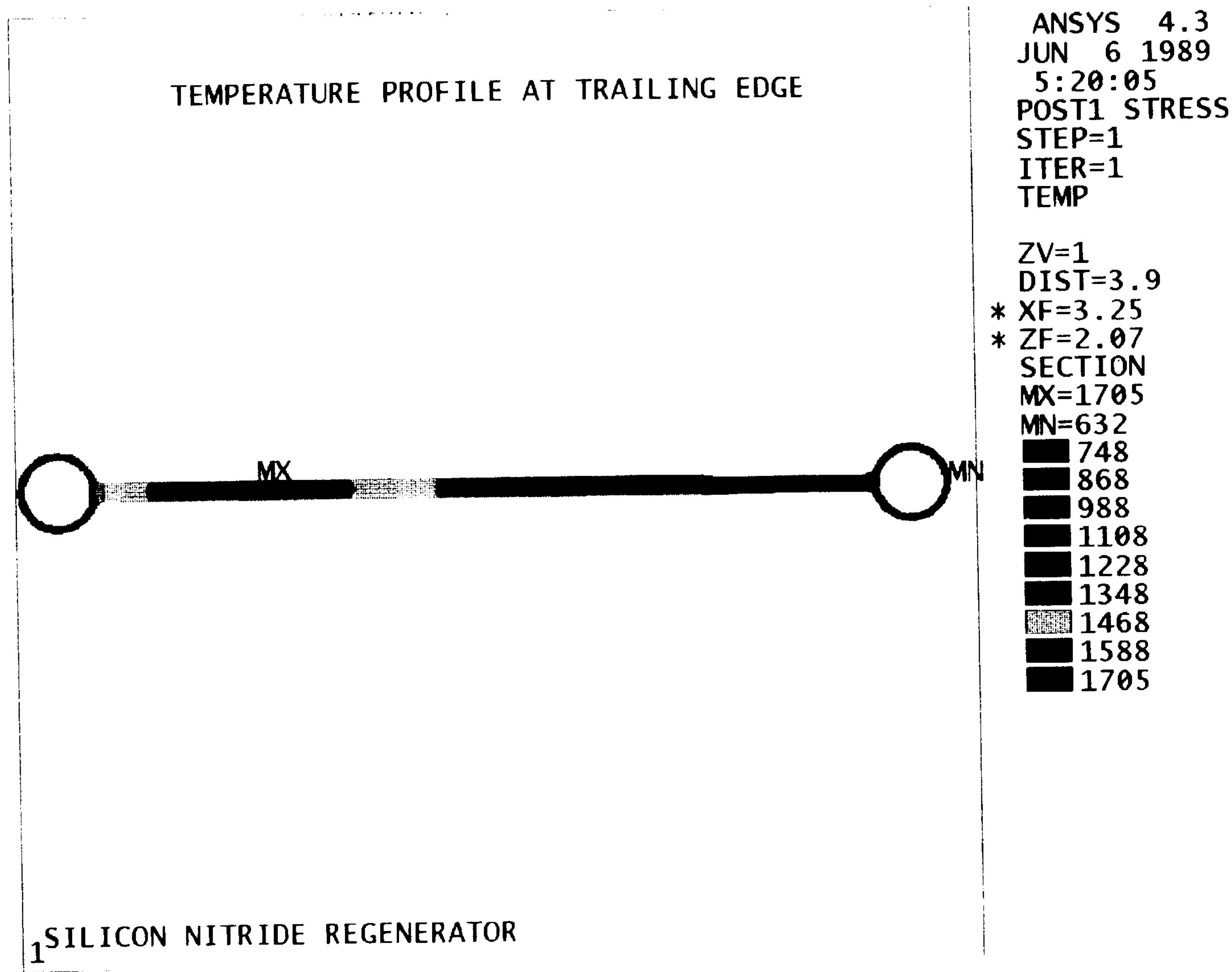

Figure 6.1.2.3 Temperature Profile at Trailing Edge

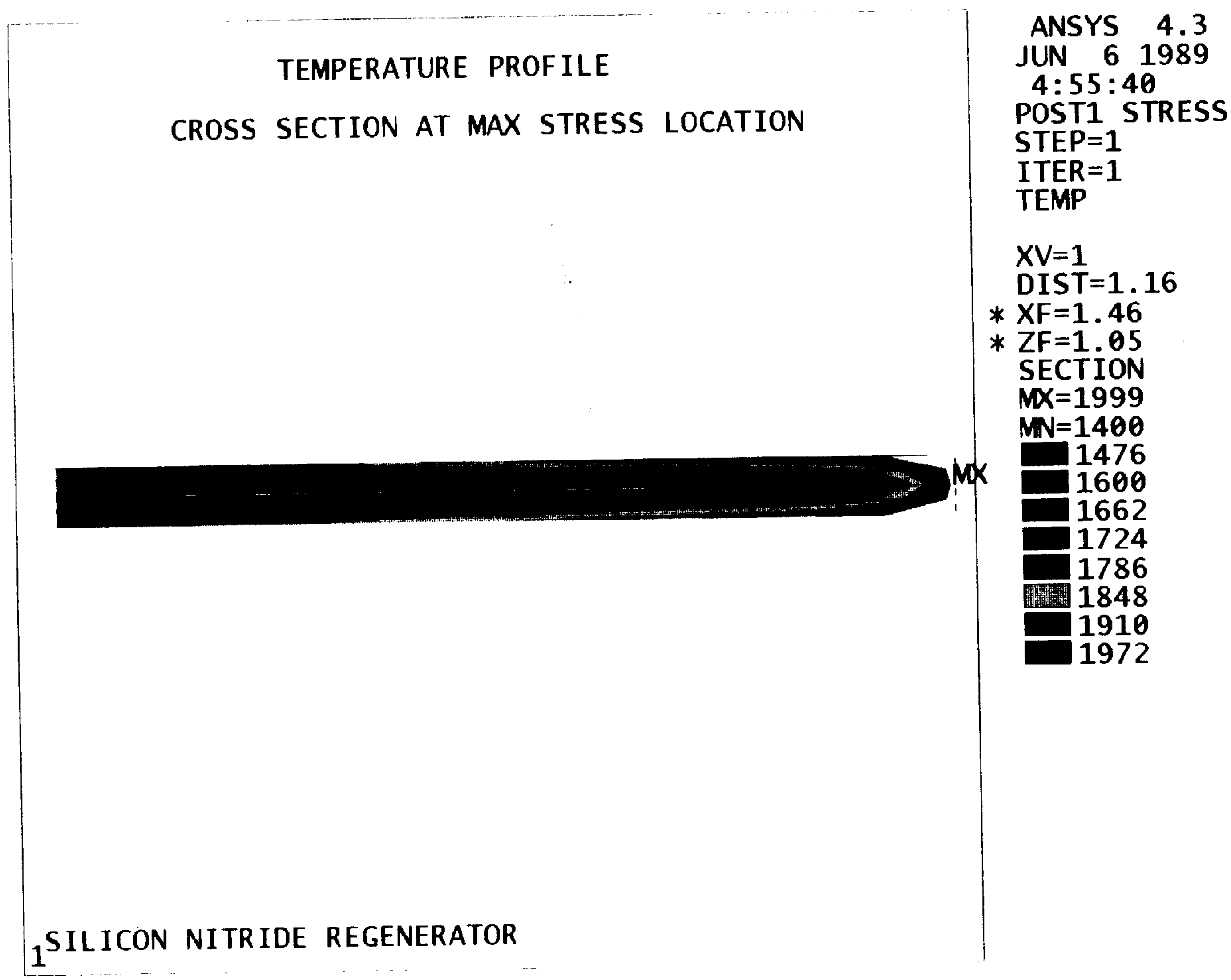

Figure 6.1.2.4 Temperature Profile Cross Section at Max Stress Location

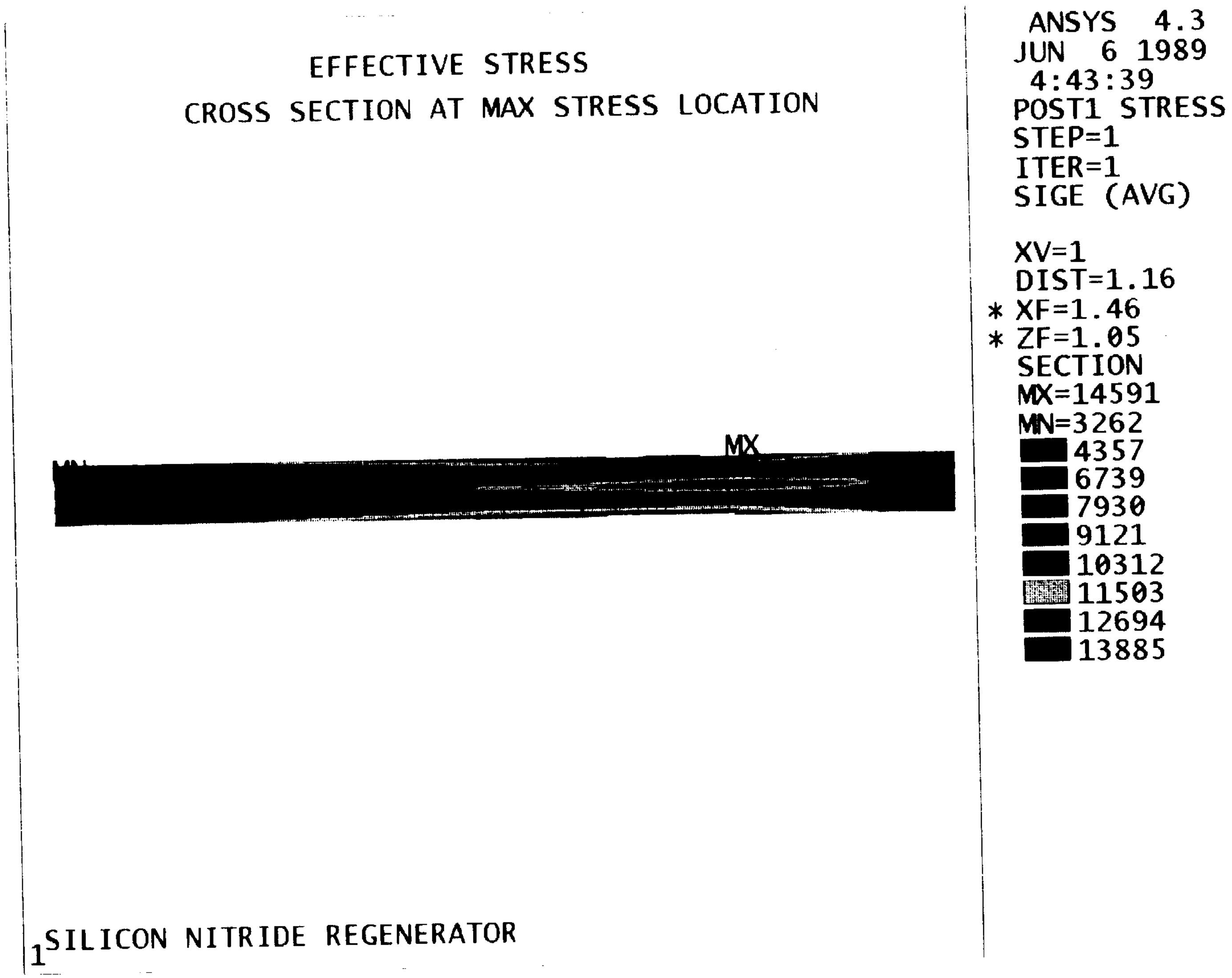

Figure 6.1.2.5 Effective Stress Cross Section at Max Stress Location

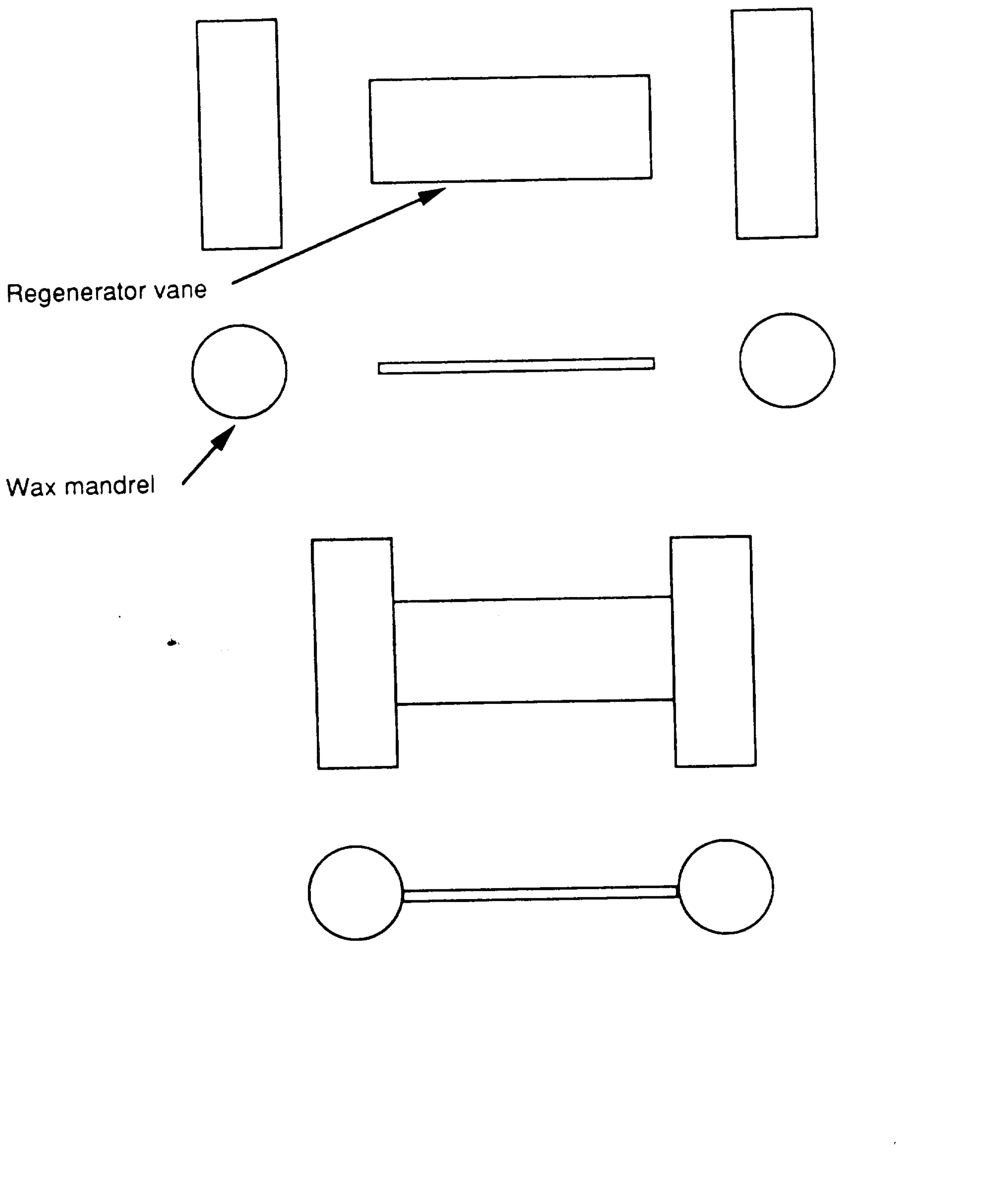

Figure 6.1.3.1 Assembly of Green Bond Regenerator Vane and Wax Cylinders. Top View is Exploded Section; Bottom View Shows Assembly Together

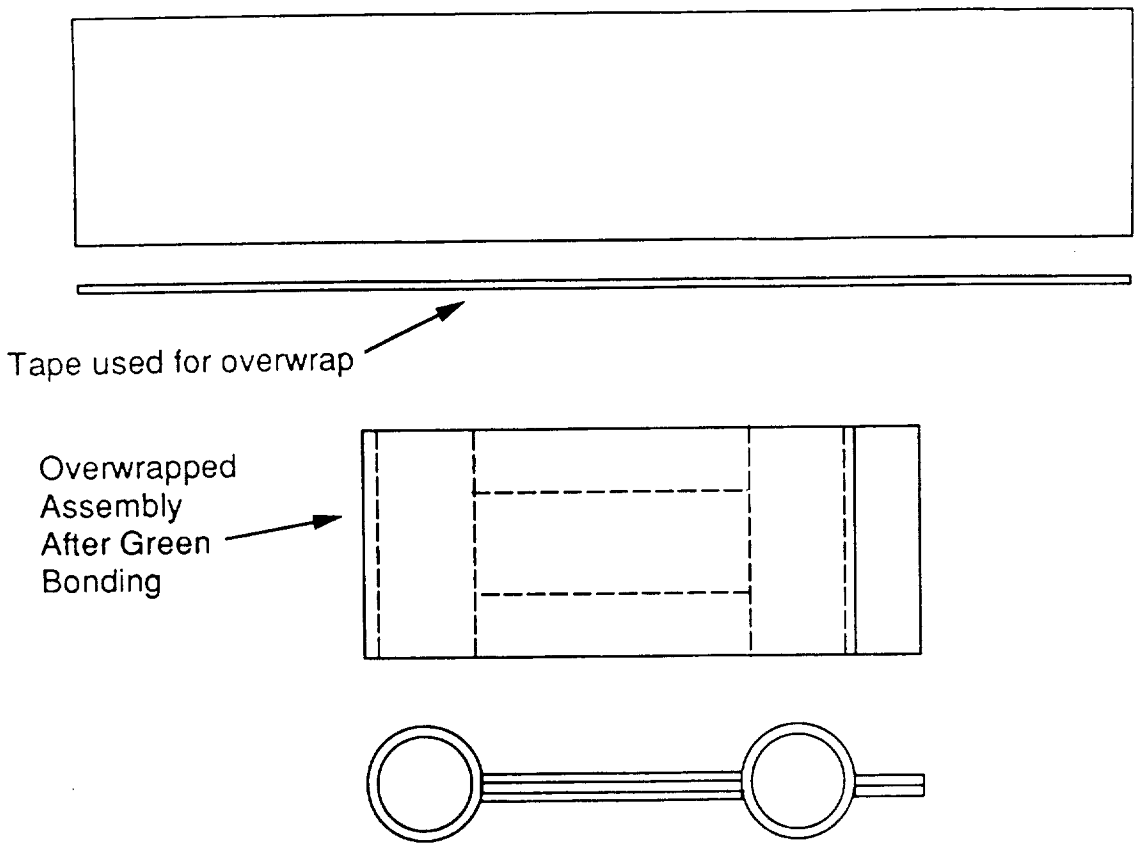

Figure 6.1.3.2a. Tape Wrapped Around Assembly From Figure 3

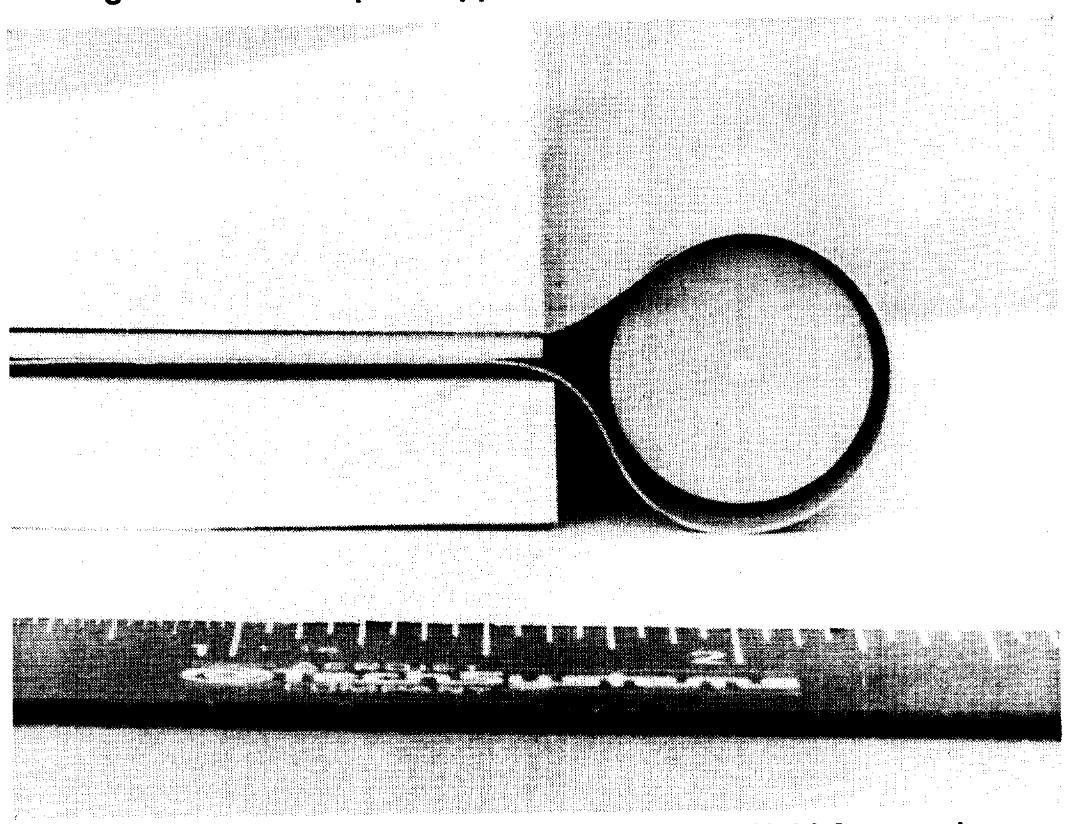

18815-4

Figure 6.1.3.2b. Detail of Tape Wrap Manifold Approach

ORIGINAL PAGE
BLACK AND WHITE PHOTOGRAPH

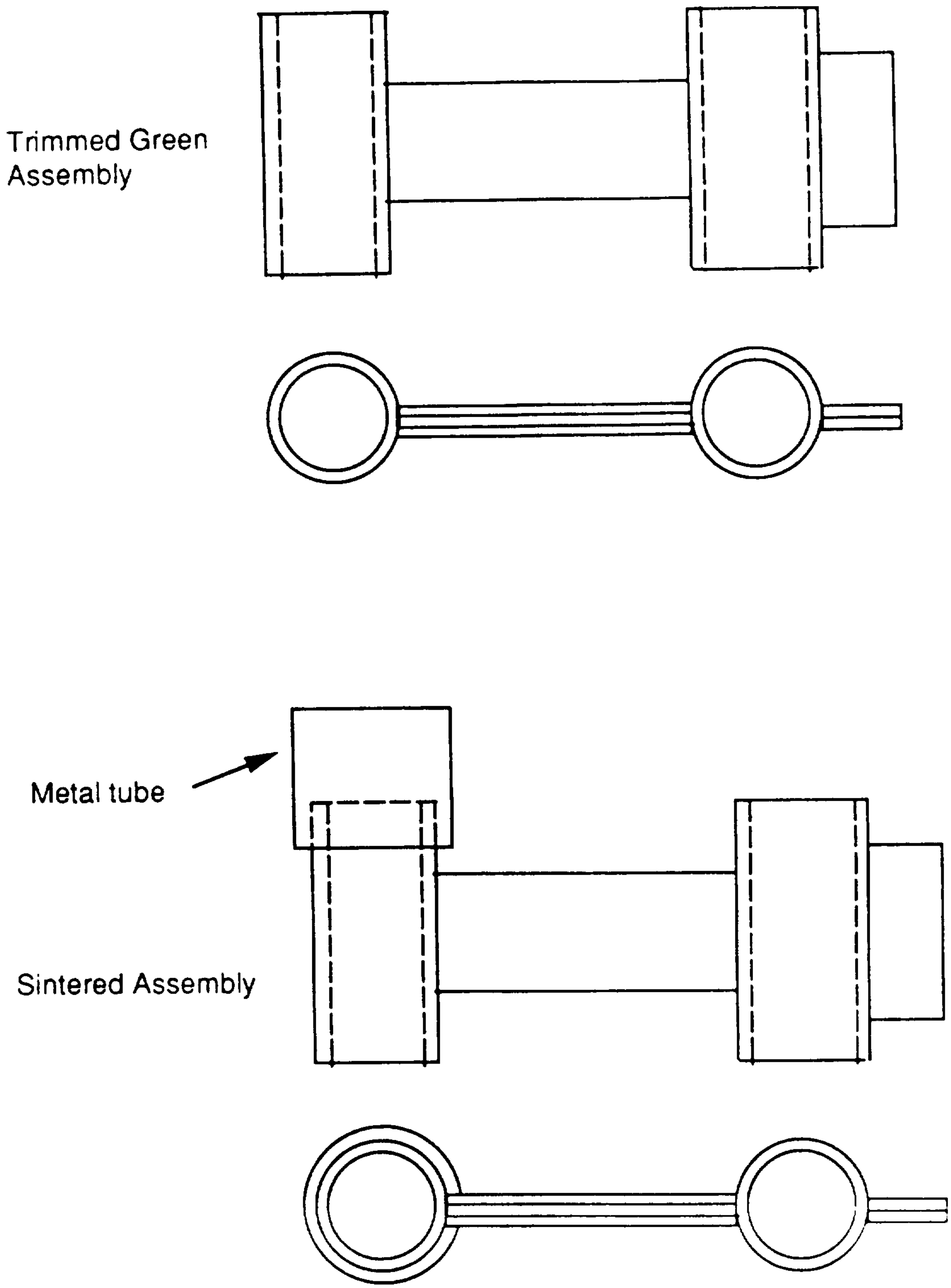

Figure 6.1.3.3 Top View Shows Overwrap Assembly After Green Machining to Trim Off Excess Material. Bottom View is Assembly After Sintering. A Metallic Tube is Shown Brazed Onto One Inlet. One Tube Was to Be Brazed to Each Outlet for Controlling Methane Flow

PAGE ________ INTENTIONALLY BLANK

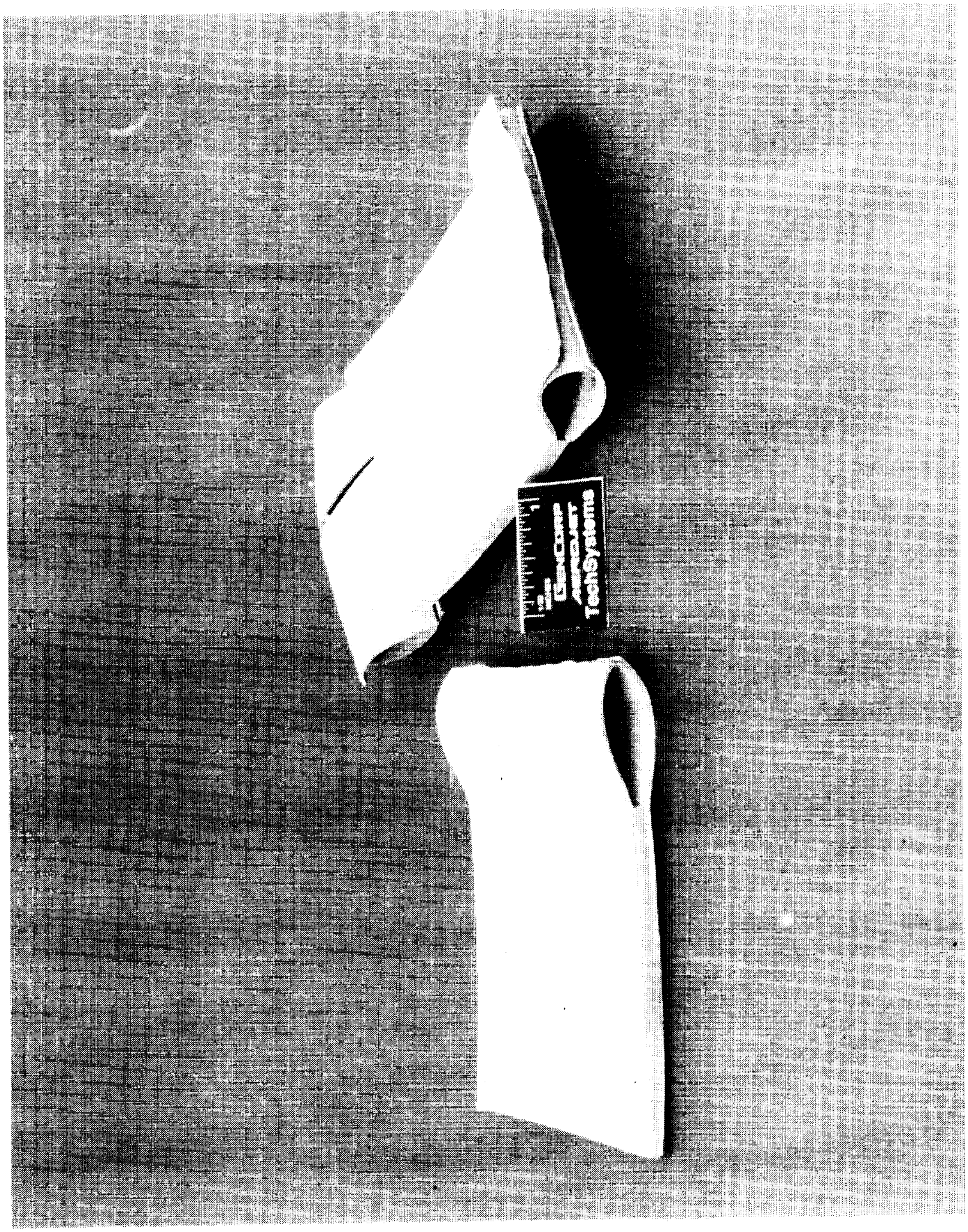

Figure 6.1.3.4 Initial Unsuccessful Tubular Manifold Design

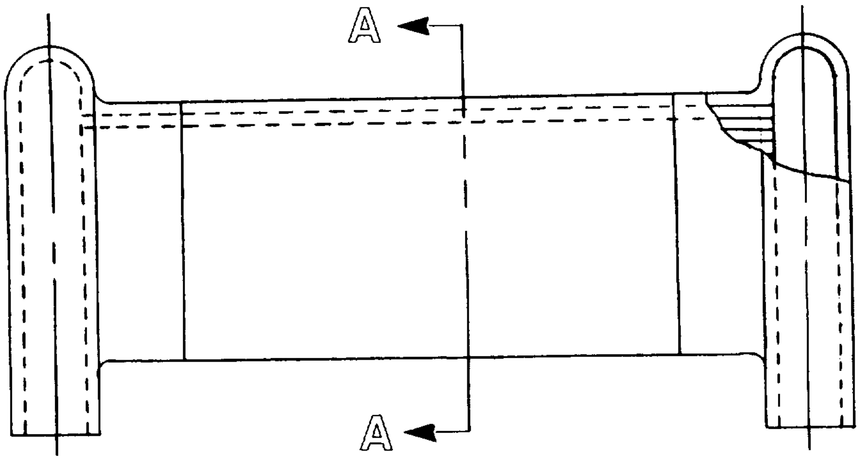

Figure 6.1.3.5a. Overall View of Ceramic Regenerator With Platelet Manifolds

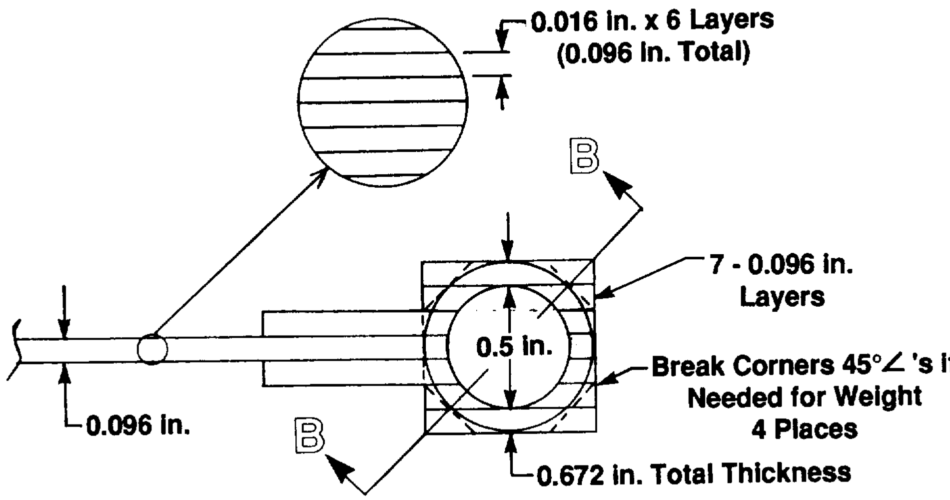

Figure 6.1.3.5b. Cross Section of Platelet Manifolds for Ceramic Regenerator. Structure is Made Up From Multiple 0.016 in. Layers, Green Bonded, Machined and Fired

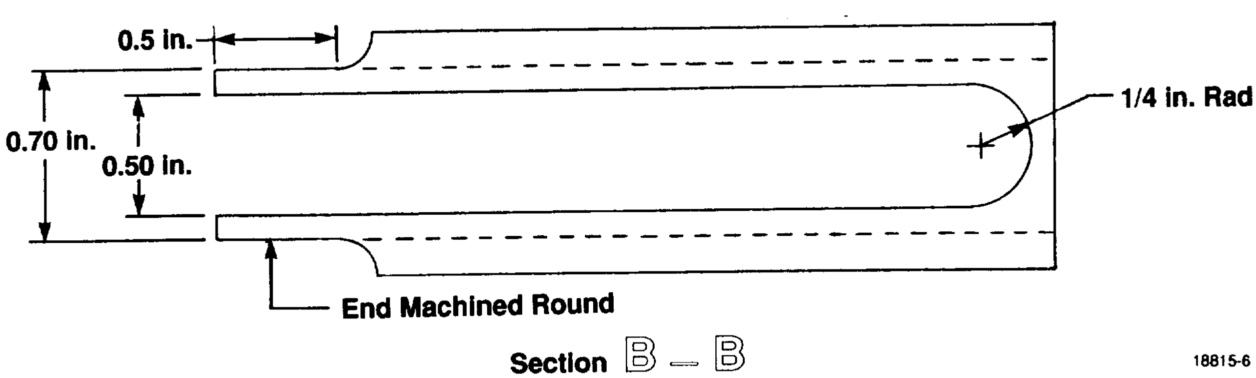

Figure 6.1.3.5c. Section B–B From Figure 6b. After Green Bonding of Manifold Stack, Manifold Tubes are Machined Into Stack, the Ends Machined Round and Parts Fired

An alternate, but similar, manifold configuration is shown in Figure 6.1.3.6. In this design the methane enters the manifolds at the sides rather than at the ends. Construction is similar to that shown in Figure 6.1.3.5, except the manifold passages are partly machined before green bonding. This will help eliminate a concern about smearing and blocking the channel ends during green machining of the concept shown in Figure 6.1.3.5. The cross section of the side entry is shown in Figure 6.1.3.6b, again, the manifold is made from multiple layers of 0.016 in. tape. A detail of the manifold configuration is shown in Figure 6.1.3.6c. The manifold was to be constructed from rectangular sections and the corners machined off and the 0.5 in. round passage bored after bonding.

The next iteration of the flat platelet manifolds concept is shown in Figure 6.1.3.7. This figure is an overall view of the platelet manifold configuration while a through view detail is shown in Figure 6.1.3.8a. The flow passage diagram, Figure 6.1.3.8b, shows the flow distribution within the manifold along with a platelet stacking sequence. The individual platelets are shown in detail in Figure 6.1.3.9 and in an exploded view in Figure 6.1.3.10.

Significant features of this manifold arrangement are: 1) Coolant enters and exits the manifolds normal to the vane by the means of clamp-on delivery lines, 2) The coolant is distributed in proportion to the expected heat input among the heat exchanger channels such that each channel has the same temperature rise, 3) All platelets are pre-cut green before stacking eliminating channel end smearing and green machining after green bonding, and, 4) Braze joints are eliminated by the use of mechanical seals on the flat manifold faces.

6.1.4 Final Design

After the completion of fabrication experiments discussed in Section 6.2.1, below, a final iteration of the design was performed. An overall through view of the final regenerator design is shown in Figure 6.1.4.1, and the individual platelets in Figures 6.1.4.2 through 6.1.4.6. The stacking sequence is shown in Figure 6.1.4.7. The stacking was simplified by reducing the cooled section to two platelets thick for both thermal and fabrication reasons.

Items to note on the design are the reduction of thickness of both the vane section and the manifold sections as well as the adjustment of the width of the widest channels. The vane section is now 0.120 in. thick and the manifold section about 0.4 in. thick. This makes for a lighter weight part. With the reduced flow area, the mass flow rate was decreased which increases the bulk temperature rise through the vane to the 600 F design goal. The advantages of two layers of tape for fabrication is discussed in the Section 6.2.1. The width of the two widest

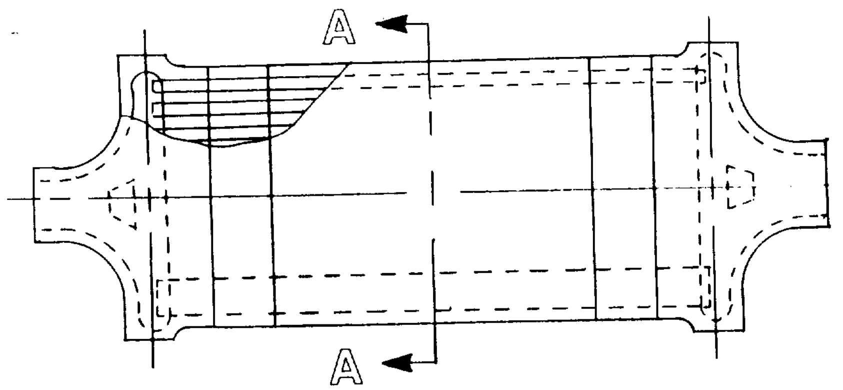

Figure 6.1.3.6a. Side Entry Ceramic Regenerator Concept. Manifolds Are Constructed From Layered Platelets

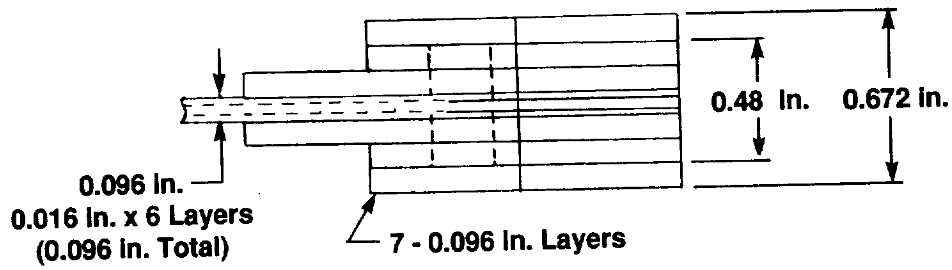

Figure 6.1.3.6b. Cross Section of Platelet Manifolds for Side Entry Manifold Concept. Manifolds are Green Machined Before Stacking and Green Bonding

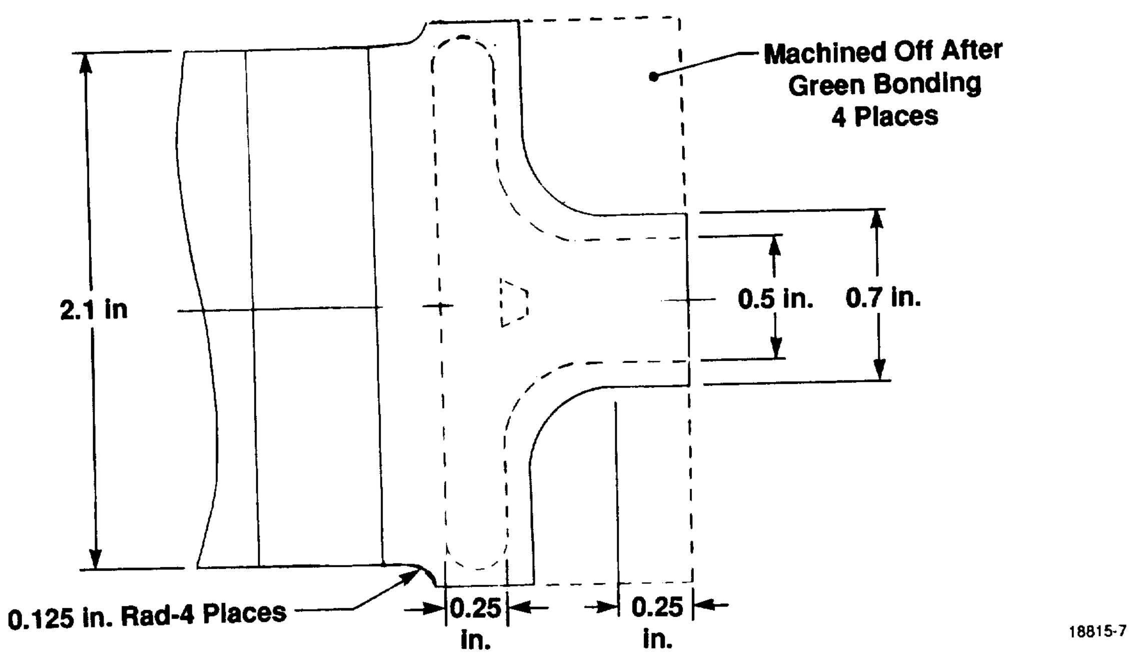

Figure 6.1.3.6c. Manifold Design of Side Entry Ceramic Regenerator. Corners and 0.5 in. Inlet are Machined After Green Bonding

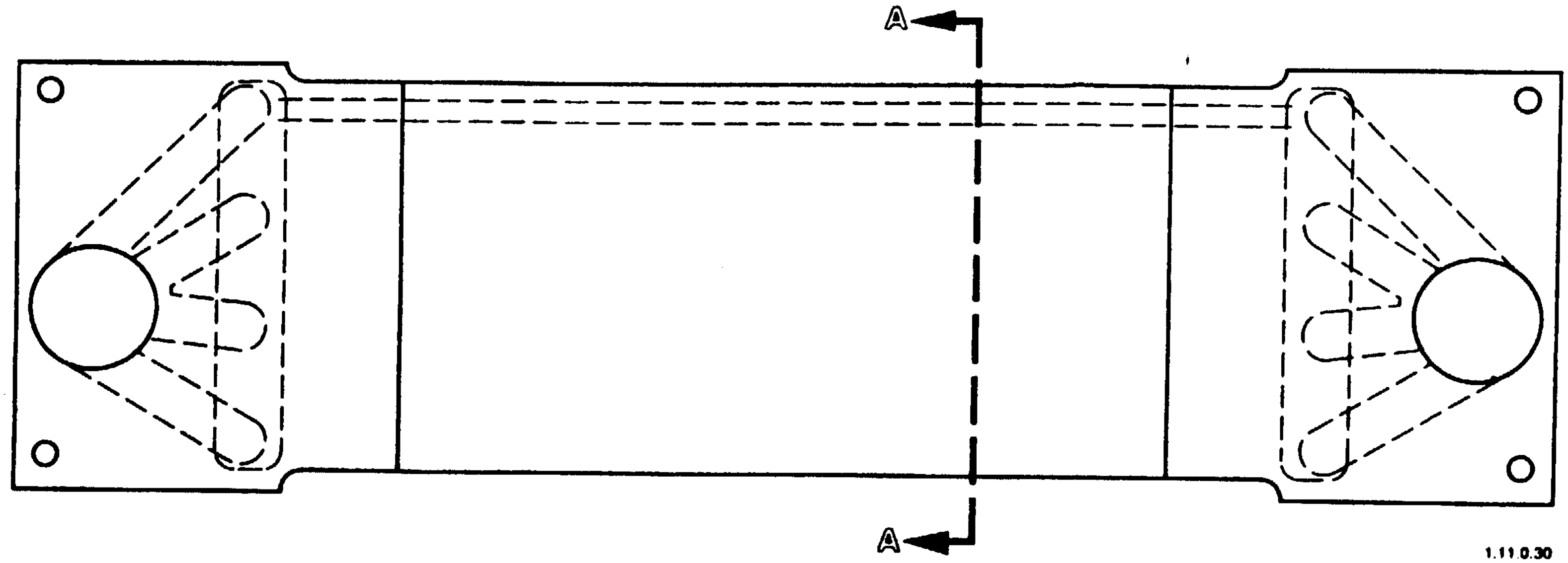

Figure 6.1.3.7a. Overall View of Improved Platelet Heat Exchanger Manifold Design

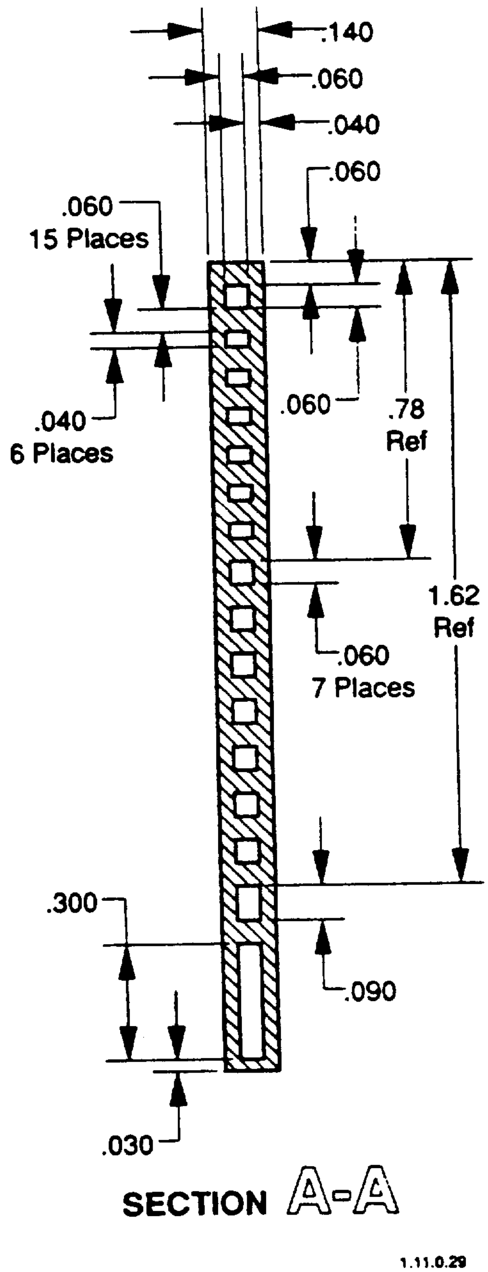

Figure 6.1.3.7b

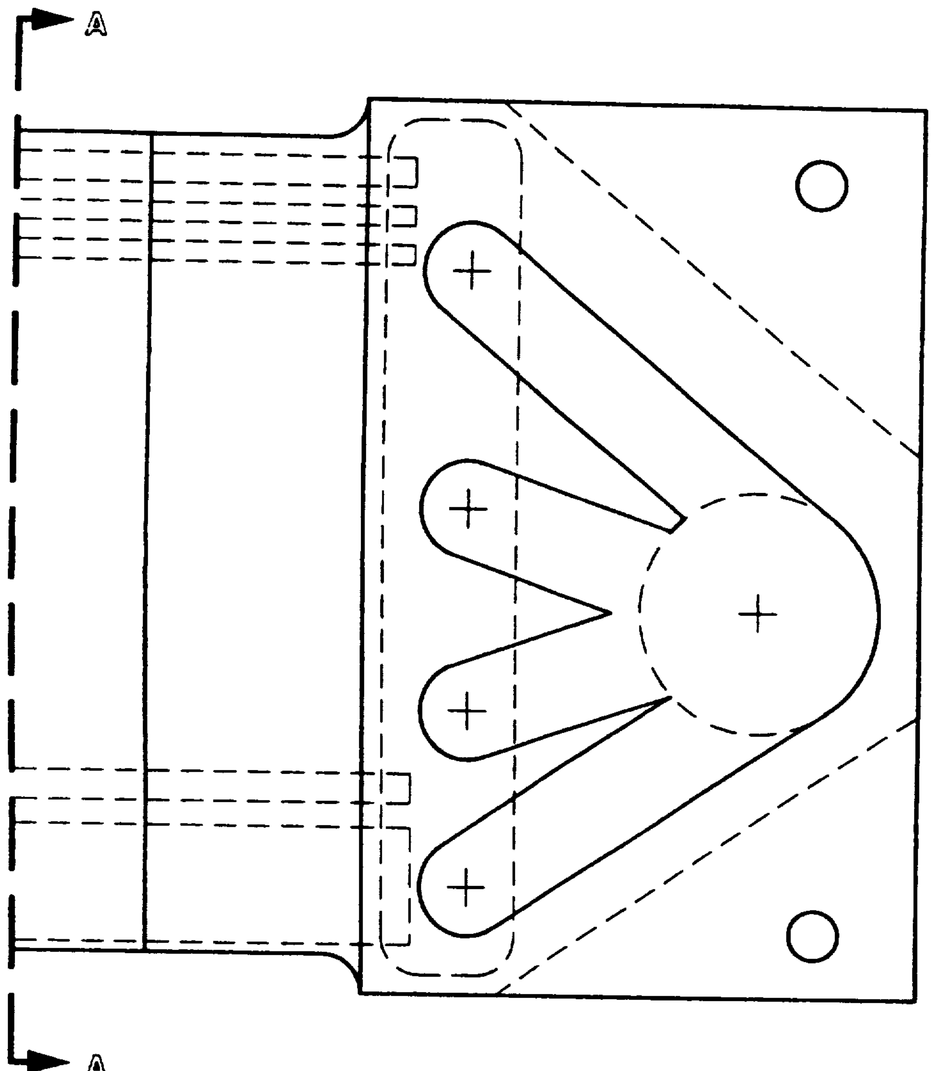

Figure 6.1.3.8a. Through View

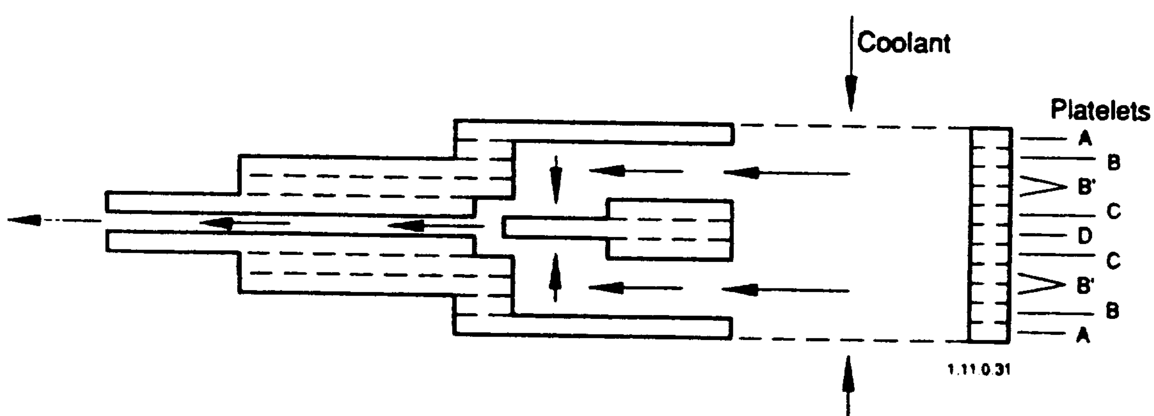

Figure 6.1.3.8b. Flow Passage

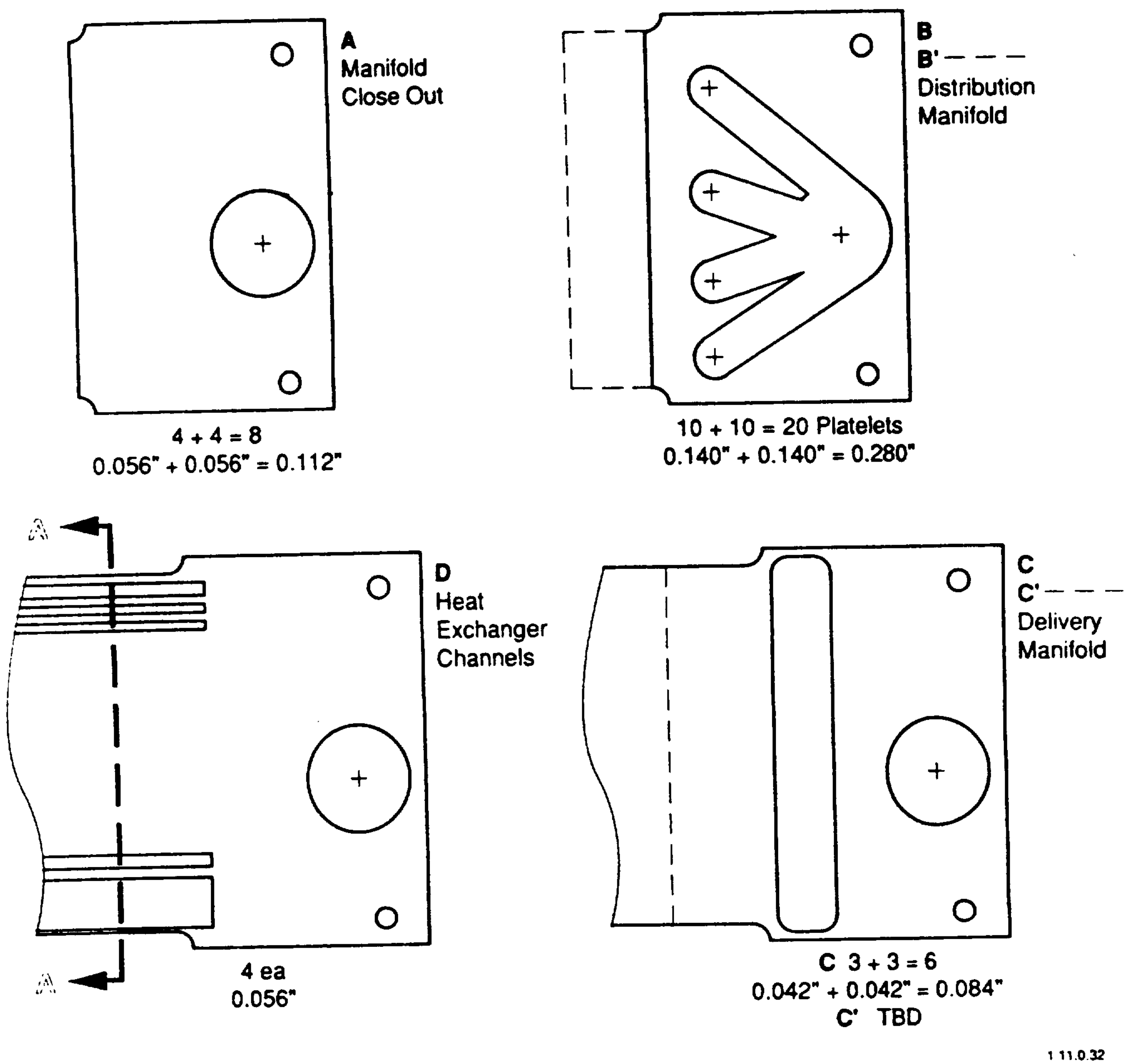

Figure 6.1.3.9 Manifold Platelet Detail

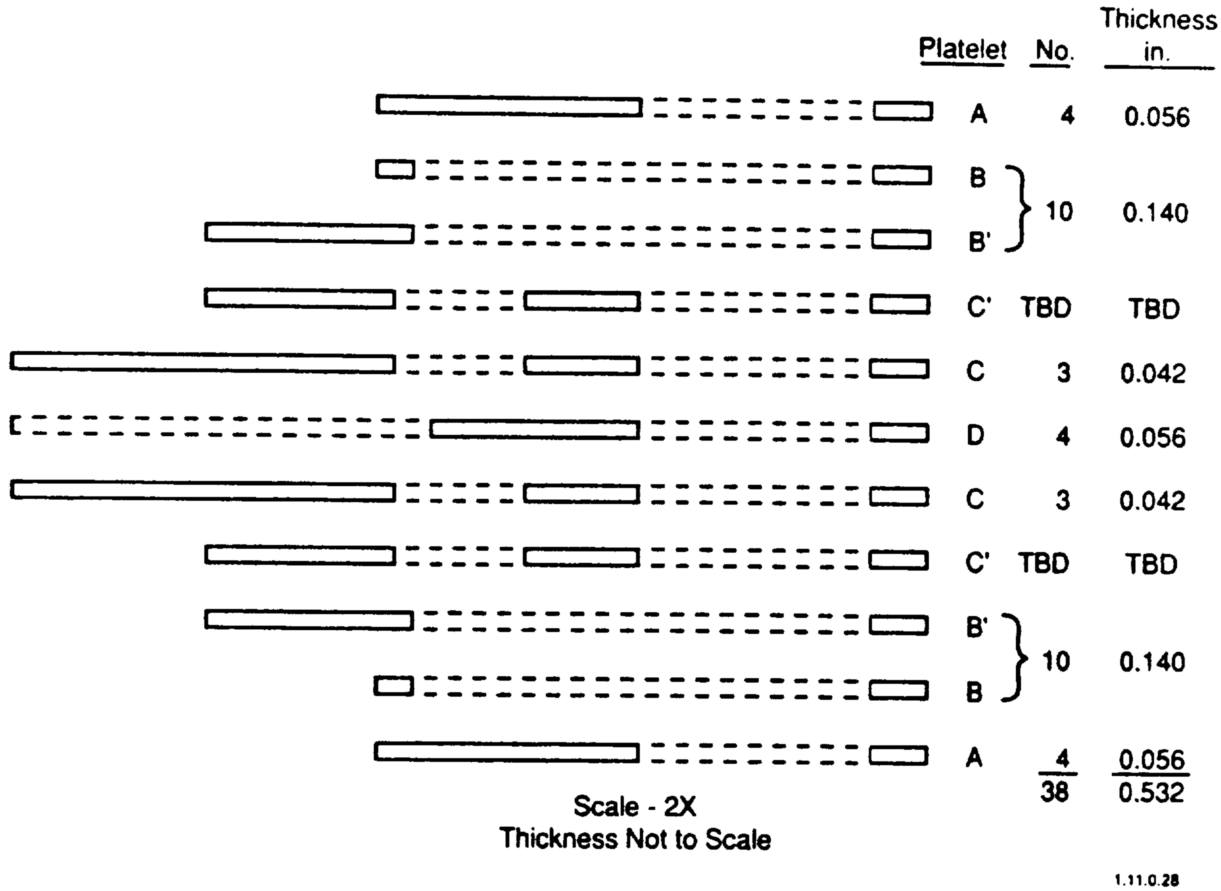

Figure 6.1.3.10 Exploded View of Manifold Ends

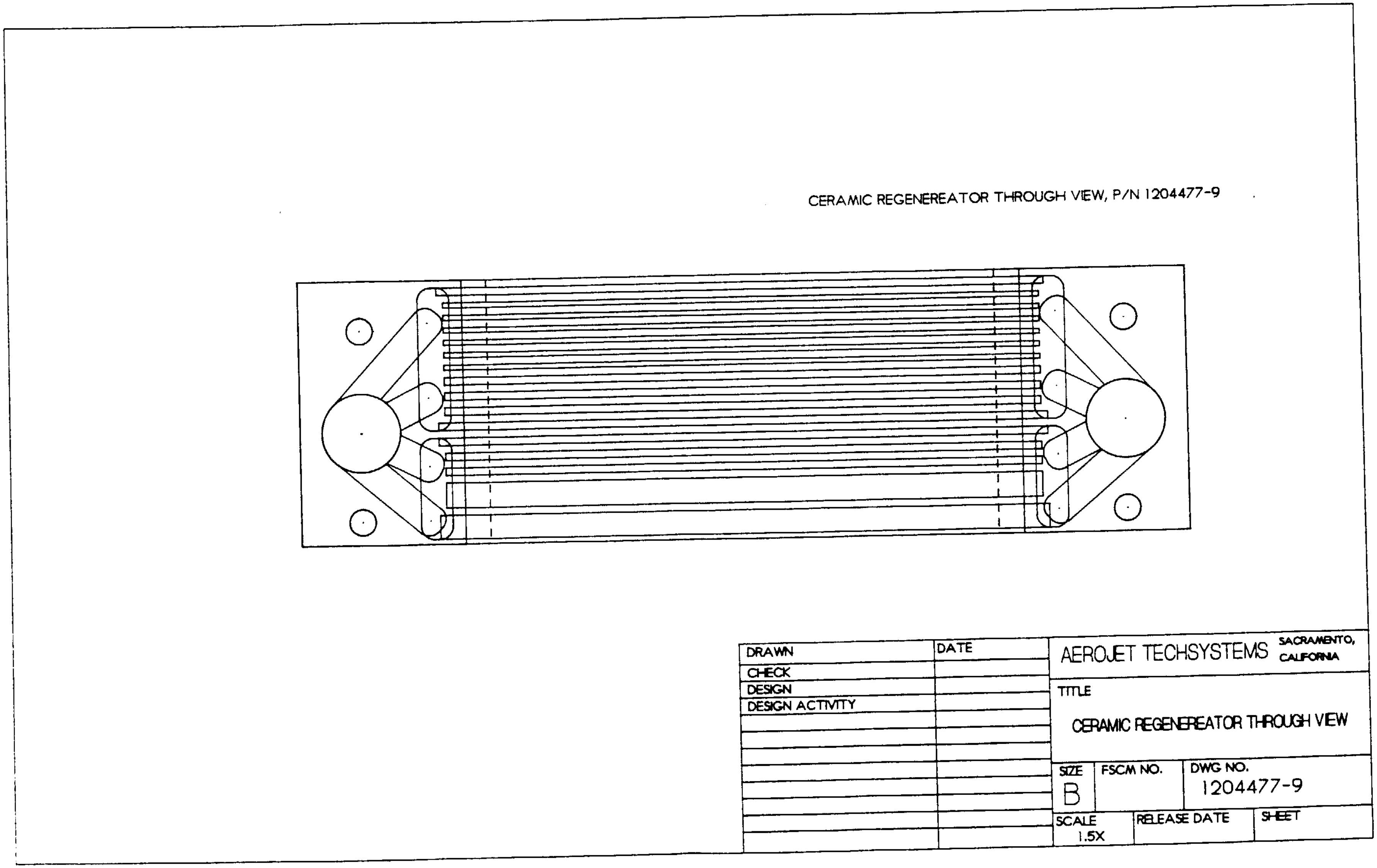

Figure 6.1.4.1 Through View of Stacked Platelets for Ceramic Regenerator

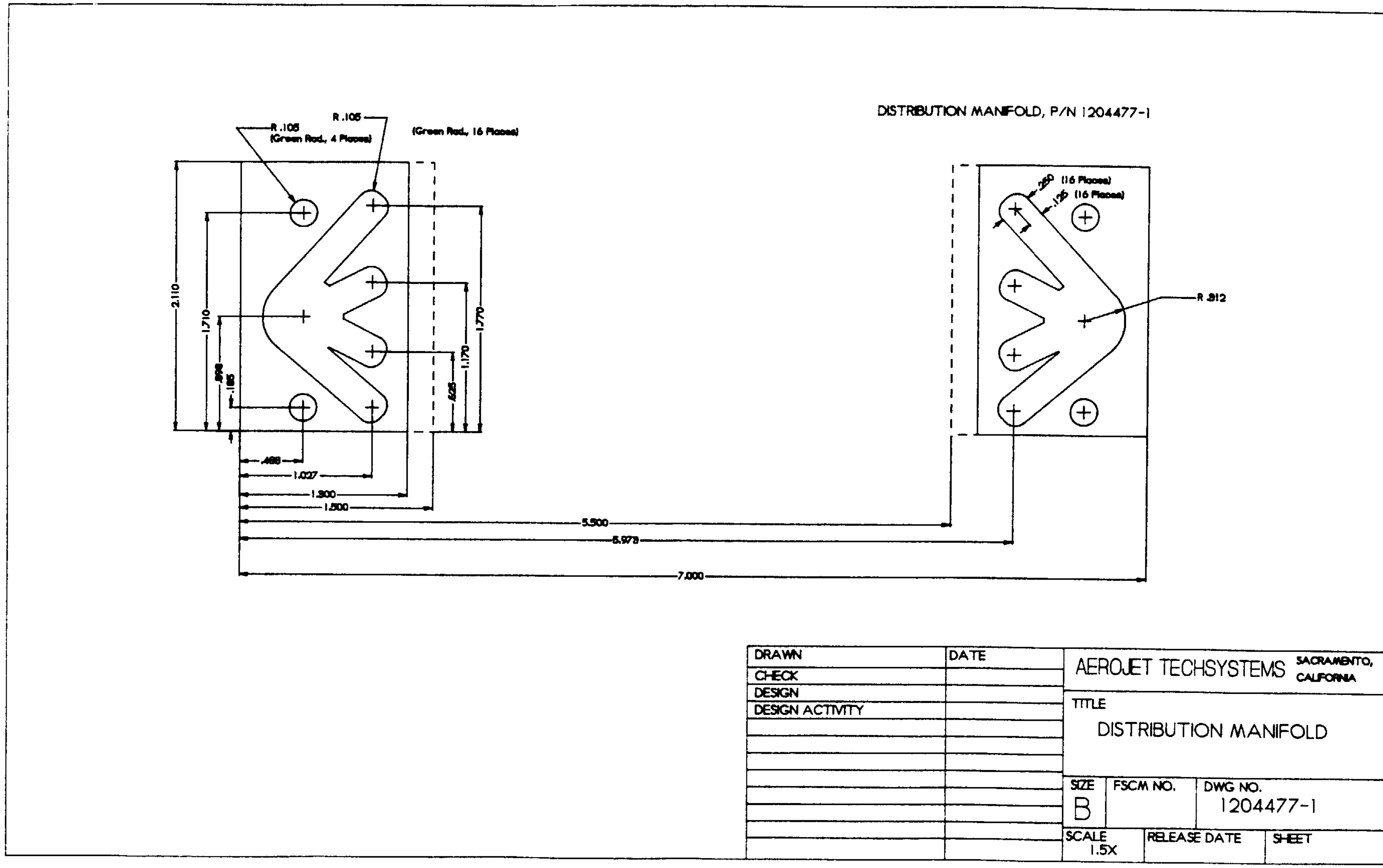

Figure 6.1.4.2 Distribution Manifold Platelets for Ceramic Regenerator

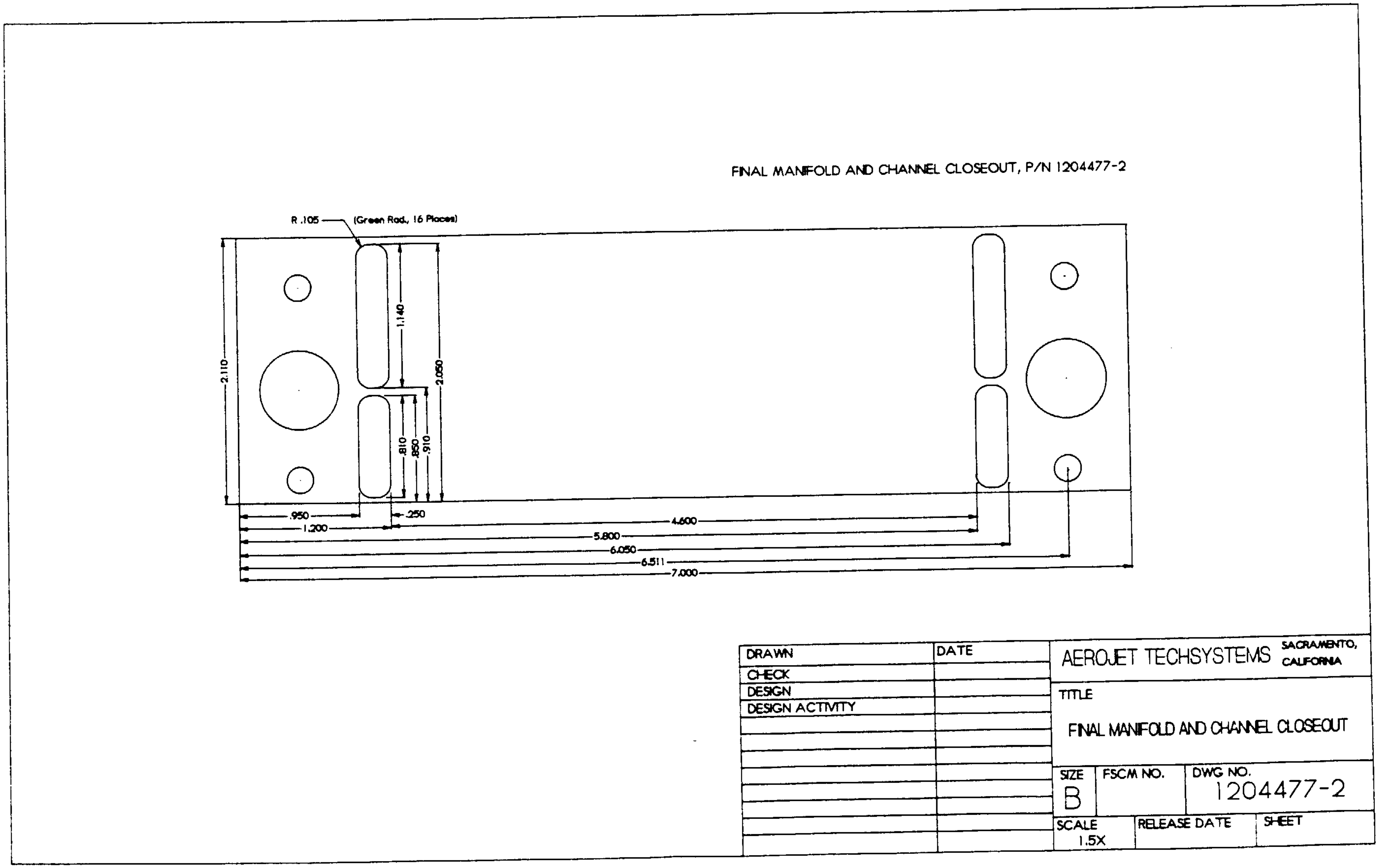

Figure 6.1.4.3 Final Manifold and Channel Closeout Platelets

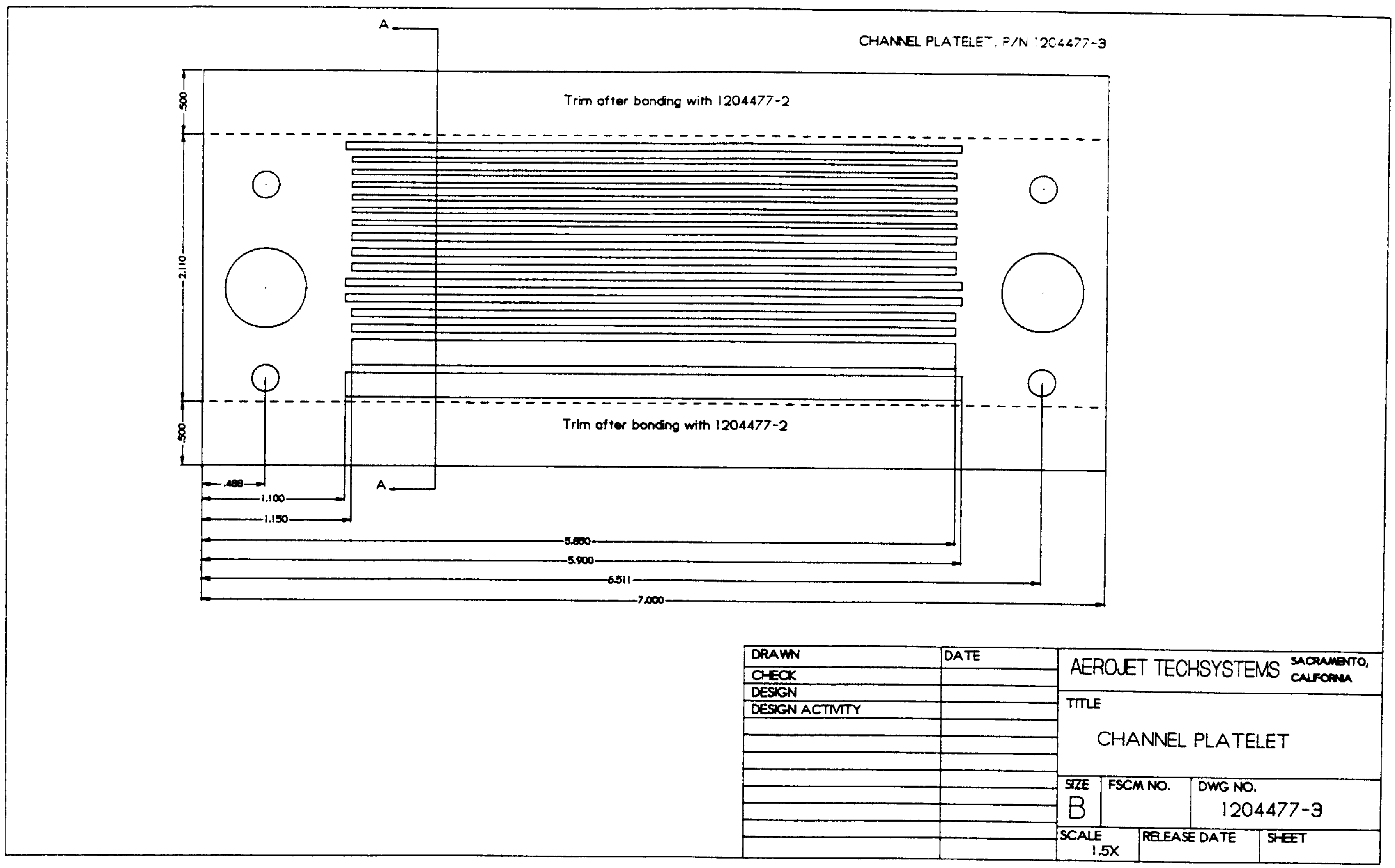

Figure 6.1.4.4 Regenerator Channel Platelet. Note the Wide Side Lands to Be Trimmed After Being Bonded

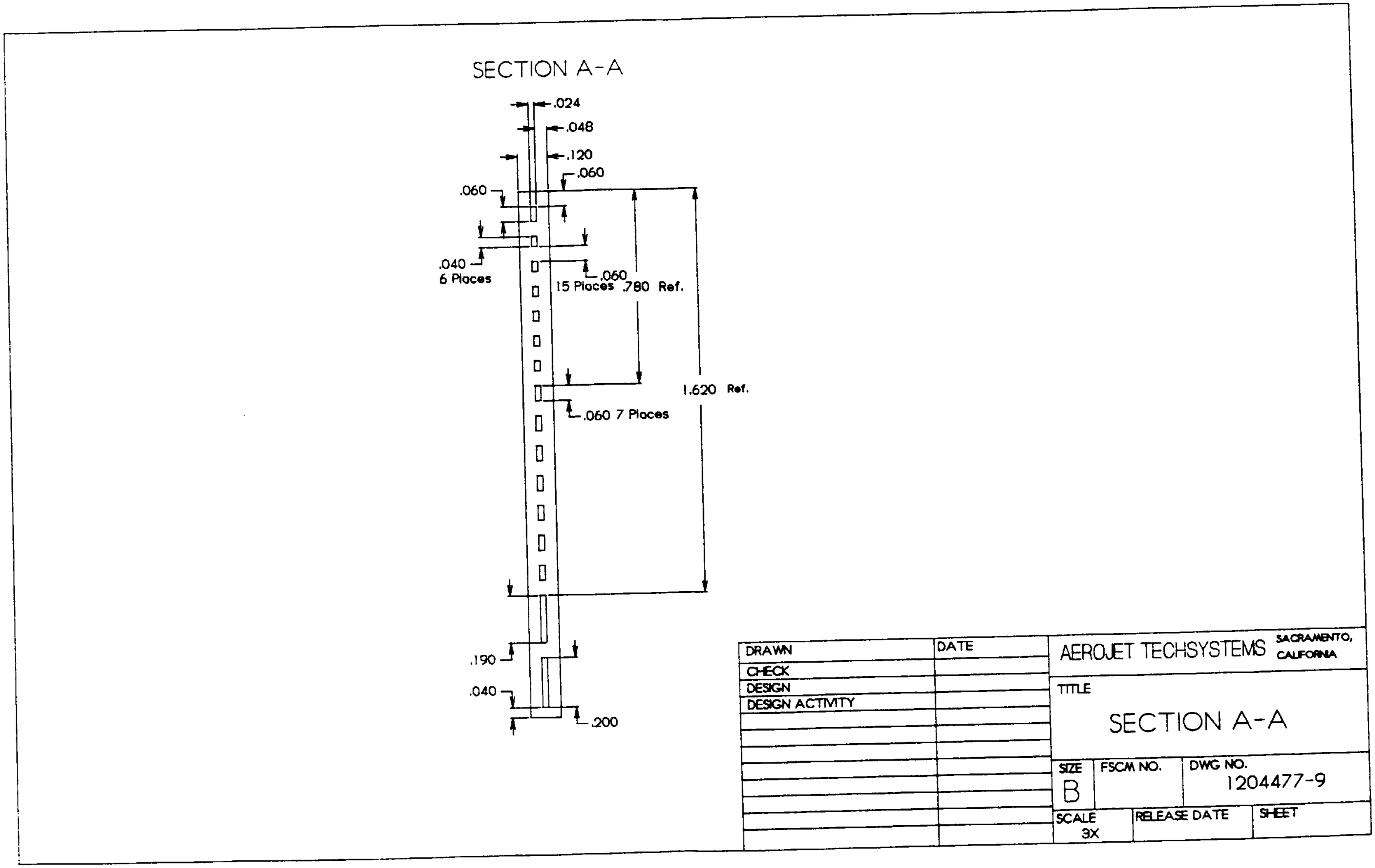

Figure 6.1.4.5 Cross Section of Regenerator Vane Section

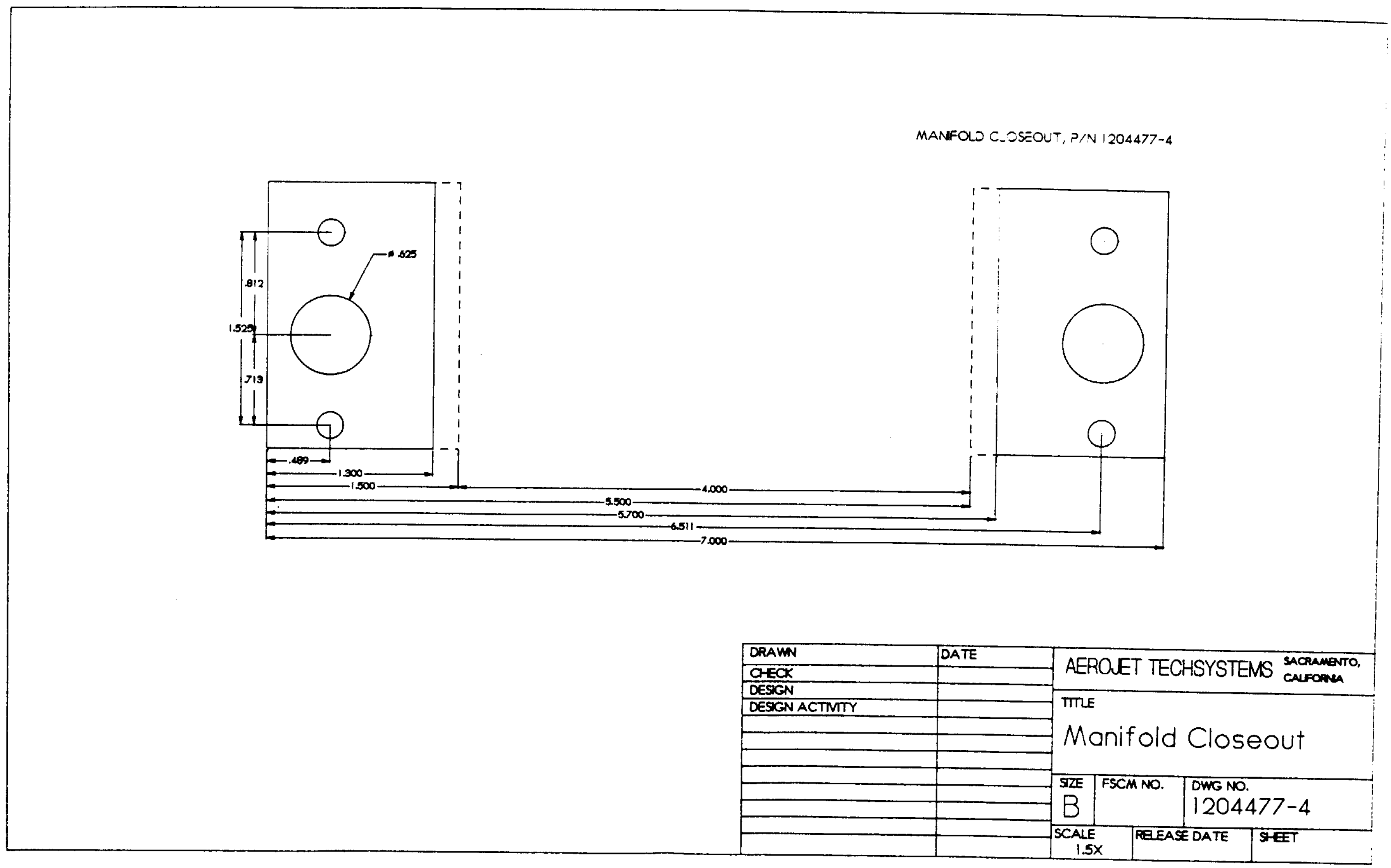

Figure 6.1.4.6 Regenerator Manifold Closeout Platelet

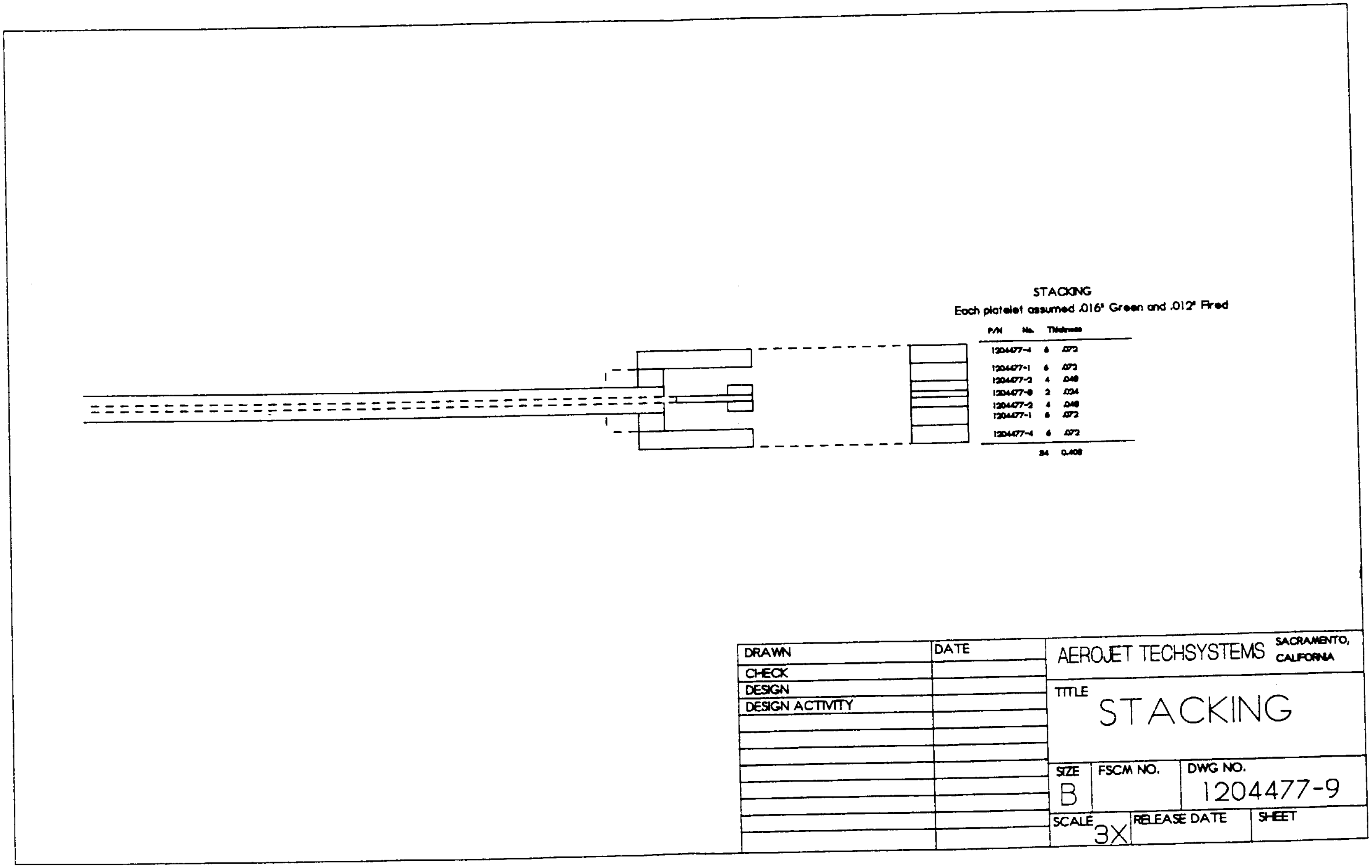

Figure 6.1.4.7 Platelet Stacking Sequence for Ceramic Regenerator. Note the Thickness of the Vane Channels (P/N 1204477-3) Has Been Reduced to 2 Platelets

channels on the leading edge were adjusted to give more support and prevent sagging of the cover sheet as seen if Figure 6.2.6. The total flow width was maintained for these two channels with a simple repositioning of the land between the two channels.

6.2 REGENERATOR FABRICATION

6.2.1 Fabrication Experimentation

The design shown in Figures 6.1.3.7 through 6.1.3.10 were evaluated by Cercom and Coors for fabrication feasibility. Initial reaction was positive and prototype platelets were fabricated. Examples of these platelets were delivered to Aerojet for evaluation and are shown in Figure 6.2.1 with the regenerator channel platelet in greater detail in Figure 6.2.2. These example platelets were punched from alumina tape.

Coors produced a prototype regenerator made from alumina for process assessment and examination purposes. Figure 6.2.3 shows this regenerator after being sectioned for evaluation. The prototype regenerator is made from alumina with some chromium oxide which gives it a pink color. Features to note on this first alumina part are the warpage of the vane section, Figure 6.2.4, some delamination in the manifold section, Figure 6.2.5, poor alignment of the lands and edges and a droop in the wide laminated channel, Figure 6.2.6.

All of these problems were addressed. The warpage and delaminations are due to the shrinkage of the part during sintering. This caused dragging of the part on the furnace furniture. This was solved by constructing the furniture from the same green material as the part such that both shrink at the same rate and eliminate any drag.

The Coors punching equipment is only able to punch two layers of tape at once. The misalignment of the lands and at edges of the channels is due to the requirement that several layers of channels be punched and then stacked together with no alignment provisions for the lands. This problem was eliminated by having the channels only two platelets thick and punching them both at once. The two platelet thickness also produces a desired increases in the temperature rise of the coolant.

The poorly aligned edge was eliminated by having an extra wide land at the edge to give lateral support. The wide land is then trimmed to the correct width after being green bonded to the cover platelet.

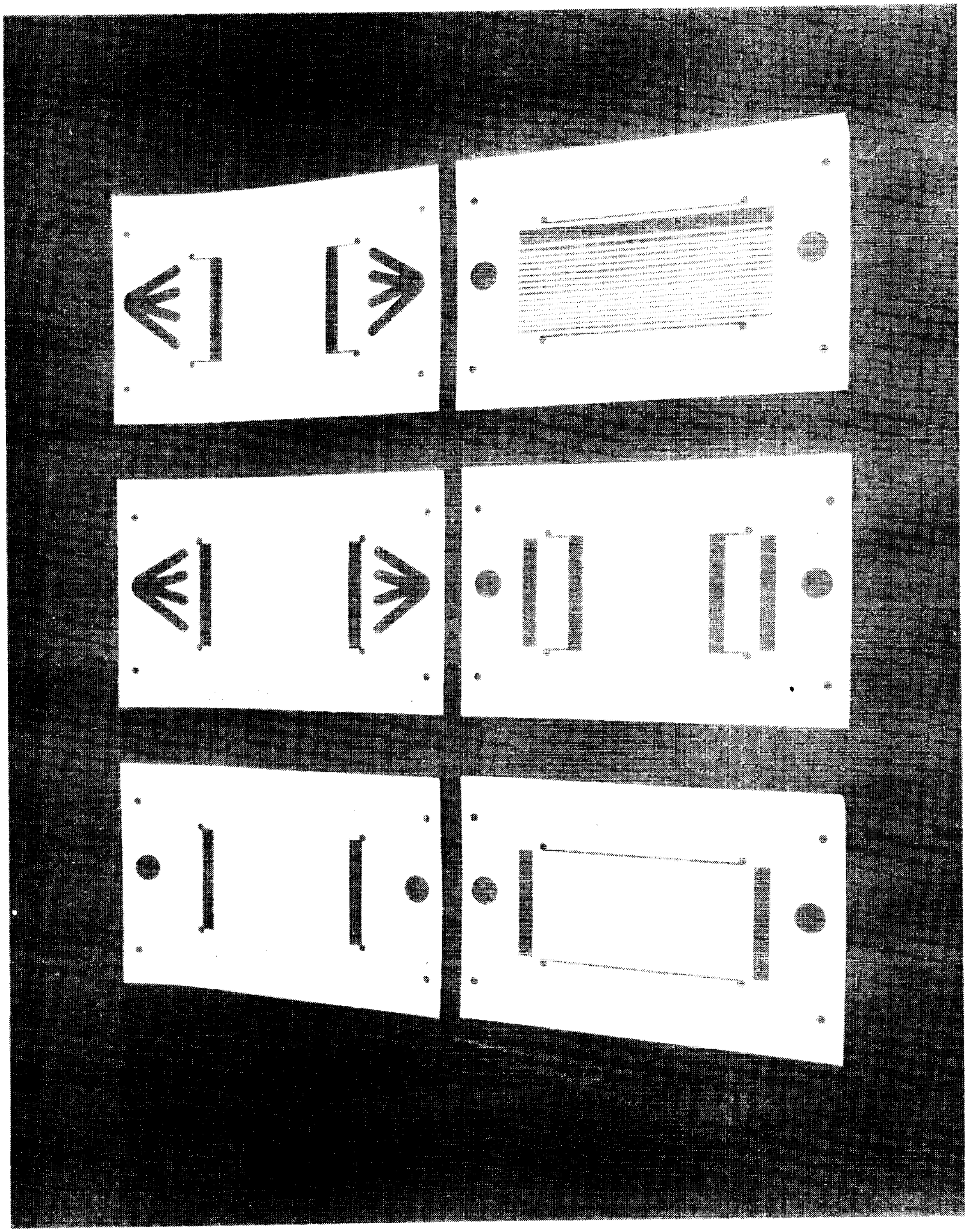

Figure 6.2.1 Prototype (Green Alumina) Regenerator Platelets Showing Manifolds and Cooling Passages

ORIGINAL PAGE
BLACK AND WHITE PHOTOGRAPH

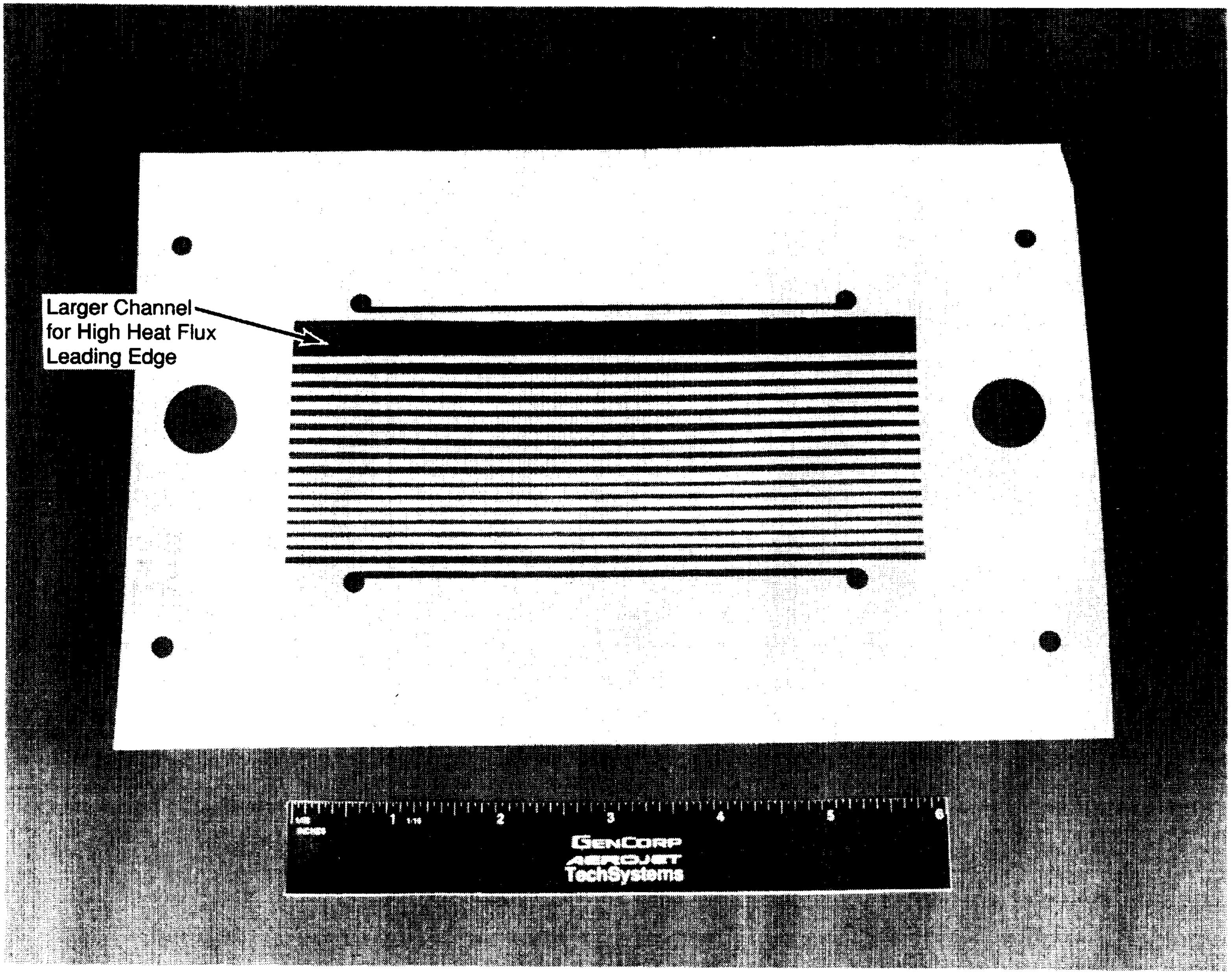

Figure 6.2.2 Green Prototype (Alumina) Cooling Passage Platelet. Passages are Optimized to Match Heat Input

ORIGINAL PAGE
BLACK AND WHITE PHOTOGRAPH

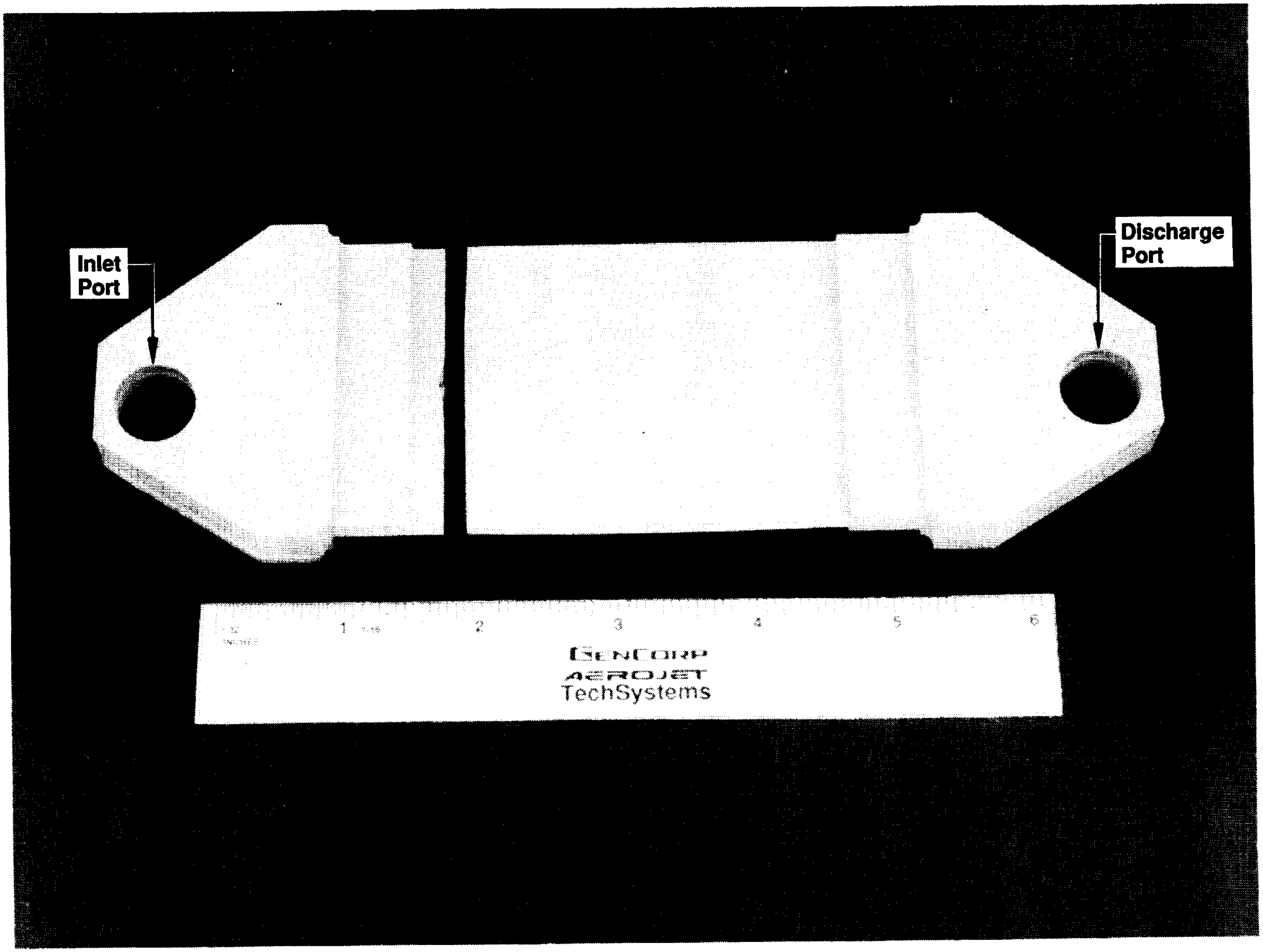

Figure 6.2.3 Overall View of Prototype Alumina Regenerator Fabricated With an Earlier Design. This Part was Sectioned for Evaluation

ORIGINAL PAGE
BLACK AND WHITE PHOTOGRAPH

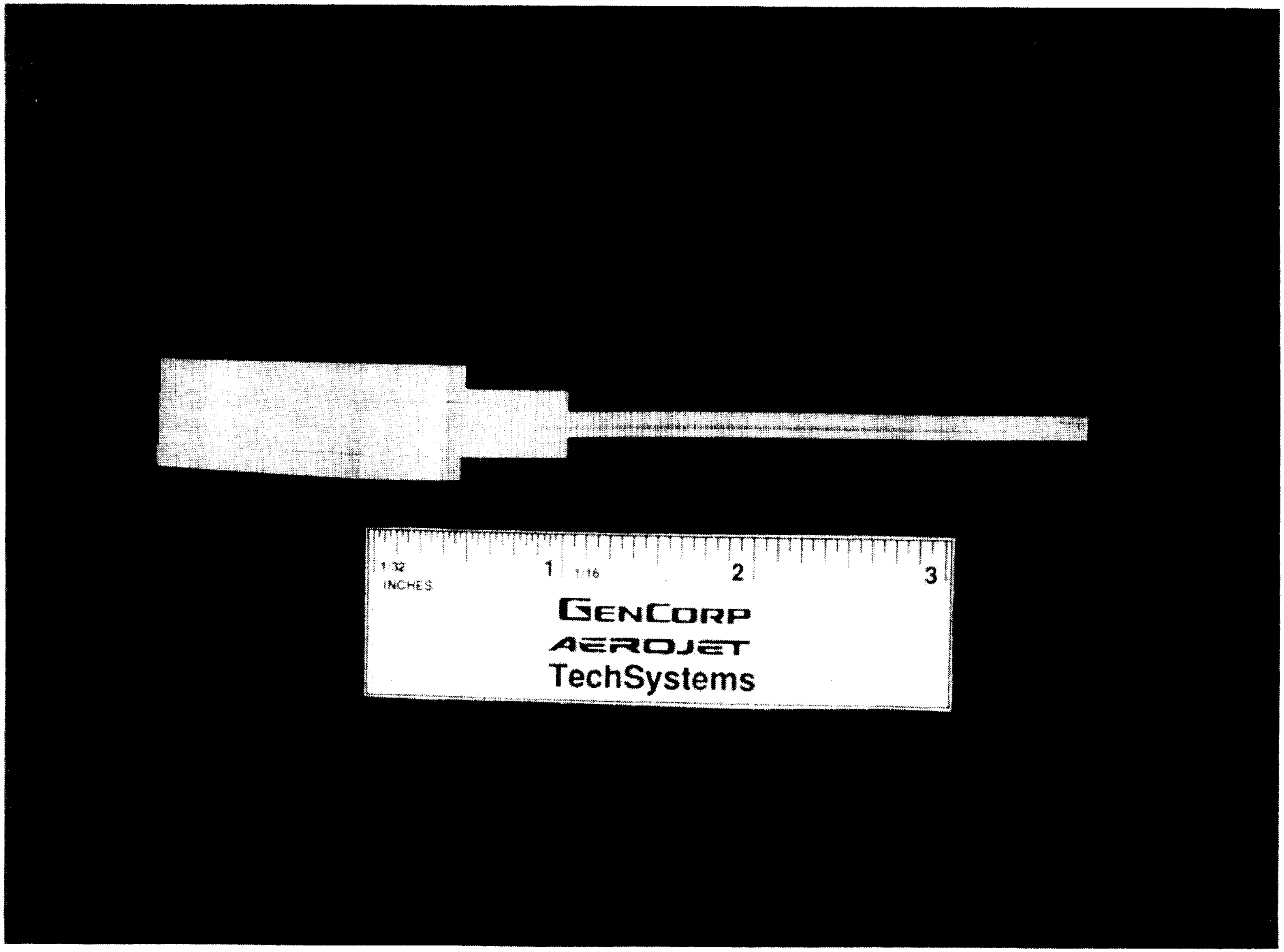

Figure 6.2.4 Edge View of Prototype Alumina Regenerator. The Warpage of the Vane Section is Due to Dragging of the Part on the Furnace Due to Shrinkage During Sintering

ORIGINAL PAGE
BLACK AND WHITE PHOTOGRAPH

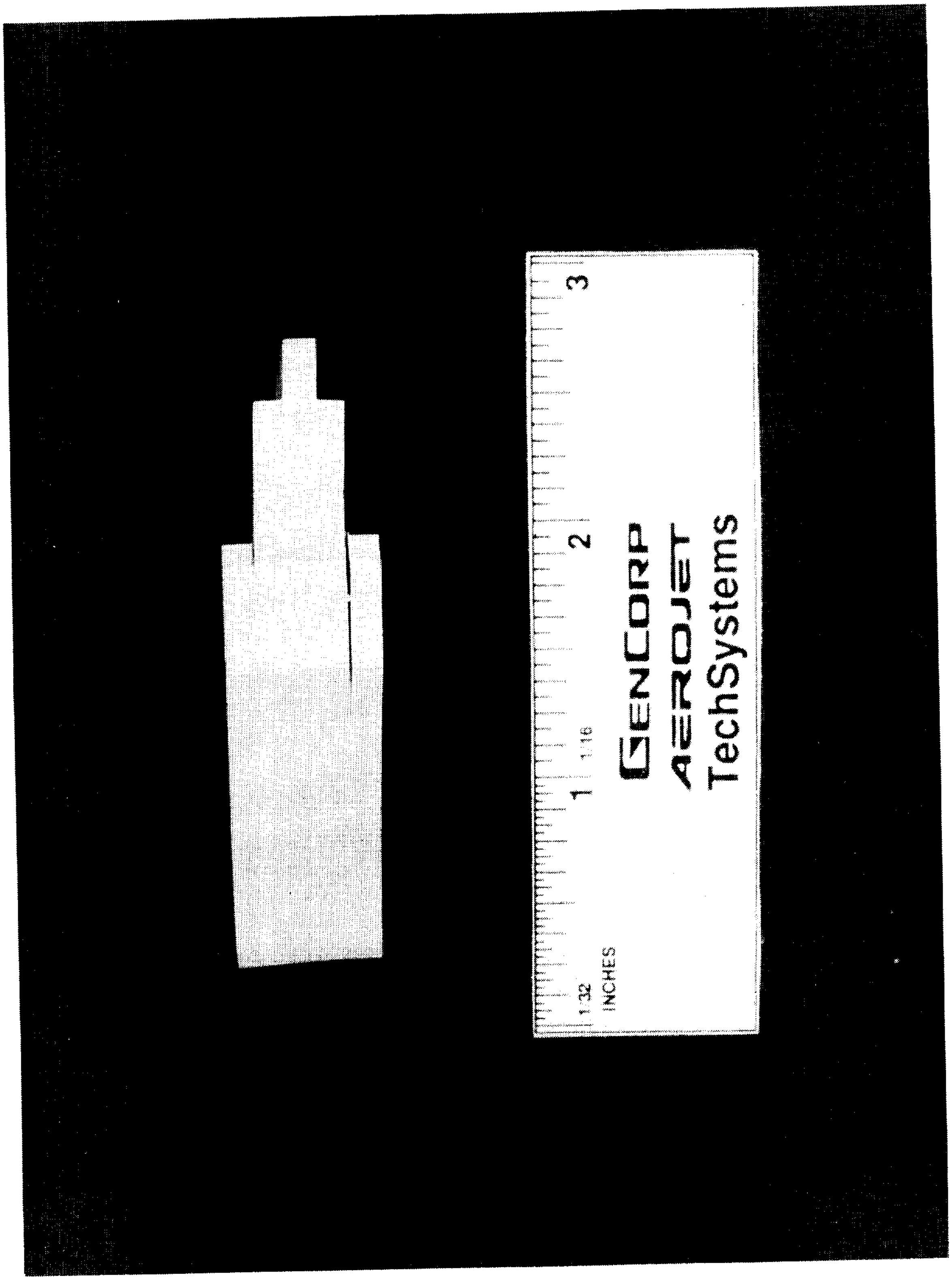

Figure 6.2.5 Edge View of Prototype Alumina Regenerator Manifold. The Delaminations is Due to Dragging of the Part on the Furnace Due to Shrinkage During Sintering

ORIGINAL PAGE
BLACK AND WHITE PHOTOGRAPH

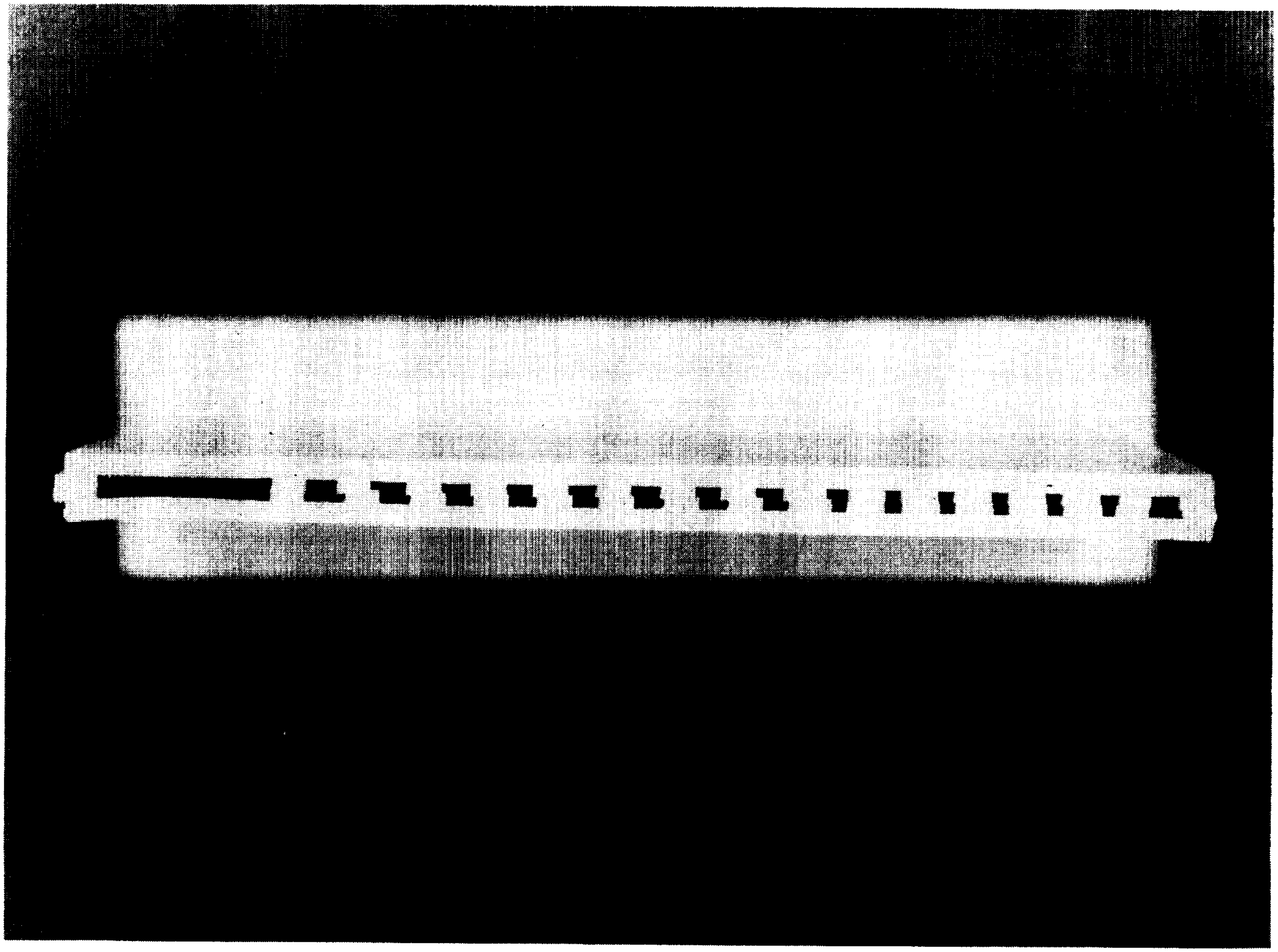

Figure 6.2.6 Cross Section of the Alumina Prototype Regenerator. Note the Misalignment of the Channels and Lands, the Droop in the Wide Channel and the Poor Alignment of the Edges of the Part. All of These Problems Have Been Addressed and Will Be Eliminated in Future Parts

ORIGINAL PAGE
BLACK AND WHITE PHOTOGRAPH

The drooping in the wide channel was addressed by reducing the width of the largest channel and widening the adjacent channel while retaining the same total flow area (see drawings, Figures 6.1.4.1, 6.1.4.4 and 6.1.4.5). It was also suggested that the parts be fired in the edge up position to prevent the drooping. Initial experiments in the edge firing position have were not successful, but the method may still have merit with further development.

During the fabrication experiments at Coors, a tape structure 0.8 inches thick was produced and sent to Aerojet for evaluation, Figure 6.2.7. This was accomplished by green bonding 5 layers of 0.016 in. tape together to produce 0.08 in. thick tapes. Ten of these tapes were then bonded together to produce the final 0.8 in. part.

The initial machining approach, using standard machine shop practices, resulted in some delamination at the edges of the large stack and were marginally successful. The punched platelet configuration eliminated the need for this fabrication technique and the work was not continued, but, it does have possibilities for future applications with some development work.

The burn out and sintering experiments on the large sections also resulted in some delamination and warping of the final part. This was due to incomplete burn out of the thick parts resulting in residual binders being present during the sintering procedure. This problem was solved by extending the burnout times to eliminate all the binders.

6.2.2 Final Regenerator Fabrication

The final manifold and vane design changes, Figures 6.1.4.1 through 6.1.4.7, were programmed into the numerical controlled punch at Coors and prototype platelets of the final design produced, Figure 6.2.2.1. The platelets were punched extra wide and trimmed after bonding in order to maintain edge registration. The holes in the corners of each platelet are used for stacking alignment pins which maintain platelet position during lamination.

Prototype regenerators of the final manifold design from alumina were produced for punching control, process assessment and examination purposes. Two of these regenerators are shown in Figure 6.2.2.2. One of the alumina regenerators was sectioned for internal inspection. The locations of the inspection sections are shown in Figure 6.2.2.3. Figure 6.2.2.4 shows the cross sections of both the first alumina prototype (top) and the final prototype version (bottom). The channel height reduction on the bottom prototype reflects a change in the coolant flow requirements in the test section. Excessive sagging and delamination in the wide channels can be noted as can excessive deformation in the smaller channels. The sagging and delamina-

PAGE_______ INTENTIONALLY BLANK

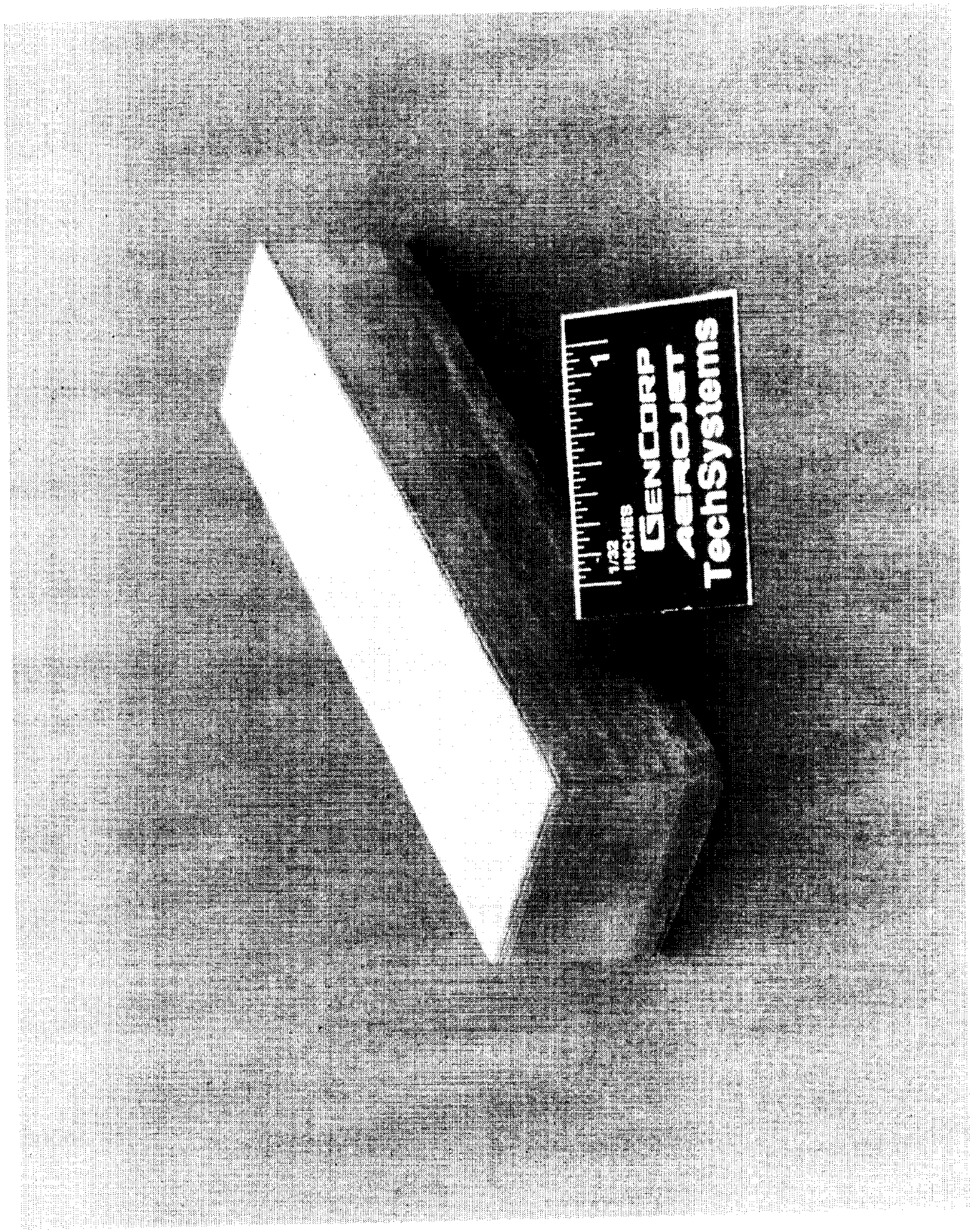

Figure 6.2.7 Large Scale "Green" Silicon Nitride Laminated Structure

ORIGINAL PAGE
BLACK AND WHITE PHOTOGRAPH

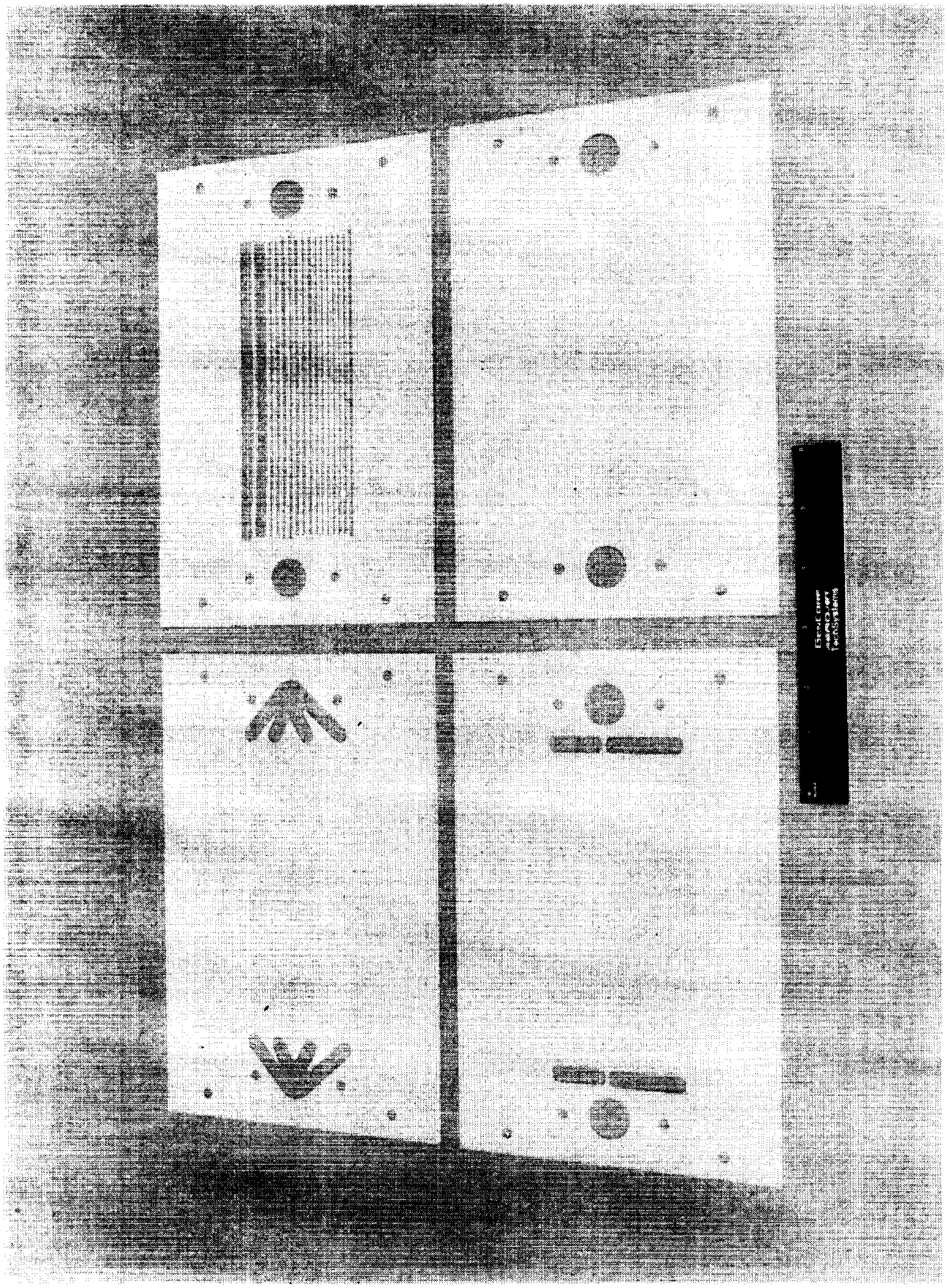

Figure 6.2.2.1 Prototype Silicone Nitride Platelets

ORIGINAL PAGE
BLACK AND WHITE PHOTOGRAPH

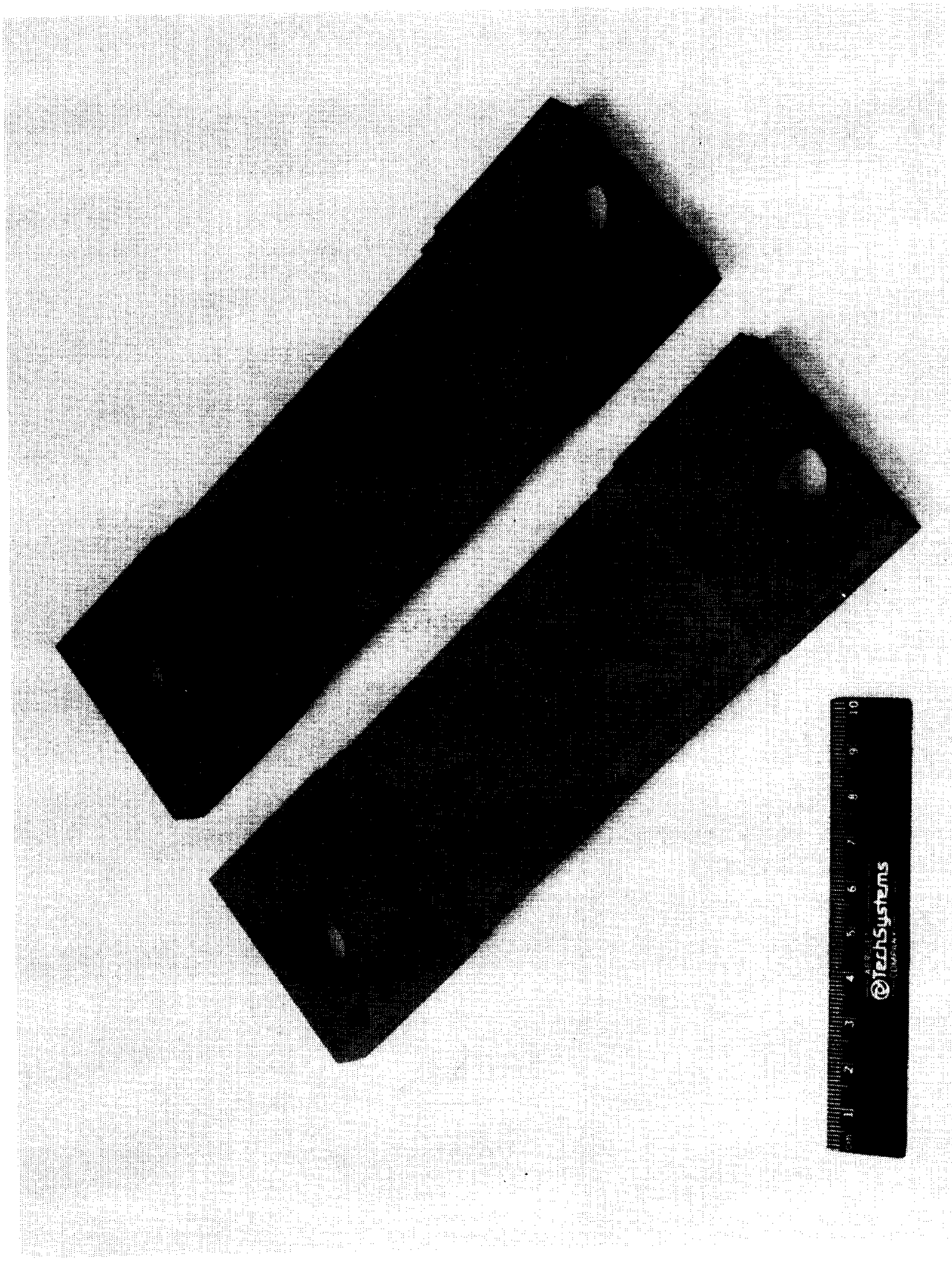

Figure 6.2.2.2 Alumina Prototype of the Final Regenerator Design

PAGE ____ INTENTIONALLY BLANK

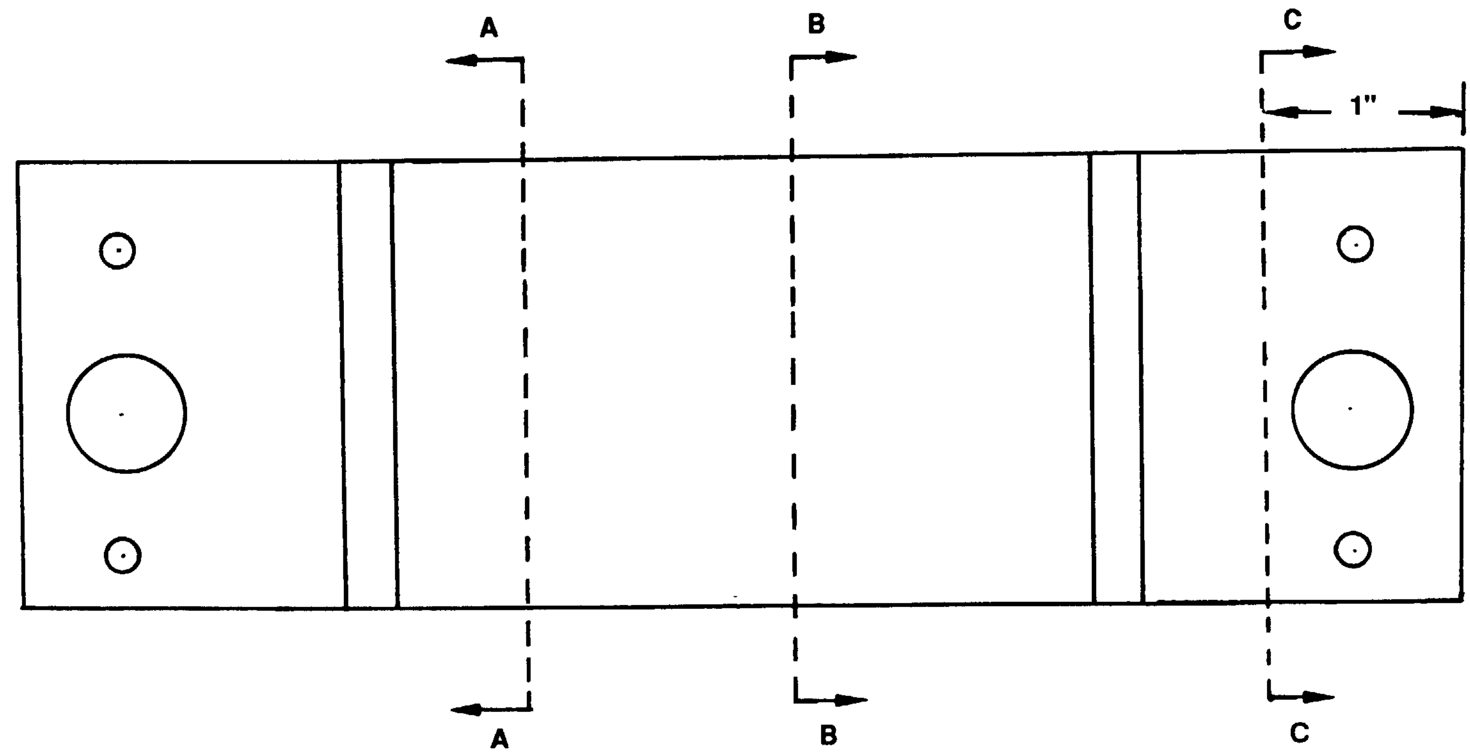

Figure 6.2.2.3 Location of Inspection Sections for Alumina Prototype Regenerator

PAGE_____INTENTIONALLY BLANK

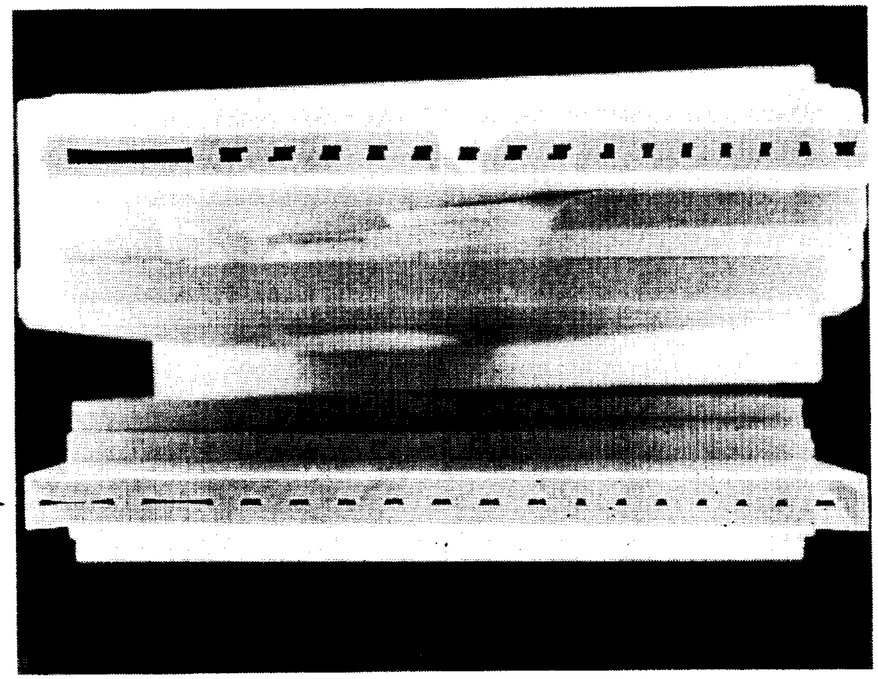

Figure 6.2.2.4 Cross Section of the First Alumina Regenerator (Top) and Current Pre-Prototype Version (Bottom)

tion of the wide channels can more easily be seen in Figure 6.2.2.5 and the excessive deformation of the smaller channels in Figure 6.2.2.6.

A temperature of 160 F was used during the lamination process. This is 10 degree F higher than the normal 150 F lamination temperature. This was done in an attempt to improve the bonding of the layers of the regenerator. With the higher temperature the bonding pressure was excessive and resulted in and the deformed channels and cracking seen in Figure 6.2.2.6.

Figure 6.2.2.7 shows the cross section of the manifold region, section C-C, Figure 6.2.2.3. Here more delamination and blistering can be seen. These are due to insufficient burn-out of the binder. If the binder is not completely removed during the burn-out step the higher temperature sintering operation can cause gases to expand without sufficient time for it to escape and bubbles or blisters are formed. This problem was alleviated in subsequent runs by allowing sufficient burn-out time before sintering.

A parametric study of the laminations of the channel section of the regenerator sections was performed at Coors in order to eliminate the sagging and cracking. The results of the study indicated that the problem was not the parameters used in the lamination but the number of times the parts experienced the pressure and temperature of lamination. In the first assembly sequence, the channel section was subjected to nine lamination cycles. A reassessment of the lamination procedure by Coors and Aerojet resulted in a lamination sequence whereby the channel section can be subjected to only one, two or three lamination cycles depending on the procedure used.

With the lamination problems resolved, three silicon nitride regenerators were punched and green laminated. These three regenerators constructed for process verification were delivered to Cercom for burnout and sintering. It was decided to confirm the burnout and sintering procedure by processing the three process verification articles one at a time. The first burned-out and sintered silicon nitride regenerator was delivered to Aerojet for evaluation. This process verification article was designated PV-1.

This first unit was slightly bowed and had a through crack in the vane section. These two features are related. Cercom reported that the crack was not present after the burnout procedure but did develop during the first sintering step. In order to be sure that the crack was not a random event the second silicon nitride part was processed in the same manner. This part was not cracked after the first sintering step but was also bowed. It is believed that the

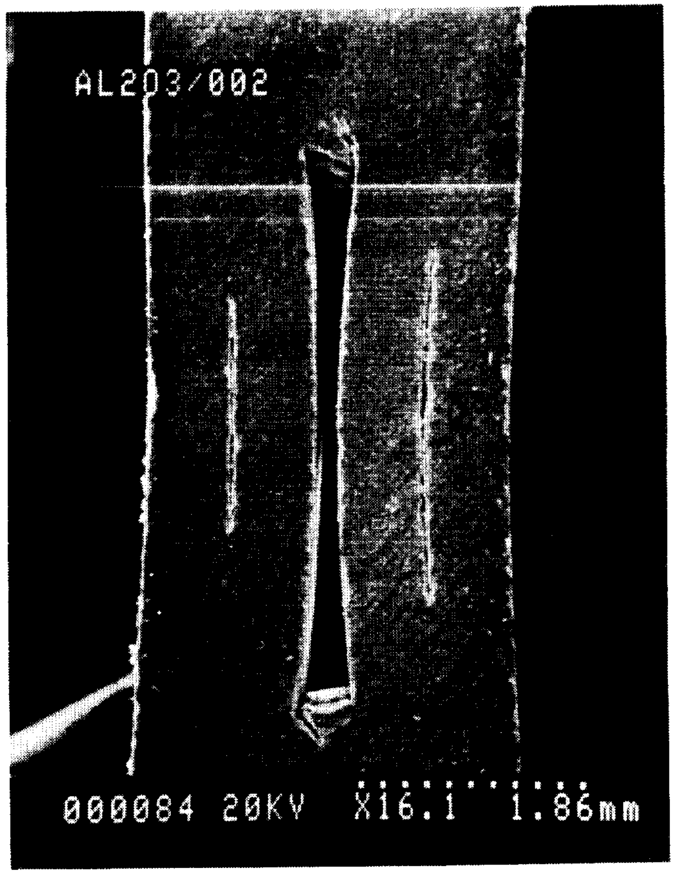

Section B-B

Figure 6.2.2.5 Detail of Sagging and Delamination of Wide Regenerator Channels

ORIGINAL PAGE
BLACK AND WHITE PHOTOGRAPH

A B

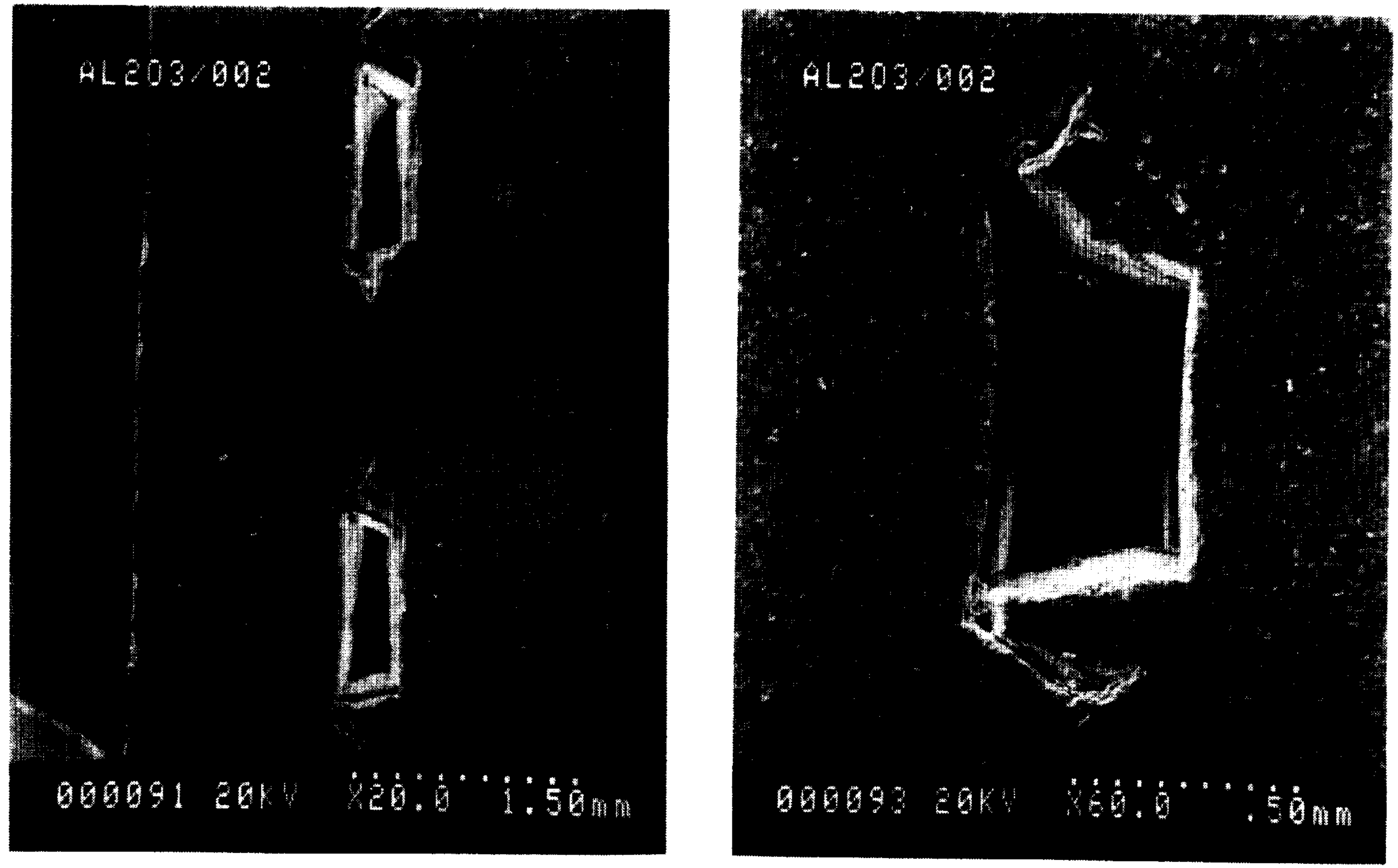

Section B-B

Figure 6.2.2.6 Prototype Alumina Regenerator. Deformation and Cracking is Due to Excessive Temperature and Pressure Used During Lamination

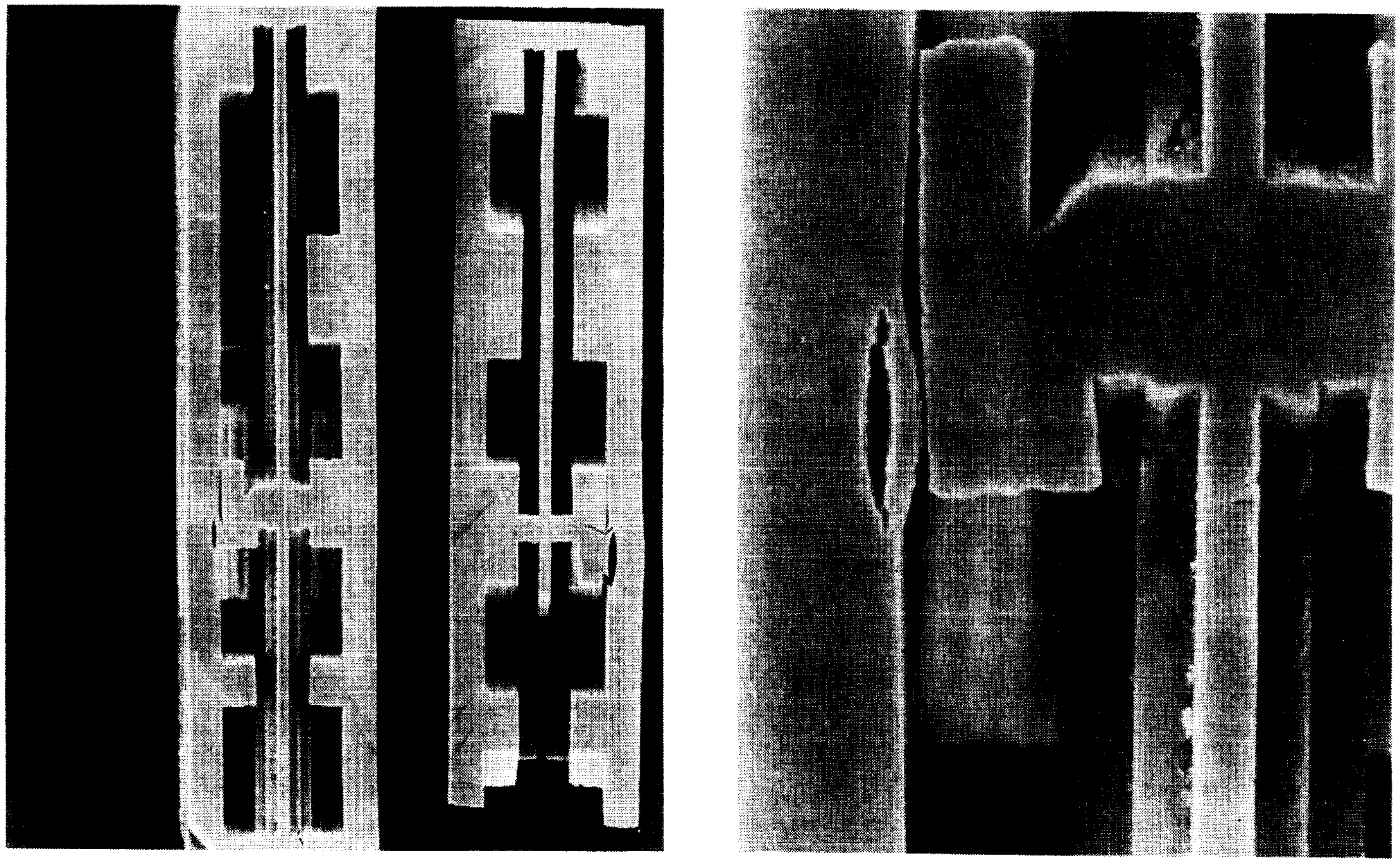

A B

Figure 6.2.2.7 Cross Section of Manifold Region, Section C-C, Figure 2. Blistering and Delamination Due to Incomplete Burn-Out

ORIGINAL PAGE
BLACK AND WHITE PHOTOGRAPH

PAGE ______ INTENTIONALLY BLANK

bowing and related cracking is due to uneven shrinking of the two sides of the regenerator during sintering. This is probably due to uneven temperature gradient in the sintering furnace or dragging of the part during sintering. In order to eliminate the possibility of a temperature distribution, the parts were packed in a sintering media during the sintering procedure. This helps distribute the heat around the part. The possible dragging of the part was addressed by a modification of the green silicon nitride furniture which is burned-out and sintered along with the regenerators.

The silicon nitride regenerator, PV-1, was sectioned through the vane and the manifolds in order to evaluate the laminations and design details. Figure 6.2.2.8a shows a macro-photograph of the cross section of the silicon nitride regenerator vane. As can be seen, it is a faithful execution of the design cross section shown in Figure 6.2.2.8b. Cross sections through the manifold are shown in Figure 6.2.2.9 and 6.2.2.10. Figure 6.2.2.9 is a section through the distribution manifold ends which sections small cords at the rounded ends. This causes the edges of the features to seem rougher than they actually are. Figure 6.2.2.10 which was sectioned normal to the edge shows the feature edges much straighter. The laminations are void free except in the areas evident in Figure 6.2.2.10. The void here is due to the lamination of an unsupported region. Above and below the void there is no support to press the platelets together and voids are formed. These voids were eliminated by an additional modification of the lamination sequence.

The second process verification article, PV-2, like PV-1, also had some bowing of the vane section, but, there is no visible cracking of the part. The third process verification article, PV-3, was destroyed during processing when a furnace controller malfunctioned.

Upon the completion of the evaluation of the process verification articles, four final articles were processed through final sintering, the seal faces diamond ground and delivered. Figures 6.2.2.11 and 6.2.2.12 shows these four regenerators ready for testing. These regenerators were measured and the dimensions are shown in Table 6.2.2.1.

6.3 REGENERATOR TESTING

6.3.1 <u>Objectives</u>

The objective of the test program is to demonstrate a proof-of-concept methane-cooled ceramic platelet regenerator. The operating conditions were selected to simulate a high speed engine environment. The temperature, pressure and chemical environment were

PAGE ____ INTENTIONALLY BLANK

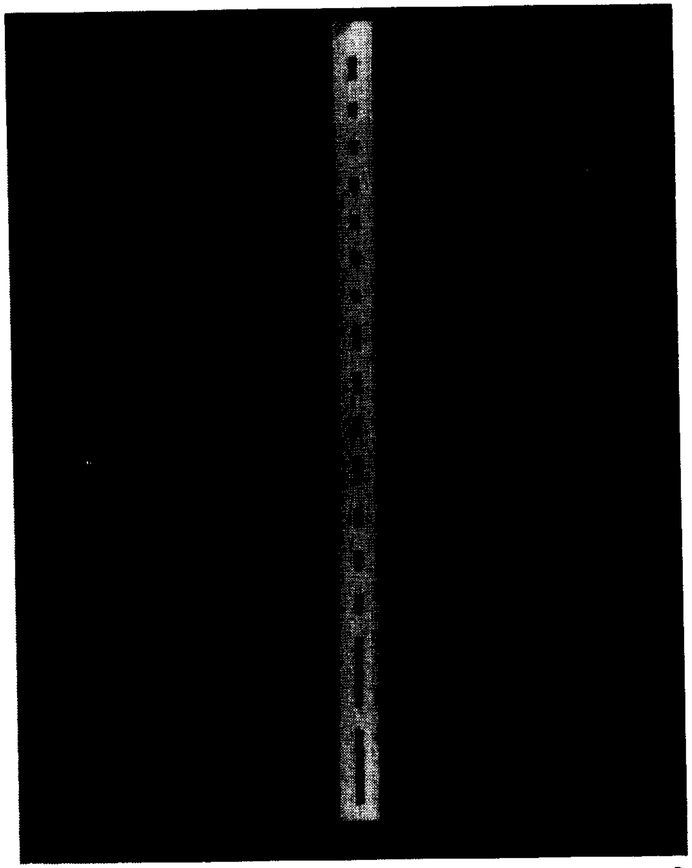

a.

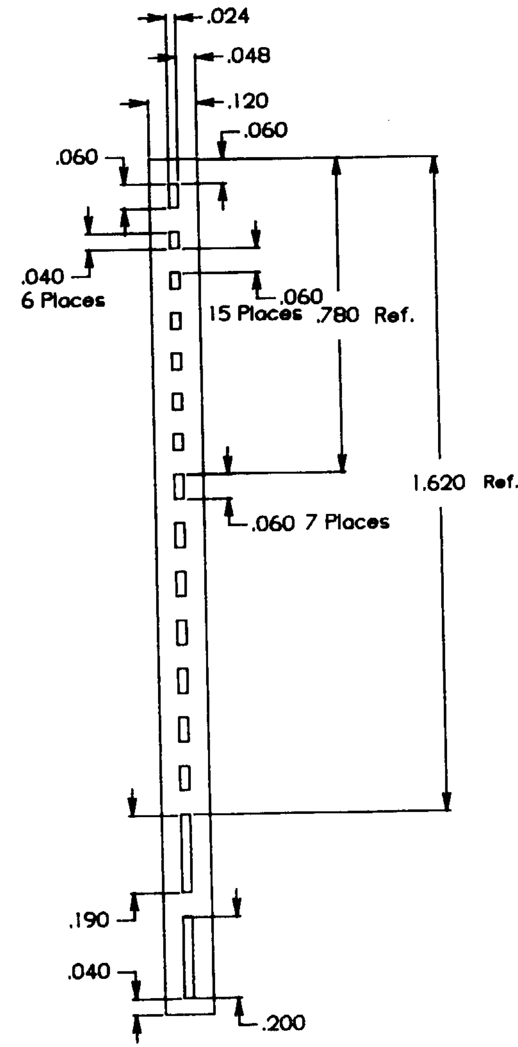

b.

Figure 6.2.2.8 (a) Cross Section of the First Article Silicon Nitride Regenerator Vane
(b) Design Cross Section of Vane Section

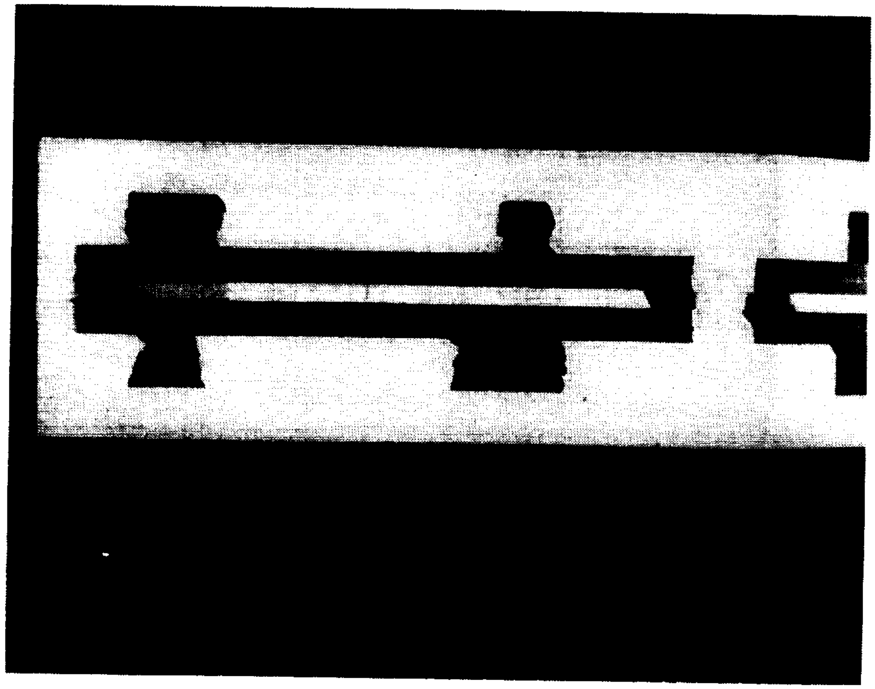

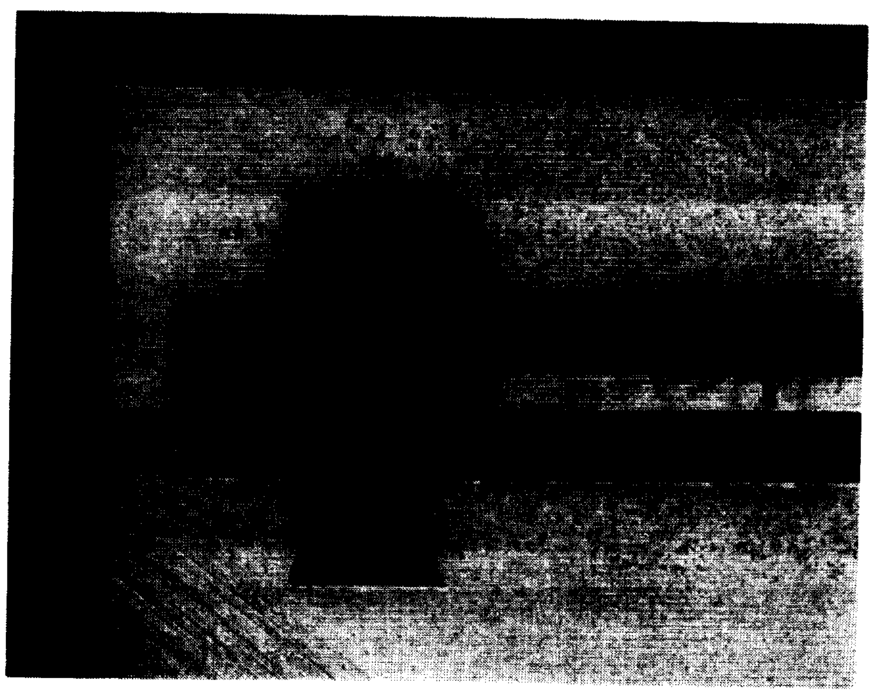

Figure 6.2.2.9 Section Through Manifold of Silicon Nitride Regenerator. Note the Laminations are Free From Voids. The Rough Feature Edges are Due to the Section Being a Small Cord Cut on Round Features

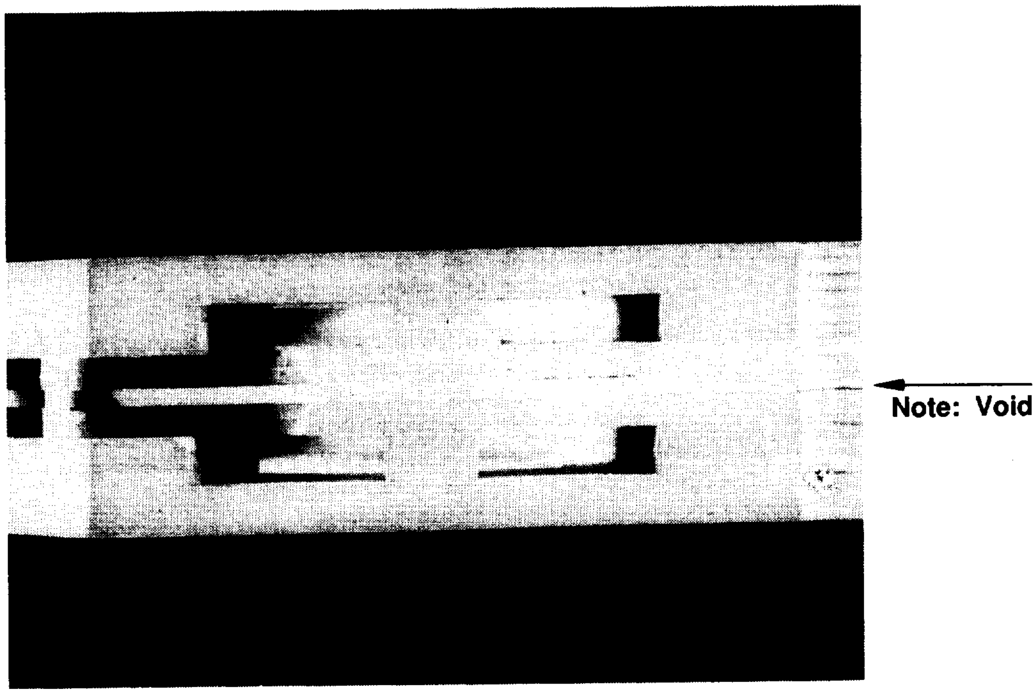

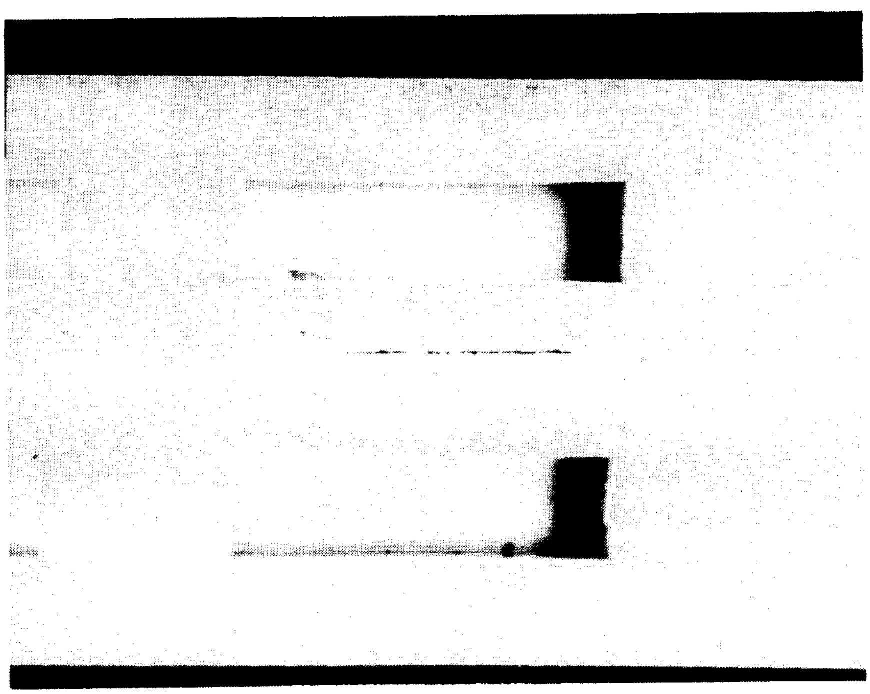

Figure 6.2.2.10 Section Through Manifold of Silicon Nitride Regenerator. Note the Straight Feature Edges. The Void is Due to the Lamination of an Unsupported Region

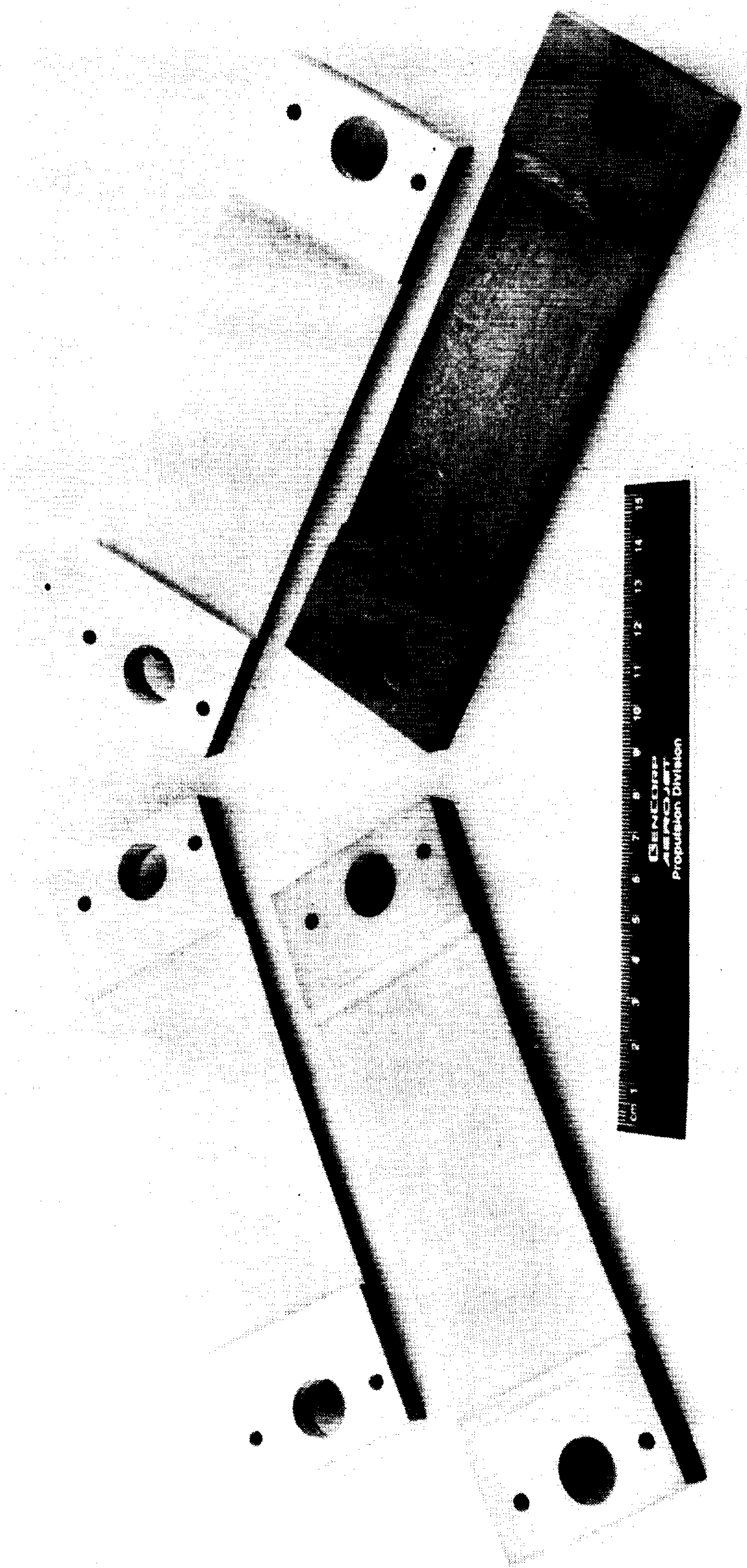

Figure 6.2.2.11 Regenerators

ORIGINAL PAGE
BLACK AND WHITE PHOTOGRAPH

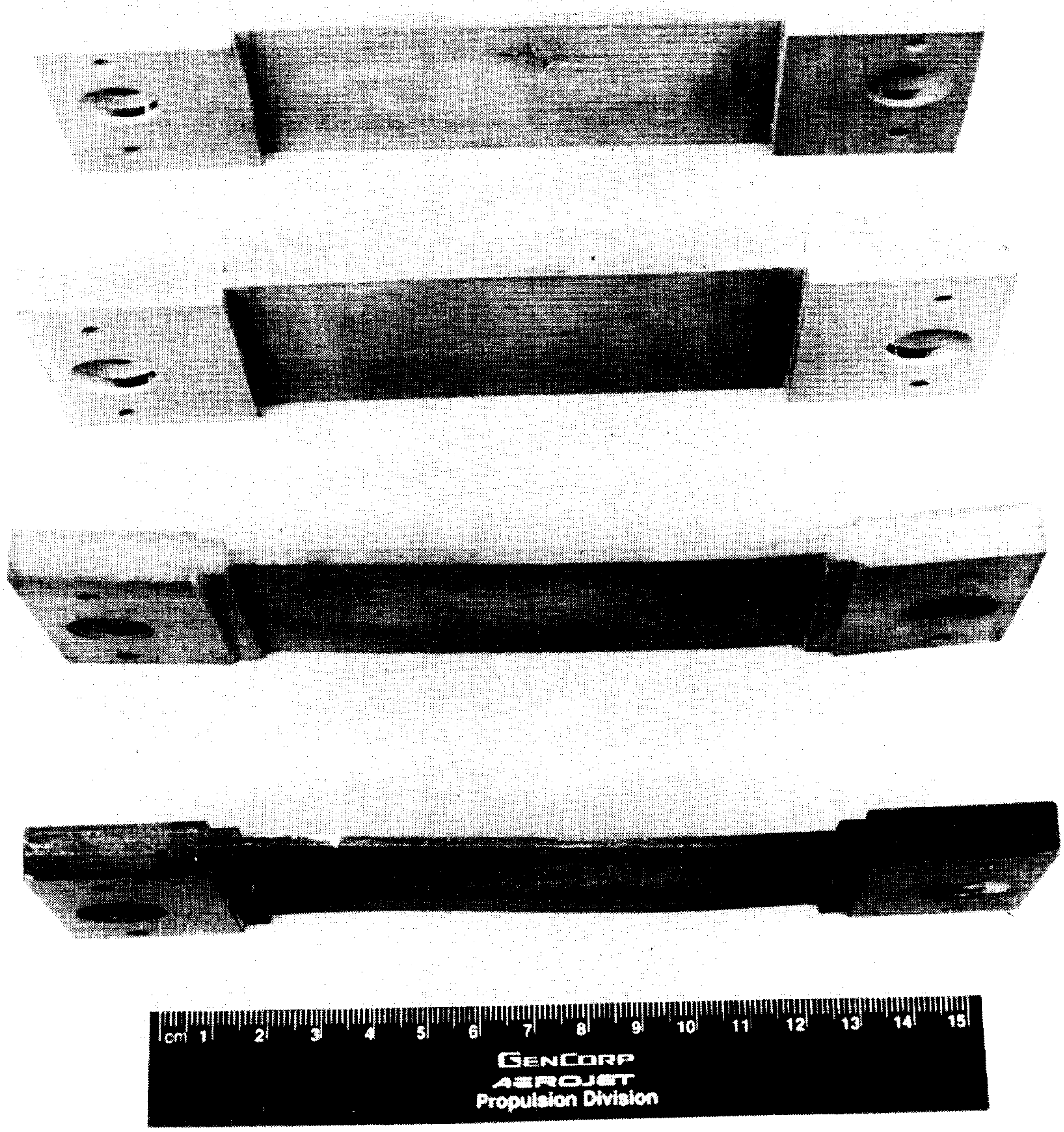

Figure 6.2.2.12 Regenerators

ORIGINAL PAGE
BLACK AND WHITE PHOTOGRAPH

PAGE ____ INTENTIONALLY BLANK

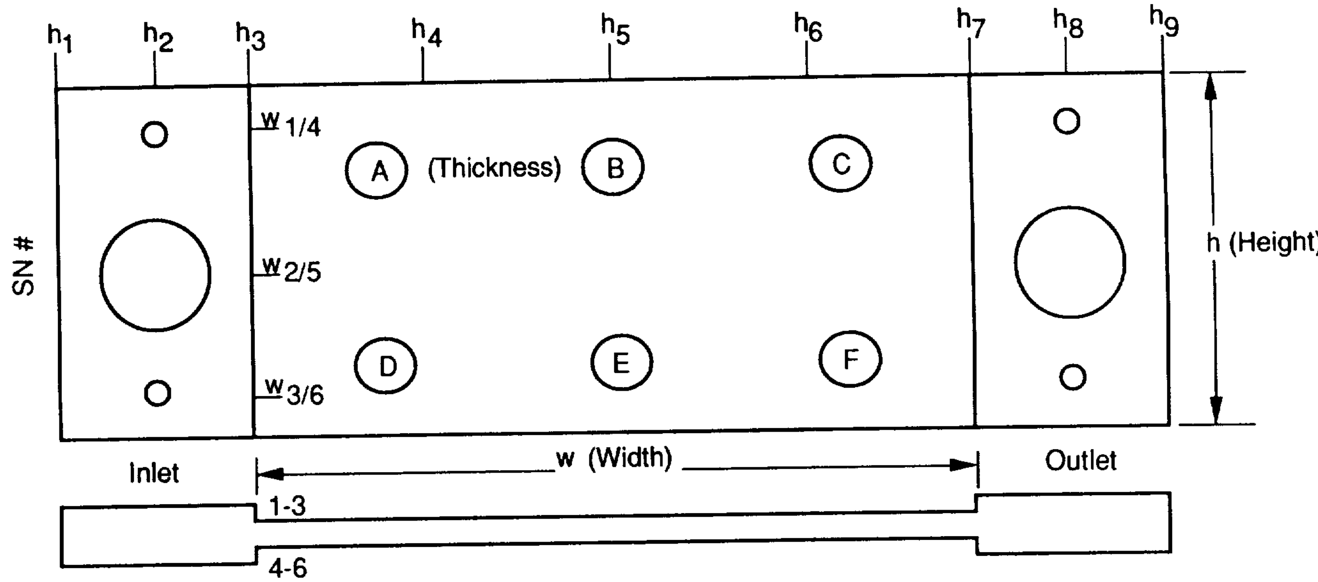

TABLE 6.2.2.1 Dimension of Regenerator Vanes SN-1, SN-2, SN-3 and SN-4

	SN-1	SN-2	SN-3	SN-4
A	.1149	.1165	.1160	.1115
B	.1142	.1155	.1165	.1115
C	.1150	.1158	.1150	.1115
D	.1130	.1157	.1175	.1145
E	.1134	.1154	.1165	.1150
F	.1138	.1161	.1155	.1140
h_1	2.148	2.206	2.2345	1.99
h_2	2.136	2.186	2.2100	1.9855
h_3	2.1285	2.178	2.192	1.9760
h_4	2.1135	2.166	2.1665	1.9600
h_5	2.110	2.156	2.1585	1.9575
h_6	2.1175	2.1640	2.1565	1.9555
h_7	2.1295	2.1865	2.1695	1.9665
h_8	2.1365	2.1950	2.1730	1.9825
h_9	2.150	2.1995	2.1745	1.9928
w_1	4.0585	4.124	4.0830	4.0065
w_2	4.0765	4.099	4.0615	4.0135
w_3	4.0970	4.094	4.0635	4.0065
w_4	4.0670	4.124	4.1195	3.9770
w_5	4.083	4.118	4.1035	3.9955
w_6	4.055	4.103	4.0950	4.0035

selected to demonstrate the feasibility of a lightweight, high-efficiency regenerator for high-speed propulsion.

6.3.2 Test Facility Description

Performance testing was accomplished in the Aerojet Heat Exchanger Test Facility. This facility uses an air-fuel burner capable of providing up to 1,250,000 Btu/hr. A forced draft blower supplies pressurized air for combustion. Combustion gases at temperatures up to 3100 F pass through a water cooled nozzle section at 500 to 600 fps, providing a realistic simulation of the ATR regenerator environment.

The test facility set up consisted of a refractory lined combustion chamber and a water cooled nozzle section to hold the test piece, Figures 6.3.2.1 and 6.3.2.2. North American Manufacturing fabricated the refractory lined combustion chamber for use with an existing burner, blower and control system, a detailed drawing of the combustion chamber is contained within the appendix. The chamber has an inside diameter of 12 inches, and outside diameter of 30 inches and a length of about 5 feet. These dimension allowed sufficient length and diameter for flame burn out and sufficient wall thickness to maintain a 3000 F wall on the inside and 350 F on the outside. Standing on two foot long legs, the chamber is high enough to mount the burner underneath and allow access for plumbing.

The water cooled section is a non-pressurized water circulation system with a flow acceleration nozzle which is located in the discharge of the combustor. This is shown in Figures 6.3.2.3 and 6.3.2.4 with detailed drawing shown in the appendix. The 3.5 in. by 0.60 in. rectangular duct increases the gas velocity to 500 to 600 fps in the test section. A water cooled 0.75 in. diameter baffle tube is positioned ahead of the test section to produce mixing and turbulence of the combustion gases. Pt-30Rh/Pt-6Rh, Type B, thermocouples positioned in the gas stream record the gas temperature. One of the side walls of the water cooled high-velocity duct contains 6 view port for monitoring the test specimen surface temperature. Surface temperatures of the regenerator were measured by a optical pyrometer and Type B thermocouples.

The test specimens were held in place by the means of stainless steel clamps fixed to the outside of the high velocity duct and by flanges containing gold coated metal seals. This arrangement is seen Figures 6.3.2.5, 6.3.2.6, 6.3.2.7 and 6.3.2.8 with the detailed drawings in the appendix. The coolant lines are affixed to the regenerator by means of flanges seen in the figures.

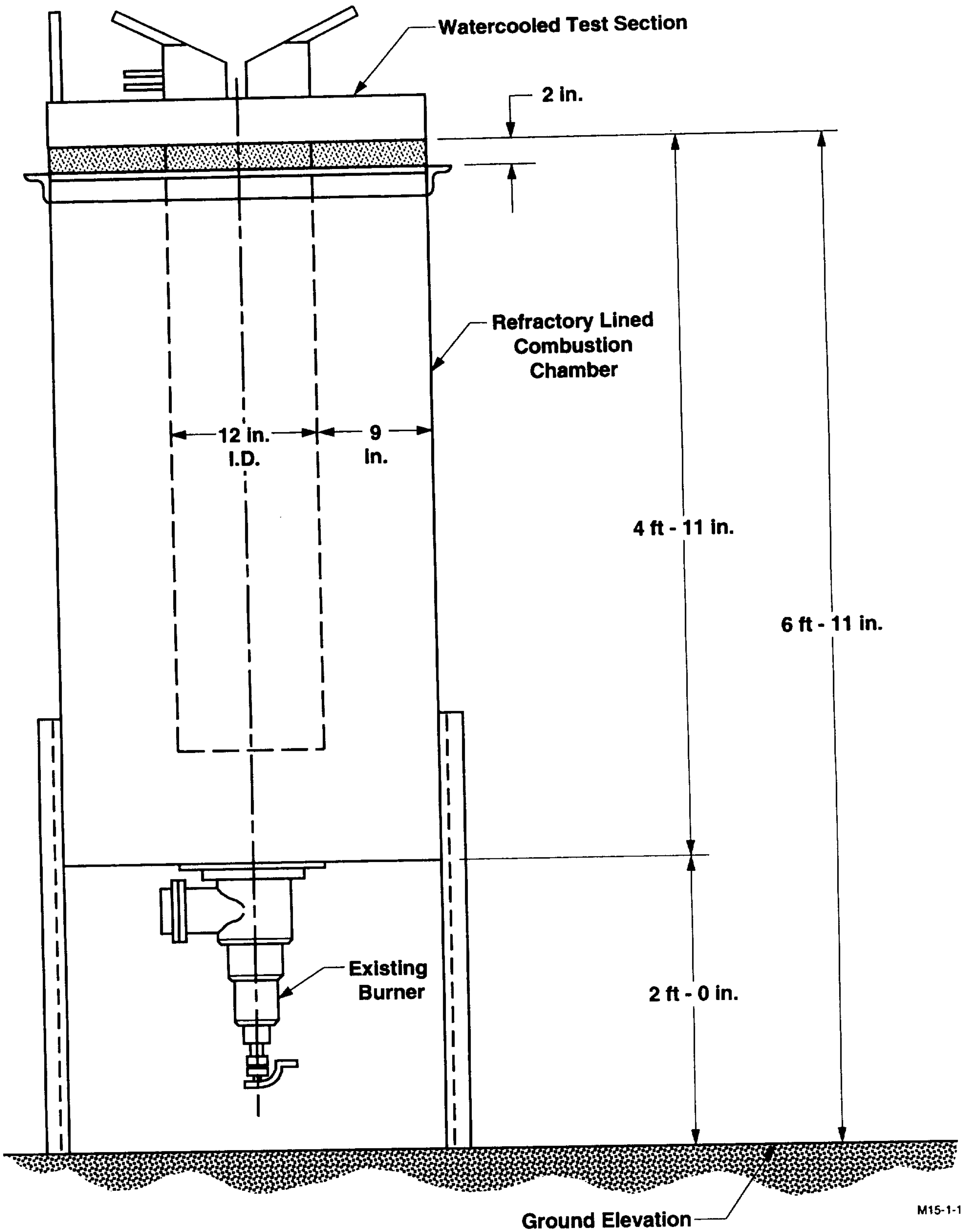

Figure 6.3.2.1 Refractory Lined Combustion Chamber and Watercooled Test Section

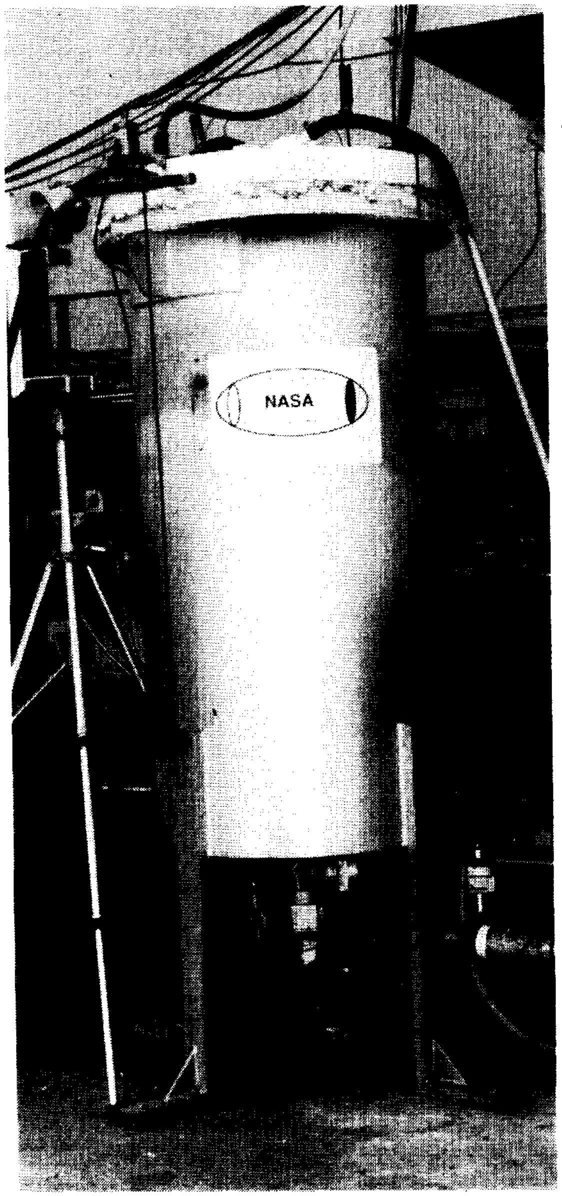

Figure 6.3.2.2a.

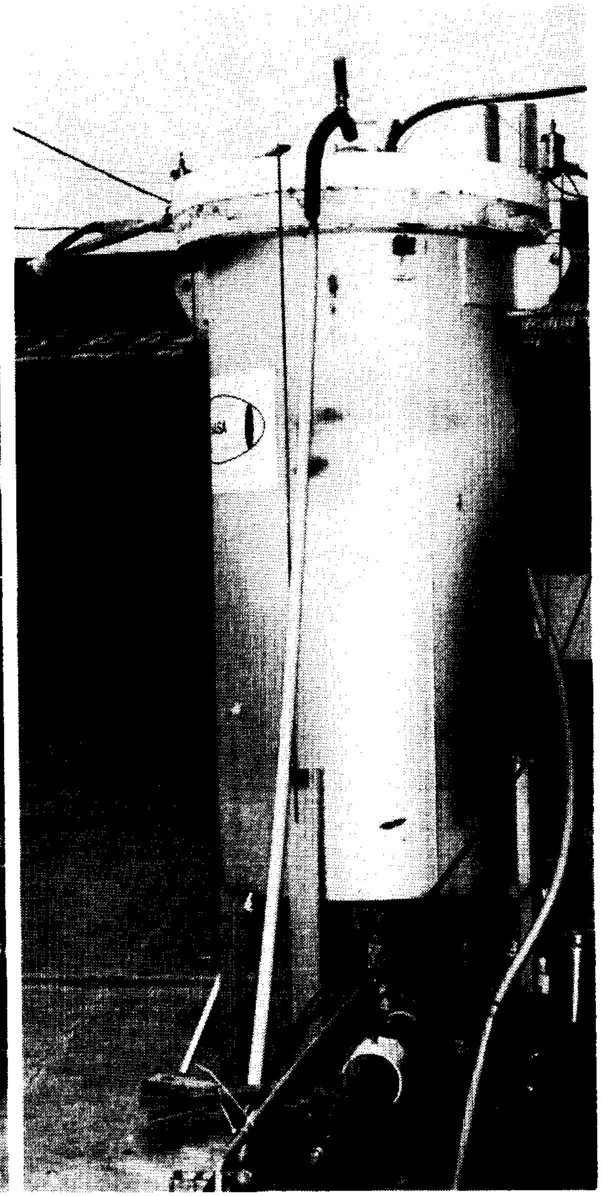

Figure 6.3.2.2b.

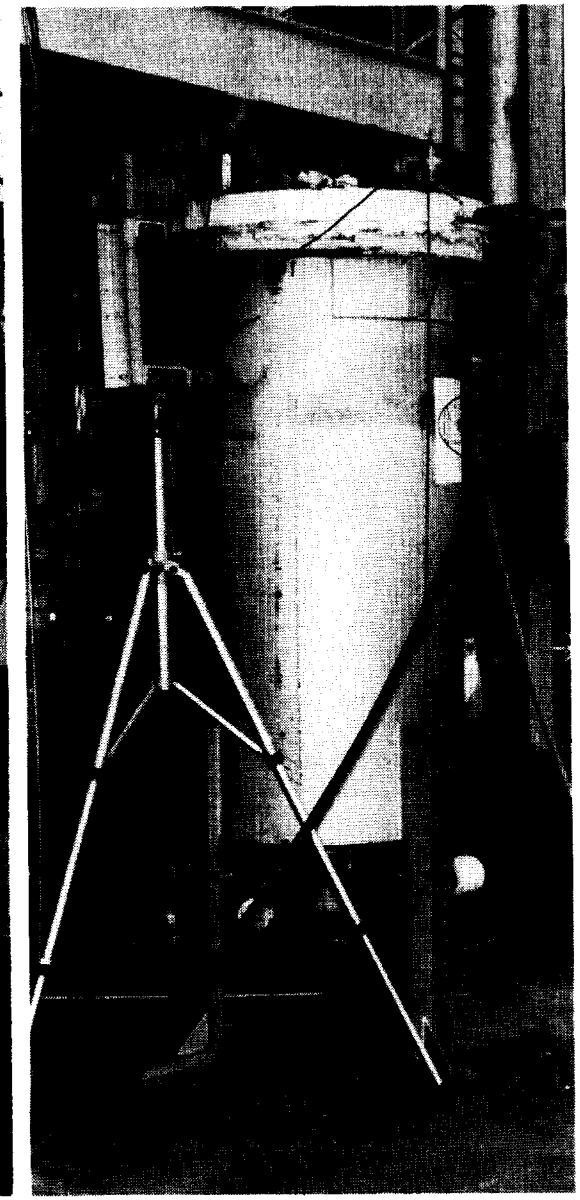

Figure 6.3.2.2c.

Figure 6.3.2.2. Combustion Chamber and Watercooled Test Section Setup in Test Area

ORIGINAL PAGE
BLACK AND WHITE PHOTOGRAPH

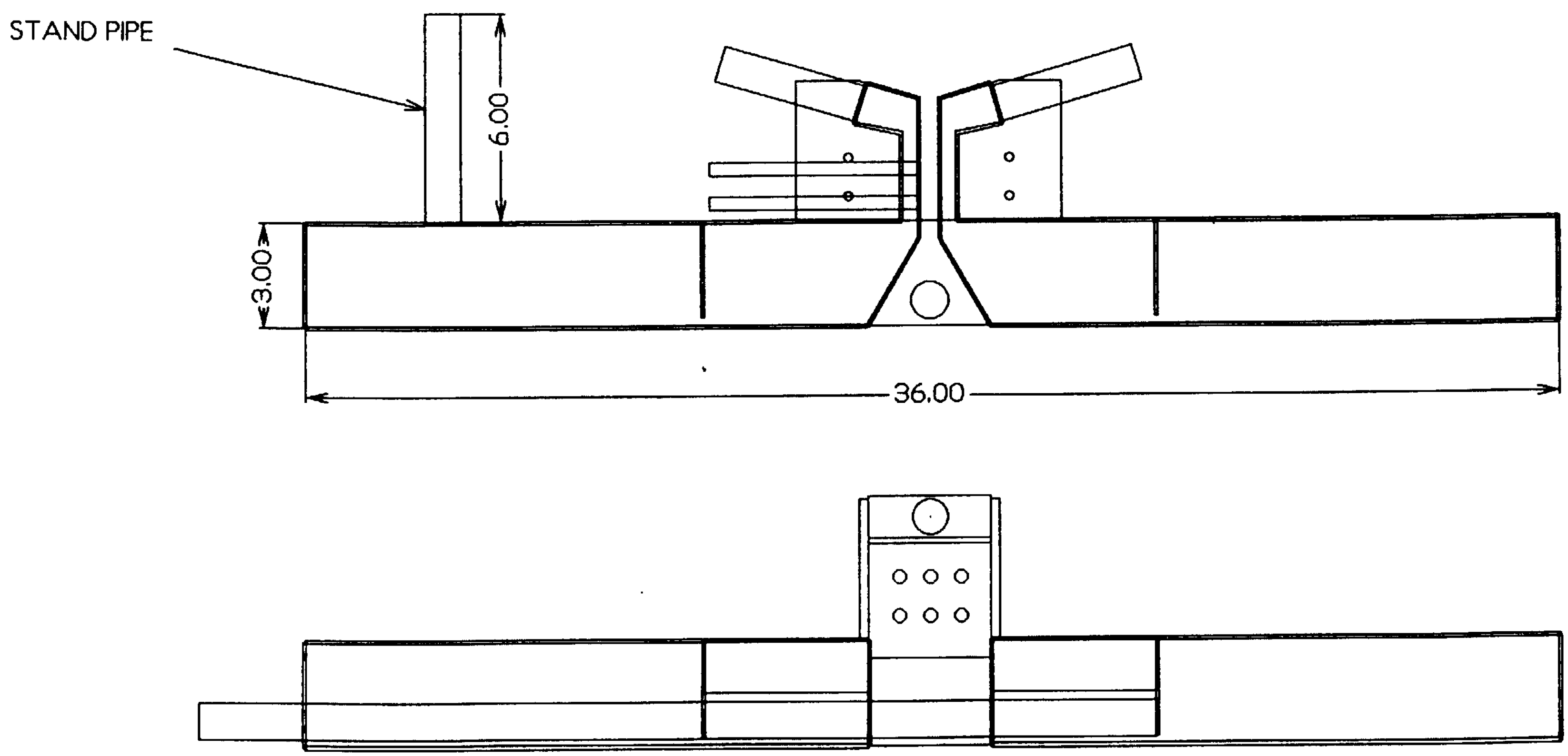

Figure 6.3.2.3. Sketch of Water Cooled Test Section

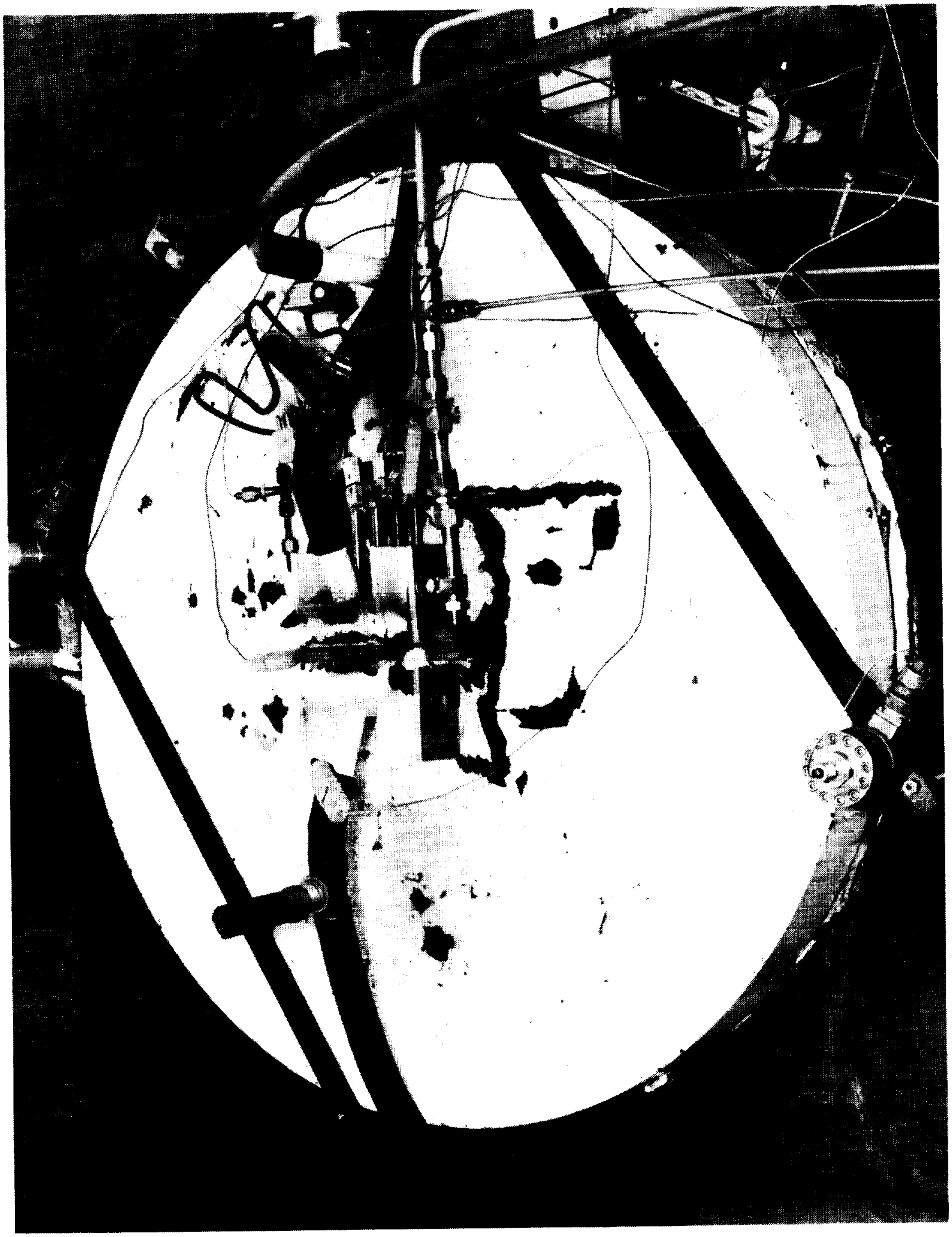

Figure 6.3.2.4. Top View of Water Cooled Test Section After Completion of Testing

ORIGINAL PAGE
BLACK AND WHITE PHOTOGRAPH

PAGE_______INTENTIONALLY BLANK

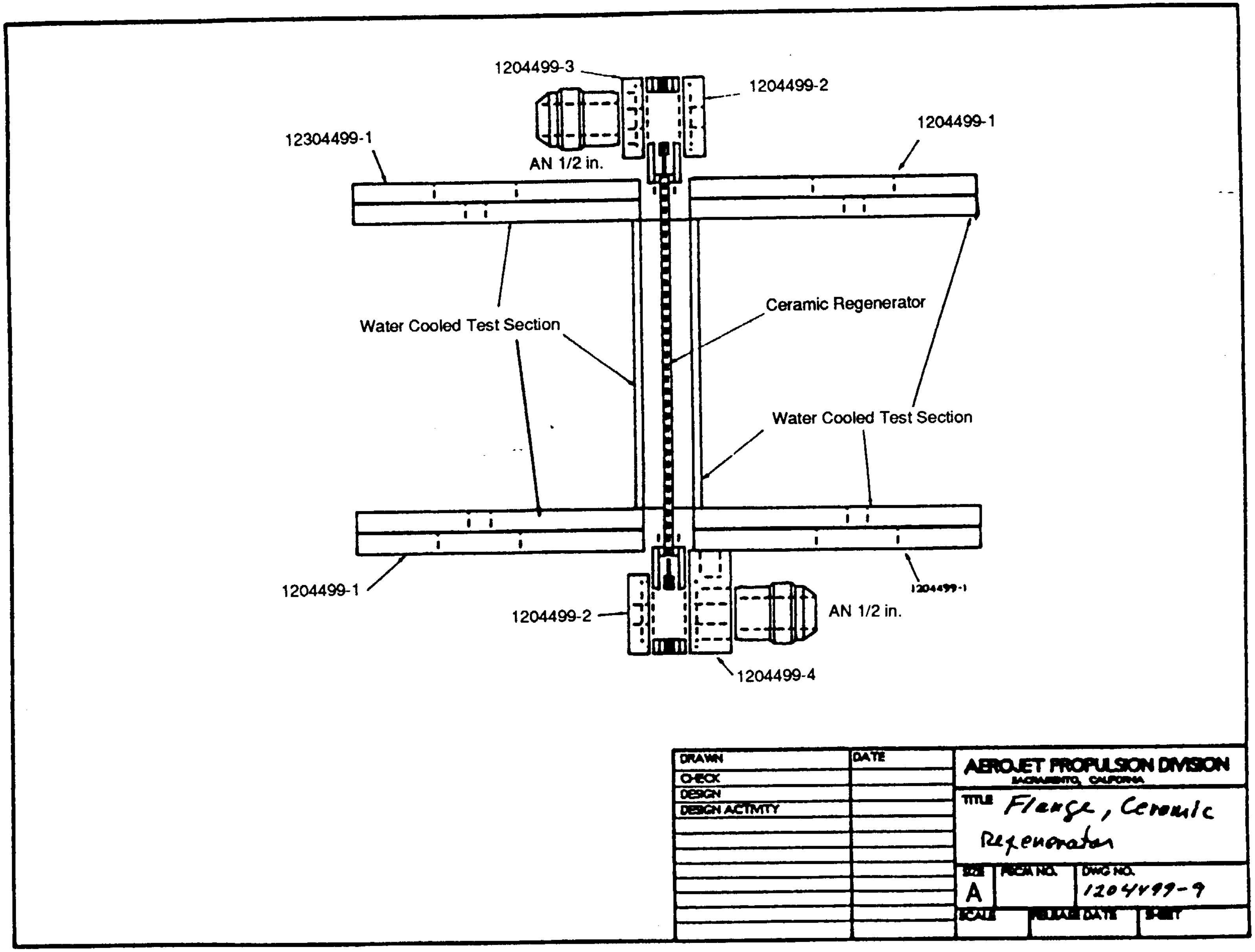

Figure 6.3.2.5. Sketch of Test Section With Vane and Flanges Exploded in Place

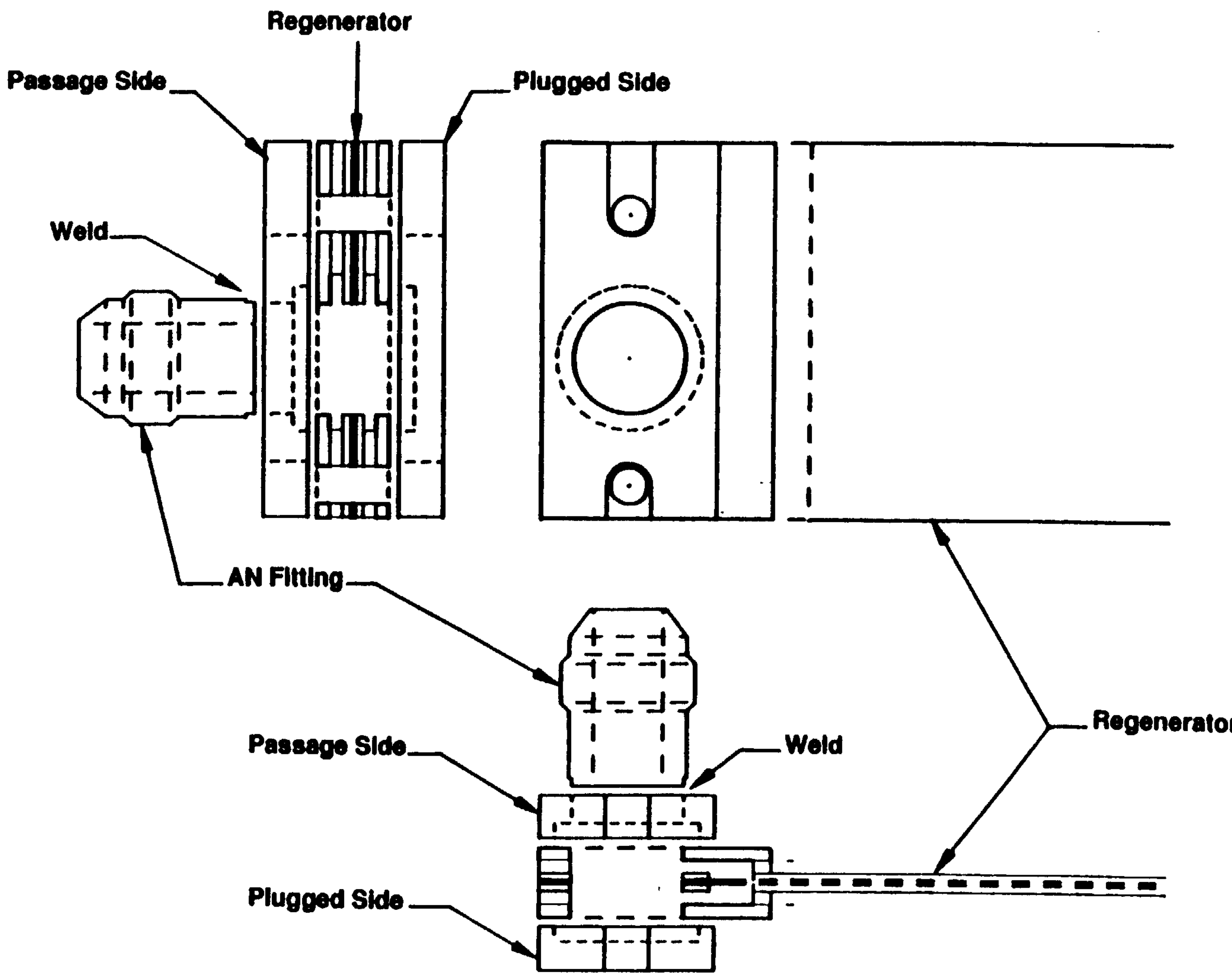

Figure 6.3.2.6 Exploded View of Inlet and Exit Flanges for Ceramic Regenerator

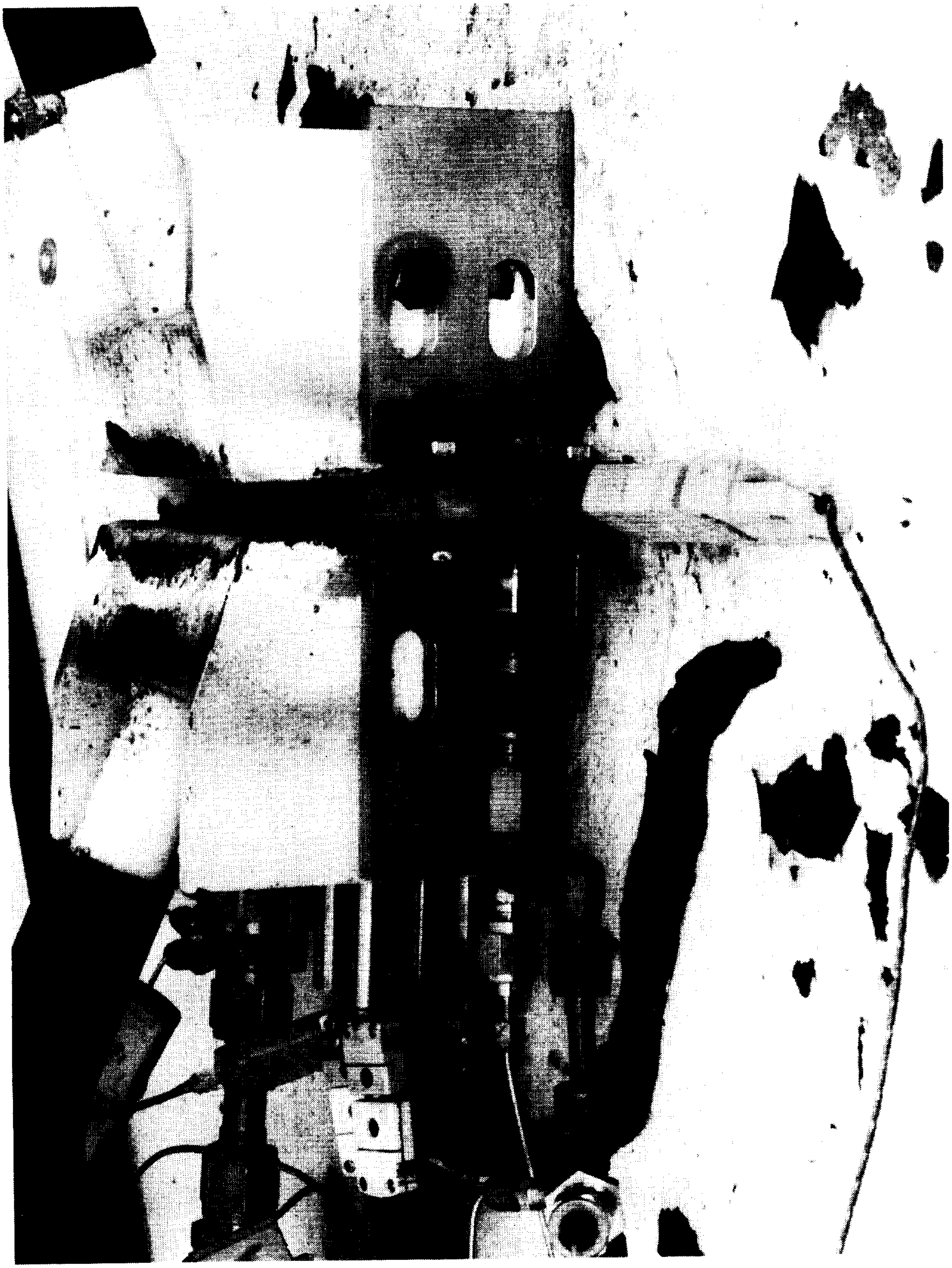

Figure 6.3.2.7 Ceramic Regenerator Vane in Place in Test Section

ORIGINAL PAGE
BLACK AND WHITE PHOTOGRAPH

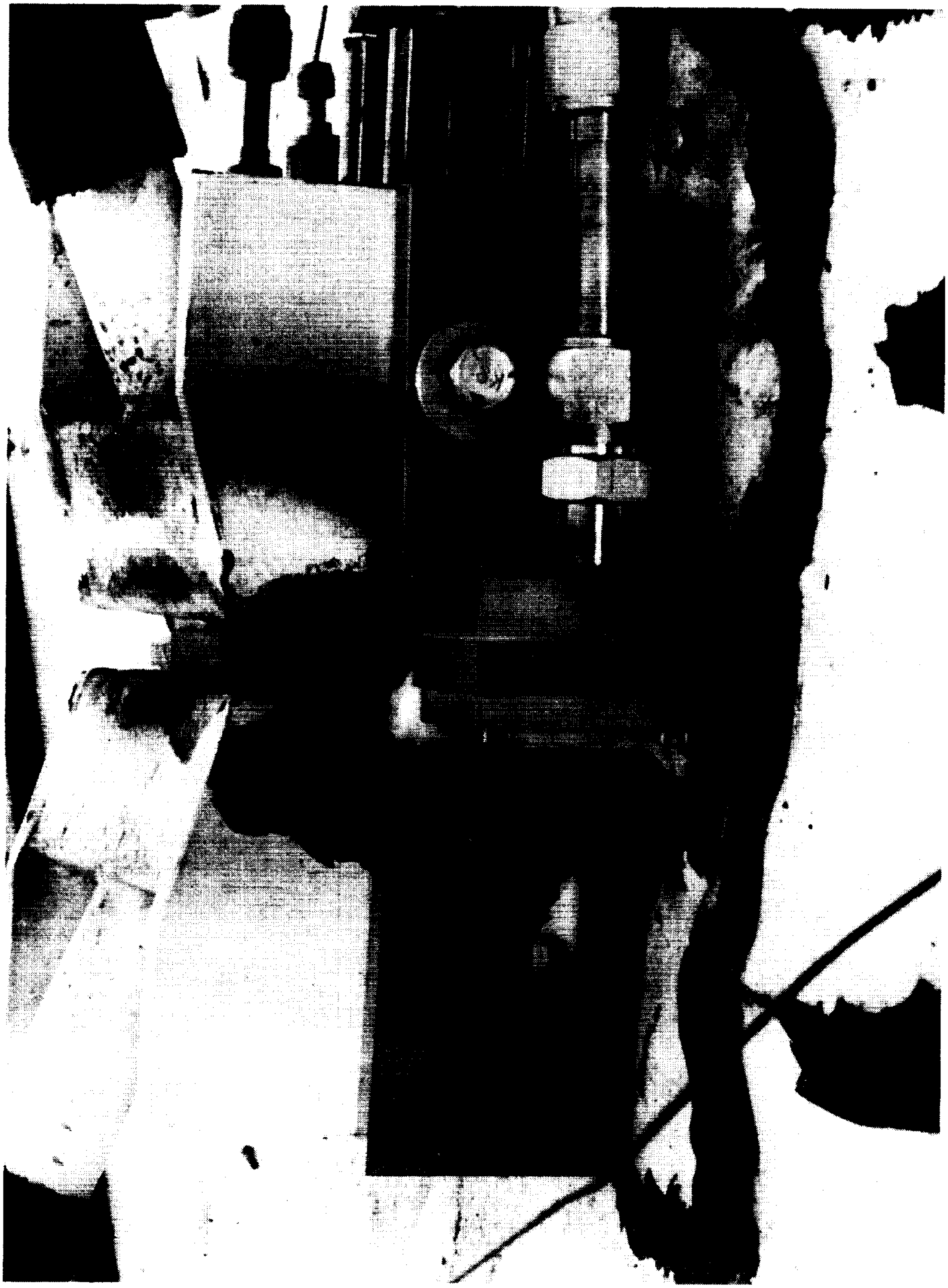

C0291 0740

Figure 6.3.2.8. Close-Up View of Regenerator Vane in Test Section

ORIGINAL PAGE
BLACK AND WHITE PHOTOGRAPH

6.3.3 Results

6.3.3.1 Leak, Proof and Burst Testing

Leak testing consisted of pressurizing the parts with 50 psig GN_2 and then applying a leak check solution and watching for bubbles. Regenerators SN-1 and SN-3 were leak free by this method while SN-2 has a small weeping leak at the manifold interface. The forth regenerator, SN-4, has a delaminated area at one of the manifolds and was not subjected to the GN_2 procedure. The delamination in SN-4 appears to be the result of a fabrication error. The edge of the part was trimmed excessively close causing a lack of support in the region and the delamination.

Proof testing consisted of pressurizing the regenerators with water to 900 psig which is 1.5 times the working pressure of 600 psig. The pressure was then held at 900 psig for five minutes. Regenerators SN-1, SN-2 and SN-3 passed this proof test, SN-4 was not tested. SN-2 which had the weeping leak did not leak when pressurized with water during this test.

Permeability testing consisted of pressurizing the two non-leaking regenerators with 600 psig GN_2 and recording the pressure decay over a period of 30 minutes. At the same time leak check solution was used on the parts. Only parts SN-1 and SN-3 were tested in this manner. SN-1 had a pressure decay of 110 psi from 606 psig to 496 psig. SN-3 had a pressure decay of 120 psi from 600 psig to 480 psig. A concerted effort was made to assure that the isolation valve and O-ring seals were leak free during this testing and the pressurized volume was small as possible. No leaks were detected with the leak check solution during the testing of these two parts. The cause of the pressure decay was not determined. The conclusion from these tests are the permeability of the silicon nitride assemblies is quite low but not quantified with the test procedure.

6.3.3.2 Hot-Fire Testing

A summary of the hot-fire tests conducted is given in Table 6.3.3.1. A summary of the program goals and accomplishments are provided in Table 6.3.3.2. Typical heat up transients during the cyclic tests are shown in Figure 6.3.3.1. In Test 32 the maximum exposed surface temperature of the $Si_3 N_4$ reaches 2023°F in 60 sec. while the GN_2 discharge temperature reached 543°F with a combustion gas temperature of 2432°F The vane surface temperature charge rate is shown in Figure 6.3.3.2 superimposed on the vane surface temperature. As can be seen, the rates of heating and cooling of the silicon nitride exceed 4000°F/min.

Table 6.3.3.1 Ceramic Regenerator Program Test Duration Summary. All Tests With GN_2 Coolant Except Where Noted With CH_4.

Ceramic Regenerator Test Summary.

I.D.	Test No.	Duration (hr:mim:sec)	I.D.		Test No.	Duration (hr:mim:sec)
SN-1	1	00:05:26	SN-3		1	00:01:46
					2	01:46:00
				CH4	3	00:10:12
SN-2	1	01:48:36			4	01:23:42
	2	00:17:16		CH4	5	00:10:19
	3	00:34:38			6	00:05:23
	4	00:37:57		CH4	7	00:10:21
	5	00:03:24			8	00:05:31
	6	00:46:26		CH4	9	00:10:28
	7	00:06:41			10	00:06:01
	8	01:30:43		CH4	11	00:01:00
	9	00:11:37			12	00:00:15
	10	00:10:02		CH4	13	00:00:12
	11	00:47:15			14	00:00:17
	12	00:12:21		CH4	15	00:05:46
	13	00:05:00			16	00:00:25
	14	00:06:01		CH4	17	00:10:58
	15	00:04:46			18	00:12:05
	16	00:06:00		CH4	19	00:10:21
	17	00:37:00			20	00:08:39
	18	00:15:00		CH4	21	00:11:58
	19	00:04:18			22	00:04:18
	20	00:04:31			23	112:04:47
	21	00:04:46				
	22	00:33:39			Total Time	117:23:44
	23	00:02:55				
	24	00:03:28				
	25	00:02:45				
	26	00:03:56				
	27	00:08:37				
	28	00:00:56				
	29	00:00:55				
	30	00:01:16				
	31	00:00:50				
	32	00:01:05				
	33	00:00:35				
	34	00:00:42				
	35	00:00:51				
	36	00:00:43				
	37	00:00:30				
	38	00:00:45				
	39	00:00:50				
	40	00:00:35				
	Total Time	09:40:11				

GN2 Used in All Tests Except Where Noted.

TABLE 6.3.3.2 ATR Ceramic Regenerator Program
Summary of Program Accomplishments

	Goal	Accomplished
Fabrication	4 Parts	6 Parts
Proof Pressure	900 psi	>900 psi
Leakage	None	None (2 Parts)
Burst Pressure	>900 psi	1575 psi (1 Part)
Hot Testing	2 Parts	2 Parts
Life	100 Hrs	>117 Hrs
Max. Surface Temperature	>2000°F	2339°F
Max. Outlet Temperature	>1250°F	1415°F
No. Thermal Cycles	36	40 (1 Part)

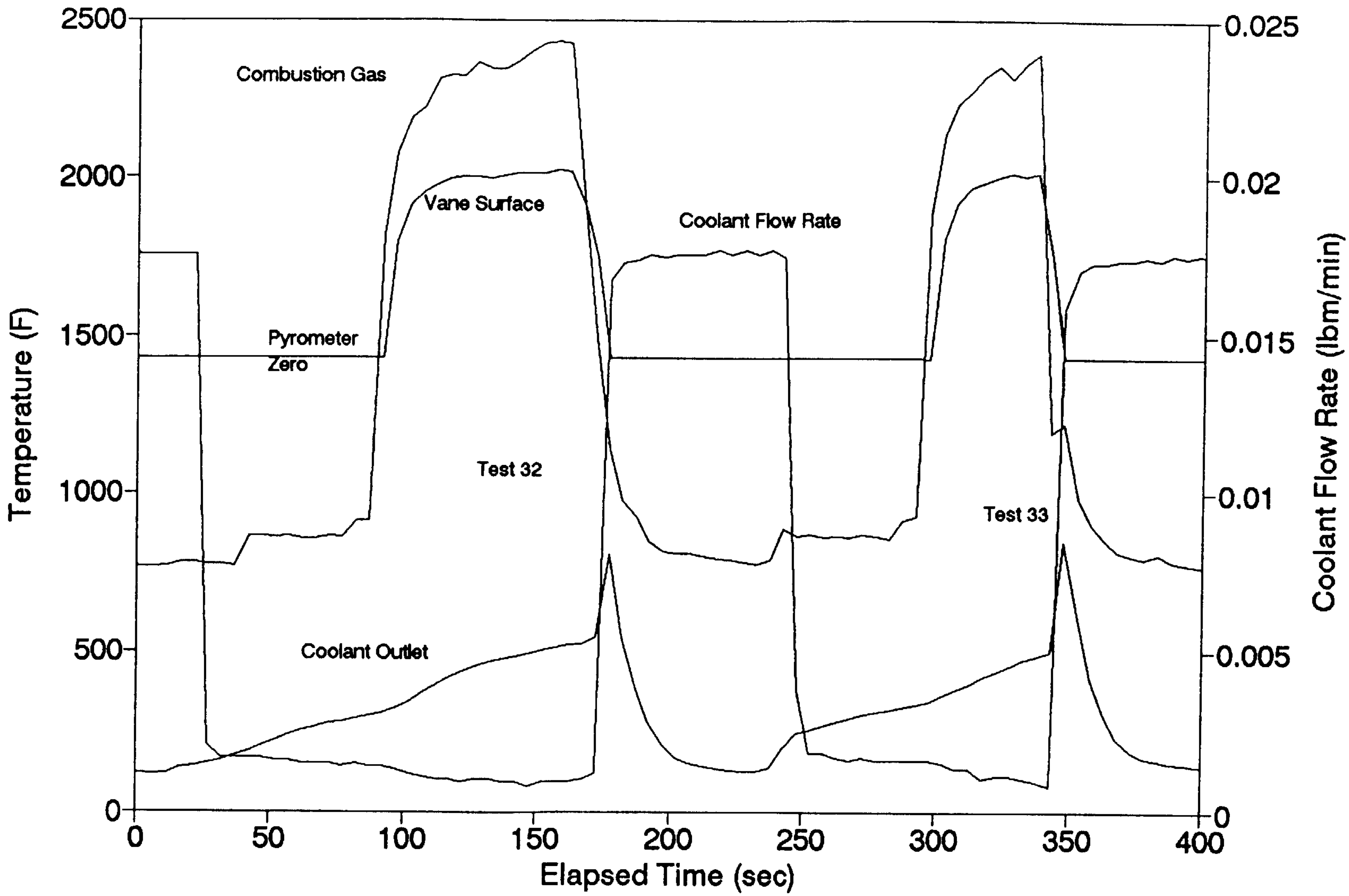

Figure 6.3.3.1 Typical Heat Up and Cooling Transients During the Thermocycling Tests. Tests 32 and 33 on Part SN-2

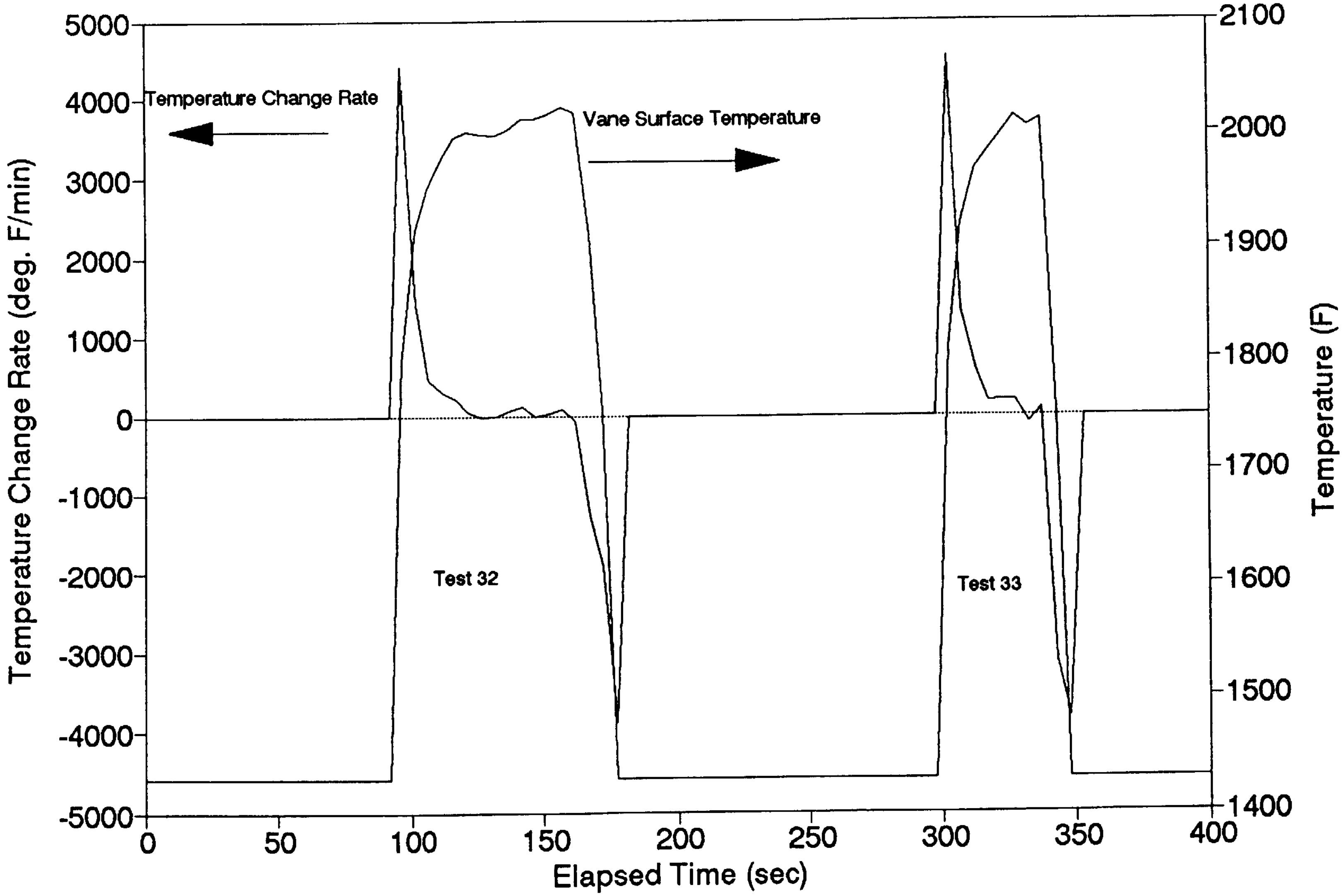

Figure 6.3.3.2 Heating and Cooling Rates of the Surface of the Silicon Nitride During Tests 32 and 33

Test part SN-1, Figures 6.3.3.3 and 6.3.3.4, fractured during an initial heat-up cycle. Figure 6.3.3.5 shows heating and cooling cycles for SN-2 tests #27 through 40. The pyrometer shows the surface to reach 2000°F and the gas temperature 2400°F. The coolant discharge temperature and heat flow corresponding to these cycles is also shown in the figure. The temperature at restart based on these measurements is about 120°F. Regenerator SN-2, Figures 6.3.3.6 and 6.3.3.7, survived 40 thermal cycles for a total test exposure time of 09:40:11 (hr:min:sec) before fracturing. Details of the fracture are shown in Figures 6.3.3.8 and 6.3.3.9. The fracture is believed to have initiated at the vane/manifold interface during the rapid heating during cycle 40.

Part number SN-3, Figures 6.3.3.10 and 6.3.3.11 underwent 10 methane exposure tests and a long duration test of 112:04:47 (hr:min:sec), for a total exposure time of 117:23:44 (hr:min:sec). The thermal maps for these tests are shown in Figure 6.3.3.12 through 6.3.3.17. Figure 6.3.3.12 shows the thermal profiles for Test 9. The combustion gas is 3250°F, the regenerator maximum temperature is 1900°F to 2000°F; and the methane is heated from 70°F to 1050°F, Figure 6.3.3.13 and 6.3.3.14. The steady temperatures during the hold period from 350 sec. to 950 sec. indicate that the methane is not decomposing as a result of the high wall temperatures. Rapid decomposition of methane into $2H_2$ + C has been reported as low as 1200°F when in contact with some metals. Post-test evaluation indicated no visual evidence of carbon on the channel surface. Figures 6.3.3.16 through 6.3.3.17 show the results of the 112 hours life/durability test. The discharge temperature of the coolant (N_2) range from 1250°F to 1300°F for the entire period, while the gas flowing over the vane at 550 FPS was 2700 to 2800°F. The cycling of the temperatures was caused by the inability to control the coolant flow rate due to pressure cycling of the facility supply. The coolant flow cycled from .001 to .0015 lbm/sec, Figure 6.3.3.16. The vane surface cycled from 2000 to as high as 2350°F. These high temperatures did not cause an observable problem. The flow cycling caused the heat flux cycling shown in Figure 6.3.3.17. The flux was calculated from the flow rate and temperature change measurements of the coolant.

During the long duration test the exterior surface of the regenerator vane accumulated a large amount of various deposits. These can be seen in the front and rear faces of the vane, Figures 6.3.3.10 and 6.3.3.11 and on the leading edge, Figure 6.3.3.18 and trailing edge, Figure 6.3.3.10. On the leading edge, Figure 6.3.3.18, there is a brownish-red deposit of primarily silicon, sodium, iron, potassium, aluminum and oxygen. Figure 6.3.3.19 shows an EDS (Energy Dispersal X-ray Spectroscopy) spectrum of this material. Most of this material is believed to have come from the refractory lined combustion chamber (alumina and silica) and the water cooled high-velocity section (iron/iron oxide). The sodium and potassium may well have

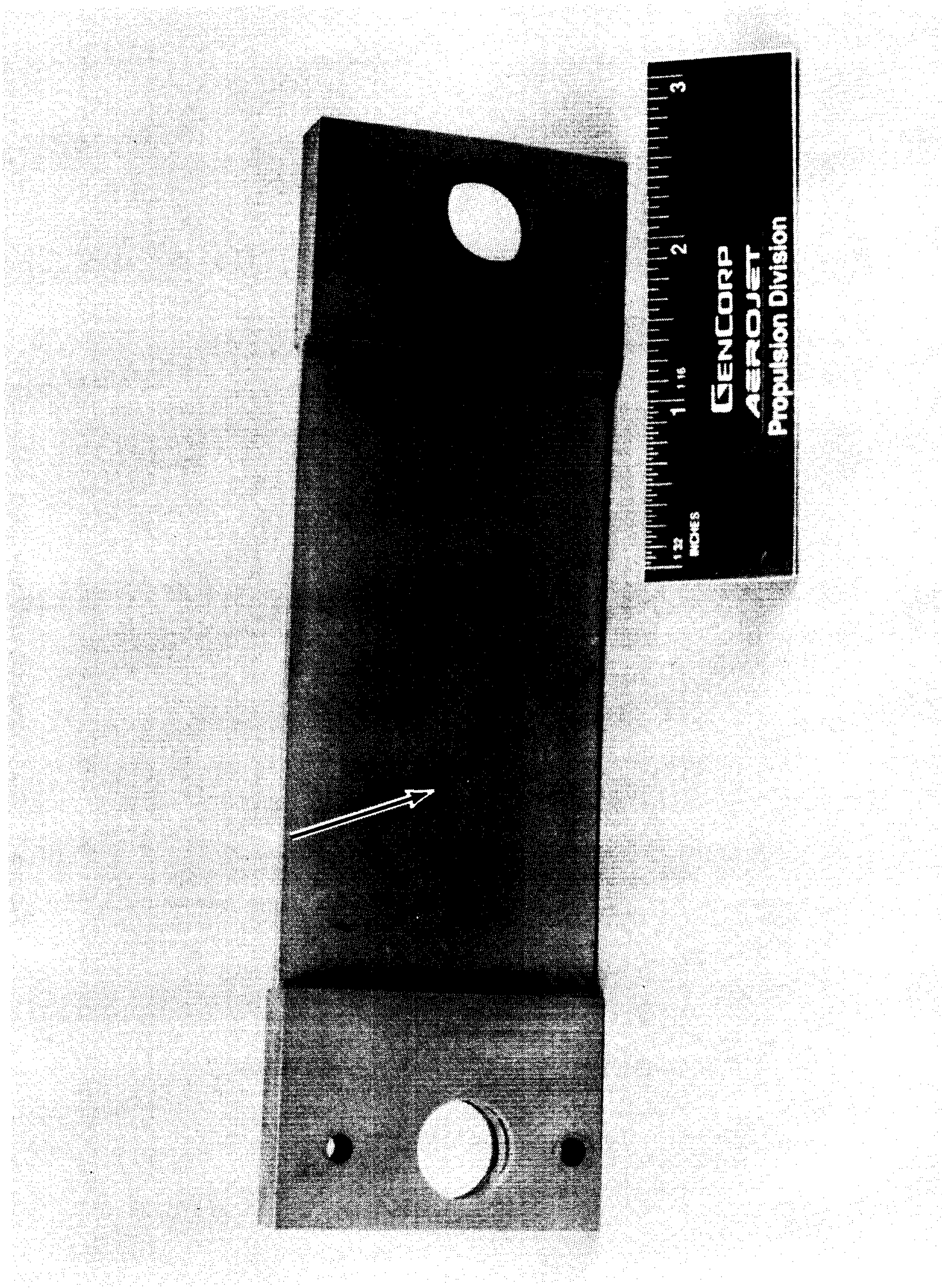

Figure 6.3.3.3 Test Part SN-1, Fractured During Initial Heat-Up Cycle. Note the Crack in Center of Vane (Front)

ORIGINAL PAGE
BLACK AND WHITE PHOTOGRAPH

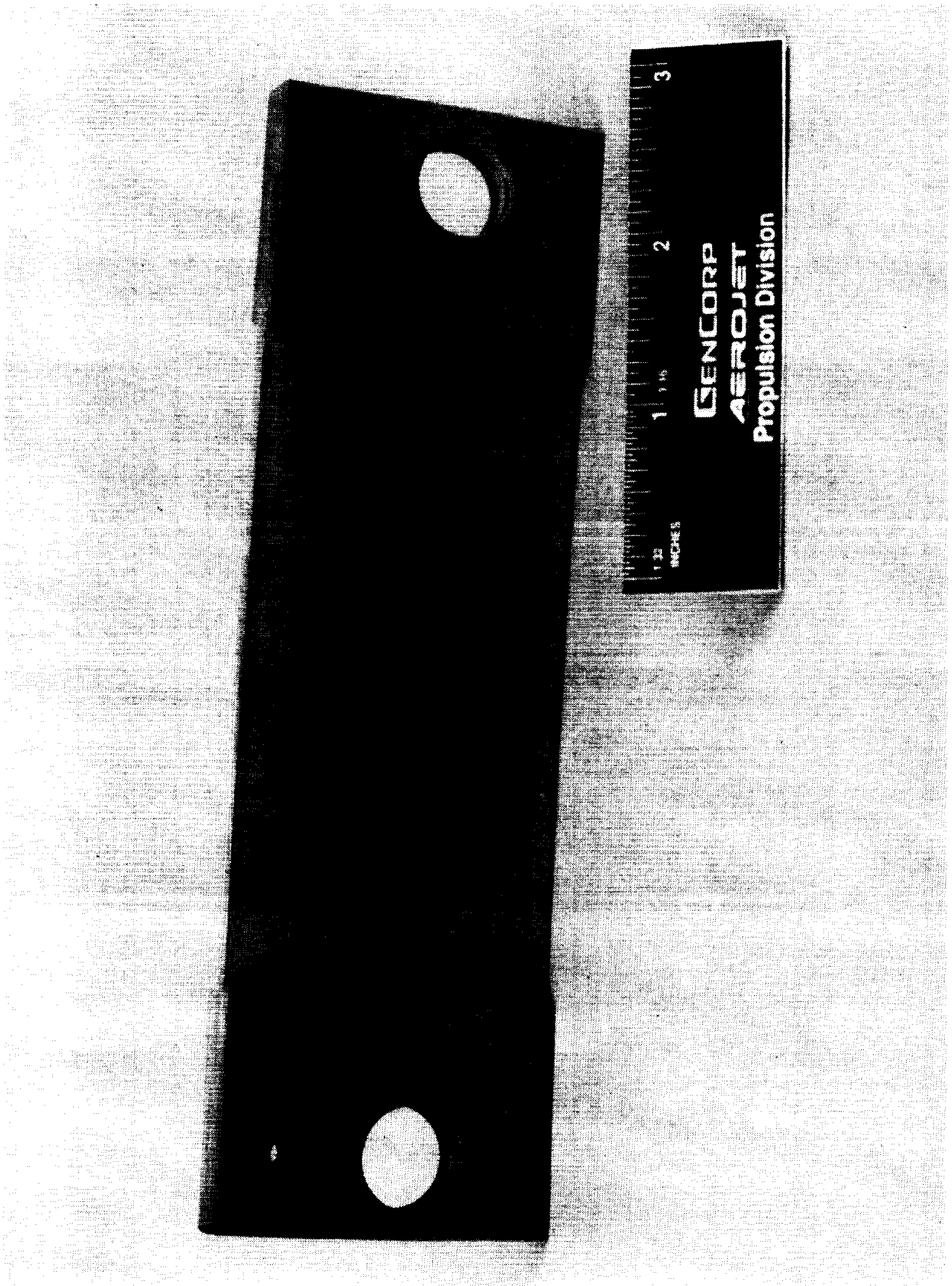

Figure 6.3.3.4 Obverse of Vane SN-1 (Rear)

ORIGINAL PAGE
BLACK AND WHITE PHOTOGRAPH

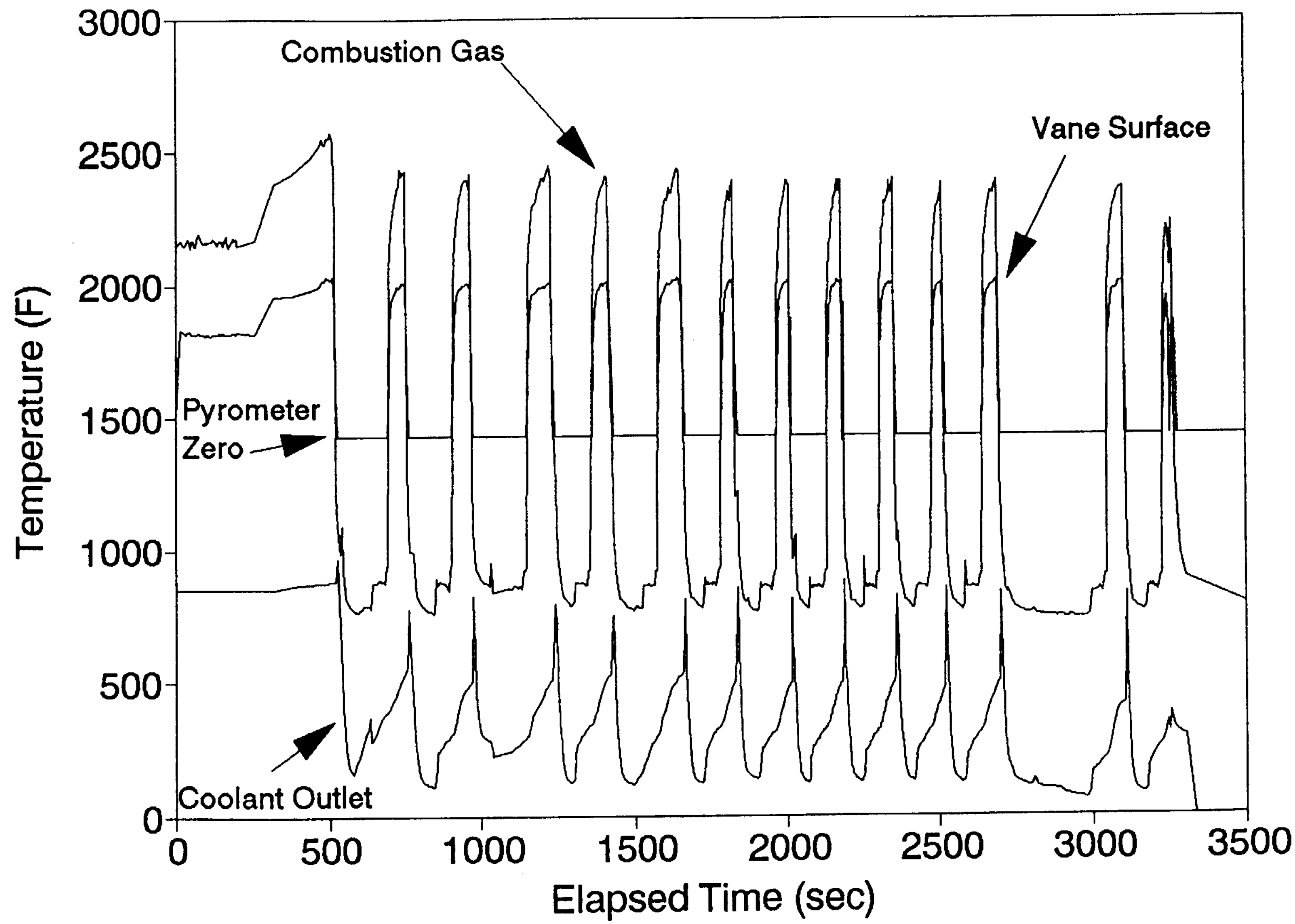

Figure 6.3.3.5 SN-2 Thermocycle Test Numbers 27 Through 40

PAGE ______ INTENTIONALLY BLANK

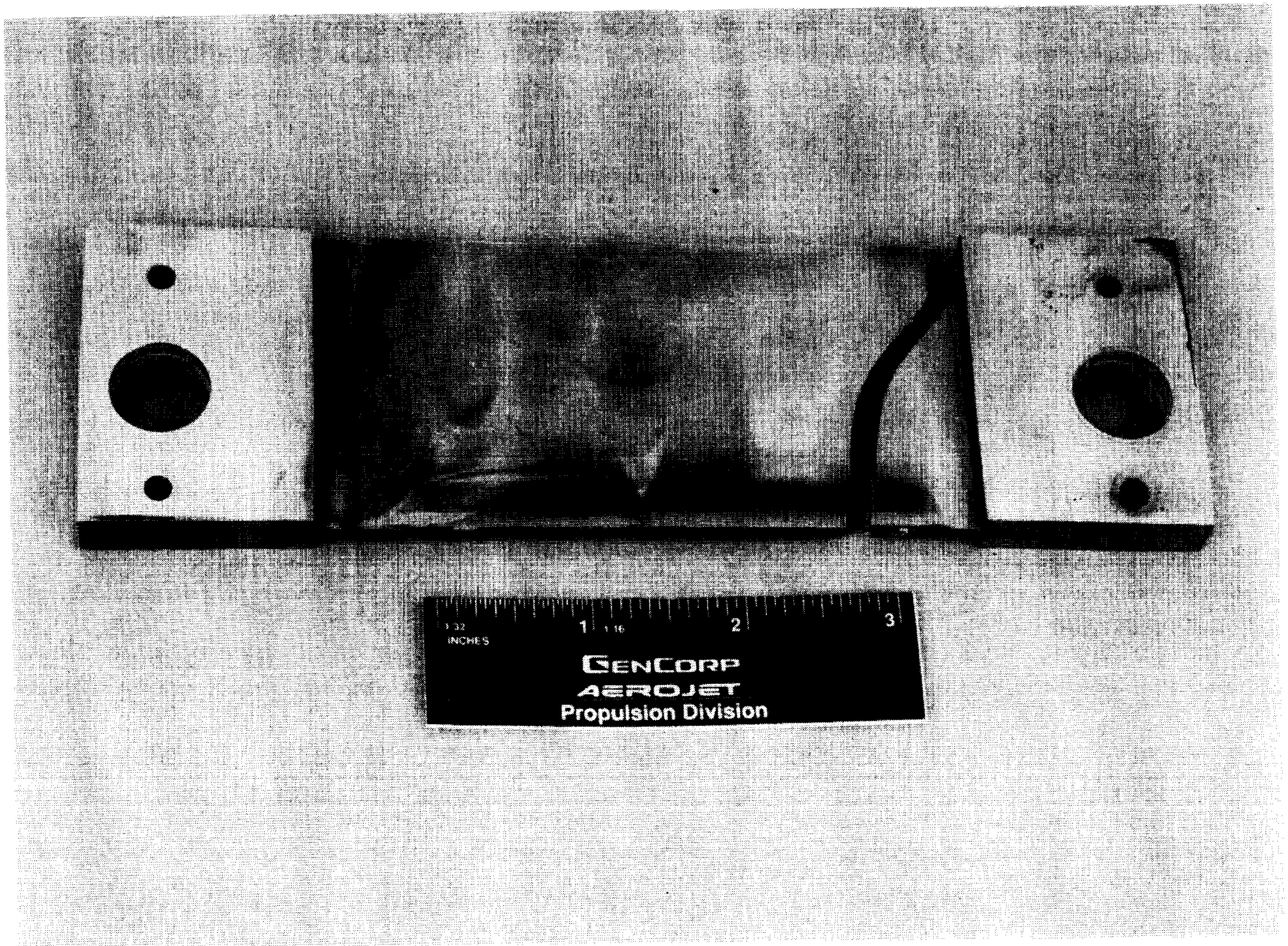

Figure 6.3.3.6 Vane SN-2 After 40 Thermal Cycles and 09:40:11 (hr:min:sec) of Exposure (Front)

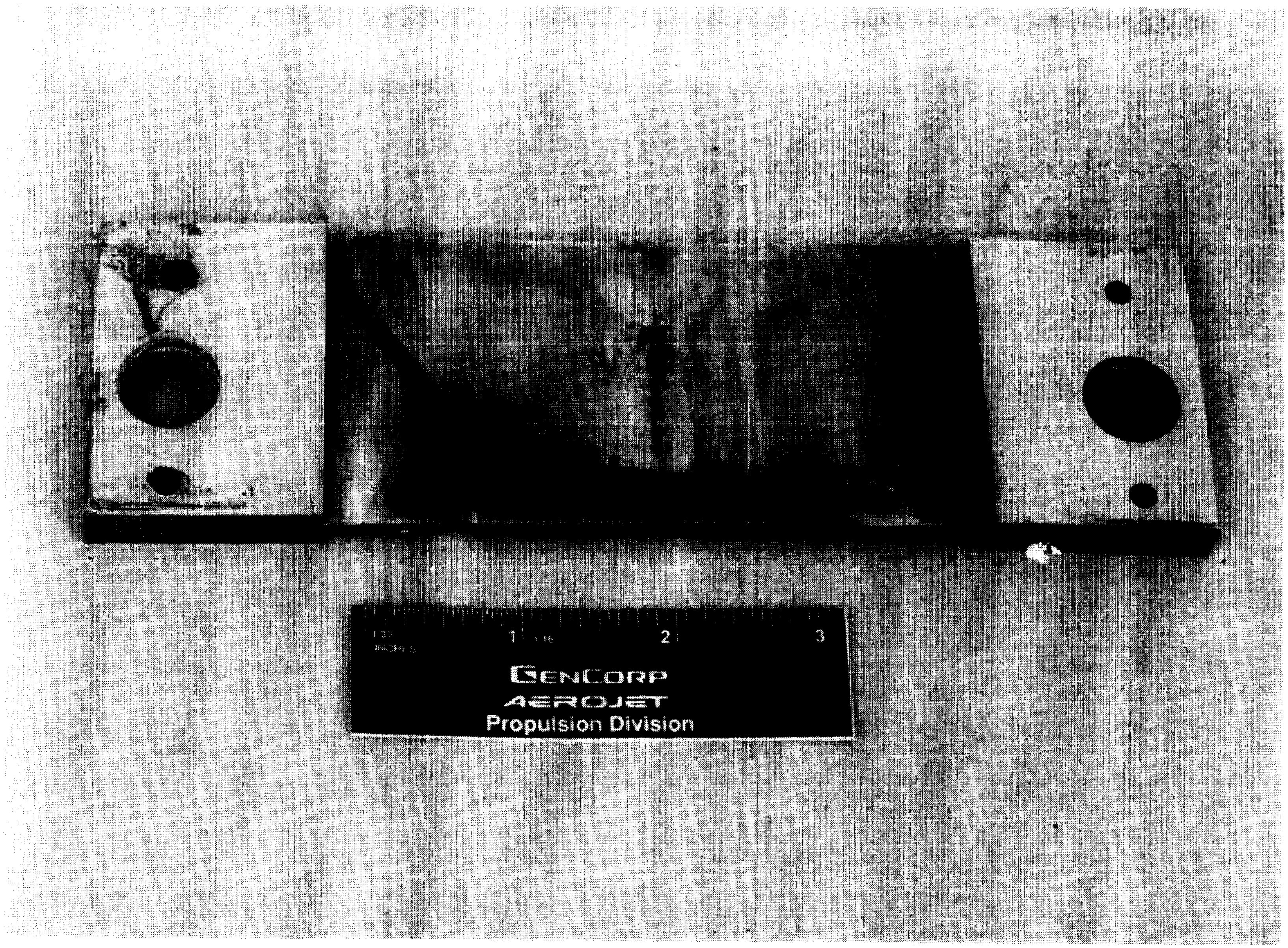

Figure 6.3.3.7 Obverse of SN-2 After Testing (Rear)

ORIGINAL PAGE
BLACK AND WHITE PHOTOGRAPH

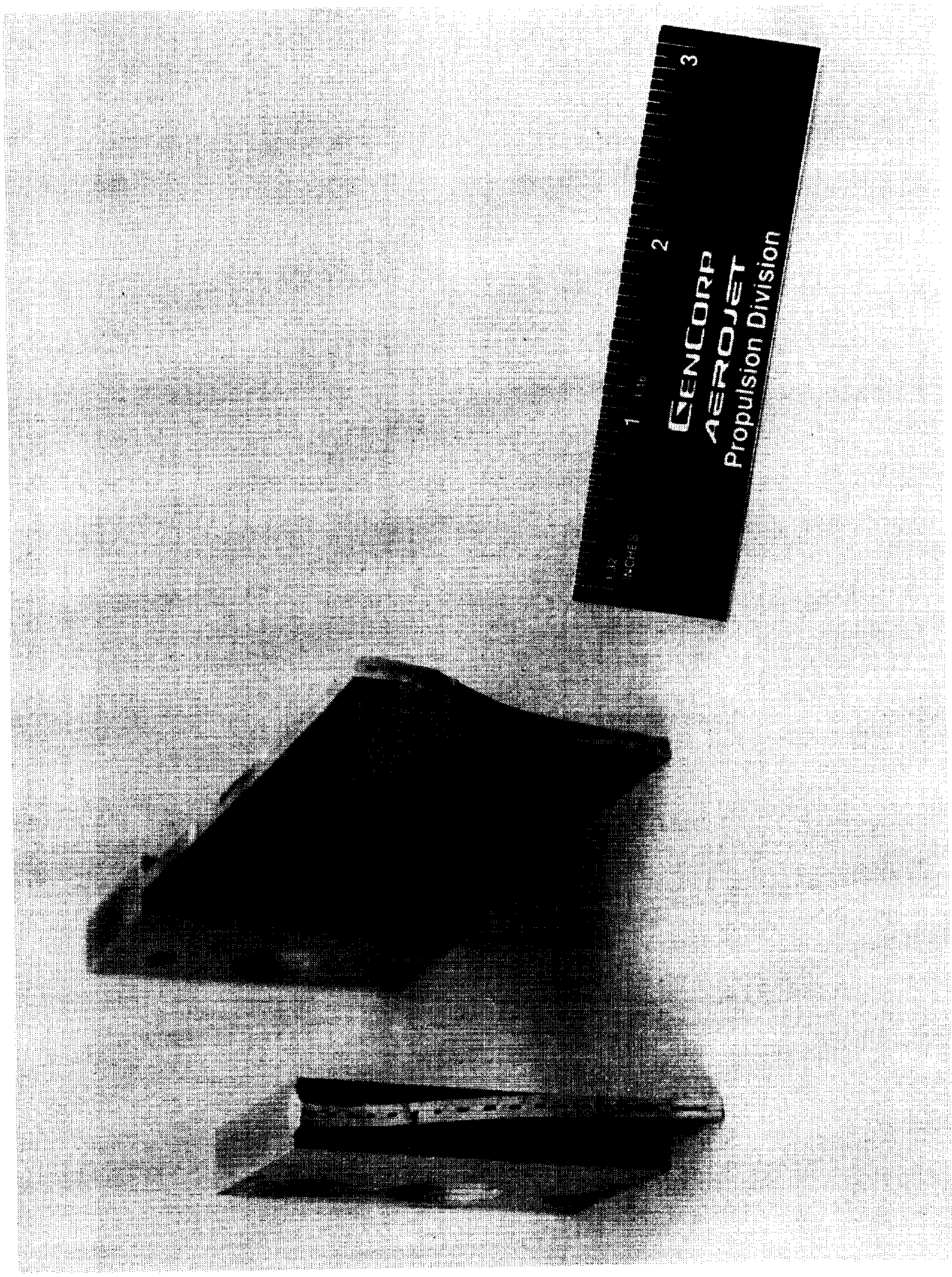

Figure 6.3.3.8 Detail of Fracture of Vane SN-2 After Testing

Figure 6.3.3.9 Profile of Fracture of SN-2

ORIGINAL PAGE
BLACK AND WHITE PHOTOGRAPH

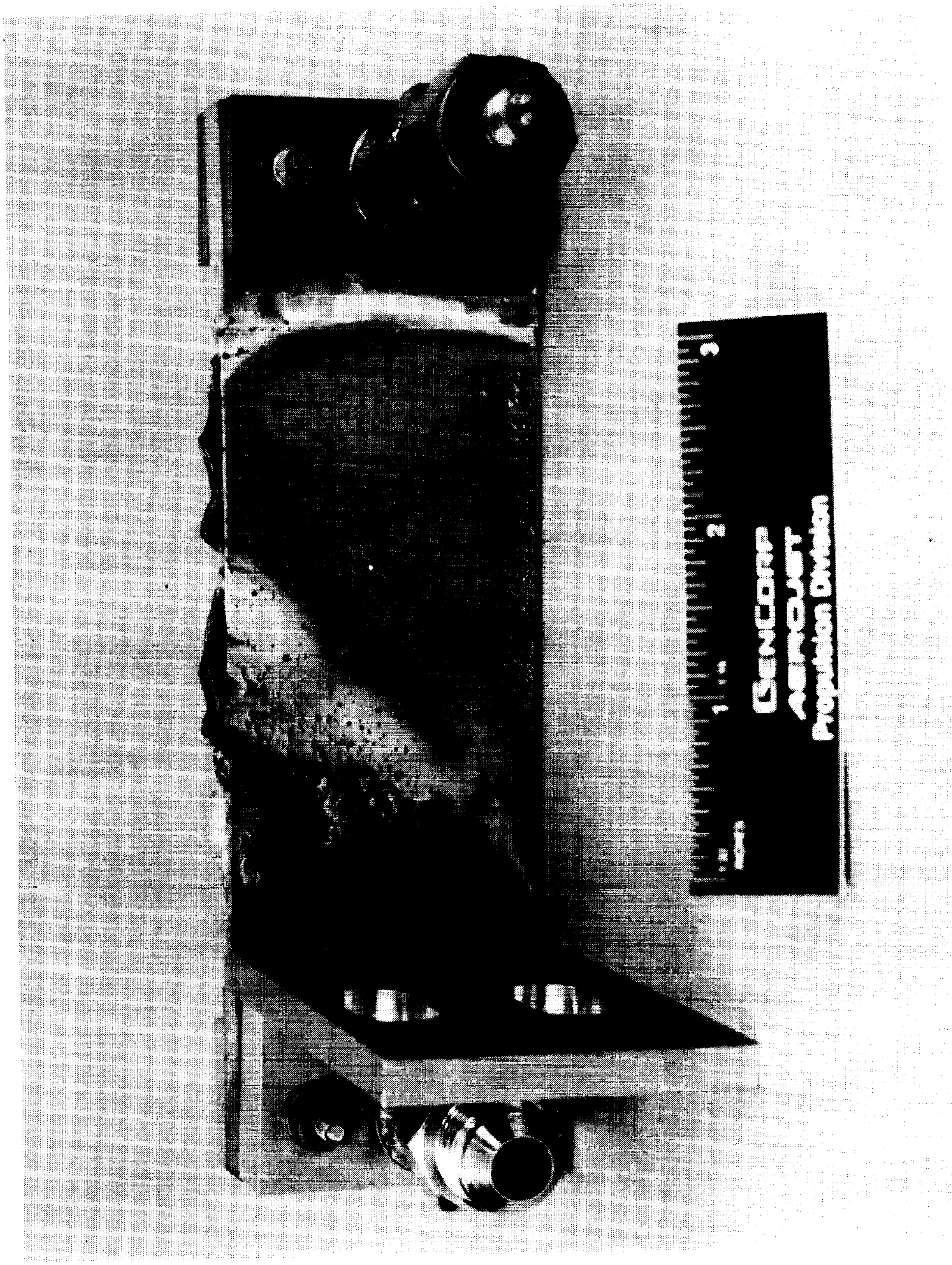

Figure 6.3.3.10 Part No. SN-3 After 117:23:44 (hr:min:sec) of Exposure to Prepare Combustion Products (Front)

ORIGINAL PAGE
BLACK AND WHITE PHOTOGRAPH

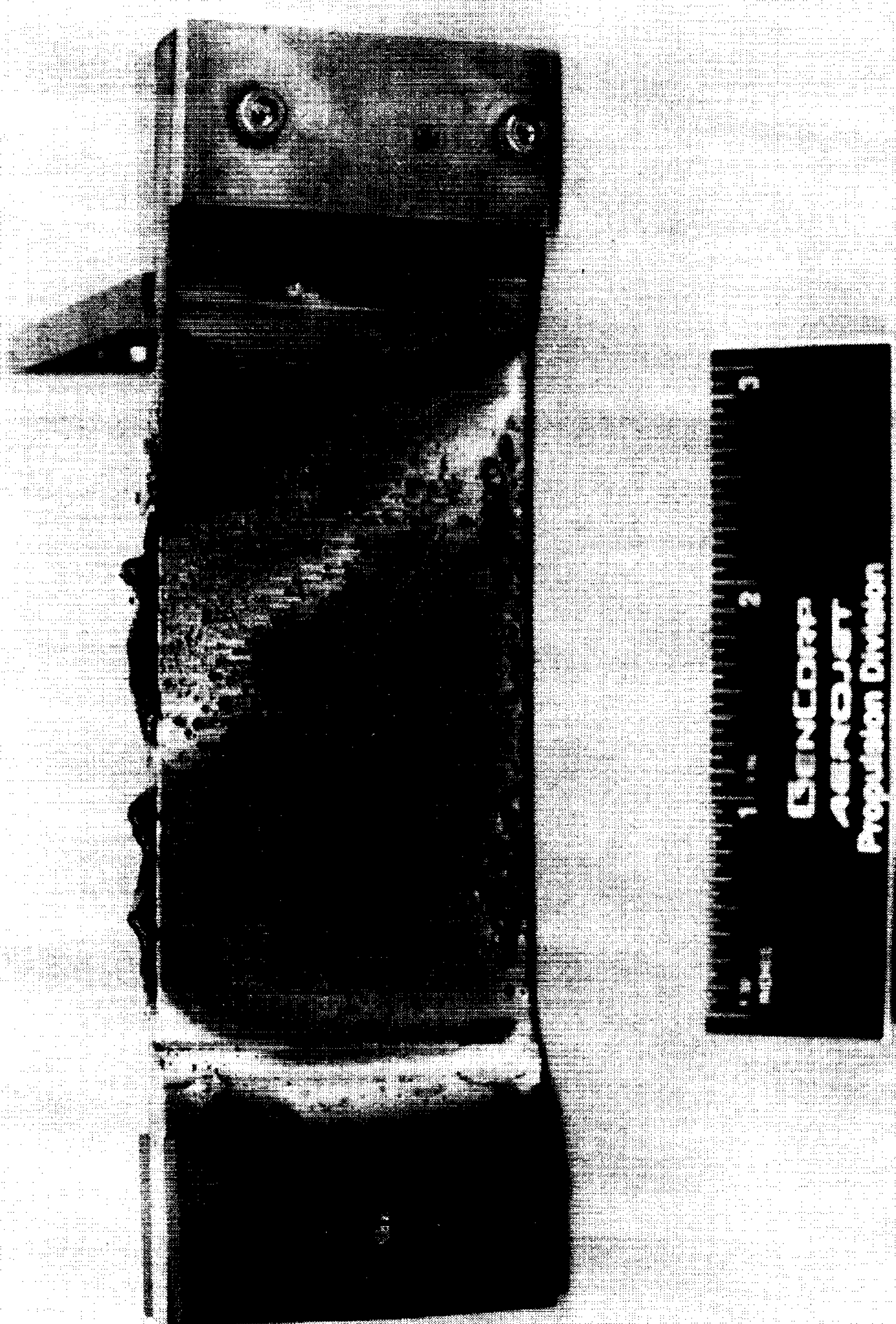

Figure 6.3.3.11 Obverse of SN-3 After Long Duration Test (Rear)

ORIGINAL PAGE
BLACK AND WHITE PHOTOGRAPH

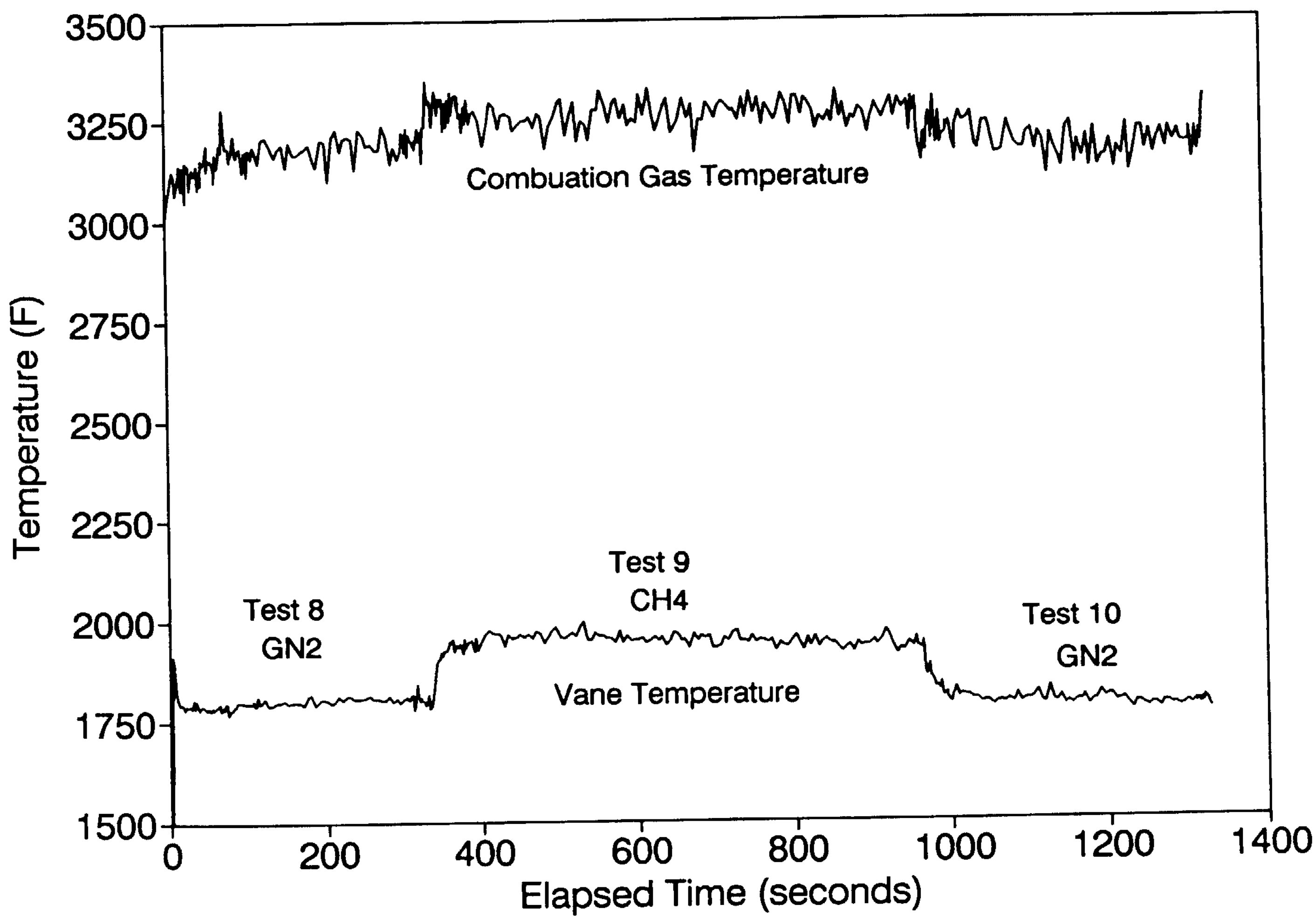

Figure 6.3.3.12 **Regenerator Vane No. SN-3, Test 9. Typical Thermal Cycle of Vane Surface Temperature During Methane Testing**

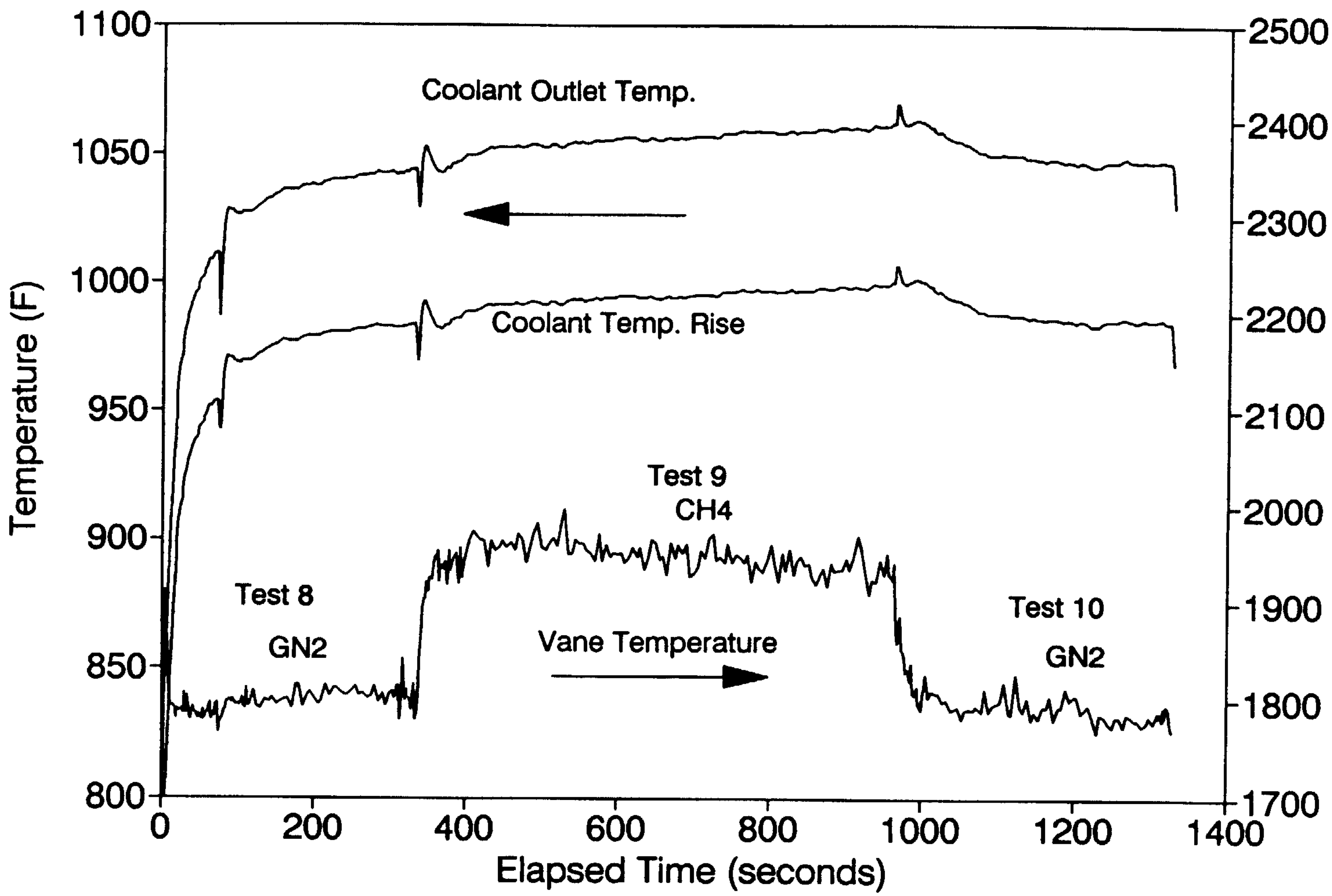

Figure 6.3.3.13 Regenerator Vane No. SN-3, Methane Test No. 9. Coolant Outlet Temperature and Vane Temperature Rise as the Coolant Passes Through the Heated Section

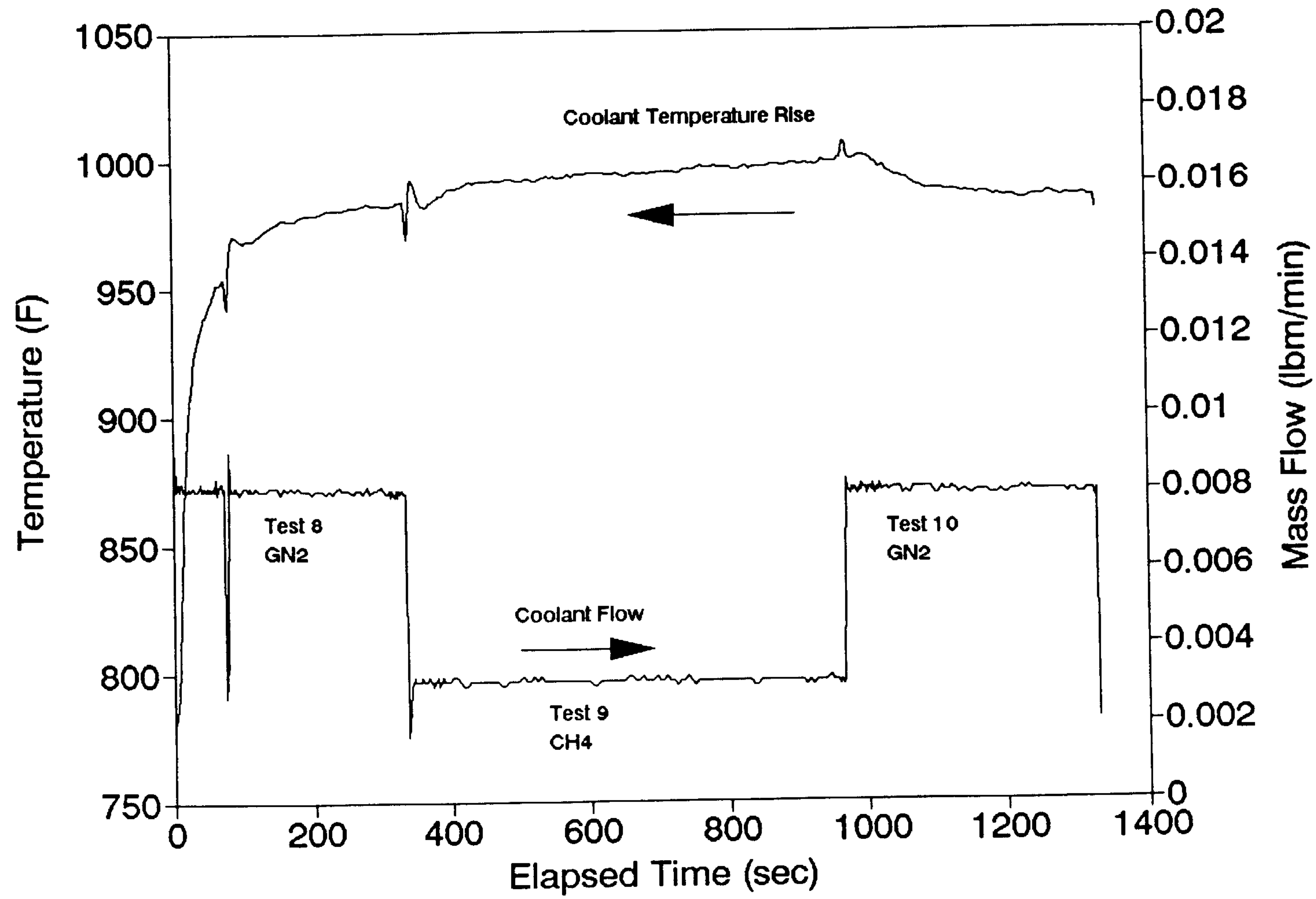

Figure 6.3.3.14 Vane SN-3 Coolant Flow Rate and Coolant Temperature Rise During Methane Test No. 9

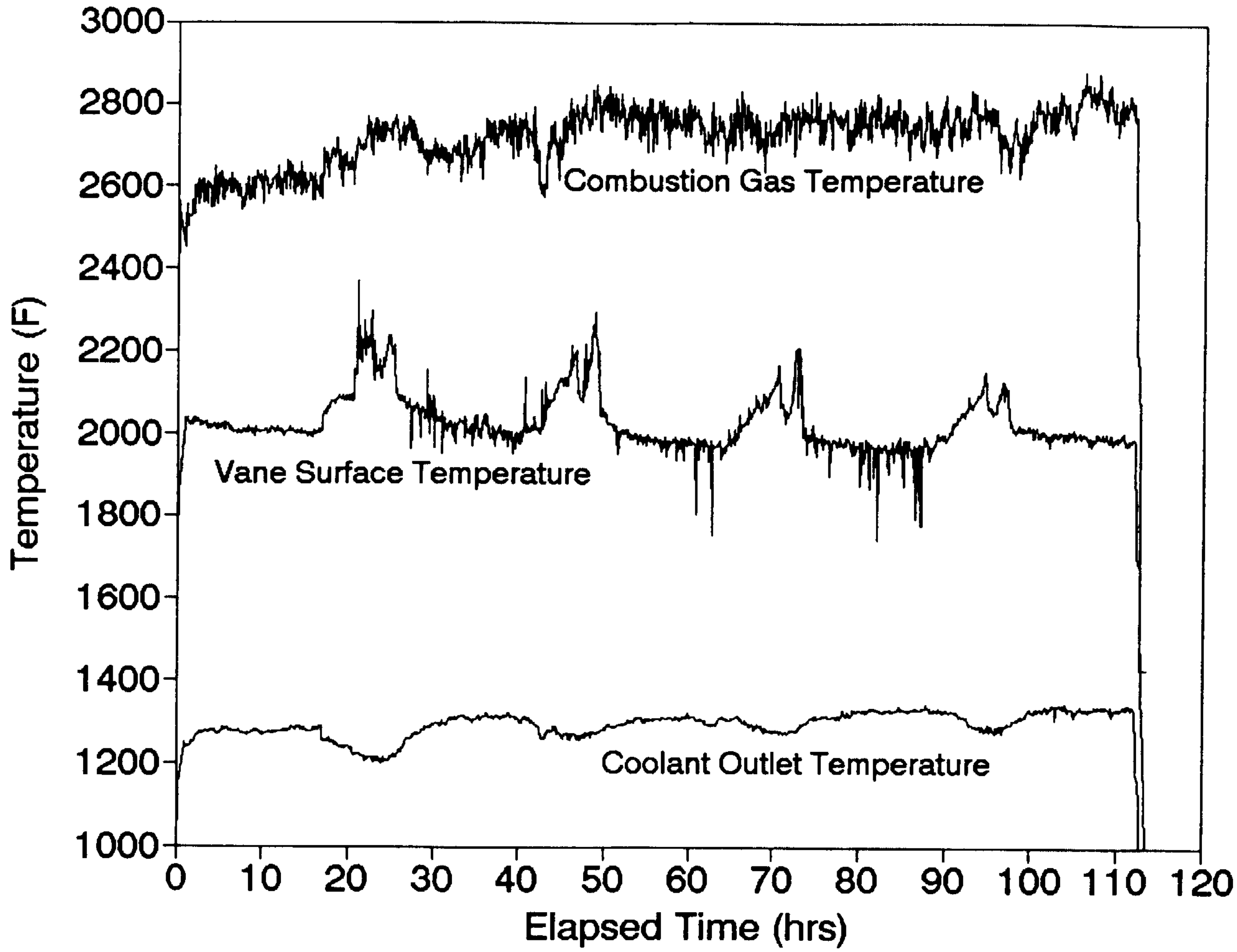

Figure 6.3.3.15 **Long Duration Testing of SN-3 With GN_2, Combustion Gas Temperature and Coolant Outlet Temperature**

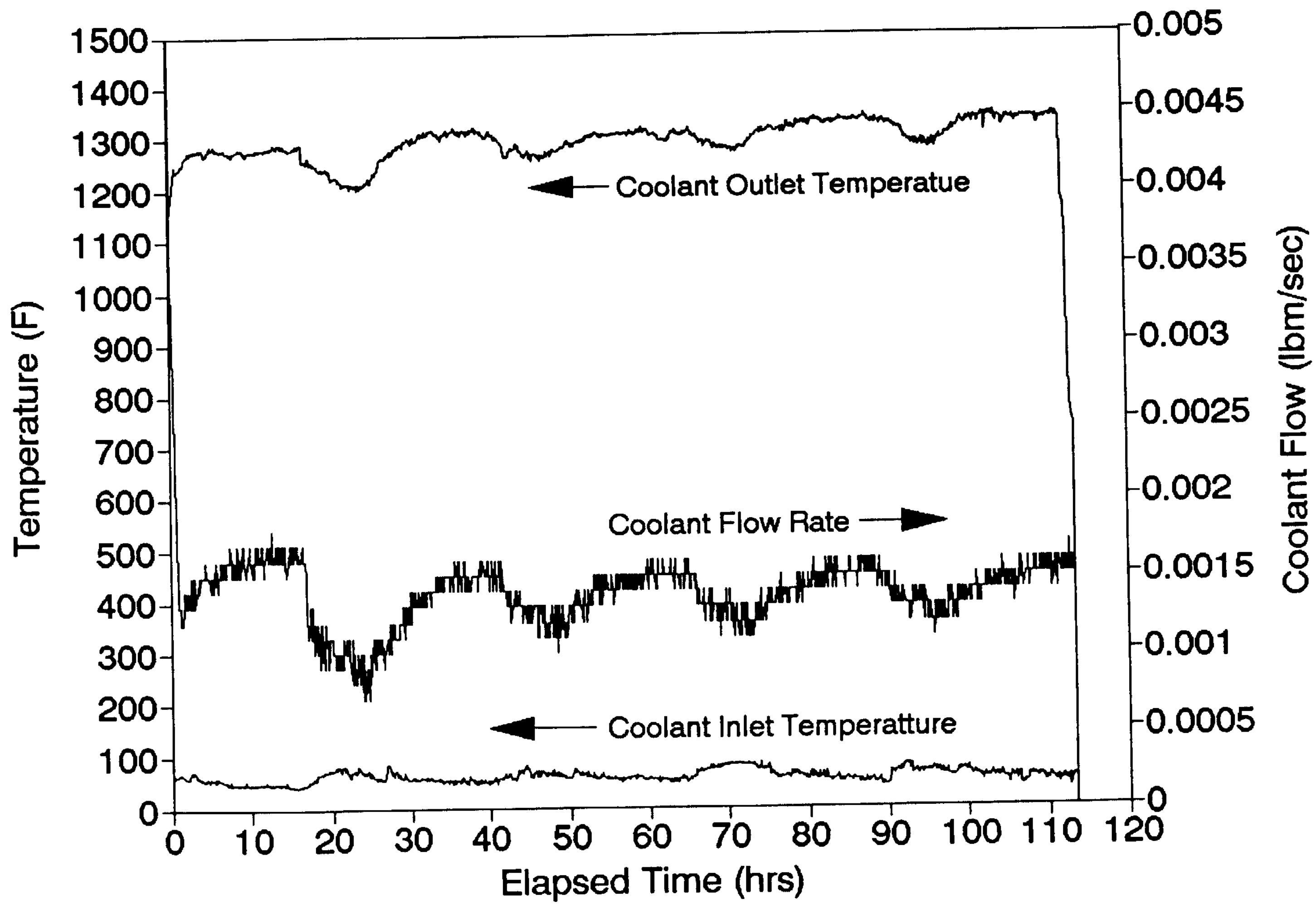

Figure 6.3.3.16 Long Duration Test of SN-3 Showing Coolant Flow Rate, Inlet, and Outlet Coolant Temperature

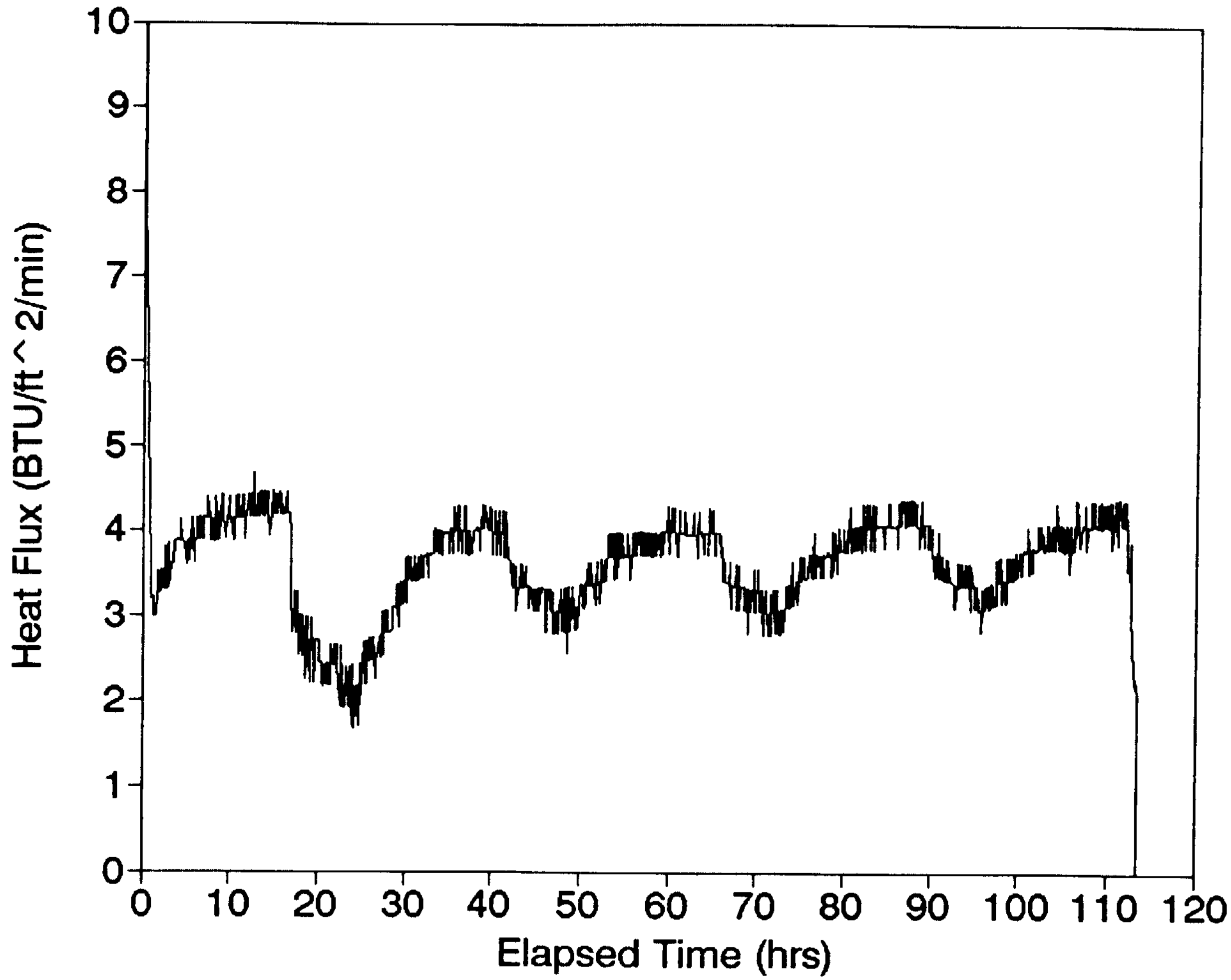

Figure 6.3.3.17 Heat Flux Variation During the Long Duration Test of SN-3

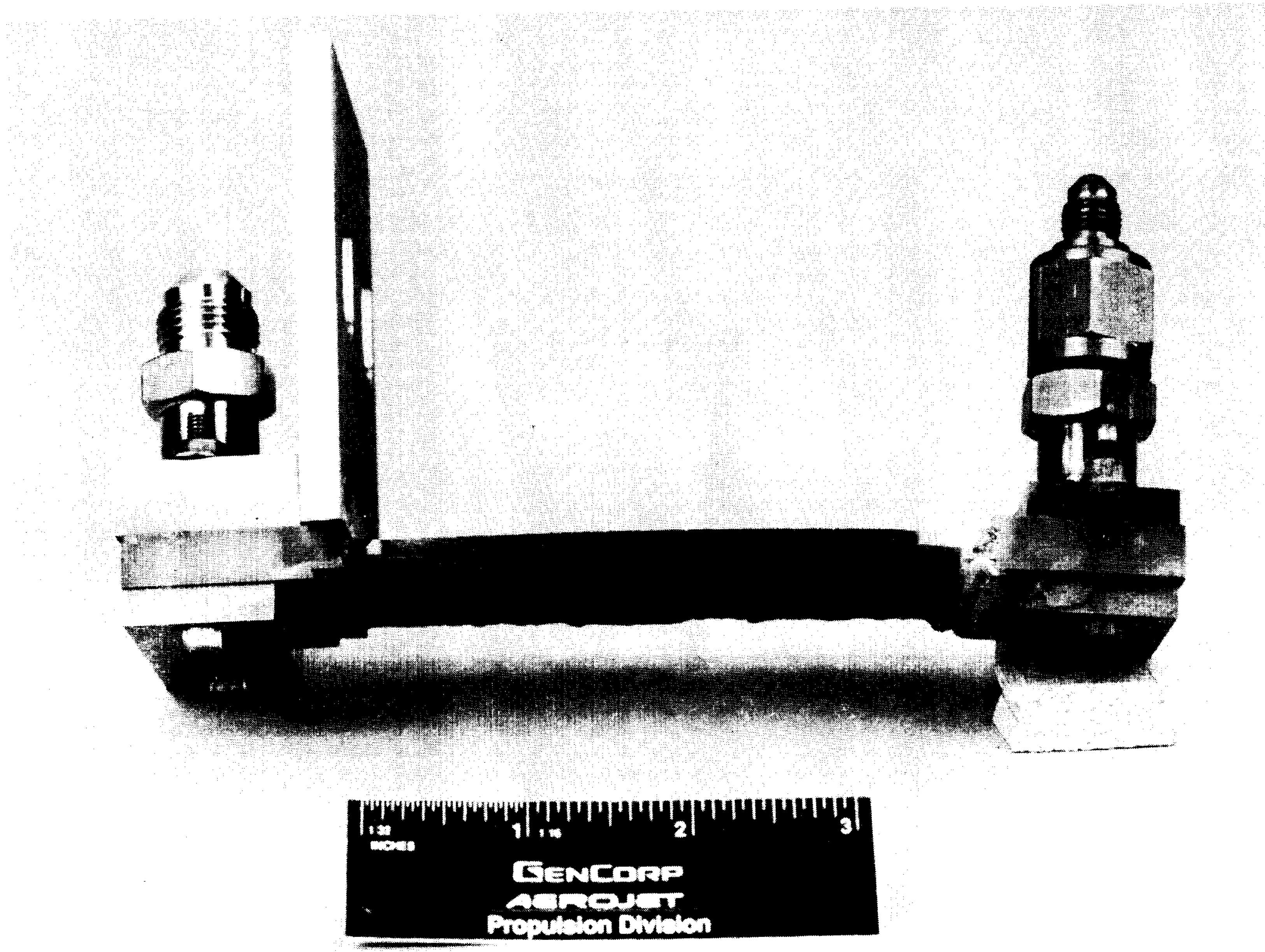

Figure 6.3.3.18 Leading Edge of SN-3 After Long Duration Test. Deposits From Tester

ORIGINAL PAGE
BLACK AND WHITE PHOTOGRAPH

PAGE_______INTENTIONALLY BLANK

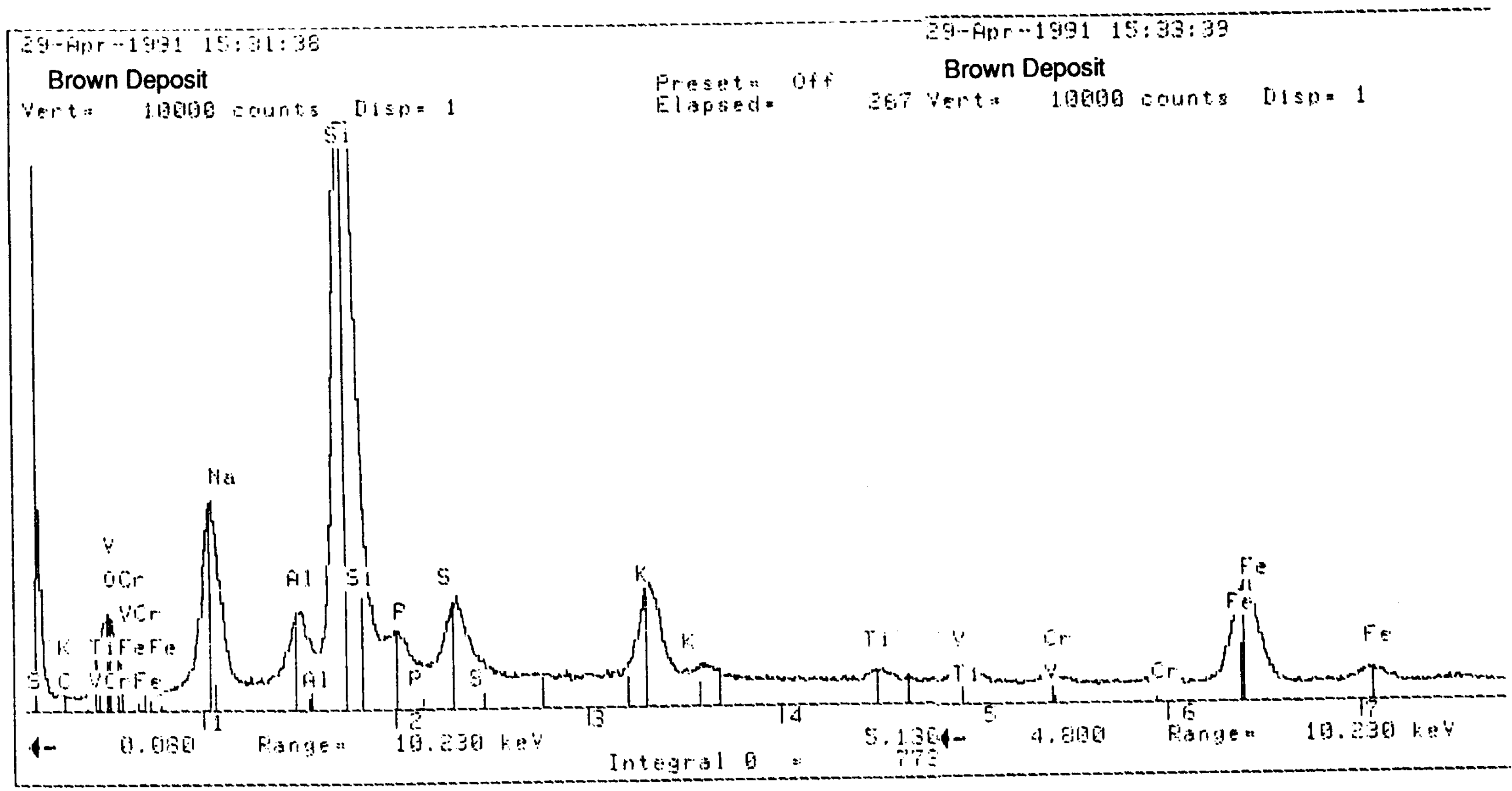

Figure 6.3.3.19. EDS Spectrum of Deposit Found on Leading Edge of SN-3. This Material is Believed to Originate in the Combustion Chamber and Water Cooled Section, and the Sulfur From the Propane Fuel

been in the refractory. The sulfur would have been in the odorized propane fuel. On the trailing edge, Figure 6.3.3.20, there were green/yellow deposits. The green deposit, Figure 6.3.3.21, was primarily silicon, oxygen and sodium, the yellow/green deposit Figure 6.3.3.22, was primarily sulfur, sodium and oxygen, again, material from the refractory and fuel. At the inlet end of the vane there were yellow/brown deposits, Figure 6.3.3.10 left end, which proved to be composed primarily of sulfur, iron and potassium, Figure 6.3.3.23, from the sources discussed above.

The possibility that the silicon/oxygen in the surface deposits was a result of the conversion of silicon nitride to silica was considered. Selective measurements taken after the duration test of part SN-3 were compared with those taken before testing, Table 6.2.2.1. This comparison was inconclusive. Not only did the post-test measurements show an increase in size of the part, the measurements were not repeatable. This was due to the frangibility of the deposits which was fretted by the measurement activity itself, resulting in inconsistent measurements. Visual inspection did not reveal any areas which were eroded except at the outlet end of leading edge where the combustion products and material from the tester impacted the part at a velocity in excess of 500 fps. From this, it was concluded that there was some surface degradation of the part except in the areas of high velocity impingement.

Part SN-3 had been previously pressure tested to 1575 psi before fracturing in the exit manifold section and was thermally tested with the fractured manifold. This was due to the untimely fracture of SN-1 after only 5:26 (min:sec). Examination of the fractured region of SN-3 after the methane and long duration tests showed no evidence of soot or coking due to methane decomposition. The area visible through the fracture is the area of highest temperature coolant flow.

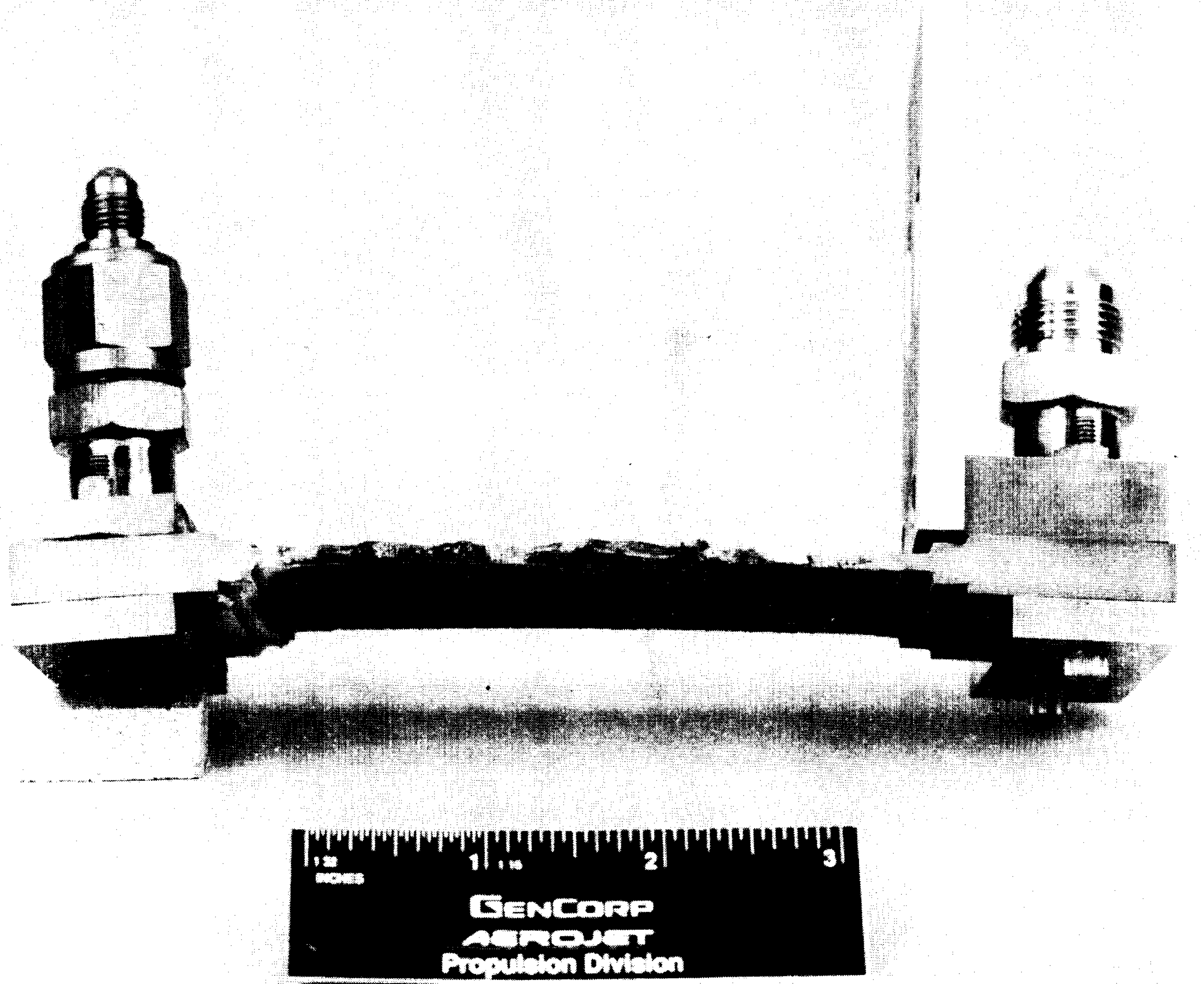

Figure 6.3.3.20. Trailing Edge of SN-3 After Long Duration Testing. Deposits are From Tester

PAGE ____ INTENTIONALLY BLANK

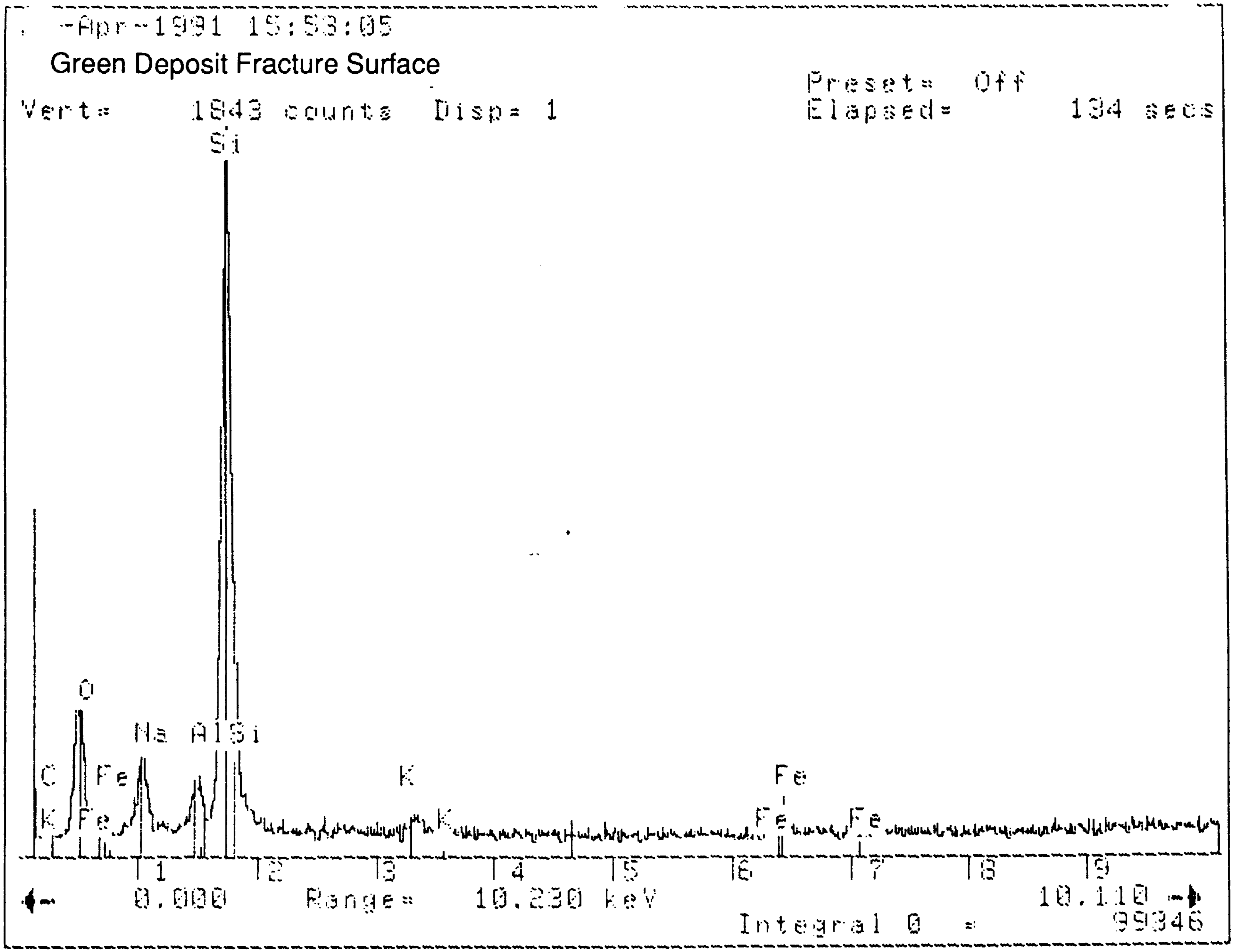

Figure 6.3.3.21 EDS Spectrum of Green Deposit on Trailing Edge of SN-3 After Testing

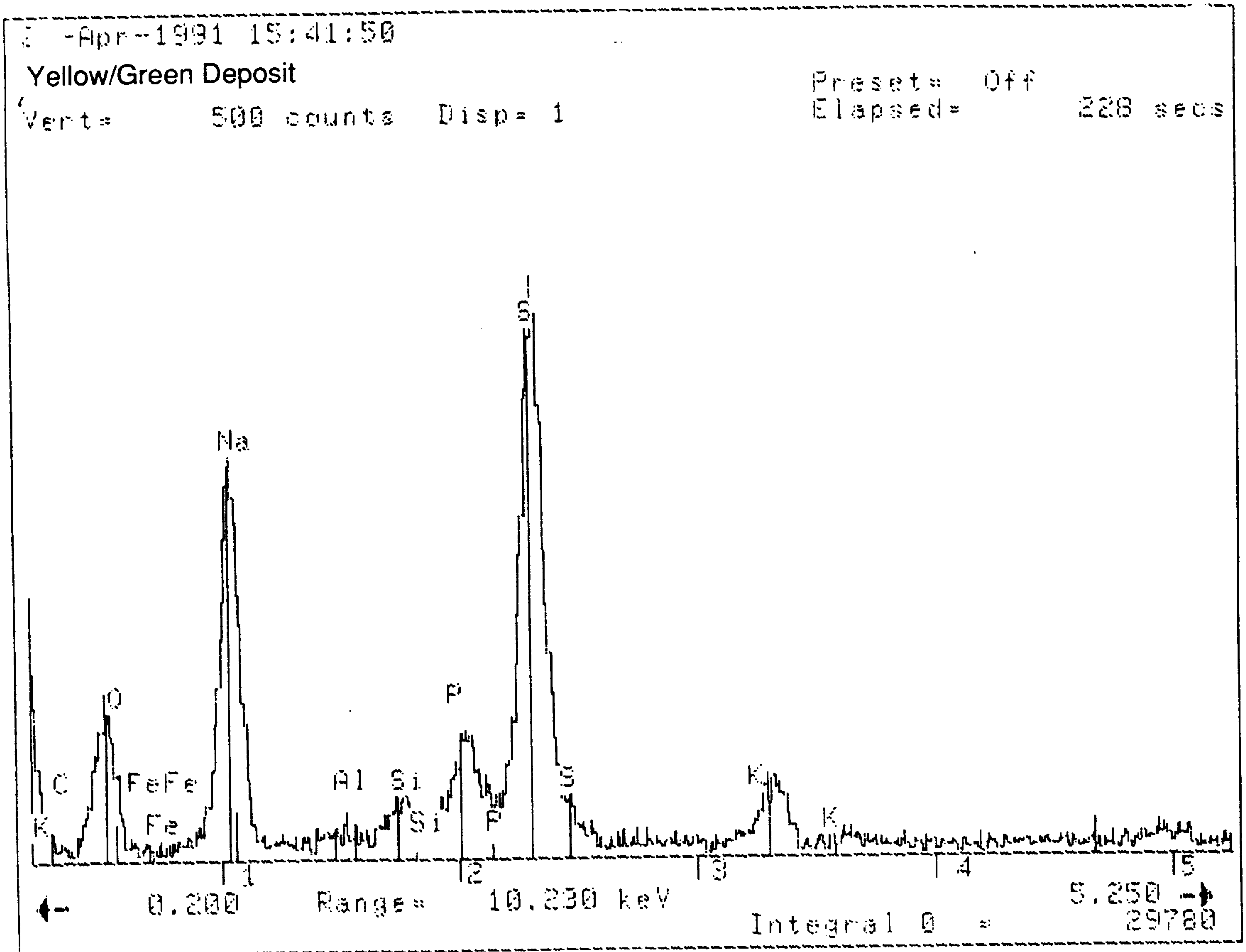

Figure 6.3.3.22 EDS Spectrum of Yellow Green Deposit Found on Trailing Edge of SN-3 After Testing

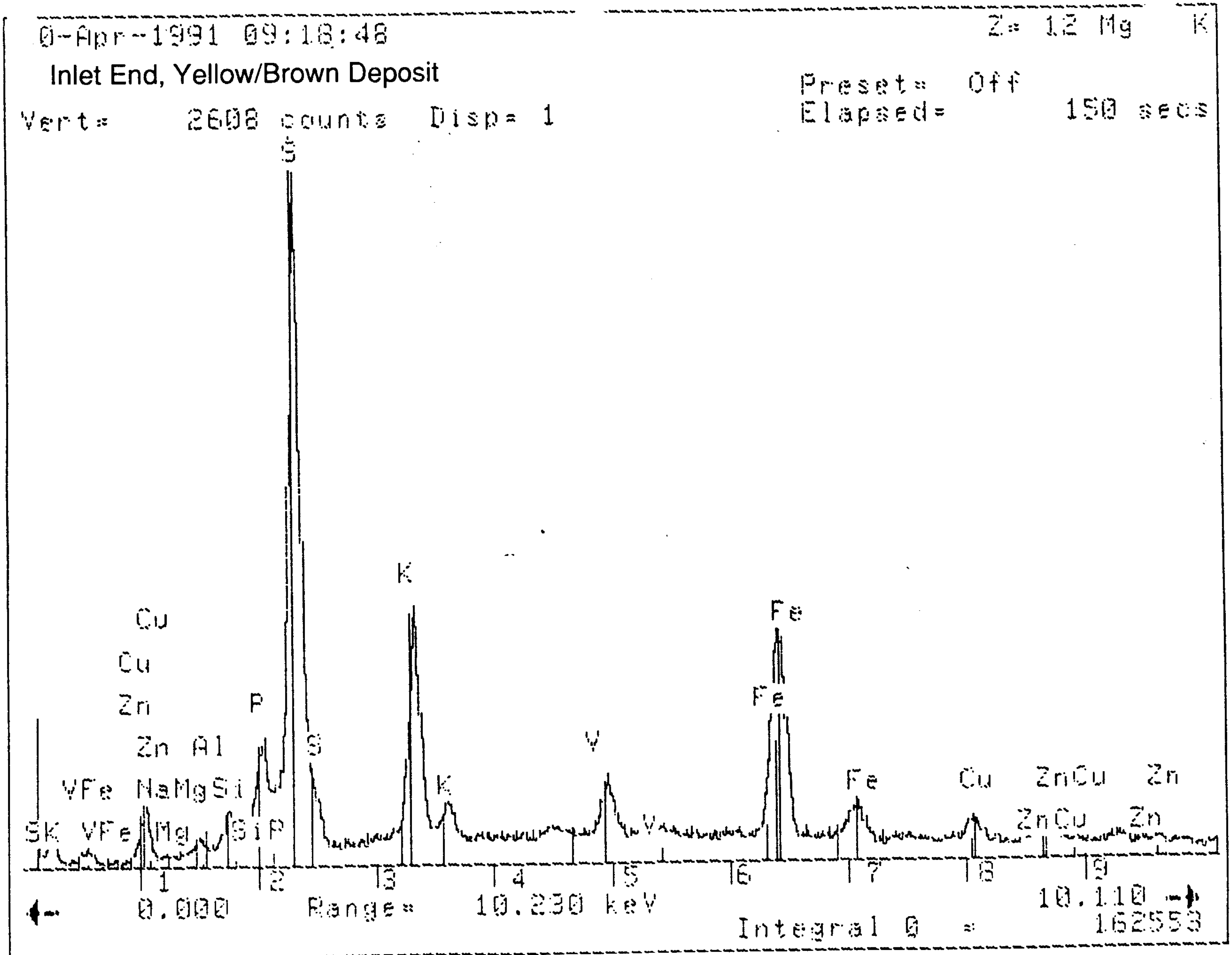

Figure 6.3.3.23 EDS Spectrum of Yellow/Brown Deposit Found on Inlet End of the Vane Face of SN-3 After Testing

PAGE________INTENTIONALLY BLANK

APPENDIX A

CERAMIC REGENERATOR TEST PLAN

INTENTIONALLY BLANK

CERAMIC REGENERATOR TEST PLAN

Contract NAS 3-25416

1.0 INTRODUCTION

Advanced materials are the key element in the development of high-speed propulsion systems for the NASP and other aeropropulsion systems such as the ATR. With the use of these materials, propulsion system thrust/weight is improved tremendously, and Mach number capability is enhanced by eliminating the need for efficiency robbing cooling air.

The selected silicon nitride ceramic regenerator for preheating liquid methane has several advantages over conventional metal regenerators. The three primary advantages are (1) low material density (30% of copper and steel), resulting in lightweight components, (2) higher operating temperature capability (up to 2500 F), and (3) improved corrosion resistance at higher temperatures. Disadvantages are a lack of ductility and low thermal shock resistance.

2.0 OBJECTIVE

The objective of this test program is to perform proof-of-concept demonstration of a methane-cooled ceramic platelet regenerator. Four prototype components are to be tested; one for mechanical capabilities and three in a simulated high-speed engine. The operating conditions of temperature, pressure, and chemical environment selected to demonstrate the feasibility of a lightweight, high-efficiency regenerator for high-speed propulsions are given in Table A-1.

3.0 TEST ARTICLE DESIGN/DESCRIPTION

The tape cast and laminated silicon nitride regenerator vane is designed to heat coolant supplied at 600 psi to gas at 1800 R with a minimum pressure loss. A conceptual design and the test configuration is shown in Figure A-1. The detailed design of the four platelet types that comprise the ceramic platelet regenerator assembly are provided in Figures A-2 through A-8. The design is a single pass cross-flow configuration, i.e., the coolant enters the vane on one end, flows through 16 channels, and discharges on the opposite end. The channels are equal to the thickness of two laminates (0.025 in.) in one direction, and the width is adjusted to match the heat input such that the fuel temperature rise in each channel is approximately equal. The high-speed hot gas flows perpendicular to the coolant flow. The gas impacts on the thin leading edge where the coolant channels are the largest, and flows across the two parallel faces of the vane,

TABLE A-1

NOMINAL TEST CONDITIONS

Combustion Gas:	
Hydrocarbon Fuel/Air	Propane/Air (O/F ≈17)
Pressure, psia	≈15
Gas Velocity, fps	500-600
Gas Temperature, R	3500
Fuel/Coolant:	
Methane, lb/sec	0.005-0.010
Inlet Pressure, psia	600
Supply Temperature, R	530-1200 (70-740 F)

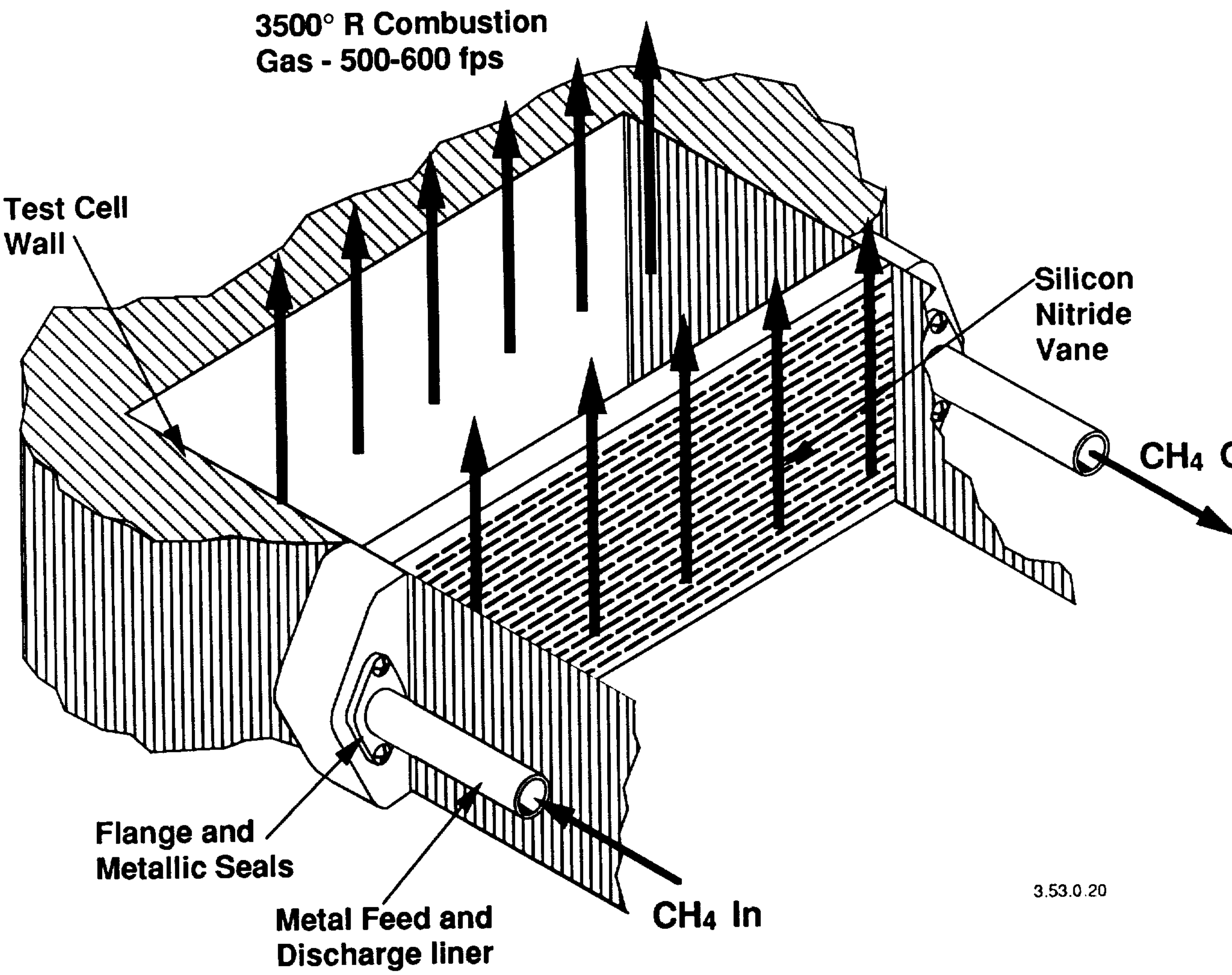

Figure A-1. Ceramic Regenerator Conceptual Design and Test Configuration

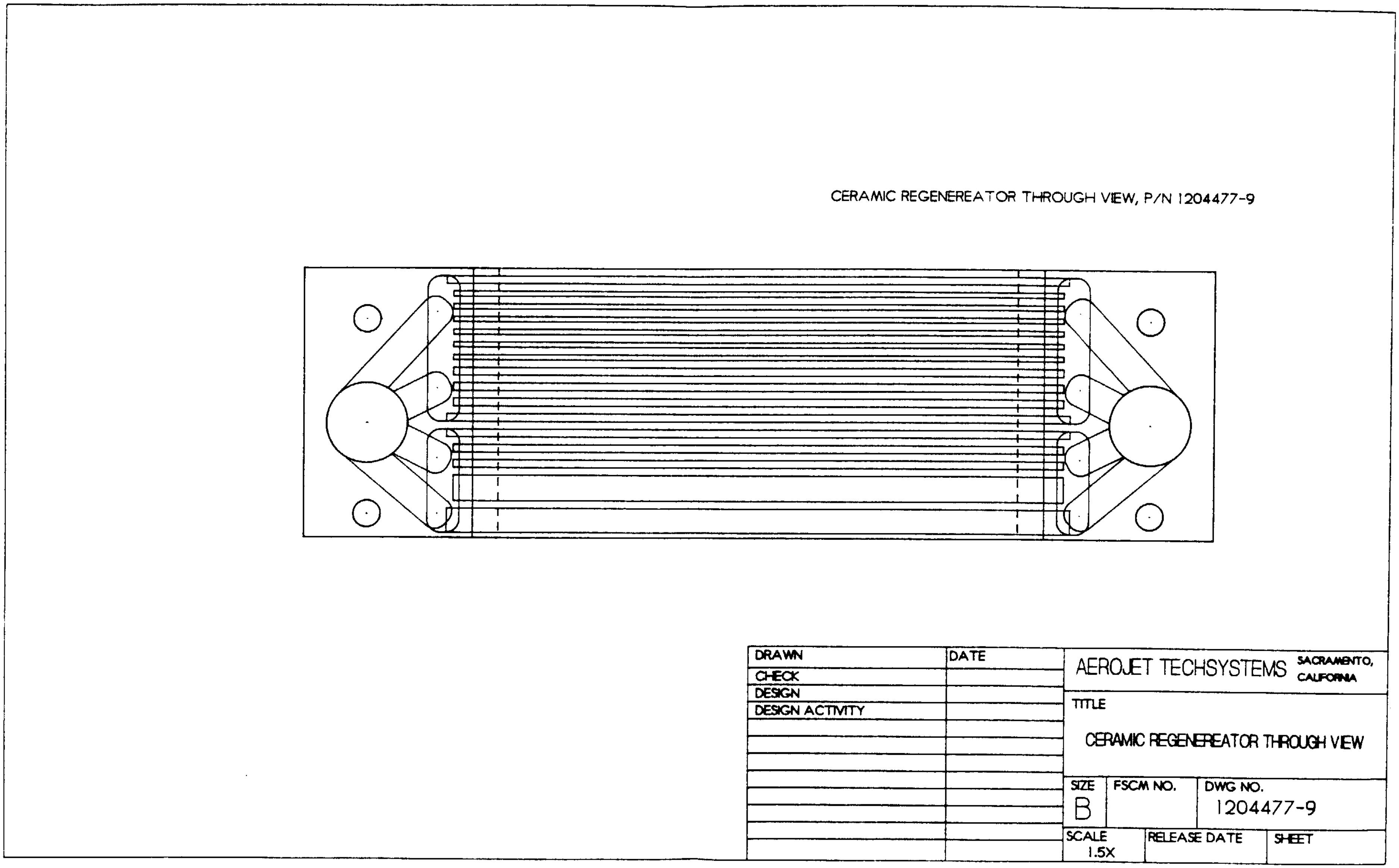

Figure A-2. Through View of Stacked Platelets for Ceramic Regenerator

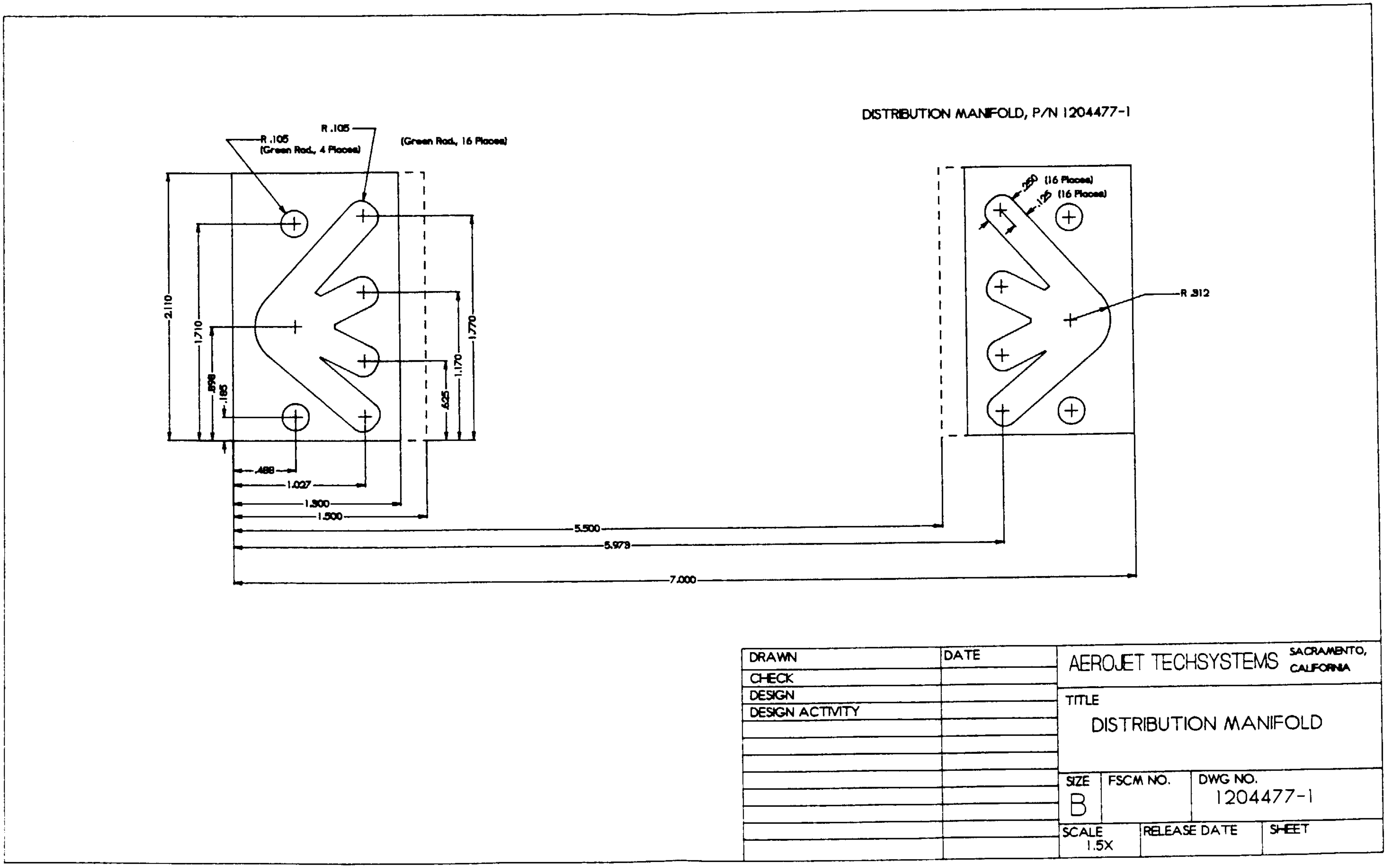

Figure A-3 Distribution Manifold Platelets for Ceramic Regenerator

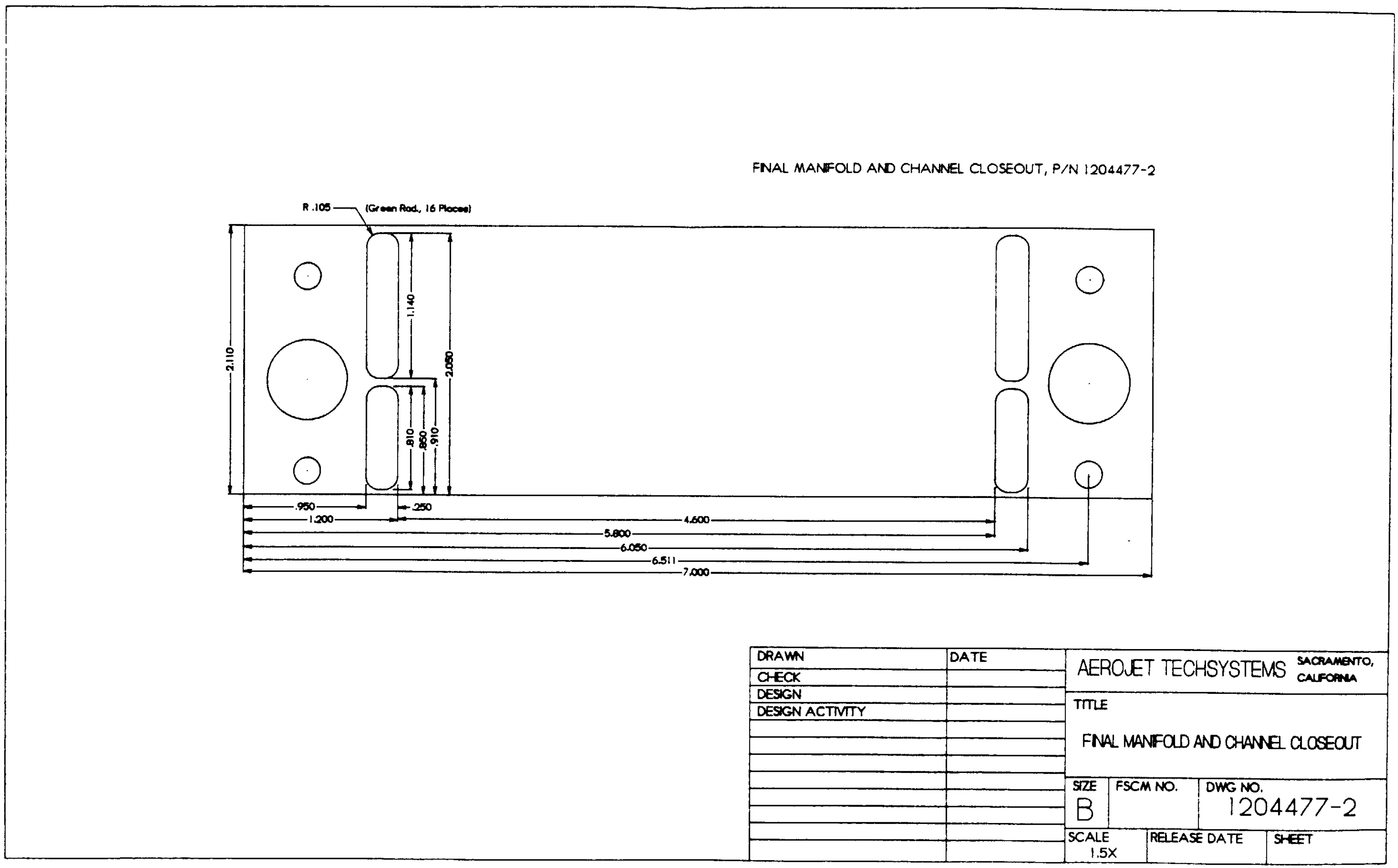

Figure A-4 Final Manifold and Channel Closeout Platelets

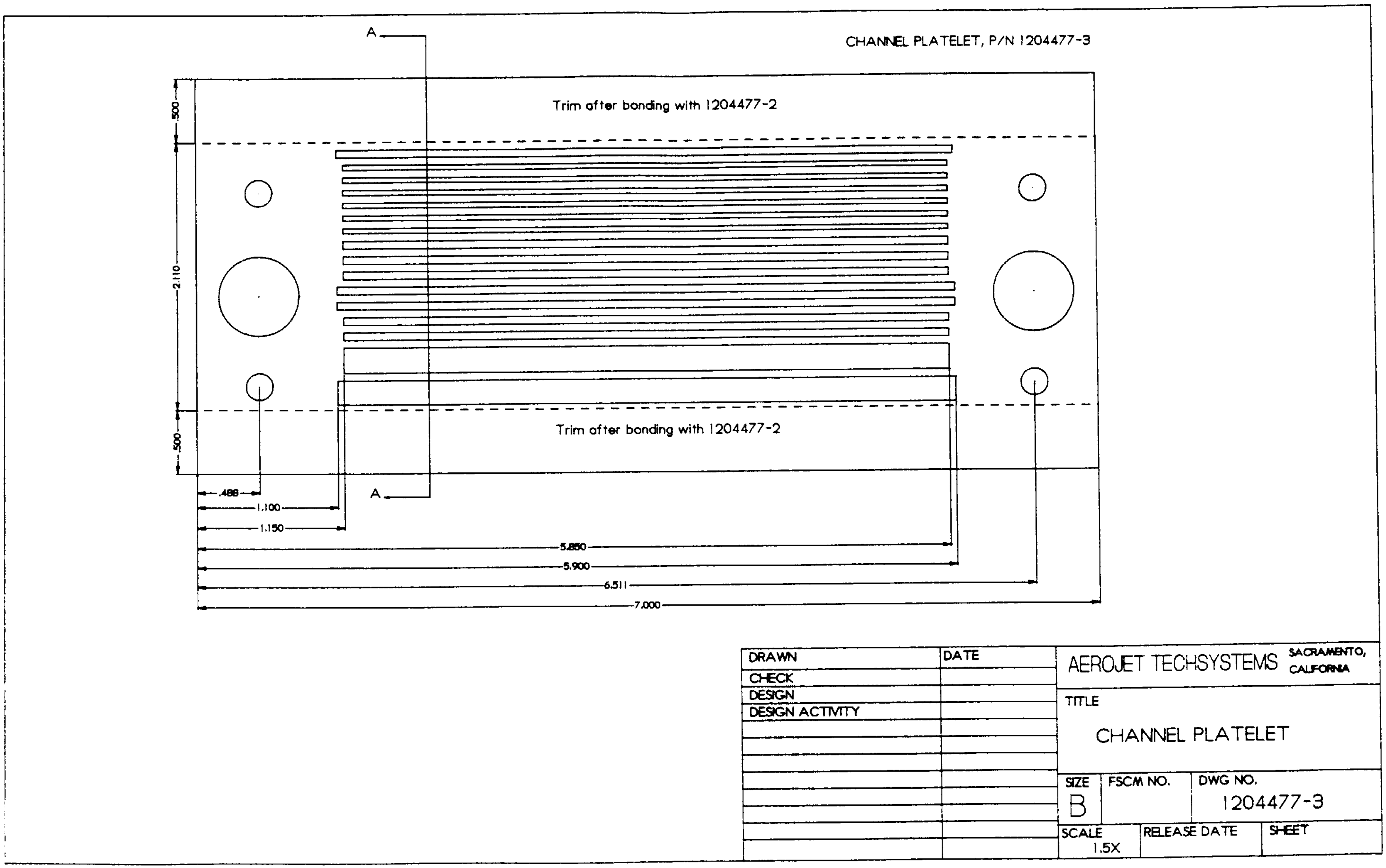

Figure A-5 Regenerator Channel Platelet. Note the Wide Side Lands to be Trimmed After Being Bonded With P/N 1204477-2, Figure 3

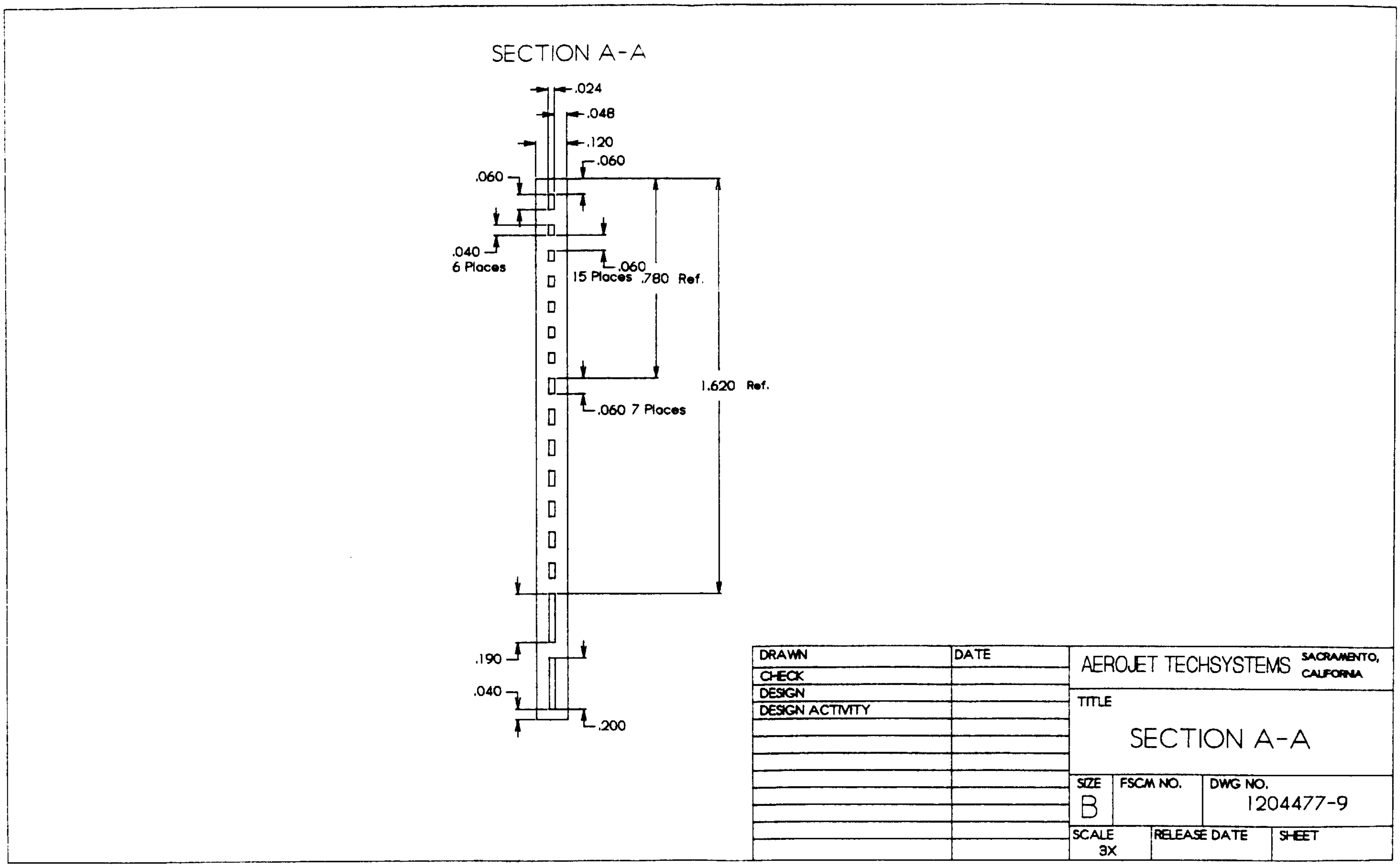

Figure A-6 Cross Section of Regenerator Vane Section

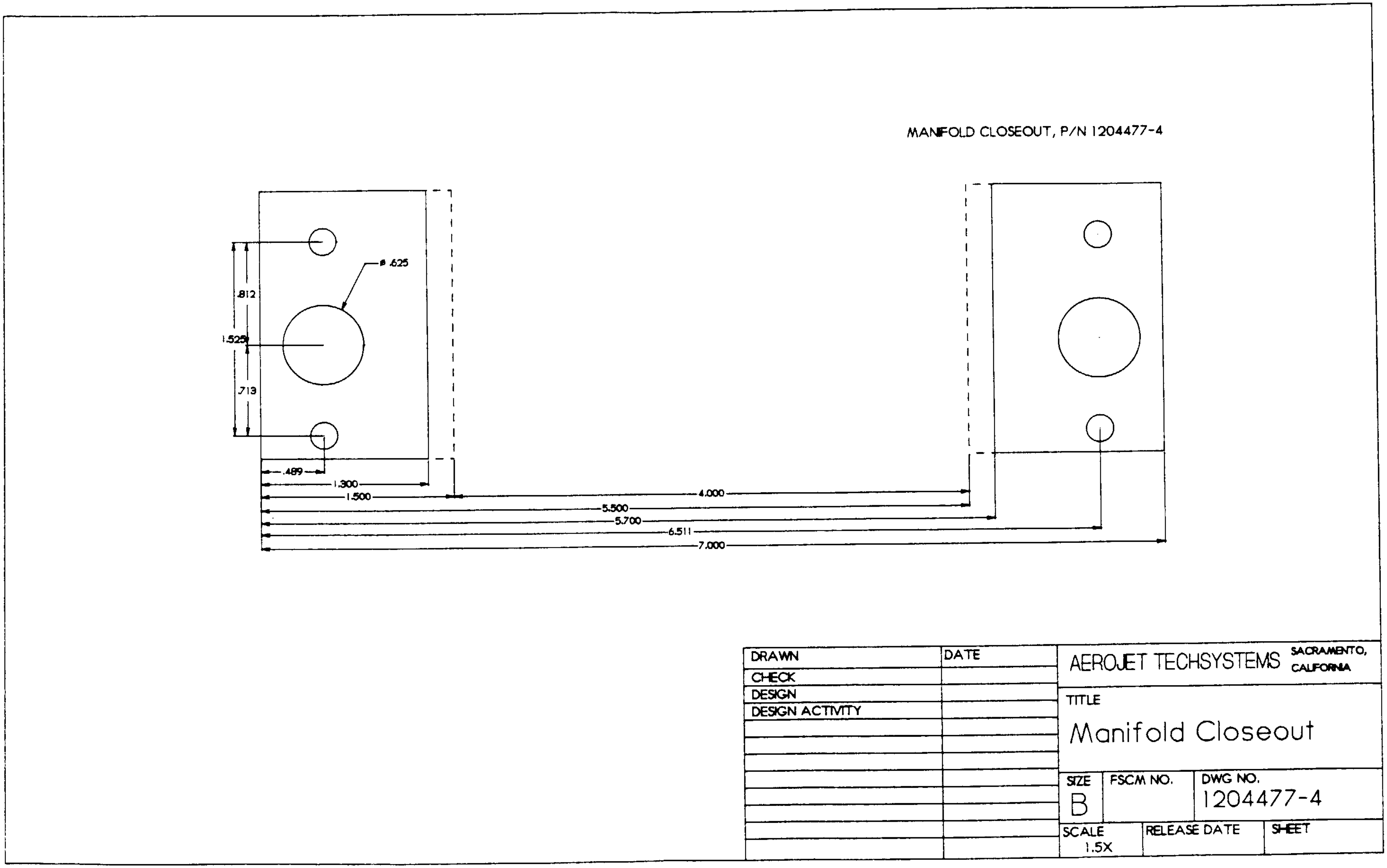

Figure A-7 Regenerator Manifold Closeout Platelet

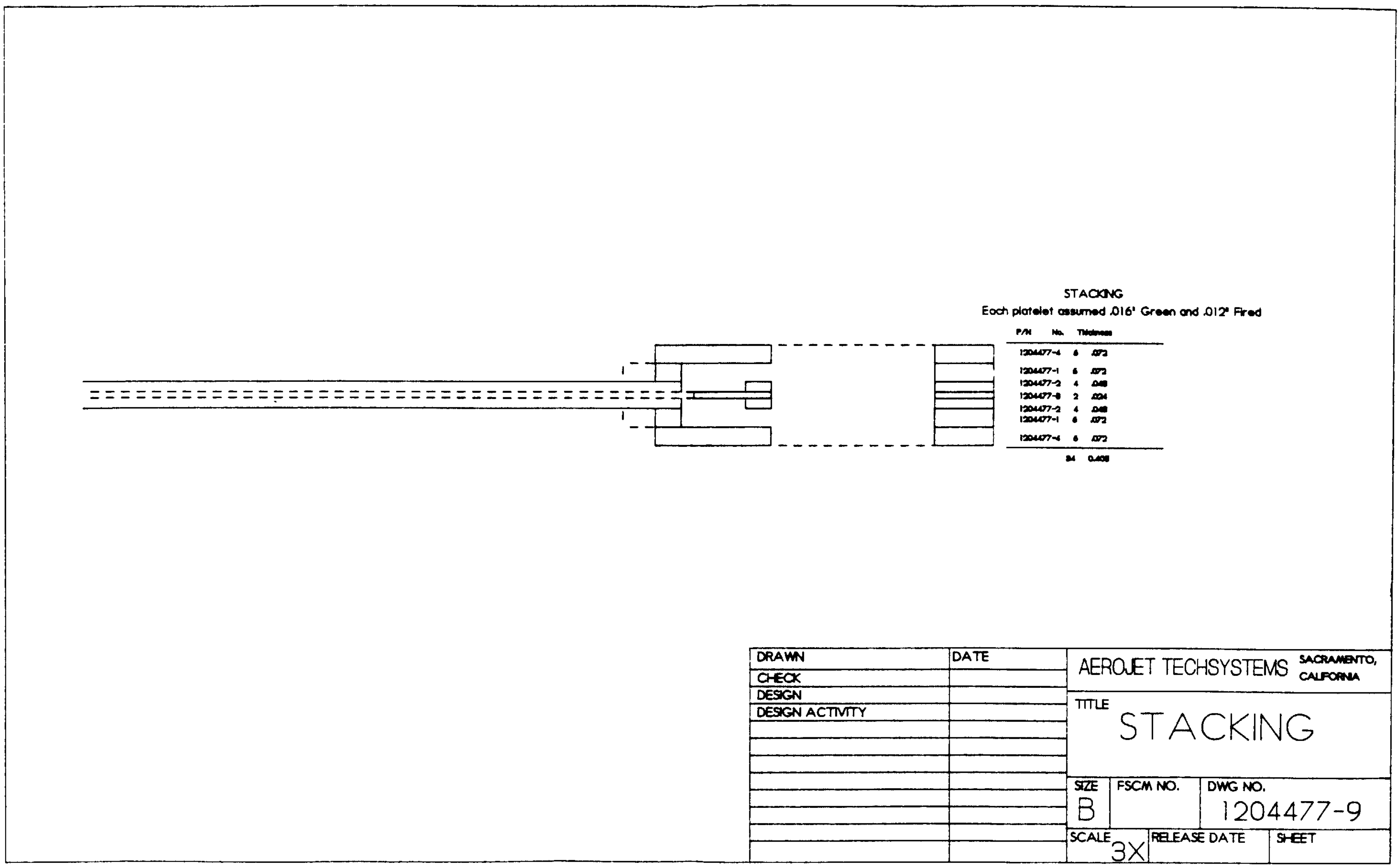

P/N	No.	Thickness
1204477-4	6	.072
1204477-1	6	.072
1204477-2	4	.048
1204477-8	2	.024
1204477-2	4	.048
1204477-1	6	.072
1204477-4	6	.072
	34	0.408

Figure A-8 Platelet Stacking Sequence for Ceramic Regenerator. Note the Thickness of the Vane Channels (P/N 1204477-3) Has Been Reduced to 2 Platelets

and discharges off the trailing edge. The thickness, width, and height of the vane in the heated zone are 0.105, 3.50, and 2.05 in., respectively.

The fuel to be heated is delivered to the inlet and removed from the discharge end via 1/2-in.-dia stainless steel tubes. The supply and discharge tubes are bolted on to the test section via flanges containing a P.S.I., Inc., gold-plated seal, P/N 663129Y-0010-2. The assembly sequence and torque specifications for attaching the feed lines are given in Appendix A-1.

Tables A-2 through A-4 define the predicted operating temperatures and pressure drops for three cooling flow rates when the methane supply temperature and pressure are 530 R and 610 psia, respectively. Tables A-5 through A-7 define the temperature and pressure drop when the methane inlet temperature is increased to 1260 R. These flow vs. temperature analyses are conducted for predetermined pressure drops of 2, 10, and 50 psig through the heated portion of the test section. The pressure loss in the supply lines is small and has been neglected.

4.0 EVALUATION AND TESTING

The product evaluation program is divided into three parts as follows:

4.1 Measurements and Nondestructive Testing
4.2 Mechanical/Hydraulic Limits Testing
4.3 Thermal Testing

4.1 MEASUREMENTS AND NONDESTRUCTIVE TESTING

The test articles will be subjected to the following measurements and tests.

4.1.1 Each specimen will be weighed to within %0.5 gm.
4.1.2 Dimensional inspection per Figure A-9.
4.1.3 The following mechanical/hydraulic testing will be conducted.

4.1.4 Low-Pressure Proof Test

A. Pressurize to 100 psi with GN_2, hold for 1 min.

B. Pressurize to 250 psi with GN_2, hold for 1 min.

TABLE A-2

INITIAL GUESS BULK TEMP = 1000.0
WIDTH OF REGENERATOR VANE= 3.500
CERAMIC THICKNESS in = 0.040
CERAMIC COND, Btu/in-s-R = 0.000081
SHAPE FACTOR = 1.00
OF CHANNEL PER VANE = 16.0
OF VANES = 1.0
HOT GAS MASS FLOW, lbm/s = 0.10
COOLANT PRESSURE, psia = 610.0
COOLANT INLET TEMP, R = 530.0
MINOR LOSS FACTOR = 2.000
COMBUSTION GAS TEMP, R = 3500.0
COMBUSTION GAS PRESS, R = 15.0
COMBUSTOR AREA, in = 2.2
COMB GAS VISC, lbm/in-s = 0.000004
COMB GAS Cp, Btu/lbm = 0.37
COMB GAS COND, Btu/in-s-R= 0.000002
COMB GAS MOLECULAR WT. = 28.40

No.	X	REx	Delta	hs	Twg	Twl	Tb	Tex	hl	q"	ITER	CHANNEL MASS FLOW
	in		in	B/in2s	R	R	R	R	B/in2sR	B/in2s		lbm/sec
1	0.14	1792.	0.015	0.00034	1890.	1567.	1053.	1575.	0.001537	0.79	211	0.00155
2	0.39	4992.	0.026	0.00021	1423.	1195.	856.	1182.	0.001462	0.50	786	0.00168
3	0.64	8193.	0.033	0.00016	1472.	1280.	955.	1380.	0.001431	0.47	396	0.00045
4	0.76	9729.	0.036	0.00015	1432.	1249.	937.	1343.	0.001428	0.45	73	0.00045
5	0.88	11265.	0.038	0.00014	1380.	1206.	915.	1299.	0.001448	0.42	89	0.00046
6	1.00	12801.	0.041	0.00013	1341.	1175.	896.	1262.	0.001441	0.40	74	0.00047
7	1.12	14337.	0.043	0.00013	1309.	1150.	882.	1233.	0.001441	0.39	60	0.00047
8	1.24	15873.	0.046	0.00012	1286.	1132.	869.	1207.	0.001414	0.37	52	0.00048
9	1.36	17409.	0.048	0.00011	1245.	1099.	852.	1174.	0.001437	0.35	68	0.00048
10	1.48	18945.	0.050	0.00011	1424.	1285.	1022.	1514.	0.001398	0.37	680	0.00019
11	1.57	20097.	0.051	0.00010	1405.	1270.	1010.	1489.	0.001375	0.36	50	0.00019
12	1.66	21249.	0.053	0.00010	1382.	1249.	1000.	1469.	0.001404	0.35	41	0.00019
13	1.75	22401.	0.054	0.00010	1378.	1247.	997.	1464.	0.001400	0.35	10	0.00019
14	1.84	23554.	0.056	0.00010	1364.	1235.	987.	1445.	0.001382	0.34	40	0.00019
15	1.93	24706.	0.057	0.00010	1350.	1224.	978.	1426.	0.001365	0.34	37	0.00020
16	2.02	25858.	0.058	0.00009	1407.	1271.	954.	1377.	0.001462	0.46	99	0.00045

No.	RE COOLANT	PRESS DROP	HEAT TRANSFER	CHANNEL H.T. AREA	GAS-SIDE AREA	RATIO	Deq	WIDTH	HEIGHT	LAND THICKNESS	q"gas	Qgas	Pr COOLANT
		psi	Btu/sec	in2	in2		in	in	in	in	B/in2s	Btu/sec	
1	13921.	2.0	1.2459	1.575	2.257	1.43	0.0444	0.200	0.025	0.040	0.55	1.25	0.696
2	18819.	2.0	0.7456	1.505	1.750	1.16	0.0442	0.190	0.025	0.060	0.43	0.75	0.678
3	11572.	2.0	0.2769	0.595	0.840	1.41	0.0353	0.060	0.025	0.060	0.33	0.28	0.688
4	11916.	2.0	0.2651	0.595	0.840	1.41	0.0353	0.060	0.025	0.060	0.32	0.27	0.686
5	12355.	2.0	0.2509	0.595	0.840	1.41	0.0353	0.060	0.025	0.060	0.30	0.25	0.684
6	12736.	2.0	0.2393	0.595	0.840	1.41	0.0353	0.060	0.025	0.060	0.28	0.24	0.682
7	13061.	2.0	0.2299	0.595	0.840	1.41	0.0353	0.060	0.025	0.060	0.27	0.23	0.681
8	13353.	2.0	0.2218	0.595	0.840	1.41	0.0353	0.060	0.025	0.060	0.26	0.22	0.679
9	13755.	2.0	0.2111	0.595	0.840	1.41	0.0353	0.060	0.025	0.060	0.25	0.21	0.677
10	7160.	2.0	0.1414	0.385	0.630	1.64	0.0273	0.030	0.025	0.060	0.22	0.14	0.694
11	7294.	2.0	0.1379	0.385	0.630	1.64	0.0273	0.030	0.025	0.060	0.22	0.14	0.693
12	7402.	2.0	0.1350	0.385	0.630	1.64	0.0273	0.030	0.025	0.060	0.21	0.14	0.692
13	7427.	2.0	0.1344	0.385	0.630	1.64	0.0273	0.030	0.025	0.060	0.21	0.13	0.692
14	7536.	2.0	0.1317	0.385	0.630	1.64	0.0273	0.030	0.025	0.060	0.21	0.13	0.691
15	7642.	2.0	0.1290	0.385	0.630	1.64	0.0273	0.030	0.025	0.060	0.20	0.13	0.690
16	11600.	2.0	0.2759	0.595	1.418	2.38	0.0353	0.060	0.025	0.060	0.19	0.28	0.688

TOTAL COOLANT FLOW, lbm/s= 0.0081
TOTAL HEAT TRANSFER, B/s = 4.77
VANE LENGTH, in = 2.030
VANE SURFACE AREA, in^2 = 15.1
CHANNEL AREA, in^2 = 10.2
HOT GAS DENSITY, lbm/ft^3= 0.0113
HOT GAS Pr, = 0.671
BLOCKAGE FACTOR = 0.169
HOT GAS VELOCITY, ft/sec = 585.
TOTAL WEIGHT OF VANE, lbm= 0.059
W.T. PER Btu/sec = 0.0123
W.T. PER in^2 = 0.0000
AVE. EXIT TEMPERATURE, R = 1342.

TABLE A-3

INITIAL GUESS BULK TEMP = 1000.0
WIDTH OF REGENERATOR VANE= 3.500
CERAMIC THICKNESS in = 0.040
CERAMIC COND, Btu/in-s-R = 0.000081
SHAPE FACTOR = 1.00
OF CHANNEL PER VANE = 16.0
OF VANES = 1.0
HOT GAS MASS FLOW, lbm/s = 0.10
COOLANT PRESSURE, psia = 610.0
COOLANT INLET TEMP, R = 530.0
MINOR LOSS FACTOR = 2.000
COMBUSTION GAS TEMP, R = 3500.0
COMBUSTION GAS PRESS, R = 15.0
COMBUSTOR AREA, in = 2.2
COMB GAS VISC, lbm/in-s = 0.000004
COMB GAS Cp, Btu/lbm = 0.37
COMB GAS COND, Btu/in-s-R= 0.000002
COMB GAS MOLECULAR WT. = 28.40

No.	X	REx	Delta	hs	Twg	Twl	Tb	Tex	hl	q'	ITER	CHANNEL MASS FLOW	RE COOLANT	PRESS DROP	HEAT TRANSFER
	in		in	B/in2s	R	R	R	R	B/in2sR	B/in2s		lbm/sec		psi	Btu/sec
1	0.14	1792.	0.015	0.00034	1527.	1131.	797.	1064.	0.002903	0.97	812	0.00440	49953.	10.0	1.5268
2	0.39	4992.	0.026	0.00021	1139.	880.	684.	837.	0.002863	0.56	455	0.00465	63167.	10.0	0.8471
3	0.64	8193.	0.033	0.00016	1149.	927.	733.	937.	0.002798	0.54	209	0.00127	41126.	10.0	0.3211
4	0.76	9729.	0.036	0.00015	1118.	907.	723.	916.	0.002794	0.51	41	0.00129	42071.	10.0	0.3050
5	0.88	11265.	0.038	0.00014	1081.	883.	711.	892.	0.002801	0.48	50	0.00130	43221.	10.0	0.2863
6	1.00	12801.	0.041	0.00013	1052.	864.	701.	872.	0.002797	0.46	46	0.00131	44177.	10.0	0.2713
7	1.12	14337.	0.043	0.00013	1029.	850.	693.	856.	0.002778	0.44	33	0.00133	44990.	10.0	0.2590
8	1.24	15873.	0.046	0.00012	1010.	837.	687.	844.	0.002789	0.42	26	0.00133	45643.	10.0	0.2494
9	1.36	17409.	0.048	0.00011	984.	821.	678.	826.	0.002786	0.40	36	0.00135	46585.	10.0	0.2359
10	1.48	18945.	0.050	0.00011	1085.	924.	765.	1001.	0.002707	0.43	349	0.00055	26451.	10.0	0.1646
11	1.57	20097.	0.051	0.00010	1069.	912.	759.	987.	0.002707	0.42	27	0.00055	26831.	10.0	0.1598
12	1.66	21249.	0.053	0.00010	1056.	904.	753.	975.	0.002679	0.40	25	0.00056	27164.	10.0	0.1558
13	1.75	22401.	0.054	0.00010	1054.	902.	750.	973.	0.002673	0.40	6	0.00056	27235.	10.0	0.1549
14	1.84	23554.	0.056	0.00010	1042.	893.	746.	963.	0.002682	0.39	21	0.00056	27520.	10.0	0.1515
15	1.93	24706.	0.057	0.00010	1030.	885.	742.	953.	0.002691	0.39	19	0.00056	27795.	10.0	0.1483
16	2.02	25858.	0.058	0.00009	1082.	924.	732.	934.	0.002751	0.54	39	0.00128	41259.	10.0	0.3188

No.	CHANNEL H.T. AREA	GAS-SIDE AREA	RATIO	Deq	WIDTH	HEIGHT	LAND THICKNESS	q"gas	Qgas	Pr COOLANT
	in2	in2		in	in	in	in	B/in2s	Btu/sec	
1	1.575	2.257	1.43	0.0444	0.200	0.025	0.040	0.68	1.53	0.670
2	1.505	1.750	1.16	0.0442	0.190	0.025	0.060	0.48	0.85	0.654
3	0.595	0.840	1.41	0.0353	0.060	0.025	0.060	0.38	0.32	0.662
4	0.595	0.840	1.41	0.0353	0.060	0.025	0.060	0.36	0.31	0.660
5	0.595	0.840	1.41	0.0353	0.060	0.025	0.060	0.34	0.29	0.659
6	0.595	0.840	1.41	0.0353	0.060	0.025	0.060	0.32	0.27	0.657
7	0.595	0.840	1.41	0.0353	0.060	0.025	0.060	0.31	0.26	0.656
8	0.595	0.840	1.41	0.0353	0.060	0.025	0.060	0.30	0.25	0.655
9	0.595	0.840	1.41	0.0353	0.060	0.025	0.060	0.28	0.24	0.654
10	0.385	0.630	1.64	0.0273	0.030	0.025	0.060	0.26	0.16	0.666
11	0.385	0.630	1.64	0.0273	0.030	0.025	0.060	0.25	0.16	0.665
12	0.385	0.630	1.64	0.0273	0.030	0.025	0.060	0.25	0.16	0.665
13	0.385	0.630	1.64	0.0273	0.030	0.025	0.060	0.25	0.15	0.664
14	0.385	0.630	1.64	0.0273	0.030	0.025	0.060	0.24	0.15	0.664
15	0.385	0.630	1.64	0.0273	0.030	0.025	0.060	0.24	0.15	0.663
16	0.595	1.418	2.38	0.0353	0.060	0.025	0.060	0.23	0.32	0.662

TOTAL COOLANT FLOW, lbm/s= 0.0229
TOTAL HEAT TRANSFER, B/s = 5.56
VANE LENGTH, in = 2.030
VANE SURFACE AREA, in^2 = 15.1
CHANNEL AREA, in^2 = 10.2
HOT GAS DENSITY, lbm/ft^3= 0.0113
HOT GAS Pr, = 0.671
BLOCKAGE FACTOR = 0.169
HOT GAS VELOCITY, ft/sec = 585.
TOTAL WEIGHT OF VANE, lbm= 0.059
W.T. PER Btu/sec = 0.0106
W.T. PER in^2 = 0.0000
AVE. EXIT TEMPERATURE, R = 923.

TABLE A-4

```
INITIAL GUESS BULK TEMP  = [illegible]
WIDTH OF REGENERATOR VANE=  3.500
CERAMIC THICKNESS in     = 0.040
CERAMIC COND, Btu/in-s-R = 0.000081
SHAPE FACTOR             =  1.00
# OF CHANNEL PER VANE    =  16.0
# OF VANES               =   1.0
HOT GAS MASS FLOW, lbm/s =  0.10
COOLANT PRESSURE, psia   =   610.0
COOLANT INLET TEMP, R    =   530.0
MINOR LOSS FACTOR        =   2.000
COMBUSTION GAS TEMP, R   =  3500.0
COMBUSTION GAS PRESS, R  =  15.0
COMBUSTOR AREA, in       =     2.2
COMB GAS VISC, lbm/in-s  = 0.000004
COMB GAS Cp, Btu/lbm     =    0.37
COMB GAS COND, Btu/in-s-R= 0.000002
COMB GAS MOLECULAR WT.   =   28.40
```

No.	X	REx	Delta	hs	Twg	Twl	Tb	Tex	hl	q"	ITER	CHANNEL MASS FLOW	RE COOLANT	PRESS DROP	HEAT TRANSFER	CHANNEL H.T. AREA	GAS-SIDE AREA	RATIO	Deq	WIDTH	HEIGHT	LAND THICKNESS	q"gas	Qgas	Pr COOLANT
	in		in	B/in2s	R	R	R	R	B/in2sR	B/in2s		lbm/sec		psi	Btu/sec	in2	in2		in	in	in	in	B/in2s	Btu/sec	
1	0.14	1792.	0.015	0.00034	1288.	845.	654.	778.	0.005670	1.08	1384	0.01191	160764.	50.0	1.7085	1.575	2.257	1.43	0.0444	0.200	0.025	0.040	0.76	1.71	0.650
2	0.39	4992.	0.026	0.00021	980.	704.	598.	666.	0.005647	0.60	225	0.01207	184794.	50.0	0.9025	1.505	1.750	1.16	0.0442	0.190	0.025	0.060	0.52	0.90	0.641
3	0.64	8193.	0.033	0.00016	966.	726.	620.	711.	0.005505	0.58	90	0.00340	127174.	50.0	0.3462	0.595	0.840	1.41	0.0353	0.060	0.025	0.060	0.41	0.35	0.645
4	0.76	9729.	0.036	0.00015	943.	716.	616.	701.	0.005505	0.55	19	0.00342	128866.	50.0	0.3276	0.595	0.840	1.41	0.0353	0.060	0.025	0.060	0.39	0.33	0.644
5	0.88	11265.	0.038	0.00014	914.	703.	610.	689.	0.005510	0.51	25	0.00344	130948.	50.0	0.3052	0.595	0.840	1.41	0.0353	0.060	0.025	0.060	0.36	0.31	0.643
6	1.00	12801.	0.041	0.00013	893.	693.	605.	680.	0.005494	0.48	19	0.00346	132549.	50.0	0.2883	0.595	0.840	1.41	0.0353	0.060	0.025	0.060	0.34	0.29	0.642
7	1.12	14337.	0.043	0.00013	876.	686.	602.	673.	0.005508	0.46	15	0.00348	133817.	50.0	0.2752	0.595	0.840	1.41	0.0353	0.060	0.025	0.060	0.33	0.28	0.642
8	1.24	15873.	0.046	0.00012	862.	680.	599.	667.	0.005491	0.44	13	0.00349	134921.	50.0	0.2639	0.595	0.840	1.41	0.0353	0.060	0.025	0.060	0.31	0.26	0.641
9	1.36	17409.	0.048	0.00011	843.	671.	595.	659.	0.005498	0.42	17	0.00351	136418.	50.0	0.2489	0.595	0.840	1.41	0.0353	0.060	0.025	0.060	0.30	0.25	0.641
10	1.48	18945.	0.050	0.00011	895.	721.	634.	739.	0.005318	0.46	158	0.00149	84762.	50.0	0.1775	0.385	0.630	1.64	0.0273	0.030	0.025	0.060	0.28	0.18	0.647
11	1.57	20097.	0.051	0.00010	884.	715.	631.	732.	0.005308	0.45	12	0.00150	85466.	50.0	0.1721	0.385	0.630	1.64	0.0273	0.030	0.025	0.060	0.27	0.17	0.646
12	1.66	21249.	0.053	0.00010	874.	710.	628.	726.	0.005301	0.43	13	0.00150	86125.	50.0	0.1672	0.385	0.630	1.64	0.0273	0.030	0.025	0.060	0.27	0.17	0.646
13	1.75	22401.	0.054	0.00010	872.	709.	628.	725.	0.005295	0.43	7	0.00151	86235.	50.0	0.1663	0.385	0.630	1.64	0.0273	0.030	0.025	0.060	0.26	0.17	0.646
14	1.84	23554.	0.056	0.00010	864.	705.	625.	720.	0.005293	0.42	11	0.00151	86792.	50.0	0.1622	0.385	0.630	1.64	0.0273	0.030	0.025	0.060	0.26	0.16	0.645
15	1.93	24706.	0.057	0.00010	856.	701.	623.	716.	0.005293	0.41	10	0.00151	87299.	50.0	0.1584	0.385	0.630	1.64	0.0273	0.030	0.025	0.060	0.25	0.16	0.645
16	2.02	25858.	0.058	0.00009	894.	725.	620.	710.	0.005516	0.58	13	0.00340	127426.	50.0	0.3434	0.595	1.418	2.38	0.0353	0.060	0.025	0.060	0.24	0.34	0.645

```
TOTAL COOLANT FLOW, lbm/s=  0.0606
TOTAL HEAT TRANSFER, B/s =     6.01
VANE LENGTH,    in       = 2.030
VANE SURFACE AREA, in^2  =     15.1
CHANNEL AREA, in^2       =     10.2
HOT GAS DENSITY, lbm/ft^3= 0.0113
HOT GAS Pr,              = 0.671
BLOCKAGE FACTOR          = 0.169
HOT GAS VELOCITY, ft/sec =  585.
TOTAL WEIGHT OF VANE, lbm=   0.059
W.T. PER Btu/sec         = 0.0098
W.T. PER in^2            = 0.0000
AVE. EXIT TEMPERATURE, R =  707.
```


ORIGINAL PAGE IS
OF POOR QUALITY

TABLE A-5

INITIAL GUESS BULK TEMP = 1600.0
WIDTH OF REGENERATOR VANE= 3.500
CERAMIC THICKNESS in = 0.040
CERAMIC COND, Btu/in-s-R = 0.000081
SHAPE FACTOR = 1.00
OF CHANNEL PER VANE = 16.0
OF VANES = 1.0
HOT GAS MASS FLOW, lbm/s = 0.10
COOLANT PRESSURE, psia = 610.0
COOLANT INLET TEMP, R = 1260.0
MINOR LOSS FACTOR = 2.000
COMBUSTION GAS TEMP, R = 3500.0
COMBUSTION GAS PRESS, R = 15.0
COMBUSTOR AREA, in = 2.2
COMB GAS VISC, lbm/in-s = 0.000004
COMB GAS Cp, Btu/lbm = 0.37
COMB GAS COND, Btu/in-s-R= 0.000002
COMB GAS MOLECULAR WT. = 28.40

No.	I	REx	Delta	hs	Twg	Twl	Tb	Tex	hl	q"	ITER	CHANNEL MASS FLOW	RE COOLANT	PRESS DROP	HEAT TRANSFER	CHANNEL H.T. AREA	GAS-SIDE AREA	RATIO	Deq	WIDTH	HEIGHT	LAND THICKNESS	q"gas	Qgas	Pr COOLANT
	in		in	B/in2s	R	R	R	R	B/in2sR	B/in2s		lbm/sec		psi	Btu/sec	in2	in2		in	in	in	in	B/in2s	Btu/sec	
1	0.14	1792.	0.015	0.00034	2251.	2001.	1649.	2037.	0.001743	0.61	605	0.00123	7901.	2.0	0.9662	1.575	2.257	1.43	0.0444	0.200	0.025	0.040	0.43	0.97	0.699
2	0.39	4992.	0.026	0.00021	1897.	1721.	1502.	1743.	0.001742	0.38	589	0.00124	8921.	2.0	0.5750	1.505	1.750	1.16	0.0442	0.190	0.025	0.060	0.33	0.58	0.705
3	0.64	8193.	0.033	0.00016	1940.	1792.	1577.	1894.	0.001665	0.36	301	0.00034	5981.	2.0	0.2131	0.595	0.840	1.41	0.0353	0.060	0.025	0.060	0.25	0.21	0.703
4	0.76	9729.	0.036	0.00015	1912.	1771.	1563.	1865.	0.001645	0.34	57	0.00034	6058.	2.0	0.2036	0.595	0.840	1.41	0.0353	0.060	0.025	0.060	0.24	0.20	0.703
5	0.88	11265.	0.038	0.00014	1872.	1738.	1546.	1832.	0.001686	0.32	67	0.00035	6147.	2.0	0.1927	0.595	0.840	1.41	0.0353	0.060	0.025	0.060	0.23	0.19	0.704
6	1.00	12801.	0.041	0.00013	1844.	1717.	1532.	1804.	0.001665	0.31	57	0.00035	6225.	2.0	0.1834	0.595	0.840	1.41	0.0353	0.060	0.025	0.060	0.22	0.18	0.704
7	1.12	14337.	0.043	0.00013	1823.	1701.	1521.	1782.	0.001649	0.30	45	0.00035	6288.	2.0	0.1761	0.595	0.840	1.41	0.0353	0.060	0.025	0.060	0.21	0.19	0.704
8	1.24	15873.	0.046	0.00012	1804.	1687.	1512.	1764.	0.001635	0.29	37	0.00035	6342.	2.0	0.1700	0.595	0.840	1.41	0.0353	0.060	0.025	0.060	0.20	0.17	0.705
9	1.36	17409.	0.048	0.00011	1774.	1662.	1500.	1740.	0.001680	0.27	49	0.00035	6413.	2.0	0.1620	0.595	0.840	1.41	0.0353	0.060	0.025	0.060	0.19	0.16	0.705
10	1.46	18945.	0.050	0.00011	1909.	1803.	1629.	1998.	0.001622	0.28	517	0.00015	3875.	2.0	0.1084	0.385	0.630	1.64	0.0273	0.030	0.025	0.060	0.17	0.11	0.700
11	1.57	20097.	0.051	0.00010	1894.	1790.	1621.	1979.	0.001609	0.27	38	0.00015	3905.	2.0	0.1056	0.385	0.630	1.64	0.0273	0.030	0.025	0.060	0.17	0.11	0.701
12	1.66	21249.	0.053	0.00010	1880.	1779.	1611.	1963.	0.001598	0.27	34	0.00015	3932.	2.0	0.1033	0.385	0.630	1.64	0.0273	0.030	0.025	0.060	0.16	0.10	0.701
13	1.75	22401.	0.054	0.00010	1678.	1777.	[illegible]	1959.	0.001596	0.27	7	0.00015	3938.	2.0	0.1028	0.385	0.630	1.64	0.0273	0.030	0.025	0.060	0.16	0.11	0.701
14	1.84	23554.	0.056	0.00010	1866.	1767.	1632.	1945.	0.001586	0.26	30	0.00015	3962.	2.0	0.1007	0.385	0.630	1.64	0.0273	0.030	0.025	0.060	0.16	0.10	0.702
15	1.93	24706.	0.057	0.00010	1855.	1759.	1596.	1932.	0.001577	0.25	27	0.00015	3984.	2.0	0.0988	0.385	0.630	1.64	0.0273	0.030	0.025	0.060	0.16	0.10	0.702
16	2.02	25858.	0.058	0.00009	1894.	1789.	1575.	1890.	0.001663	0.26	83	0.00034	5991.	2.0	0.2118	0.595	1.418	2.38	0.0353	0.060	0.025	0.060	0.15	0.21	0.703

TOTAL COOLANT FLOW, lbm/s= 0.0061
TOTAL HEAT TRANSFER, B/s = 3.67
VANE LENGTH, in = 2.030
VANE SURFACE AREA, in^2 = 15.1
CHANNEL AREA, in^2 = 10.2
HOT GAS DENSITY, lbm/ft^3= 0.0113
HOT GAS Pr, = 0.671
BLOCKAGE FACTOR = 0.169
HOT GAS VELOCITY, ft/sec = 585.
TOTAL WEIGHT OF VANE, lbm= 0.059
W.T. PER Btu/sec = 0.0160
W.T. PER in^2 = 0.0000
AVE. EXIT TEMPERATURE, R = 1869.

TABLE A-6

INITIAL GUESS BULK TEMP = 1800.0
WIDTH OF REGENERATOR VANE= 3.500
CERAMIC THICKNESS in = 0.040
CERAMIC COND, Btu/in-s-R = 0.000081
SHAPE FACTOR = 1.00
OF CHANNEL PER VANE = 16.0
OF VANES = 1.0
HOT GAS MASS FLOW, lbm/s = 0.10
COOLANT PRESSURE, psia = 610.0
COOLANT INLET TEMP, R = 1260.0
MINOR LOSS FACTOR = 2.000
COMBUSTION GAS TEMP, R = 3500.0
COMBUSTION GAS PRESS, R = 15.0
COMBUSTOR AREA, in = 2.2
COMB GAS VISC, lbm/in-s = 0.000004
COMB GAS Cp, Btu/lbm = 0.37
COMB GAS COND, Btu/in-s-R= 0.000002
COMB GAS MOLECULAR WT. = 28.40

No.	I	REx	Delta	hs	Twg	Twl	Tb	Tex	hl	q"	ITER	CHANNEL MASS FLOW	RE COOLANT	PRESS DROP
	in		in	B/in2s	R	R	R	R	B/in2sR	B/in2s		lbm/sec		psi
1	0.14	1792.	0.015	0.00034	1978.	1673.	1457.	1654.	0.003466	0.75	1372	0.00318	22293.	10.0
2	0.39	4992.	0.026	0.00021	1695.	1498.	1373.	1486.	0.003439	0.43	336	0.00315	24105.	10.0
3	0.64	8193.	0.033	0.00016	1705.	1535.	1411.	1562.	0.003321	0.41	151	0.00088	16696.	10.0
4	0.76	9729.	0.036	0.00015	1683.	1522.	1404.	1547.	0.003297	0.39	30	0.00088	16830.	10.0
5	0.88	11265.	0.038	0.00014	1655.	1504.	1394.	1528.	0.003324	0.37	38	0.00089	16992.	10.0
6	1.00	12801.	0.041	0.00013	1636.	1492.	1387.	1514.	0.003301	0.35	29	0.00089	17117.	10.0
7	1.12	14337.	0.043	0.00013	1619.	1483.	1382.	1503.	0.003283	0.33	24	0.00089	17221.	10.0
8	1.24	15873.	0.046	0.00012	1606.	1474.	1377.	1493.	0.003267	0.32	20	0.00090	17307.	10.0
9	1.36	17409.	0.048	0.00011	1586.	1462.	1370.	1480.	0.003302	0.30	27	0.00090	17427.	10.0
10	1.48	18945.	0.050	0.00011	1663.	1541.	1436.	1612.	0.003111	0.33	262	0.00038	11070.	10.0
11	1.57	20097.	0.051	0.00010	1650.	1531.	1431.	1602.	0.003172	0.32	19	0.00038	11125.	10.0
12	1.66	21249.	0.053	0.00010	1640.	1524.	1426.	1593.	0.003158	0.31	18	0.00038	11175.	10.0
13	1.75	22401.	0.054	0.00010	1638.	1523.	1426.	1591.	0.003155	0.31	4	0.00038	11186.	10.0
14	1.84	23554.	0.056	0.00010	1630.	1517.	1422.	1583.	0.003144	0.30	16	0.00039	11228.	10.0
15	1.93	24706.	0.057	0.00010	1622.	1512.	1418.	1576.	0.003133	0.29	15	0.00039	11268.	10.0
16	2.02	25858.	0.058	0.00009	1653.	1533.	1416.	1569.	0.003317	0.41	34	0.00088	16718.	10.0

No.	HEAT TRANSFER	CHANNEL H.T. AREA	GAS-SIDE AREA	RATIO	Deq	WIDTH	HEIGHT	LAND THICKNESS	q"gas	Qgas	Pr COOLANT
	Btu/sec	in2	in2		in	in	in	in	B/in2s	Btu/sec	
1	1.1776	1.575	2.257	1.43	0.0444	0.200	0.025	0.040	0.52	1.18	0.706
2	0.6463	1.505	1.750	1.16	0.0442	0.190	0.025	0.060	0.37	0.65	0.707
3	0.2452	0.595	0.840	1.41	0.0353	0.060	0.025	0.060	0.29	0.24	0.706
4	0.2328	0.595	0.840	1.41	0.0353	0.060	0.025	0.060	0.28	0.23	0.707
5	0.2179	0.595	0.840	1.41	0.0353	0.060	0.025	0.060	0.26	0.22	0.707
6	0.2067	0.595	0.840	1.41	0.0353	0.060	0.025	0.060	0.25	0.21	0.707
7	0.1974	0.595	0.840	1.41	0.0353	0.060	0.025	0.060	0.24	0.20	0.707
8	0.1898	0.595	0.840	1.41	0.0353	0.060	0.025	0.060	0.22	0.19	0.707
9	0.1793	0.595	0.840	1.41	0.0353	0.060	0.025	0.060	0.21	0.18	0.707
10	0.1253	0.385	0.630	1.64	0.0273	0.030	0.025	0.060	0.20	0.13	0.706
11	0.1218	0.385	0.630	1.64	0.0273	0.030	0.025	0.060	0.19	0.12	0.706
12	0.1186	0.385	0.630	1.64	0.0273	0.030	0.025	0.060	0.19	0.12	0.706
13	0.1179	0.385	0.630	1.64	0.0273	0.030	0.025	0.060	0.19	0.12	0.706
14	0.1152	0.385	0.630	1.64	0.0273	0.030	0.025	0.060	0.18	0.12	0.706
15	0.1128	0.385	0.630	1.64	0.0273	0.030	0.025	0.060	0.18	0.11	0.706
16	0.2432	0.595	1.418	2.38	0.0353	0.060	0.025	0.060	0.17	0.24	0.707

TOTAL COOLANT FLOW, lbm/s= 0.0158
TOTAL HEAT TRANSFER, B/s = 4.25
VANE LENGTH, in = 2.030
VANE SURFACE AREA, in^2 = 15.1
CHANNEL AREA, in^2 = 10.2
HOT GAS DENSITY, lbm/ft^3= 0.0113
HOT GAS Pr, = 0.671
BLOCKAGE FACTOR = 0.169
HOT GAS VELOCITY, ft/sec = 585.
TOTAL WEIGHT OF VANE, lbm= 0.059
W.T. PER Btu/sec = 0.0139
W.T. PER in^2 = 0.0000
AVE. EXIT TEMPERATURE, R = 1553.

ORIGINAL PAGE IS
OF POOR QUALITY

<u>TABLE A-7</u>

INITIAL GUESS BULK TEMP = 1600.0
WIDTH OF REGENERATOR VANE= 3.500
CERAMIC THICKNESS in = 0.040
CERAMIC COND, Btu/in-s-R = 0.000081
SHAPE FACTOR = 1.00
OF CHANNEL PER VANE = 16.0
OF VANES = 1.0
HOT GAS MASS FLOW, lbm/s = 0.10
COOLANT PRESSURE, psia = 610.0
COOLANT INLET TEMP, R = 1260.0
MINOR LOSS FACTOR = 2.000
COMBUSTION GAS TEMP, R = 3500.0
COMBUSTION GAS PRESS, R = 15.0
COMBUSTOR AREA, in = 2.2
COMB GAS VISC, lbm/in-s = 0.000004
COMB GAS Cp, Btu/lbm = 0.37
COMB GAS COND, Btu/in-s-R= 0.000002
COMB GAS MOLECULAR WT. = 28.40

No.	I	REx	Delta	hs	Twg	Twl	Tb	Tex	hl	q'	ITER
	in		in	B/in2s	R	R	R	R	B/in2sR	B/in2s	
1	0.14	1792.	0.015	0.00034	1811.	1473.	1351.	1442.	0.006819	0.83	1795
2	0.39	4992.	0.026	0.00021	1586.	1377.	1310.	1360.	0.006787	0.45	165
3	0.64	8193.	0.033	0.00016	1577.	1395.	1327.	1395.	0.006593	0.44	69
4	0.76	9729.	0.036	0.00015	1559.	1387.	1324.	1387.	0.006566	0.42	15
5	0.88	11265.	0.038	0.00014	1539.	1379.	1320.	1379.	0.006590	0.39	18
6	1.00	12801.	0.041	0.00013	1524.	1372.	1316.	1372.	0.006568	0.37	14
7	1.12	14337.	0.043	0.00013	1511.	1367.	1314.	1367.	0.006550	0.35	12
8	1.24	15873.	0.046	0.00012	1501.	1363.	1311.	1362.	0.006535	0.34	10
9	1.36	17409.	0.048	0.00011	1488.	1357.	1309.	1357.	0.006568	0.32	12
10	1.48	18945.	0.050	0.00011	1526.	1394.	1338.	1417.	0.006279	0.35	119
11	1.57	20097.	0.051	0.00010	1518.	1390.	1336.	1412.	0.006263	0.34	9
12	1.66	21249.	0.053	0.00010	1510.	1386.	1334.	1407.	0.006249	0.33	9
13	1.75	22401.	0.054	0.00010	1509.	1386.	1333.	1406.	0.006246	0.33	3
14	1.84	23554.	0.056	0.00010	1503.	1383.	1332.	1403.	0.006235	0.32	8
15	1.93	24706.	0.057	0.00010	1497.	1380.	1330.	1400.	0.006294	0.31	7
16	2.02	25858.	0.058	0.00009	1522.	1393.	1327.	1394.	0.006588	0.44	13

No.	CHANNEL MASS FLOW	RE COOLANT	PRESS DROP	HEAT TRANSFER	CHANNEL H.T. AREA	GAS-SIDE AREA	RATIO	Deq	WIDTH	HEIGHT	LAND THICKNESS	q"gas	Qgas	Pr COOLANT
	lbm/sec		psi	Btu/sec	in2	in2		in	in	in	in	B/in2s	Btu/sec	
1	0.00797	58926.	50.0	1.3035	1.575	2.257	1.43	0.0444	0.200	0.025	0.040	0.58	1.31	0.707
2	0.00773	61224.	50.0	0.6835	1.505	1.750	1.16	0.0442	0.190	0.025	0.060	0.39	0.69	0.706
3	0.00219	43466.	50.0	0.2634	0.595	0.840	1.41	0.0353	0.060	0.025	0.060	0.31	0.26	0.707
4	0.00220	43662.	50.0	0.2479	0.595	0.840	1.41	0.0353	0.060	0.025	0.060	0.30	0.25	0.706
5	0.00220	43872.	50.0	0.2315	0.595	0.840	1.41	0.0353	0.060	0.025	0.060	0.28	0.23	0.706
6	0.00220	44034.	50.0	0.2189	0.595	0.840	1.41	0.0353	0.060	0.025	0.060	0.26	0.22	0.706
7	0.00221	44172.	50.0	0.2083	0.595	0.840	1.41	0.0353	0.060	0.025	0.060	0.25	0.21	0.706
8	0.00221	44285.	50.0	0.1995	0.595	0.840	1.41	0.0353	0.060	0.025	0.060	0.24	0.20	0.706
9	0.00221	44424.	50.0	0.1889	0.595	0.840	1.41	0.0353	0.060	0.025	0.060	0.22	0.19	0.706
10	0.00096	29331.	50.0	0.1347	0.385	0.630	1.64	0.0273	0.030	0.025	0.060	0.21	0.13	0.707
11	0.00096	29411.	50.0	0.1304	0.385	0.630	1.64	0.0273	0.030	0.025	0.060	0.21	0.13	0.707
12	0.00096	29484.	50.0	0.1266	0.385	0.630	1.64	0.0273	0.030	0.025	0.060	0.20	0.13	0.707
13	0.00097	29500.	50.0	0.1257	0.385	0.630	1.64	0.0273	0.030	0.025	0.060	0.20	0.13	0.707
14	0.00097	29557.	50.0	0.1228	0.385	0.630	1.64	0.0273	0.030	0.025	0.060	0.20	0.12	0.707
15	0.00097	29606.	50.0	0.1202	0.385	0.630	1.64	0.0273	0.030	0.025	0.060	0.19	0.12	0.707
16	0.00219	43502.	50.0	0.2605	0.595	1.418	2.38	0.0353	0.060	0.025	0.060	0.15	0.26	0.707

TOTAL COOLANT FLOW, lbm/s= 0.0391
TOTAL HEAT TRANSFER, B/s = 4.57
VANE LENGTH, in = 2.030
VANE SURFACE AREA, in^2 = 15.1
CHANNEL AREA, in^2 = 10.2
HOT GAS DENSITY, lbm/ft^3= 0.0113
HOT GAS Pr, = 0.671
BLOCKAGE FACTOR = 0.169
HOT GAS VELOCITY, ft/sec = 585.
TOTAL WEIGHT OF VANE, lbm= 0.059
W.T. PER Btu/sec = 0.0129
W.T. PER in^2 = 0.0000
AVE. EXIT TEMPERATURE, R = 1392.

ORIGINAL PAGE IS
OF POOR QUALITY

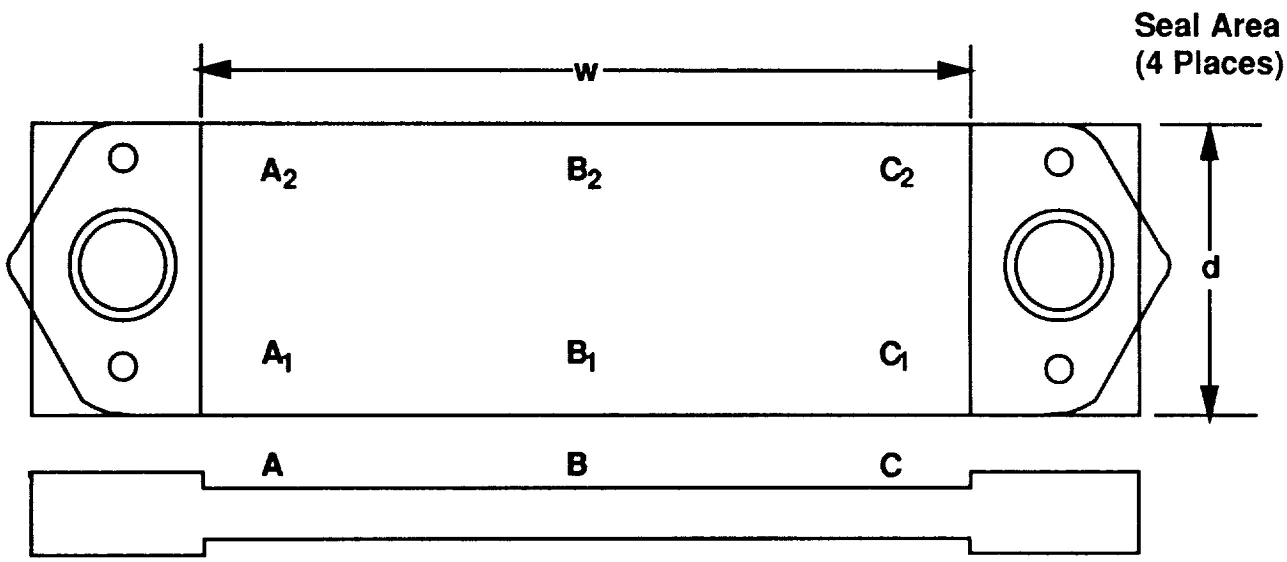

Vane SN	1			2			3			4			5			6		
	A	B	C	A	B	C	A	B	C	A	B	C	A	B	C	A	B	C
Thickness 1																		
2																		
Depth (d)																		
Width 1																		
2																		
Flatness (w)																		
Flatness (d)																		
Seal Area Flatness																		
Seal Area Surface Roughness																		
Weight (gm)																		

3.53.0.21

All Measurements to be Within 0.001 in. Roughness Resolution ±5 min. Weight ±0.5 gm

Figure A-9. Dimensional Inspection

4.1.5 Low-Pressure Leak Test

A. Pressurize with 50 psig GN_2.

B. Submerge in water and measure cc/min leakage rate for TBD min.

C. Document location of all visible leak areas.

4.1.6 High-Pressure Proof Testing

At the conclusion of the low pressure leak tests, each vane assembly will be proof tested with water to 1.5 the nominal operating pressure. The proof test will be conducted in the following steps, with one-minute holds at each pressure level except at 900 psi where the hold will be one-hour.

- 250 psi
- 400 psi
- 600 psi
- 800 psi
- 900 psi

The parts will be vacuum dehydrated at 150 F for 12 hr after proof testing.

4.1.7 Permeability Testing

All non-leaking units will be pressurized to the design point of 600 psia with nitrogen (a nitrogen molecule is about the same size as a methane molecule) and held for one hour. During this period, the pressure decay will be monitored and recorded. The volume of the pressurized system will be estimated to allow computation of the leakage rate. This test will give a more accurate assessment of permeability.

4.2 BURST TESTING

Burst testing will be conducted using water or other noncompressible fluid.

The pressure in one of the vanes will be increased in steps of 200 psi for each test and held for one-minute at pressures of 800, 1000, 1200, 1400, 1600, 1800 and 2000 psia. If rupture does not occur, the testing will continue until failure using the same stepped procedure.

Appropriate safety precautions will be provided during the above testing.

4.3 THERMAL TESTING

Thermal testing of the prototype regenerator has two basic objectives:

- To demonstrate the ability to withstand at least 50 thermal cycles in which the component goes from cold to steady-state operating temperatures.
- To simulate a working life in excess of 100 hours under realistic conditions of inside and outside environments, temperatures, and pressures.

Performance and durability testing will consist of two series of tests. In the first series, the cyclic thermal performance of one regenerator will be evaluated. In the second series, the duration capability of a second regenerator will be verified.

Testing will be performed in the Aerojet Heat Exchanger Test Facility described in Section 6.0. The facility uses an air-breathing fuel burner with a muffled forced draft fan that supplies pressurized air for combustion from stoichiometric up to approximately 50% excess air. The fuel for these tests will be commercial grade propane. An analysis of the propane will be made to establish the heating value and composition, including sulfur. Diluent air may be injected using outer ring nozzles to provide additional gas temperature control at the combustor outlet from 800 to 3100 F. The combustion gases will be passed through the test section, providing a realistic simulation of the regenerator environment. The combustor will be operated with sufficient excess air to avoid excessive CO and unburned hydrocarbons in the exhaust. The O2 content in the exhaust will be 2-5%.

In the initial check out tests the coolant will be high-purity nitrogen. This will avoid the possibility of methane coking the small cooling channels and reduces the test costs. It also reduces the fire safety hazards associated with operating with pressurized methane. In these tests the discharged methane will be burned off in the exit gas stream. High-purity methane, Table A-8, will be required to evaluate the performance and potential coking characteristics within the silicon nitride regenerator during the high temperature tests. Methane containing as little as 5 ppm H_2S was found to be capable of plugging copper cooling channels at a wall temperatures as low as 750 F. The methane coolant should operate coke-free up to about 1250 F.

Initial thermal cycle testing will consist of heating the prototype component in propane combustion products, using nitrogen as the coolant. Table A-9 shows the approximate factors to be used when substituting nitrogen for methane. The thermal cycle test matrix for the first test article is presented in Table A-10. This series of tests will establish the maximum temp-

<u>TABLE A-9</u>

APPROXIMATE FACTORS TO BE USED WHEN SUBSTITUTING NITROGEN FOR METHANE WITHOUT CHANGING WALL TEMPERATURE

Bulk Temperature, °F	$\dot{w}\ N_2/\dot{w}\ CH_4$ for Same Coefficient	$\dot{w}\ N_2 w\ \dot{C}H_4$ for Same Bulk Temperature Rise
640	3.65	3.06
1340	4.61	3.79
1700	5.85	4.03

$$\left(\dot{w}\ N_2 = \frac{\dot{w}\ N_2}{\dot{w}\ CH_4\ x}\right)^*$$

* The actual flow required may be slightly lower because the N_2 bulk temperature rise will be reduced.

TABLE A-10

PERFORMANCE CHARACTERIZATION AND THERMAL CYCLE TEST MATRIX

Test No.	Coolant Type	Estimated Flow lb/sec	Max Wall Temp.	Coolant Supply Temp. F	Coolant Disch Temp. F	Number Cycles	Time, Min. Heat	Time, Min. Cool	Notes
1	N_2	0.12-0.07	1250 to 1500	70	400-500	1	120	--	Adjust flow
2	N_2	0.048	1750	70	700	5	15	15	Inspect after test
3	N_2	0.032	2000	10	850	5	15	15	
4	N_2	TBD	Max	TBD	TBD	25	15	15	Max temp and thermal cycles
5	CH_4	0.008 0.004	2000 2000	800 70	1250 1250	5	2	15	Cycles and channel plugging
6	CH_4	TBD	Max	800 70	TBD	10	2	15	Cycles and channel plugging
						51			

erature capabilities of the design. This is accomplished by systematically reducing the coolant flow and then preheating the coolant if necessary. The test unit will be cycled from 70 F to the maximum acceptable temperature, which is expected to be 2500 F.

Test 1 will consist of one check out and instrumentation calibration cycle of 120 minutes. The coolant flow will be adjusted down ward during this period until the test section is 1500 F. The combustor will be turned off and the regenerator will cool rapidly by maintaining full coolant flow. The coolant flow will then be reduce to a trickle purge and the regenerator will be visually inspected. Three subsequent thermal cycle tests will establish the maximum temperature that the ceramic regenerator can withstand in the repeated rapid heating and cooling found in an engine. Test article instrumentation will provide all required data to calculate heat and mass balances and heat transfer parameters. Temperature measurements will be compared to the predicted values.

Methane will be substituted for nitrogen starting with Test 5. The initial methane test will limit the coolant to 1100 F in order to minimize the possibility of coking due to fuel decomposition. The final test will be for 10 cycles with the wall and coolant temperatures at maximum acceptable values. The second test section will be install following this test.

The extended-duration tests will consist of operating one prototype regenerator at the maximum acceptable temperature established in the first test series. The test will consist of heating the regenerator to full temperature and maintaining this condition for a goal of 100 hours. This duration exceeds the total test time for the component tested in thermal cycling. After the test, the regenerator will be visually inspected. This test will evaluate the performance of the regenerator for long-duration service at high temperature to determine the extent, if any, of reaction of the ceramic material with either the combustion products or the coolant.

5.0 POSTTEST EVALUATION

The tested regenerators will be examined visually for surface condition, warping, and cracking. The weight of the units after testing will be compared with weights measured before testing to determine mass changes, if any, due to surface oxidation from exposure to the combustion products. Dimensions of the components will also be compared with those measured prior to testing to determine the extent of any erosion or warpage. The units will be pressurized with nitrogen to determine the extent of leaks, if any, due to degradation caused by the testing.

After the nondestructive evaluation is completed, the prototype regenerators will be sectioned and examined for the condition of the internal channels, the extent of corrosion, fouling, and tolerances.

6.0 TEST FACILITY

6.1 DESIGN

Test objectives will be accomplished using the Aerojet Heat Exchanger Test Facility. The operating map for the propane burner-combustor has been well characterized and is defined in Figure A-10.

The facility uses an air-breathing fuel burner capable of providing up to 1,480,000 Btu/hr. A muffled forced draft fan supplies pressurized air for combustion from stoichiometric up to approximately 50% excess air. Diluent air may be injected using outer ring nozzles to provide additional gas temperature control at the combustor outlet from 800 to 3100 F. The combustion gases will be passed through the water-cooled flow section at 500 to 600 fps, providing a realistic simulation of the ATR regenerator environment and then exhausted directly to the atmosphere.

6.2 SYSTEM FLOW SCHEMATIC AND TEST INSTRUMENTATION

A facility flow schematic and the instrumentation required to control and monitor the combustor operation and conduct test article diagnostics are provided in Figure A-11. The hardware diagnostics includes coolant flow rate, inlet and discharge temperatures and pressures, and surface temperature measurements. Facility instrumentation includes gas temperature, composition, flow rate, and other control parameters. A complete list of instrumentation function, nomenclature, instrumentation type, and range is given in Table A-11.

6.3 FLOW SECTION AND SPECIMEN HOLDER

The water-cooled flow acceleration nozzle shown in Figure A-12 will be placed on the discharge of the combustor. The 3.5 in. by 0.62 in. rectangular duct will increase the gas velocity to 500-600 fps in the test section. A water-cooled 0.75 in. OD baffle tube will be positioned ahead of the test section to produce mixing and turbulence of the combustion gas. Three Pt-30 Rh vs. Pt-6 Rh Type B thermocouples positioned in the gas stream will record the gas temperature.

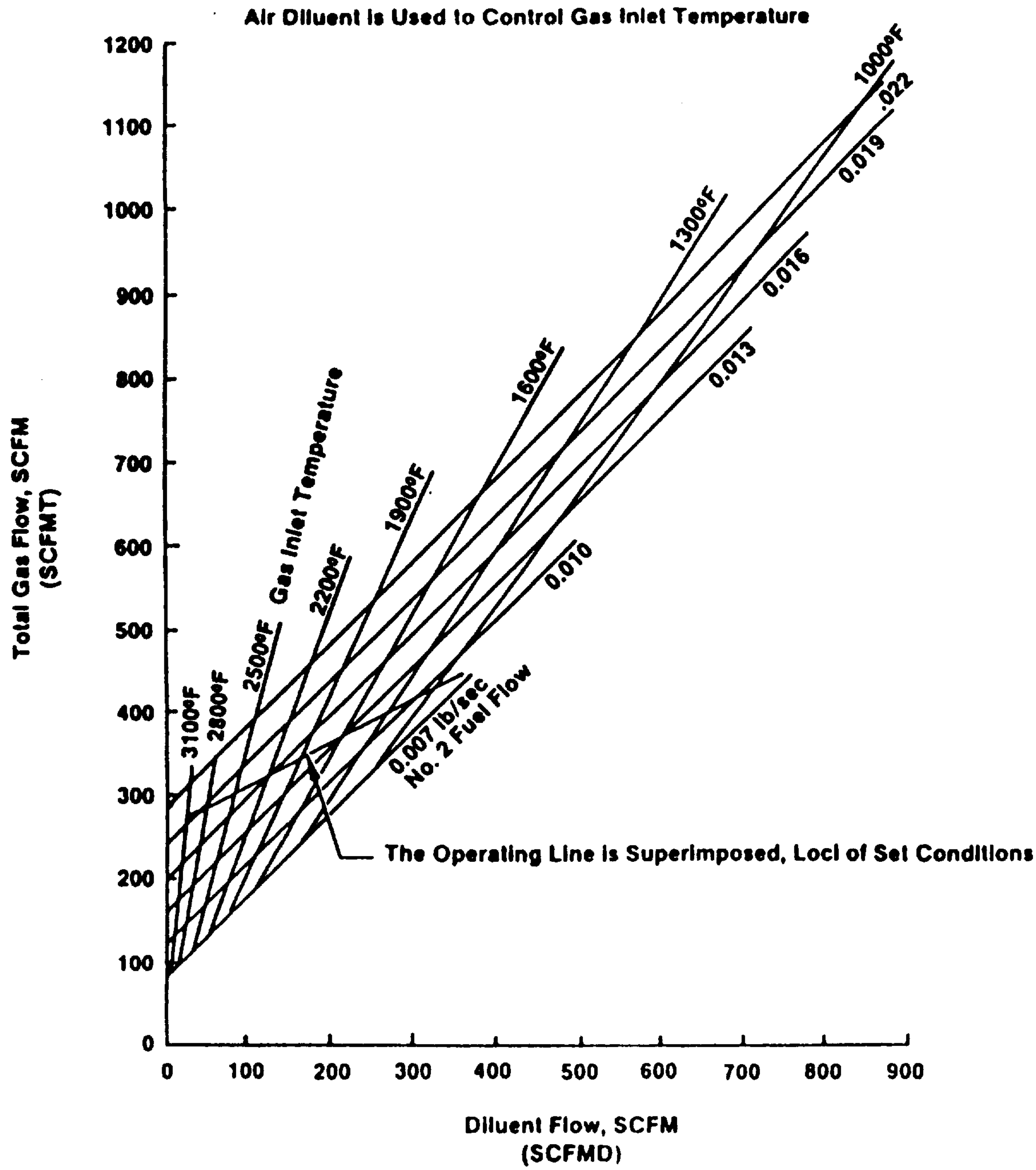

Figure A-10 Test Facility Operating Map

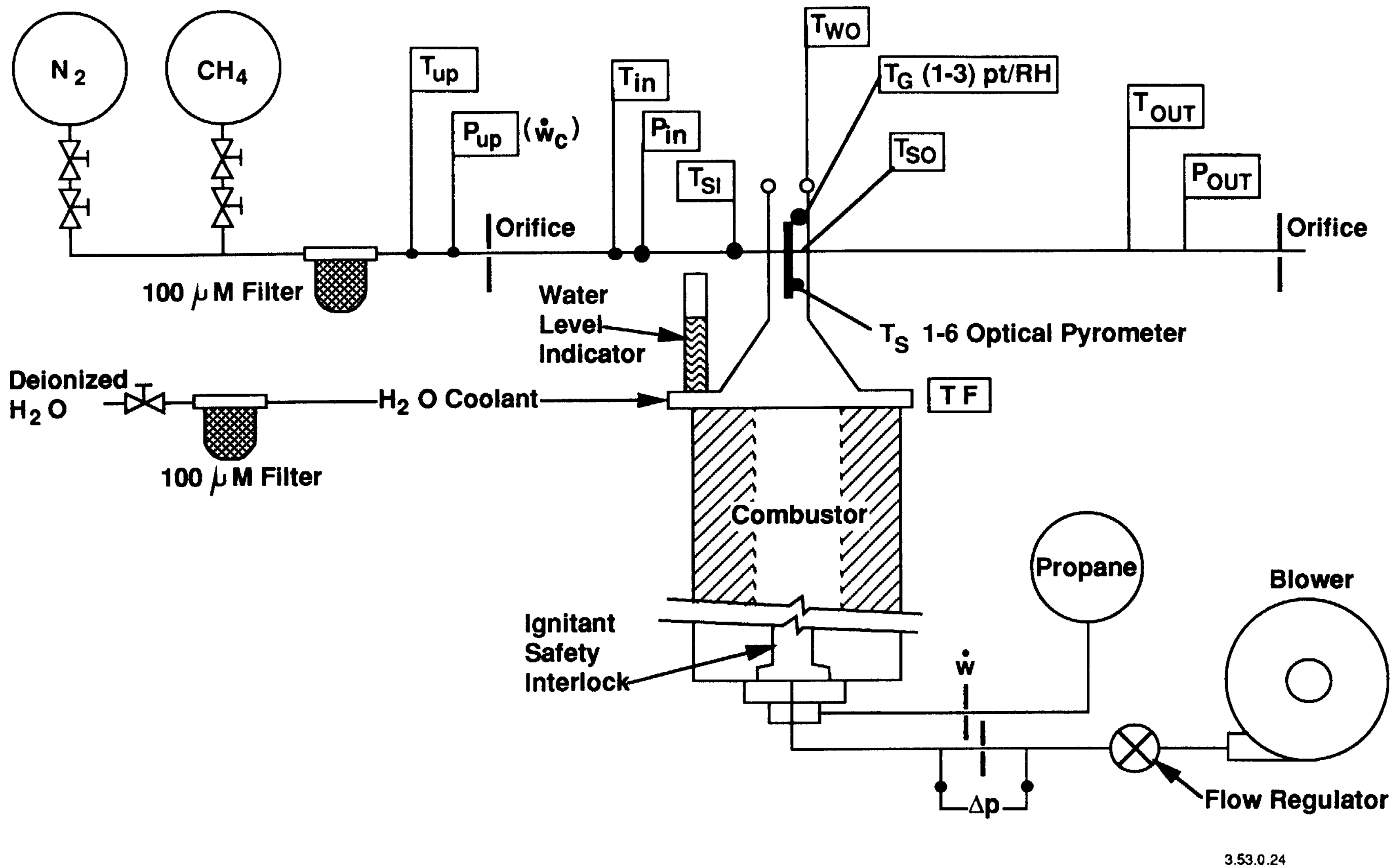

Figure A-11. Facility Flow Schematic

TABLE A-11

CERAMIC REGENERATOR INSTRUMENTATION

Test Parameter	Designation	Nominal Values	Range	Instrumentation
Hardware:				
Coolant Flow Rate, lb/sec	w_c	Var.	0.003-0.010	---
Coolant Inlet Temp, F	$T_{in.}$	Var.	70-1000	TC-K
Coolant Discharge Temp, F	T_{out}	Var.	70-1500	TC-K
Coolant Inlet Pressure, psia	P_{in}	600	400-800	Tab 206
Coolant Discharge Pressure, psia	P_{out}	600	400-800	Tab 206
Coolant Pressure Drop, psia	ΔP_c	Var.	5-40	TBD
Vane Surface Temp, F	TS-1	Var.	750-2000	Opt Pyro
	TS-2	Var.	750-2000	Opt Pyro
	TS-3	Var.	750-2000	Opt Pyro
	TS-4	Var.	750-2000	Opt Pyro
	TS-5	Var.	750-2000	Opt Pyro
	TS-6	Var.	750-2000	Opt Pyro
Inlet Seal Temp, F	TSI	Var.	70-1000	---
Outlet Seal Temp, F	TSO	Var.	70-1000	---
Facility				
Coolant Tank Pressure, psia	P_{ft}	Var.	200-2200	Tab 206
Air Pressure, psig	PA	TBD	0-1.0	---
Air Flow, cfm	wA	48	40-60	---
Propane Flow, lb/hr	wP	13.6	A/F 17 lb/air/lb fuel min	Orifice Pump
Gas Temp, F	Tg1	3000	2700-3100	Pt-30 Rh vs. Pt-6 Rh Type B
	Tg2	3000	2700-3100	Pt-30 Rh vs. Pt-6 Rh Type B
	Tg3	3000	2700-3100	Pt-30 Rh vs. Pt-6 Rh Type B
Exhaust Gas, O_2, %	VO_2	3	2-5	Batch Sample
Exhaust Gas, CO, %	VCO	<0.1	0-1	Batch Sample
Exhaust Gas, H/C, %	VH/C	<0.1	0-1	Batch Sample
Water Flow, lb/hr, 80 F	w_w	930	900-1500	For Design Only
Water Temp, F	T_{wo}	180	70-212	---
Flange Temp, F	TF	TBD	70-3000	
Preheater Power, KW	PH	Var.	0-10	For Design Only

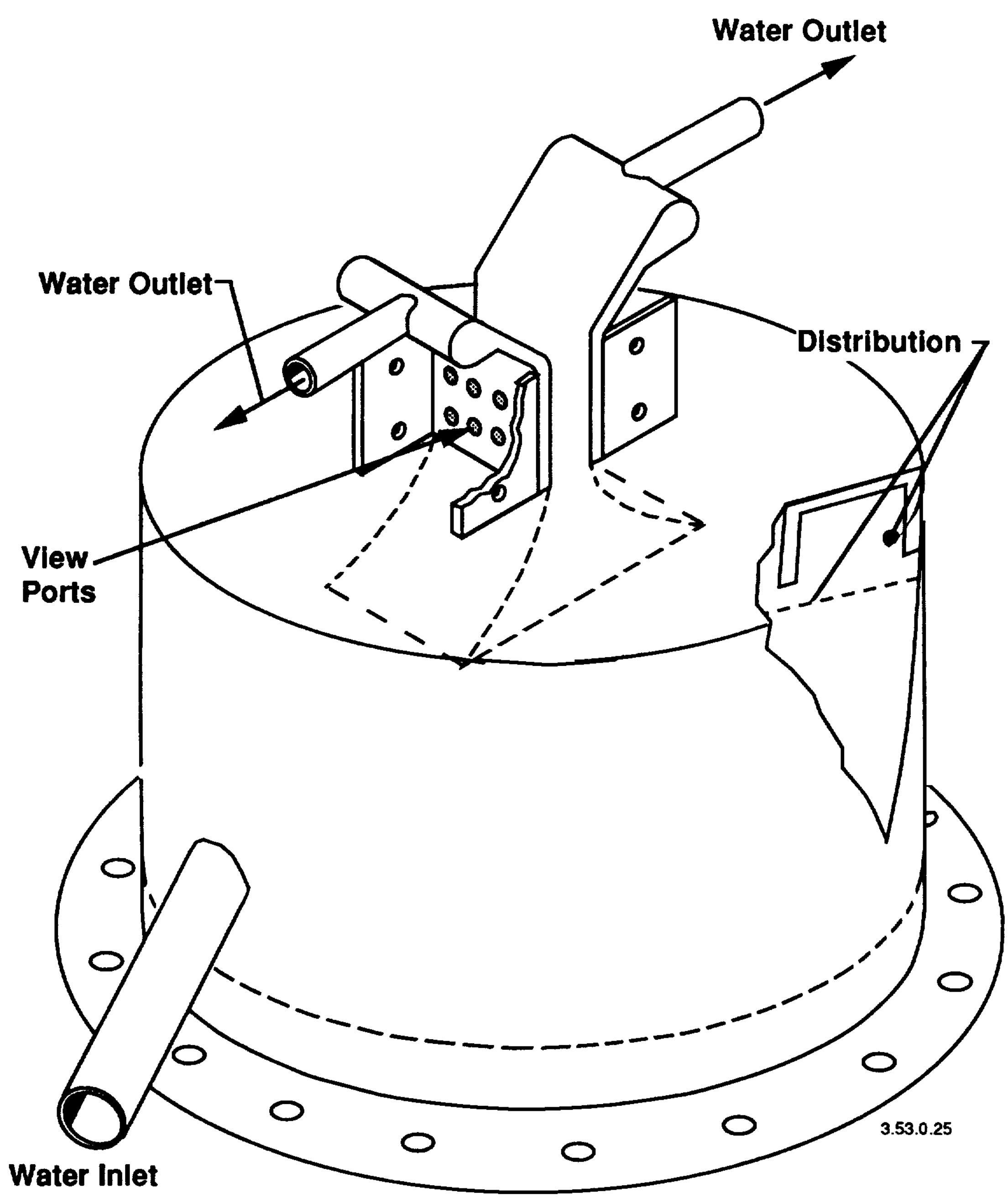

Figure A-12. Conceptual Design - Water-Cooled Specimen holder

One side-wall of the water-cooled high-velocity duct will contain 6 view ports for monitoring the test specimen surface temperature. Temperature will be measured by fiber optic pyrometers. Heat shields made of CRES 304 will be placed on the side-walls of the accelerator as shown. Holes will be provided in the shields to allow optical temperature measurement of the vane.

Four adjustable stainless steel clamps are provided to position the silicon nitride vane in the center of the gas stream, as shown in Figure A-13. The clamps are bolted to the water-cooled section on one end. A zirconia felt gasket is positioned between the test sample and the clamp, as shown in the figure. Two stainless steel brackets bridge the test section (one on each end) to prevent vertical motion. The zirconia insulation is provided above and below the test section to minimize clamp heating and gas leakage. The horizontal clamps are attached and locked in position first, then the vertical clamps are installed. Consideration will be given to the use of springs rather than bolts to maintain compression if thermal expansion loads are predicted to be a problem.

6.4 OPERATION/TEST PROCEDURES

Thermal cycle testing requires rapid heating and cooling transients in the test regenerator. Realistic thermal transients will be accomplished by cycling the fuel burner on and off as required while maintaining coolant flow through the regenerator.

It is required to bring the combustor refractory lining to thermal steady state prior to initiation of regenerator thermal cycling. This heat-up time will be based on the recommendation of the combustion vendor and is expected to be on the order of several hours.

A damper placed in the duct will allow the test section to be installed after the combustor has been preheated and removed without waiting for the refractory to cool down. The damper will be closed after the burner is shut off allowing access to the test section.

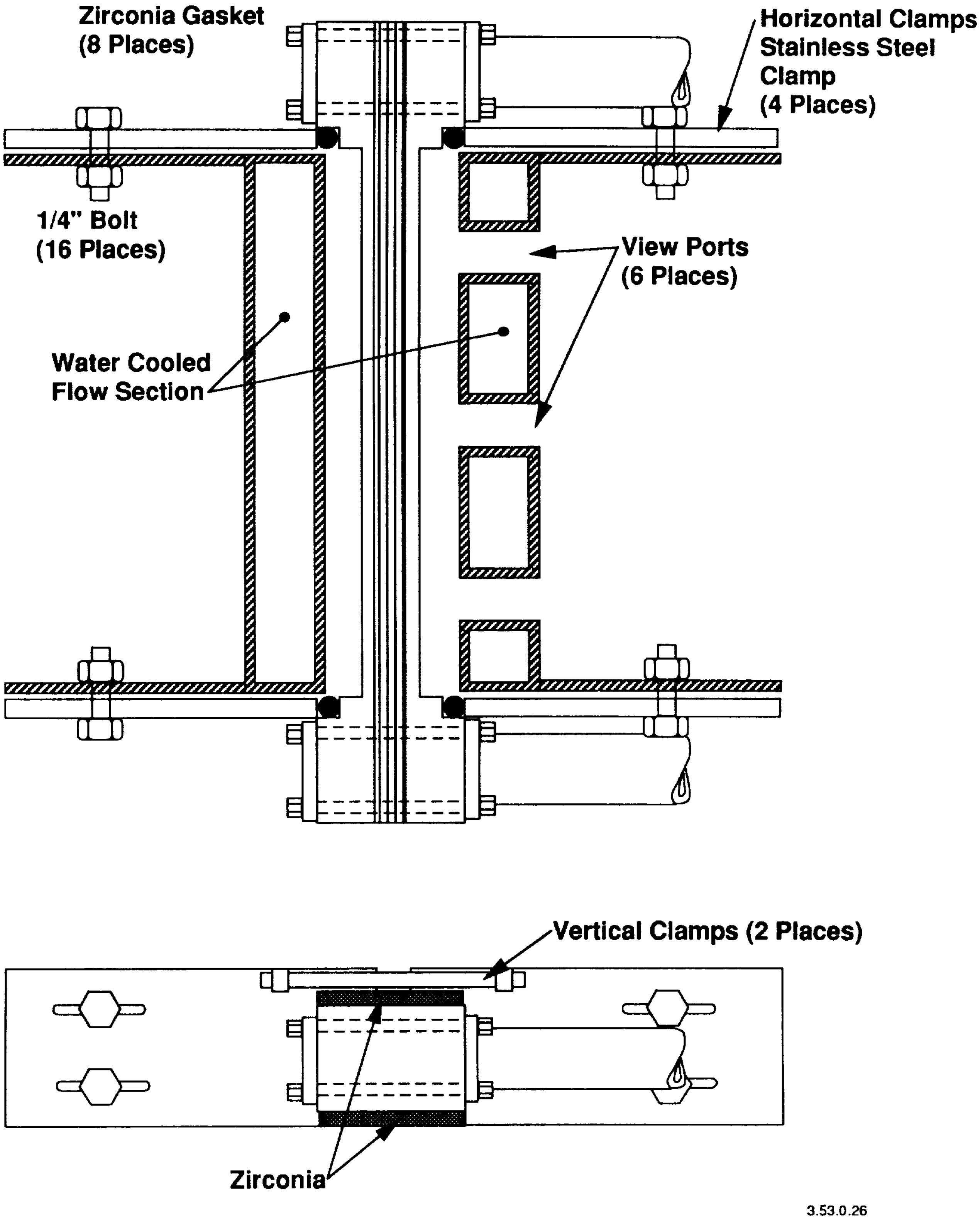

Figure A-13. Section Clamping Design

APPENDIX A-1

ASSEMBLY PROCEDURES FOR CONNECTING MANIFOLDS

TO CERAMIC VANES

PAGE________INTENTIONALLY BLANK

ASSEMBLY PROCEDURES FOR CONNECTING MANIFOLDS TO CERAMIC VANES

Surface preparation on ceramic.

Check for flatness and scratches

Flat to %0.0002 in seal area.

Install discharge orifice in discharge line before assembly. Check thermocouple and pressure tap on discharge line

Install seals in seal groove (2 on each end).

Center flange in bolt pattern.

Install bolts with Belville springs, as shown in Figure A-14.

Assemble mating flange-seal assembly and torque to TBD in. lb.

Check thermocouple spot welded to inlet and discharge flanges.

Cap discharge line and conduct leak check of seal assembly at 300 psi.

Remove cap.

Install subassembly in test apparatus and lock inlet line clamp in position, insuring vane is centered within 0.62 in. in wide duct. Note discharge end must remain free to expand.

Install 2-in. zirconia felt gasket in 4 locations and slide side wing seals to lightly contact and compress zirconia against vane.

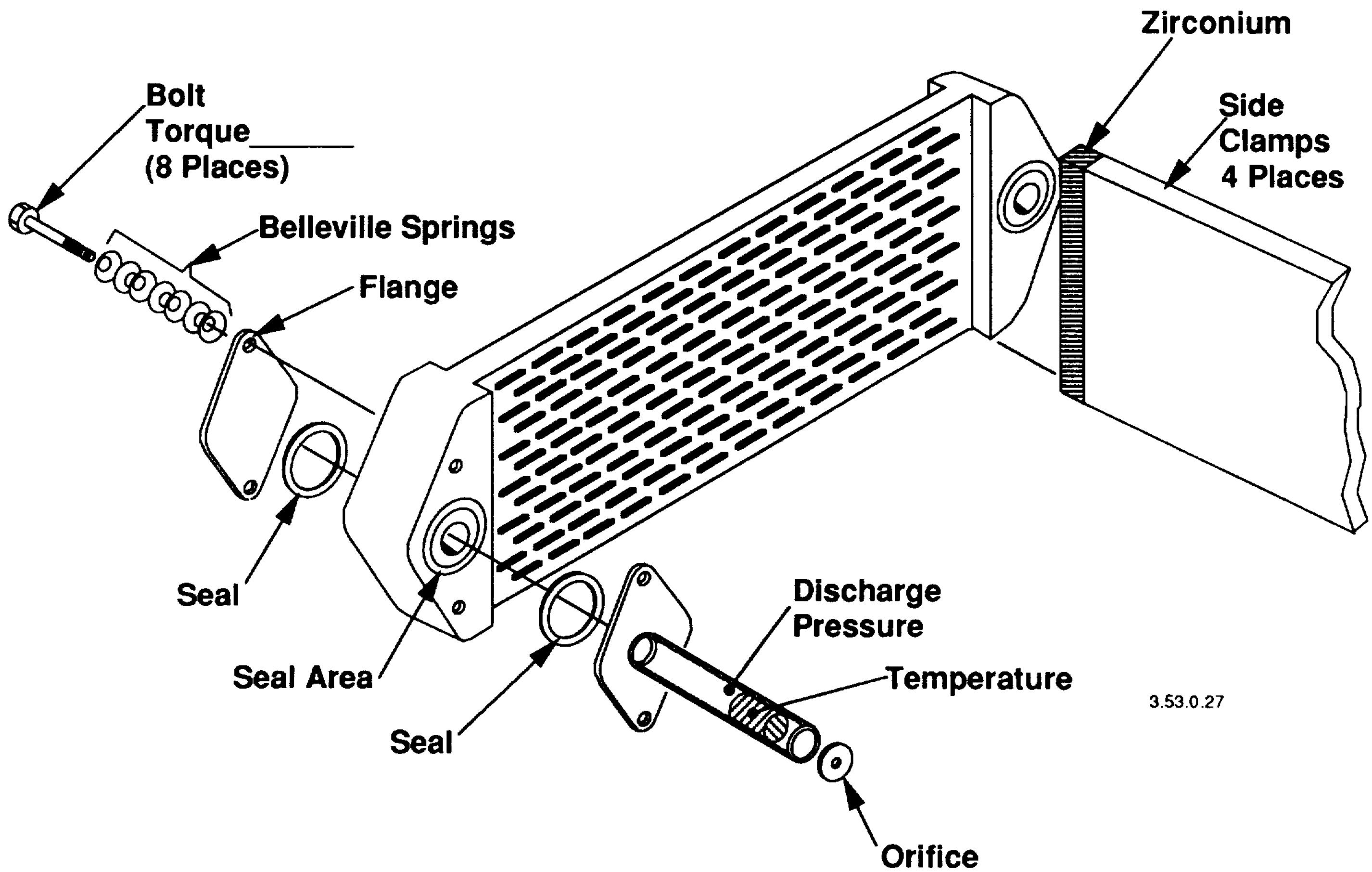

Figure A-14. Exploded View

Install 0.62-in. zirconia gasket in location and fix and lock vertical hold-down brackets on inlet and discharge end. Caution: Do not apply excessive sealing force on discharge end, as vane must be free to expand axially.

Connect inlet and discharge pressure transducers to feed line 1/8-in.-dia tubing. A minimum of one 3-in.-dia coil must be used to avoid restricting the discharge line.

Connect inlet line to coolant supply.

Activate coolant purge flow.

Connect instrumentation and check.

APPENDIX A-2

START AND SHUT DOWN SEQUENCE CHECK LIST

PAGE ____ INTENTIONALLY BLANK

START AND SHUT DOWN SEQUENCE CHECK LIST

START SEQUENCE

1. Check water level, flow rate and temperature.

2. Activate GN_2 or CH_4 coolant flow and check flow rate and pressure.

3. Open damper.

4. Follow purge and ignition sequence required by safety.

5. Check hot gas temperature and adjust O/F as required to obtain specified temperature.

6. Check test section optical pyrometers and adjust coolant flow as required.

7. Monitor coolant temperature and pressures at discharge throughout test.

SHUT DOWN SEQUENCE (full shut down)

1. Close fuel valve.

2. Stop blower, open vent valve.

3. Close damper.

4. Monitor test section temps, when under 300 F, change to GN_2 purge flow.

SHUT DOWN SEQUENCE FOR CYCLE TESTING USING N_2 COOLING

1. Use steps 1 & 2 only.

2. Hold full cooling flow until next start cycle.

APPENDIX A-3

EMERGENCY SHUT DOWN PARAMETERS

PAGE ____ INTENTIONALLY BLANK

EMERGENCY SHUT DOWN PARAMETERS

1. Loss of test section coolant or pressure. Initiate full shut down sequence.

2. Inability to prevent test section over heating by adjusting coolant flow. Initiate full shut down sequence.

APPENDIX B

DETAILED DESIGN DRAWINGS

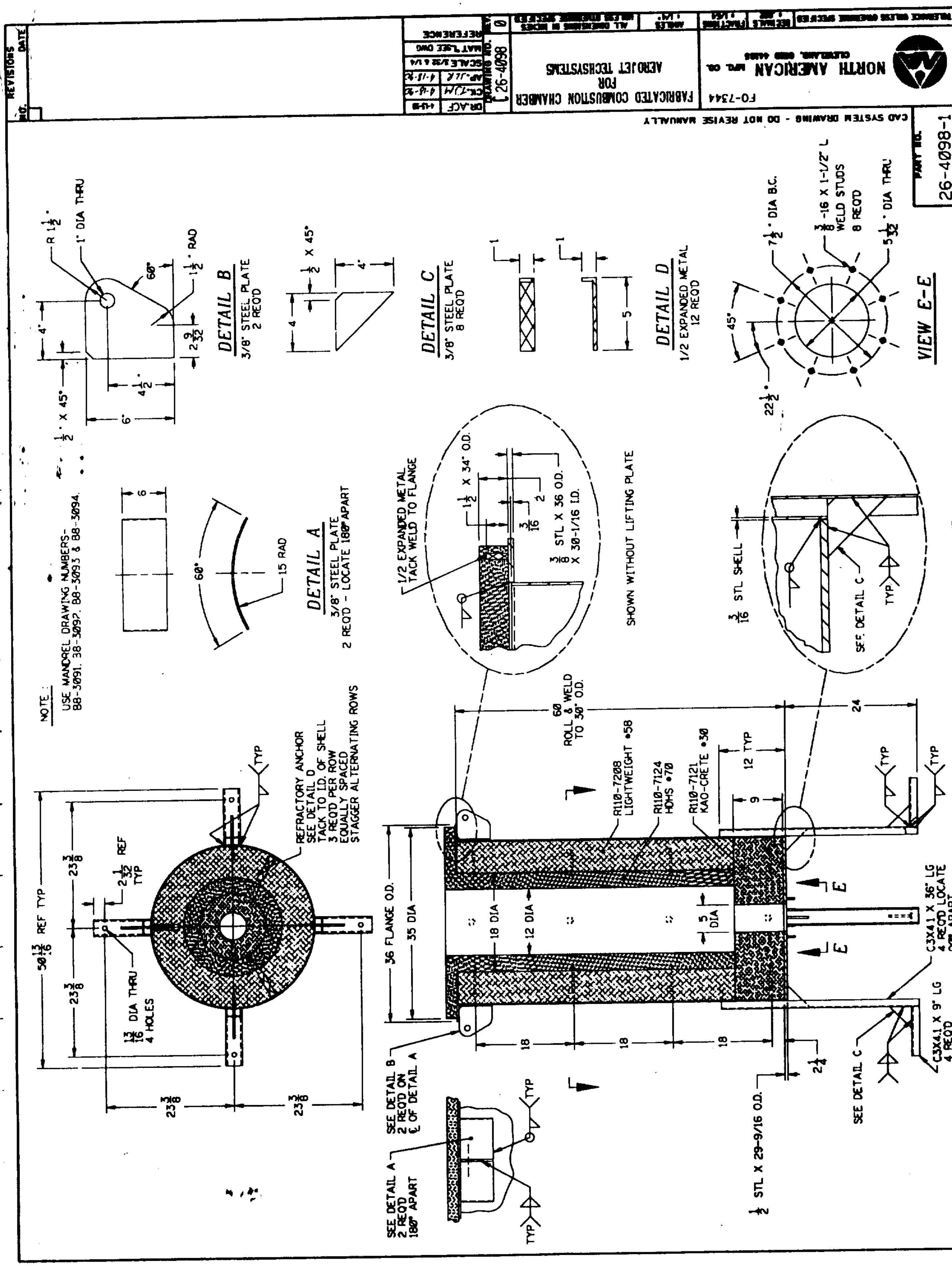

NORTH AMERICAN MFG. CO.
CLEVELAND, OHIO 44105
FO-7344
FABRICATED COMBUSTION CHAMBER
FOR
AEROJET TECHSYSTEMS
DRAWING NO. 26-4098
REV. 0
CAD SYSTEM DRAWING - DO NOT REVISE MANUALLY
PART NO. 26-4098-1
NOTE :
USE MANDREL DRAWING NUMBERS-
B8-3091. 38-3092. B8-3093 & B8-3094.
DETAIL A
3/8" STEEL PLATE
2 REQ'D - LOCATE 180° APART
15 RAD
60°
DETAIL B
3/8" STEEL PLATE
2 REQ'D
R 1½"
1" DIA THRU
1½" RAD
½" X 45°
DETAIL C
3/8" STEEL PLATE
8 REQ'D
DETAIL D
1/2 EXPANDED METAL
12 REQ'D
VIEW E-E
7½" DIA B.C.
⅜"-16 X 1-1/2" L
WELD STUDS
8 REQ'D
5 3/32" DIA THRU
22½°
45°
1/2 EXPANDED METAL
TACK WELD TO FLANGE
1½ X 34" O.D.
⅜ STL X 36 O.D.
X 30-1/16 I.D.
SHOWN WITHOUT LIFTING PLATE
3/16 STL SHELL
SEE DETAIL C
TYP
REFRACTORY ANCHOR
SEE DETAIL D
TACK TO I.D. OF SHELL
3 REQ'D PER ROW
EQUALLY SPACED
STAGGER ALTERNATING ROWS
50 13/16 REF TYP
23⅜
2 1/32 REF TYP
13/16 DIA THRU
4 HOLES
36 FLANGE O.D.
35 DIA
18 DIA
12 DIA
5 DIA
60
ROLL & WELD
TO 30" O.D.
R110-7208
LIGHTWEIGHT •58
R110-7124
HDHS •70
R110-7121
KAO-CRETE •30
24
12 TYP
9
E
C3X4.1 X 36" LG
4 REQ'D LOCATE
90° APART
C3X4.1 X 9" LG
4 REQ'D
SEE DETAIL C
½ STL X 29-9/16 O.D.
SEE DETAIL B
2 REQ'D ON
℄ OF DETAIL A
SEE DETAIL A
2 REQ'D
180° APART

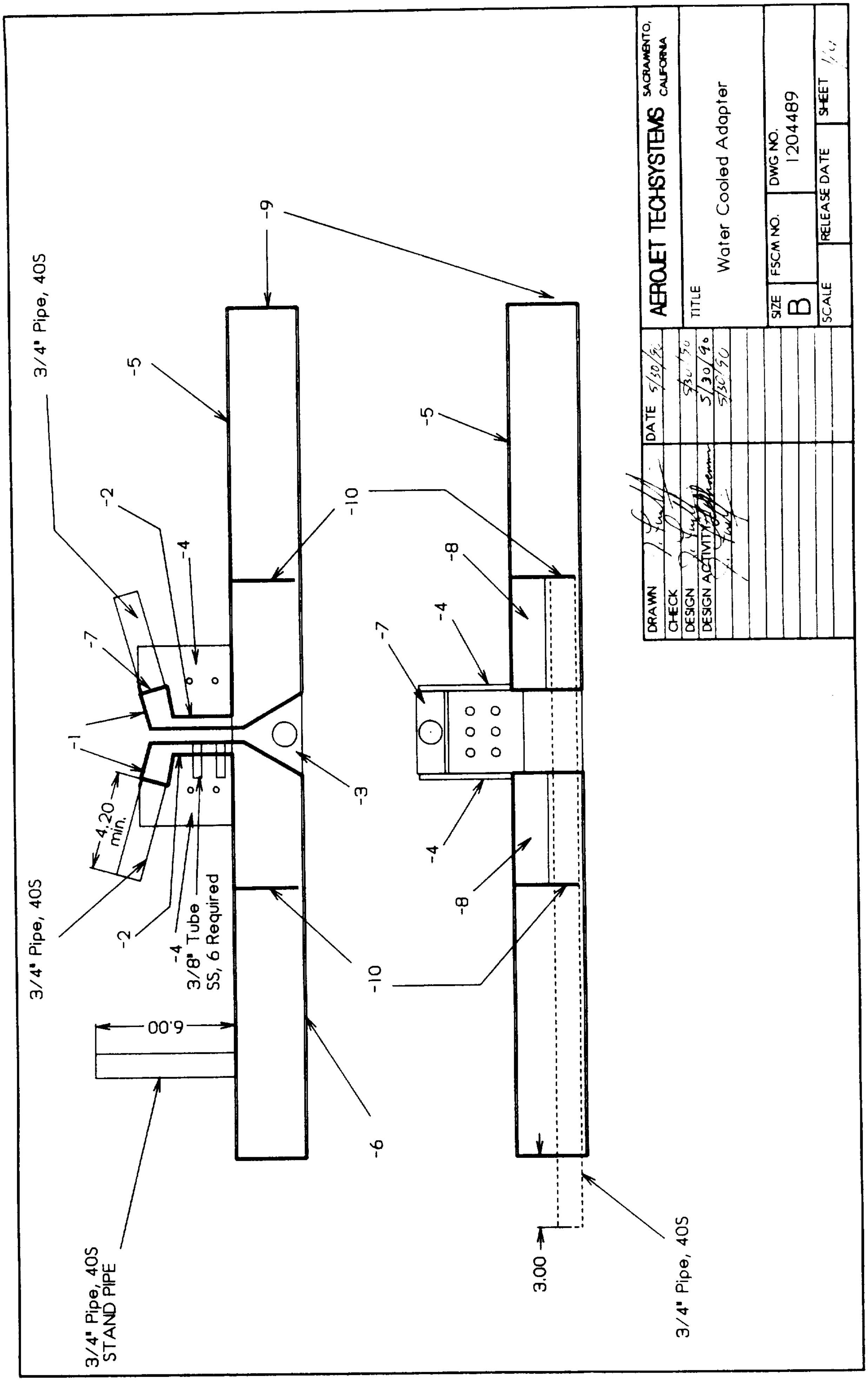
AEROJET TECHSYSTEMS
SACRAMENTO, CALIFORNIA
TITLE
Water Cooled Adapter
SIZE
B
FSCM NO.
DWG NO.
1204489
SCALE
RELEASE DATE
SHEET
DRAWN
CHECK
DESIGN
DESIGN ACTIVITY
DATE
5/30/90
5/30/90
5/30/90
5/30/90
3/4" Pipe, 40S
3/4" Pipe, 40S
3/4" Pipe, 40S
STAND PIPE
3/4" Pipe, 40S
3/8" Tube
SS, 6 Required
4.20
min.
6.00
3.00
-1
-2
-3
-4
-5
-6
-7
-8
-9
-10

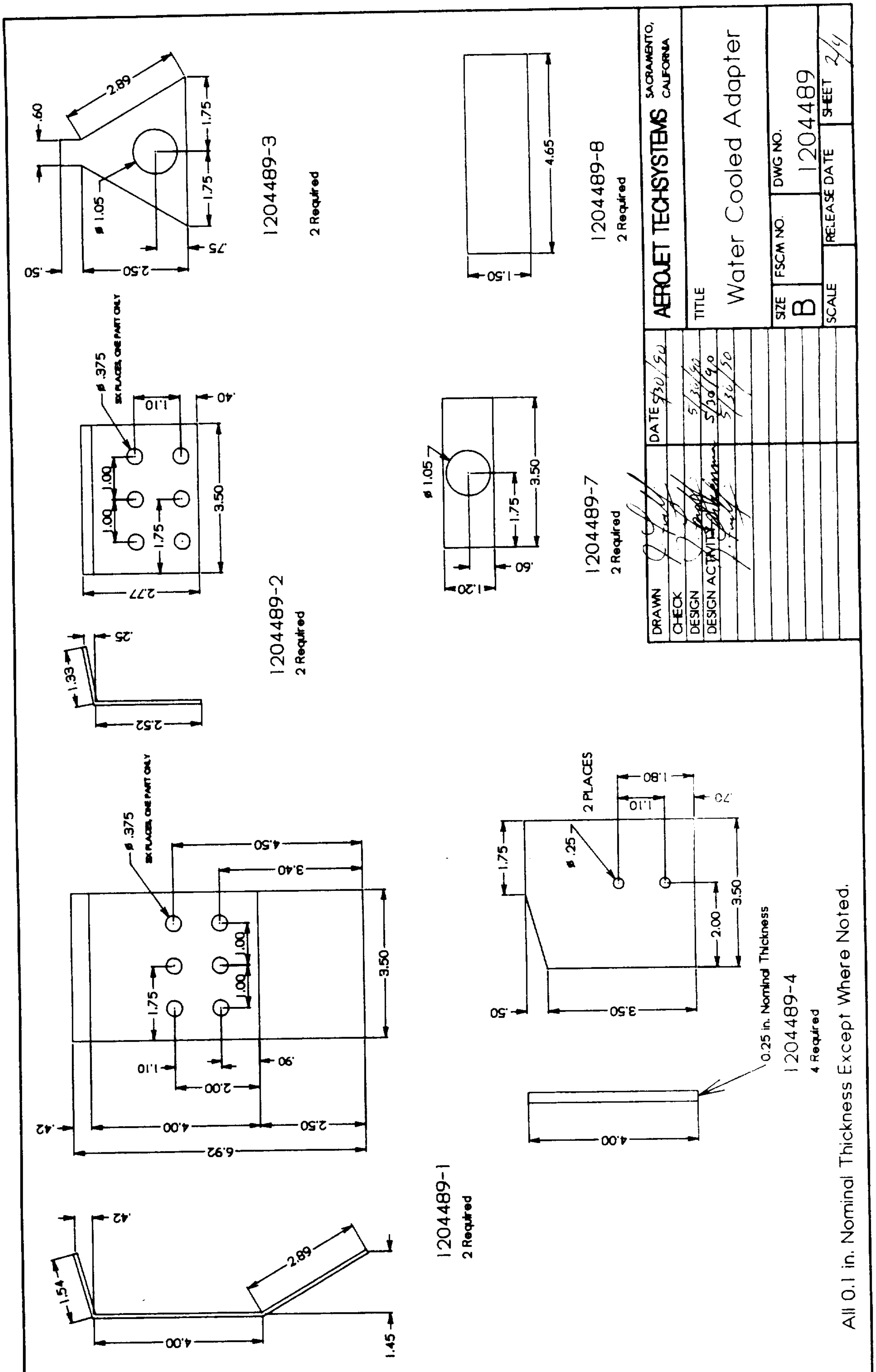
AEROJET TECHSYSTEMS SACRAMENTO, CALIFORNIA
TITLE
Water Cooled Adapter
SIZE B
FSCM NO.
DWG NO. 1204489
SCALE
RELEASE DATE
SHEET 2/4
DRAWN
CHECK
DESIGN
DESIGN ACTIVITY
DATE
1204489-1
2 Required
1204489-2
2 Required
1204489-3
2 Required
1204489-4
4 Required
1204489-7
2 Required
1204489-8
2 Required
ø .375
SIX PLACES, ONE PART ONLY
ø 1.05
ø .25
2 PLACES
0.25 in. Nominal Thickness
All 0.1 in. Nominal Thickness Except Where Noted.

PAGE ____ INTENTIONALLY BLANK

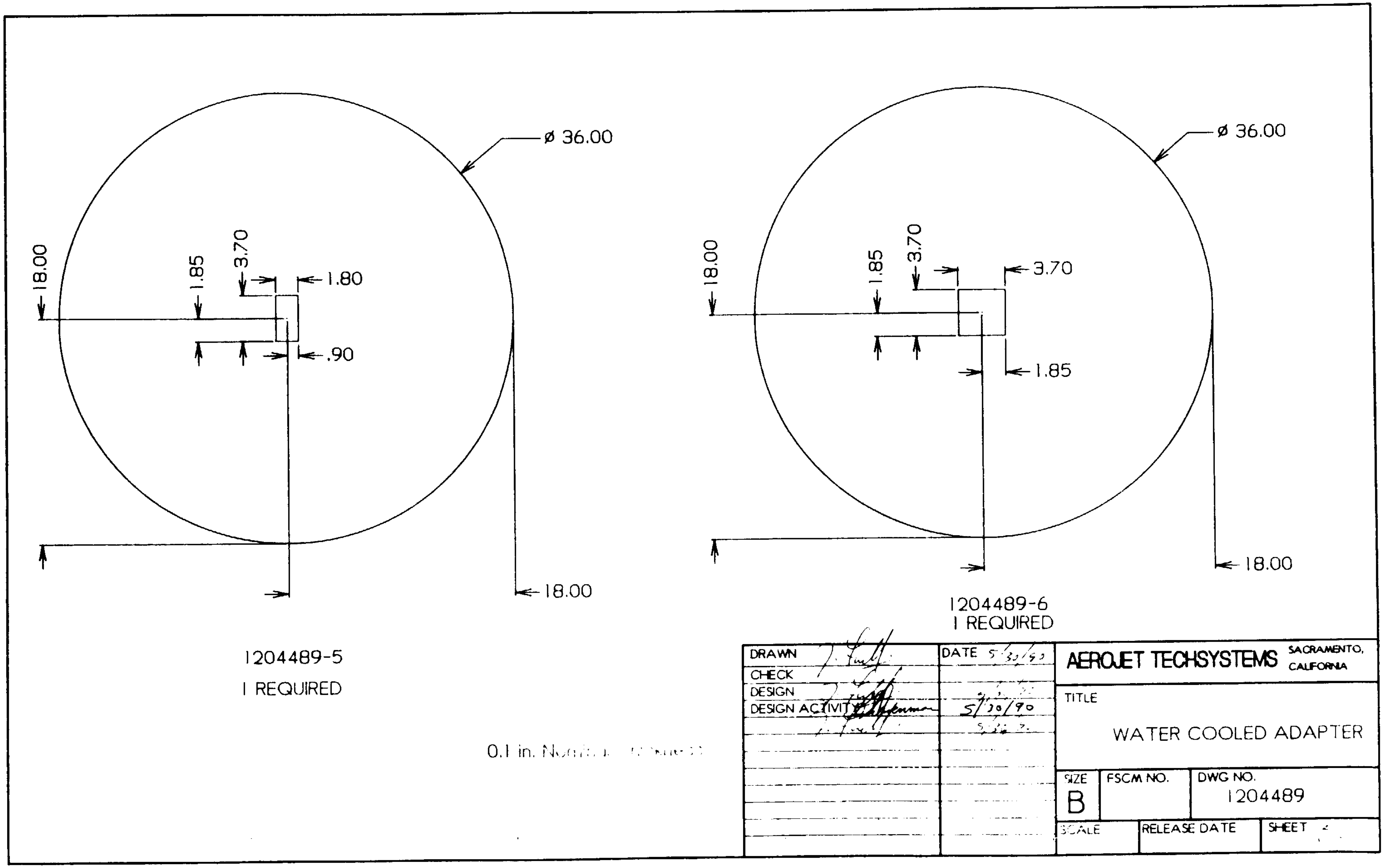
ø 36.00
18.00
1.85
3.70
1.80
.90
18.00
1204489-5
1 REQUIRED
ø 36.00
18.00
1.85
3.70
3.70
1.85
18.00
1204489-6
1 REQUIRED
0.1 in. Nominal
DRAWN
CHECK
DESIGN
DESIGN ACTIVITY
DATE
5/30/90
AEROJET TECHSYSTEMS SACRAMENTO, CALIFORNIA
TITLE
WATER COOLED ADAPTER
SIZE
B
FSCM NO.
DWG NO.
1204489
SCALE
RELEASE DATE
SHEET

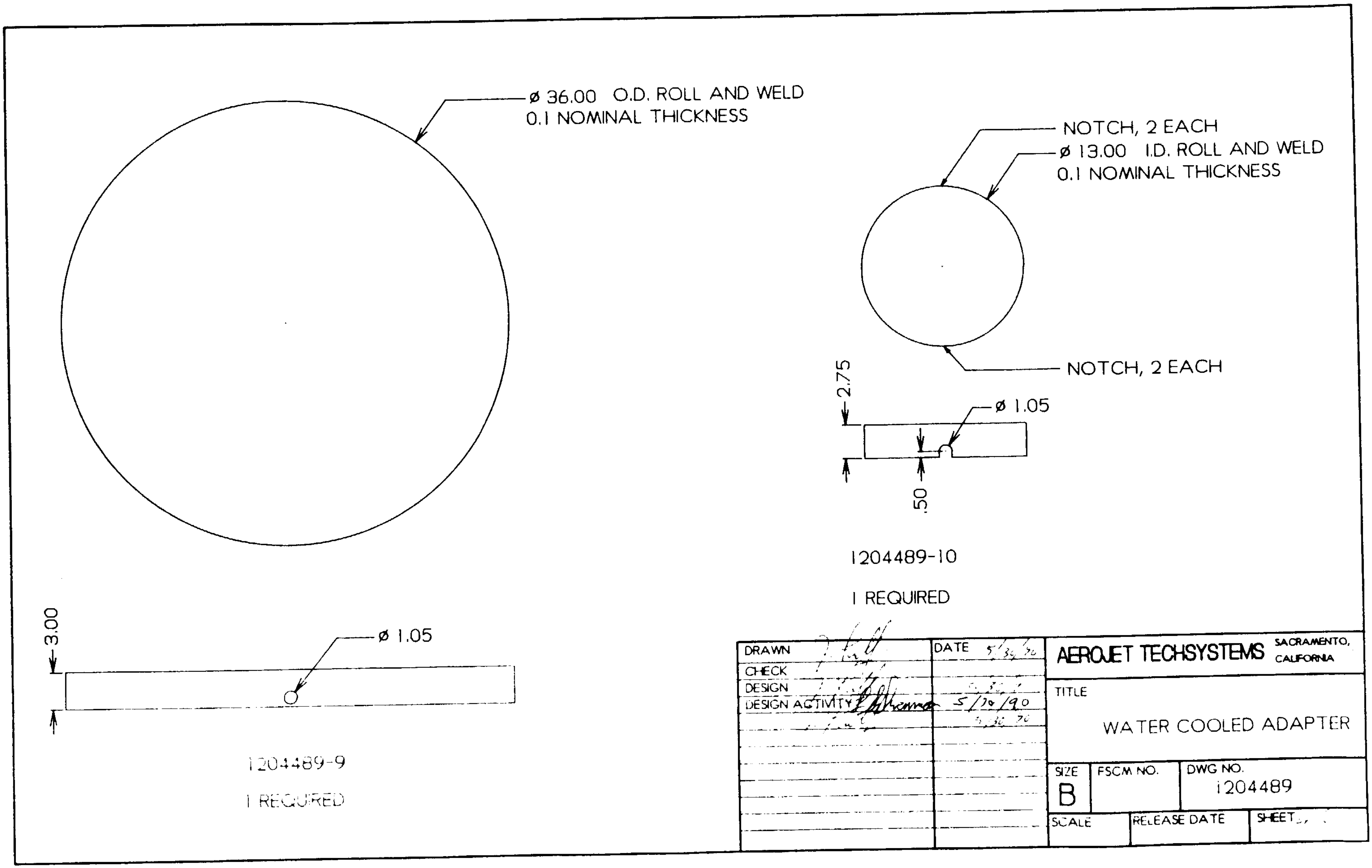
ø 36.00 O.D. ROLL AND WELD
0.1 NOMINAL THICKNESS
NOTCH, 2 EACH
ø 13.00 I.D. ROLL AND WELD
0.1 NOMINAL THICKNESS
NOTCH, 2 EACH
2.75
ø 1.05
.50
1204489-10
1 REQUIRED
3.00
ø 1.05
1204489-9
1 REQUIRED
DRAWN
CHECK
DESIGN
DESIGN ACTIVITY
DATE
5/30/90
5/30/90
AEROJET TECHSYSTEMS SACRAMENTO, CALIFORNIA
TITLE
WATER COOLED ADAPTER
SIZE
B
FSCM NO.
DWG NO.
1204489
SCALE
RELEASE DATE
SHEET

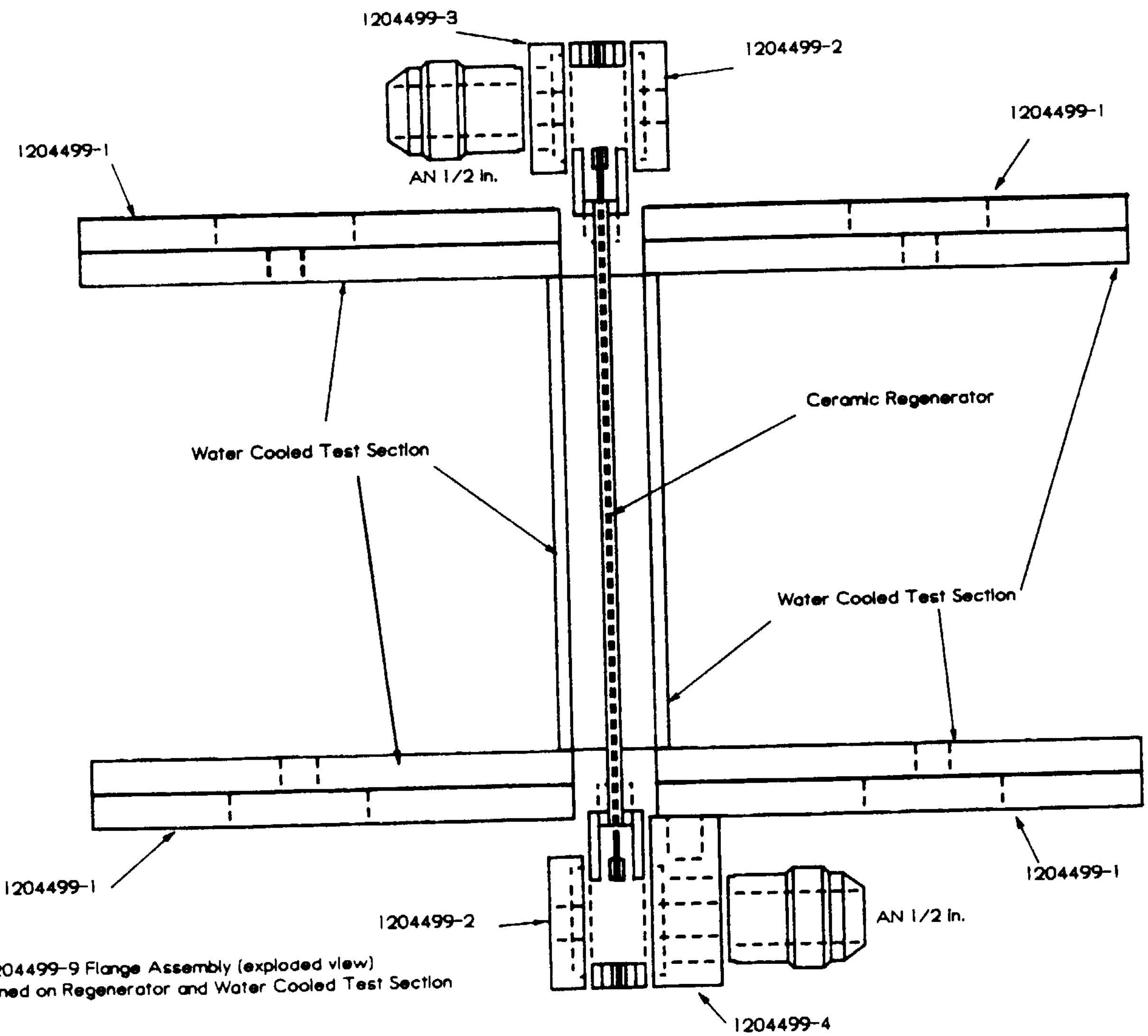

P/N 1204499-9 Flange Assembly (exploded view)
Positioned on Regenerator and Water Cooled Test Section

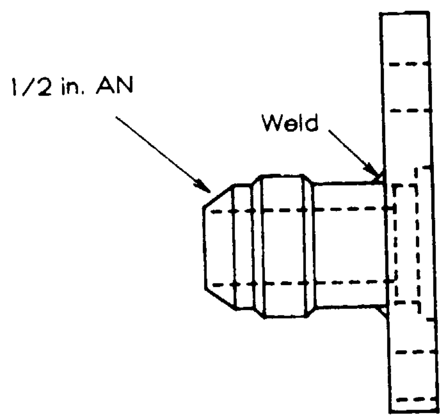

P/N 1204499-3

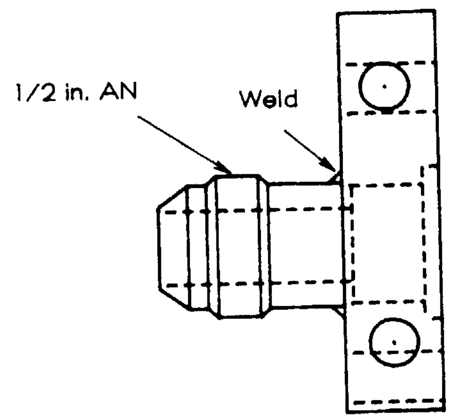

P/N 1204499-4

1. Bore .625 through hole.
2. Weld Fitting.
3. Flatten flange as needed.
4. Surface face opposite of weld.
5. Drill 1/4" holes and cut counter bore.

P/N 1204499-9 Assembly

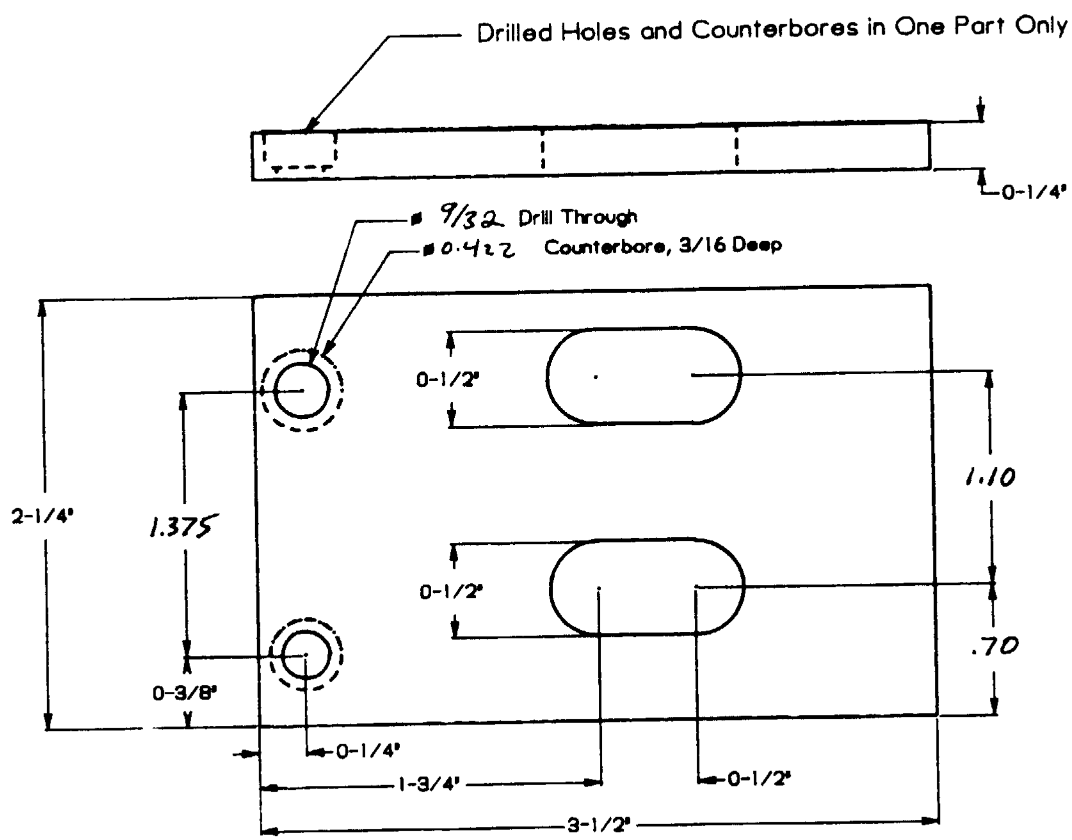

Ceramic Regenerator Flange Bracket
P/N 1204499-1, 4 Required
Fabricate from 300 series CRES

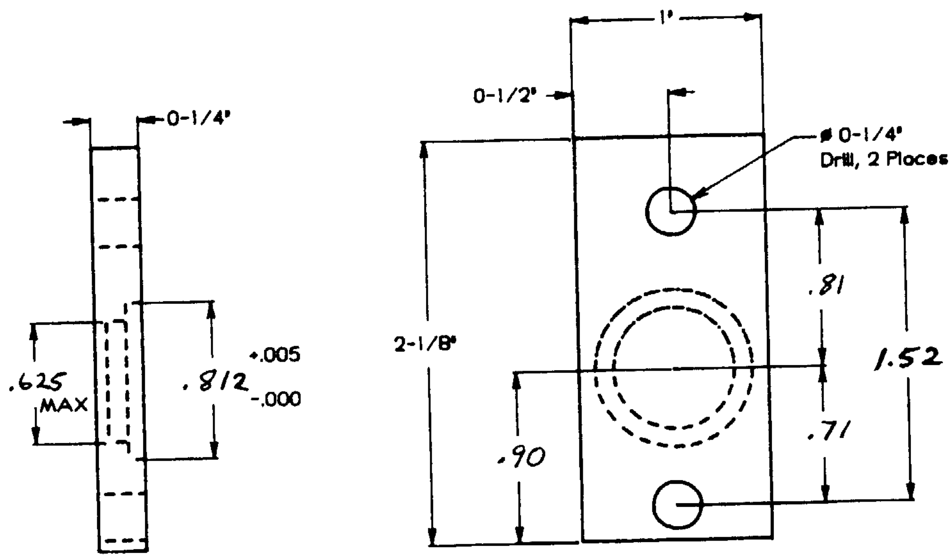

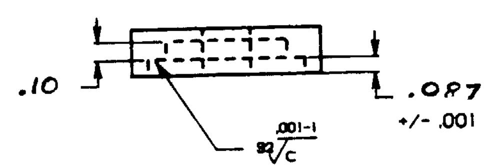

Ceramic Regenerator Flange
Plugged Side
P/N 1204499-2, 2 Required
Fabricate from 300 series CRES

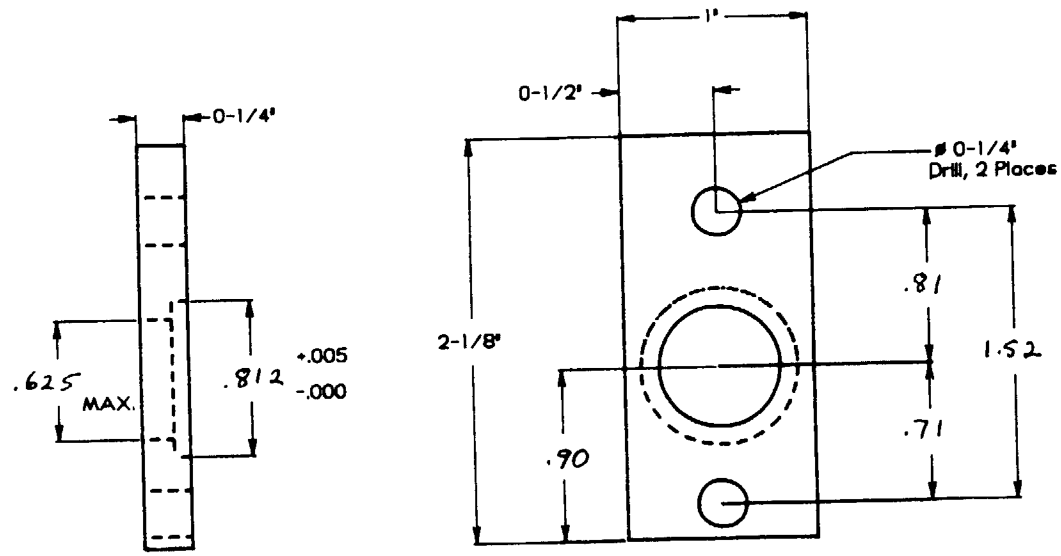

Ceramic Regenerator Flange
Passage Side, Outlet
P/N 1204499-3, 1 Required
Fabricate from 300 series CRES

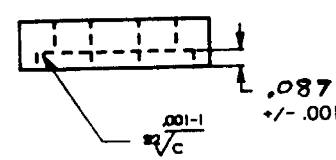

PAGE ____ INTENTIONALLY BLANK

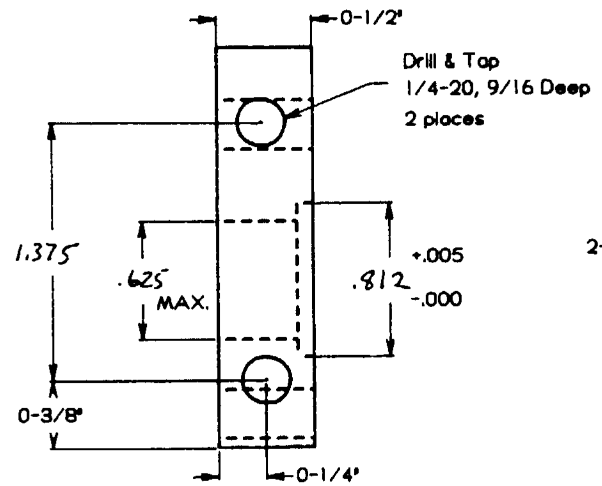

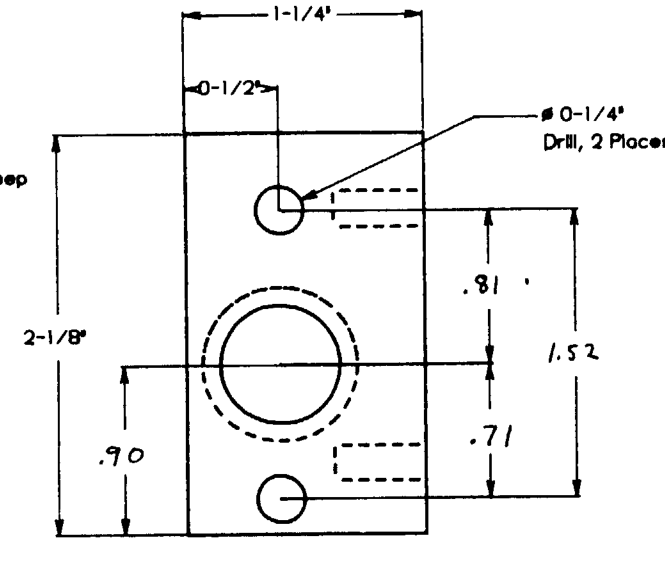

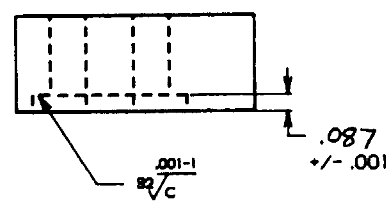

Ceramic Regenerator Flange
Passage Side, Inlet
P/N 1204499-4, 1 Required
Fabricate from 300 series CRES

PAGE ___ INTENTIONALLY BLANK

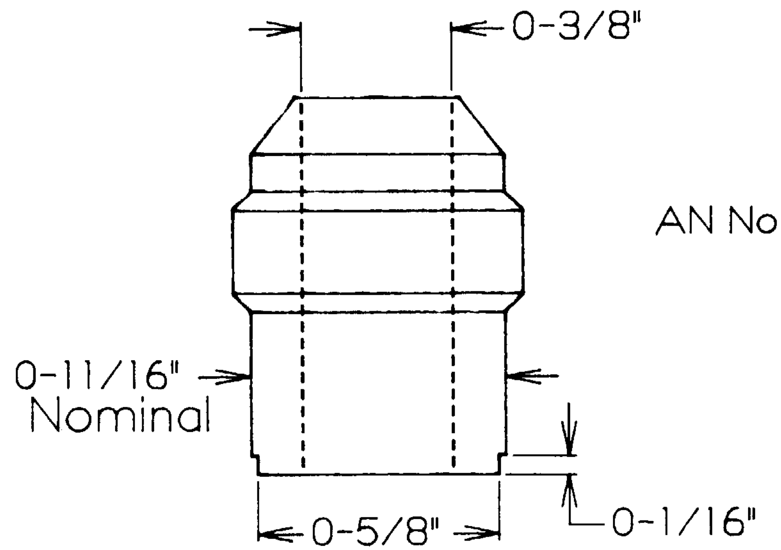

AN No. 8, 1/2 in. tube

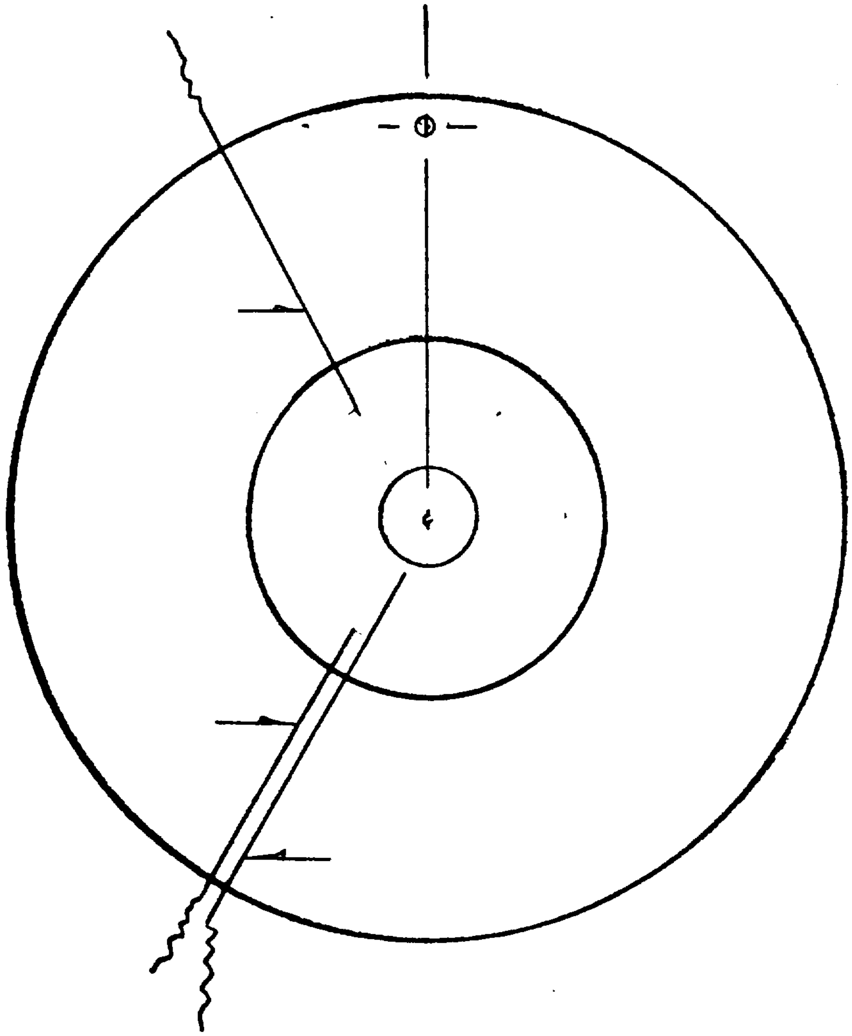

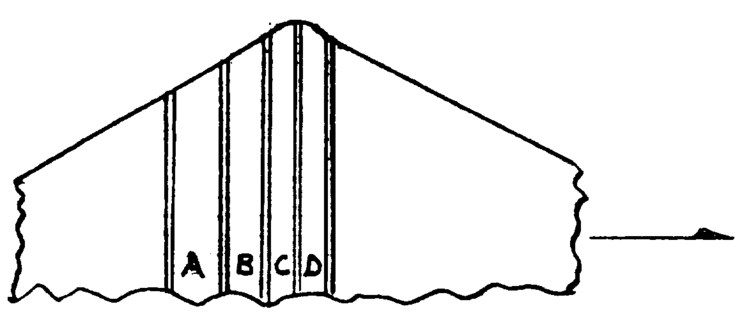
A
B
C
D

PAGE________ INTENTIONALLY BLANK

NASA
National Aeronautics and Space Administration

REPORT DOCUMENTATION PAGE

1. Report No. NASA CR 189053	2. Government Accession No.	3. Recipient's Catalog No.
4. Title And Subtitle Ceramic Regenerator Program Final Report		5. Report Date November 1991
		6. Performing Organization Code
7. Author(s) Jerrold E. Franklin		8. Performing Organization Report No. KFF-FR
		10. Work Unit No.
9. Performing Organization Name and Address Aerojet Propulsion Division P.O. Box 13222 Sacramento, CA 95813		11. Contract or Grant No. NAS 3-25416
12. Sponsoring Agency Name and Address NASA/Lewis Research Center 21000 Brookpark Road Cleveland, Ohio 44135		13. Type of Report and Period Covered Aug. 1988 thru June 1991
		14. Sponsoring Agency Code

15. Supplementary Notes

16. Abstract

The feasibility of fabricating an Air Turbo Ramjet (ATR) regenerator containing intricate hydraulic passages from a ceramic material in order to allow operation with high temperature combustion gas and to reduce weight as compared with metallic materials has been demonstrated. platelet technology, ceramic tape casting and multilayer ceramic packaging techniques were used in this fabrication of subscale silicon nitride components. Proof-of-concept demonstrations were performed to simulate a methane cooled regenerator for an ATR engine. The regenerator vane was designed to operate at realistic service conditions, i.e., 600 psi in a 3500 R (3040 F), 500 fps combustion gas environment. A total of six regenerators were fabricated and tested. The regenerators were shown to be able to withstand internal pressurization to 1575 psi. They were subjected to testing in 500 fps, 3560 R (3100 F) air/propane combustion products and were operated satisfactorily for an excess of 100 hr and 40 thermal cycles which exceeded 2460 R (2000 F).

17. Key Words (Suggested by Author(s)) Air Turbo Ramjet, ATR, Regenerator, Silicon Nitride, Ceramic Regenerator, Silicon Nitride Regenerator, Platelet Technology		18. Distribution Statement	
19. Security Classif. (of this report) Unclassified	20. Security Classif. (of this page) Unclassified	21. No. of pages 156	22. Price

NASA FORM 1626 OCT 86

RPT/I-0094 93A RDP